POLYCYCLIC AROMATIC HYDROCARBONS (PAHs):

SOURCES OF AMBIENT QUINONES

Final Report to California Air Resources Board
Contract No. 03-314
for the period January 1, 2004 to November 30, 2006

Janet Arey and Roger Atkinson, <u>Co-Principal Investigators</u>

Air Pollution Research Center
University of California
Riverside, CA 92521

May 2007

DISCLAIMER

The statements and conclusions in this Report are those of the contractor and not necessarily those of the California Air Resources Board. The mention of commercial products, their sources, or their use in connection with material reported herein is not to be construed as actual or implied endorsement of such products.

ACKNOWLEDGEMENTS

We thank the following for their contributions to the research described in this report:

TABLE OF CONTENTS

TABLE OF CONTENTS (CONT)

LIST OF FIGURES

LIST OF TABLES

LIST OF SCHEMES

ABSTRACT

It has been hypothesized that much of the high morbidity and mortality associated with fine particulate matter is due to quinones, such as 9,10-phenanthrenequinone, which have the ability to form reactive oxygen species (ROS) and cause oxidative stress. During this experimental program, we used the facilities and expertise available at the Air Pollution Research Center, University of California, Riverside, to investigate atmospheric reactions of alkylnaphthalenes and phenanthrene and to assess their potential to contribute to the ambient PAH-quinone burden. Based on our measured yields, calculations suggest that daytime OH radical-initiated and nighttime NO_3 radical-initiated reactions of gas-phase phenanthrene will be significant sources of 9,10-phenanthrenequinone in ambient atmospheres. In contrast, the ozone reaction with phenanthrene is unlikely to contribute significantly to ambient 9,10-phenanthrenequinone. The high yield (>30%) of 9,10-phenanthrenequinone from the NO_3 radical-initiated reaction implies the potential for high concentrations of this quionone to be formed in areas where nighttime NO_3 radical chemistry is important, such as Southern California.Hydroxyl radical-initiated reactions of naphthalene, naphthalene-d_8, 1- and 2-methylnaphthalene (1- and 2-MN), 1- and 2-ethylnaphthalene (1- and 2-EN) and the 10 isomeric dimethylnaphthalenes (DMNs) were conducted in a large volume Teflon chamber with analysis by atmospheric pressure ionization – mass spectrometry (API-MS). Quinone products were very minor, but the major products were ring-opened dicarbonyls that are 32 mass units higher in molecular weight than the parent compound, one or more ring-opened dicarbonyls of lower molecular weight resulting from loss of two β-carbons and associated alkyl groups, and ring-containing compounds that may be epoxides. The isomer-specific identifications and, importantly, the genotoxicity of these novel oxygenated species should be determined as well as their presence in ambient atmospheres. Gas-phase NO_3 radical-initiated reactions of naphthalene, the MNs, ENs and DMNs were conducted, and for the first time, the dimethylnitronaphthalene and ethylnitronaphthalene isomers formed were identified and their yields measured. Radical-initiated reactions of a mixture of ENs/DMNs proportioned to mimic ambient concentrations gave profiles of the ENNs and DMNNs expected to be formed from OH and NO_3 radical-initiated reactions. Comparing these ENN/DMNN profiles with those from ambient samples collected in Mexico City, Mexico, Riverside, CA and Redlands, CA, it is apparent that the nitro-PAH formation in Mexico City was dominated by OH radical reaction, while the ENN/DMNN profiles from Southern California could only be explained by the occurrence of nighttime NO_3 radical chemistry. This research suggests that nighttime NO_3 chemistry can be a significant source of toxic nitro-PAHs and PAH-quinones in ambient atmospheres.

EXECUTIVE SUMMARY

Background. It has been hypothesized that much of the high morbidity and mortality associated with fine particulate matter is due to quinones, such as 9,10-phenanthrenequinone, which have the ability to form reactive oxygen species (ROS) and cause oxidative stress. We investigated atmospheric reactions of alkylnaphthalenes and phenanthrene to assess their potential to contribute to the ambient quinone burden. For the alkylnaphthalenes, hydroxyl (OH) radical and nitrate (NO_3) radical reactions were investigated, including the formation of nitro-alkylnaphthalenes with the potential to photolyze and produce quinones as secondary products. For phenanthrene, the OH and NO_3 radical-initiated reactions and reaction with ozone (O_3) were investigated.

Methods. During this experimental program, we used the facilities and expertise available at the Air Pollution Research Center, University of California, Riverside, including Teflon chambers to simulate atmospheric reactions with OH and NO_3 radicals and O_3. We used a variety of mass spectrometric and chromatographic techniques for product identification.

Results.

Phenanthrene. The reported concentrations of 9,10-phenanthrenequinone on urban airborne particulates range up to 1 ng m^{-3} and the majority of ROS generation by extracts from ambient particles collected in Fresno, CA has recently been attributed to 9,10-phenanthrene-quinone (Chung *et al.*, 2006, Environ. Sci. Technol., 40, 4880-4886). Phenanthrene, a 3-ring polycyclic aromatic hydrocarbon exists in the atmosphere mainly in the gas-phase and has been observed in numerous ambient studies at concentrations higher than the ≥ 4-ring PAHs with, for example, phenanthrene concentrations measured in Southern California during 2003 ranging from 5-20 ng m^{-3}. Reactions with OH and NO_3 radicals are the most important daytime and nighttime atmospheric loss processes for phenanthrene, respectively and 9,10-phenanthrene-quinone was previously identified from the gas-phase reaction of phenanthrene with OH radicals. In this work we measured the 9,10-phenanthrenequinone yields to be ~3%, 33 ± 9%, and ~2% from the gas-phase OH radical, NO_3 radical and O_3 reactions, respectively. Calculations suggest that daytime OH radical-initiated and nighttime NO_3 radical-initiated reactions of gas-phase phenanthrene will be significant sources of 9,10-phenanthrenequinone in ambient atmospheres. In contrast, the ozone reaction with phenanthrene is unlikely to contribute significantly to ambient 9,10-phenanthrenequinone.

Alkylnaphthalenes. Naphthalene and the C_1- and C_2-alkylnaphthalenes are emitted by vehicle traffic and are the most abundant polycyclic aromatic hydrocarbons (PAHs) in urban atmospheres. For example, for a 5-day period in January 2003 at a heavily traffic-impacted site in Los Angeles, CA, the average morning concentrations for naphthalene, the sum of the methylnaphthalenes, and the sum of the dimethyl- and ethyl-naphthalenes were ~1600 ng m^{-3}, ~1000 ng m^{-3}, and ~160 ng m^{-3}, respectively, while co-located particle-associated benzo[*ghi*]perylene concentrations were ~2 ng m^{-3}. Hydroxyl radical-initiated reactions of naphthalene, naphthalene-d_8, 1- and 2-methylnaphthalene (1- and 2-MN), 1- and 2-ethylnaphthalene (1- and 2-EN) and the 10 isomeric dimethylnaphthalenes (DMNs) were conducted in a large volume Teflon chamber with analysis by atmospheric pressure ionization – mass spectrometry (API-MS). Quinone products were very minor, but the major products were ring-opened dicarbonyls that are 32 mass units higher in molecular weight than the parent compound, one or more ring-opened dicarbonyls of lower molecular weight resulting from loss of two β-carbons and associated alkyl groups, and ring-containing compounds that may be

epoxides. The isomer-specific identifications and, importantly, the genotoxicity of these novel oxygenated species should be determined. Interestingly, while OH radical addition appeared to occur mainly on the ring position *ortho* to the alkyl group(s), for 1,2-DMN *ipso* addition (i.e., addition to the carbon with the methyl group) explained the observed products.

Investigation of photolysis and OH radical reaction of ring-opened dicarbonyls resulting from loss of two β-carbons and associated alkyl groups, including phthaldialdehyde (formed from naphthalene, 2-MN, 2-EN and 2,3-DMN) and 2-acetylbenzaldehyde (formed from 1-MN, 1,2-DMN and 1,3-DMN) suggest that photolysis is the major atmospheric loss process for these aromatic dialdehyde and keto-aldehyde and confirmed that phthalic anhydride and alkyl-substituted phthalic anhydrides observed in the OH reactions of the naphthalene and the alkylnaphthalenes were second generation products. Considering the relatively high ambient concentrations of naphthalene and the alkylnaphthalenes, the potential health risks of the polar oxygenated products from their OH radical-initiated reactions should be investigated.

Nitrated polycyclic aromatic hydrocarbons (nitro-PAHs). Nitro-PAHs in ambient atmospheres are of concern because nitro-PAHs have been found to be mutagenic and carcinogenic. Isomer-specific nitro-PAH analyses are required to assess ambient air toxicity, and knowledge of the specific nitro-isomers present in ambient samples can also provide information on their sources. Like PAHs, nitro-PAHs may be emitted from combustion sources, but the nitronaphthalenes and alkylnitronaphthalenes present in ambient air have been attributed largely to *in situ* atmospheric formation from gas-phase reaction of naphthalene and the alkylnaphthalenes with OH radicals and NO_3 radicals. To allow identification of the dimethylnitronaphthalenes (DMNNs) and ethylnitronaphthalenes (ENNs) formed, in particular, from the NO_3 radical-initiated reactions in which high yields of nitro-products were anticipated, sub-mg to mg amounts of the 42 DMNN and 14 ENN isomers were synthesized by nitration of the parent alkylnaphthalene with N_2O_5 in CCl_4 solution. A combination of proton nuclear magnetic resonance (^1H NMR) analyses and gas chromatography/mass spectrometry (GC/MS) analyses with electron impact ionization allowed unequivocal identification of all DMNN isomers and of all but 3 ENN isomers. Retention indices (RI) on a 5% phenylmethyl-polysiloxane capillary GC column were measured.

Gas-phase NO_3 radical-initiated reactions of naphthalene, the MNs, ENs and DMNs were conducted, and for the first time, the dimethylnitronaphthalene and ethylnitronaphthalene isomers formed were identified and their yields measured. The measured yields for the ENNs from 1-EN and 2-EN were 12% and 19%, respectively, and the yields of the DMNNs ranged from 4-21%. A mechanism has been postulated to explain the most abundant isomer formed in each of these reactions which involves addition of the NO_3 at the most electrophilic position followed by *ortho* or *para* addition of NO_2 and subsequent loss of HNO_3.

Radical-initiated reactions of a mixture of ENs/DMNs proportioned to mimic ambient concentrations gave profiles of the ENNs and DMNNs expected to be formed from OH and NO_3 radical-initiated reactions. Comparing these ENN/DMNN profiles with those from ambient samples collected in Mexico City, Mexico, Riverside, CA and Redlands, CA, it is apparent that the nitro-PAH formation in Mexico City was dominated by OH radical reaction, while the ENN/DMNN profiles from Southern California could only be explained by the occurrence of nighttime NO_3 radical chemistry.

In addition to nitro-derivatives, quinones were also direct products of the NO_3 radical reaction with ENs and DMNs. Quinone formation was favored for isomers with β-alkyl-substitution. The yield of 1,4-naphthoquinone measured from naphthalene was 3.6%, the 2-

methyl-1,4-naphthoquinone (menadione) yield from 2-MN was 3.4% and the sum of the yields of the two quinone isomers formed from 2-EN was 2.2%. The quinone yields measured from 2,3-DMN, 2,6-DMN and 2,7-DMN were 4.1%, 2.2% and 3.9%, respectively.

Photolysis of 2-M-1NN produced 2-methyl-1,4-naphthoquinone, but apparently required the presence of NO_x at ppbv levels to obtain a maximum yield of 18%. 2,6-Dimethyl-1-nitronaphthalene photolyzed in the presence of 9 ppbv NO_2 produced 2,6-dimethyl-1,4-naphthoquinone. While ppbv levels of NO_x are realistic urban ambient conditions, the dependence on NO_x could be an experimental artifact and needs to be elucidated.

Conclusions. Nitro-PAHs and quinones are formed in higher yields from NO_3 radical-initiated reactions than from OH radical-initiated reactions. While the OH radical is ubiquitous during daylight hours, NO_3 is significant only at night (NO_3 photolyzes with a lifetime at solar noon of ~5 s) and requires the presence of both O_3 and NO_2 to form. Our NO_3 radical reaction yield data allow predictions on a relative basis of quinone formation from 2-3 ring PAH and of alkylnitronaphthalenes. Ambient measurements can be used to confirm these predictions and establish the importance of the NO_3 radical-initiated formation pathway in ambient atmospheres. Photolysis of the DMNNs/ENNs formed from atmospheric reactions may be another source of ambient quinones, but the apparent NO_x dependence of these reactions needs to be understood before this pathway can be reliably evaluated.

I. INTRODUCTION AND BACKGROUND

It has been hypothesized that much of the high morbidity and mortality associated with fine particulate matter (PM) is due to quinones (Froines, 2003). Quinones cause a variety of toxic effects *in vivo* through mechanisms involving (1) covalent binding to cellular proteins and/or DNA and (2) redox cycling with their semiquinone radicals, leading to formation of reactive oxygen species [ROS] (Bolton *et al.*, 2000). Demonstrating the former, human bronchial epithelial cells were arylated *in vitro* by 1,4-naphthoquinone at multiple protein targets (Lame *et al.*, 2003). Suggesting the latter, 9,10-phenanthrenequinone, 1,4- and 1,2-naphthoquinone, and 2-methyl-1,4-naphthoquinone have all been shown to be active in suppressing neuronal nitric oxide synthase (nNOS) activity, with phenanthrenequinone being most potent (Kumagai *et al.*, 1998) and also capable of inhibiting endothelial nitric oxide synthase activity and suppressing vasorelaxation (Kumagai *et al.*, 2001). Recent studies provided further support for the redox cycling capability of phenanthrenequinone with authors of one study concluding that "phenanthrenequinone may be, at least partially, responsible for diesel exhaust particle-induced oxidative stress" (Kumagai *et al.*, 2002) and other researchers attributing toxic action in aerobic yeast systems to ROS from 9,10-phenthrenequinone (Rodriguez *et al.*, 2004; 2005). Redox cycling, with rapid and sequential reduction back to the quinone and the formation of reactive oxygen species potentiates the toxic effect with one equivalent of quinone generating multiple equivalents of toxic reactive oxygen species.

PAH-quinones in ambient air may have as their sources: (a) direct emissions, for example, in diesel exhaust (Choudhury, 1982; Schuetzle, 1983) and (b) *in situ* atmospheric formation from radical-initiated reaction of the parent PAHs (Sasaki *et al.*, 1997a) or photolysis of nitro-PAHs (Atkinson *et al.*, 1989; Arey *et al.*, 1990). Thus, we have previously shown that 1,4-naphthoquinone is formed from the hydroxyl (OH) radical and nitrate (NO_3) radical-initiated reactions of naphthalene in a 1-2% yield (Sasaki *et al.*, 1997a) and the photolysis of 1-nitronaphthalene and 2-methyl-1-nitronaphthalene lead to the formation of 1,4-naphthoquinone and 2-methyl-1,4-naphthoquinone, respectively, with a ~20% yield (Atkinson *et al.*, 1989; Arey *et al.*, 1990).

Both nitro-PAHs and PAH-quinones are present in diesel emissions in small concentrations in comparison with the PAHs emitted. It has been shown that in California, nitro-PAH formation from atmospheric gas-phase PAH reactions completely dominates over nitro-PAH emissions from vehicle exhaust (Arey, 1998; Arey and Atkinson, 2003; Reisen *et al.*, 2003, 2005). Additionally, these atmospherically-formed nitro-PAH and nitro-PAH derivatives (Sasaki *et al.*, 1995 Helmig *et al.*, 1992a,b) make significant contributions to the bacterial (Arey *et al.*, 1988; Gupta, 1995; Gupta *et al.*, 1996; Sasaki *et al.*, 1995; Helmig *et al.*, 1992a,b) and human cell (Sasaki *et al.*, 1997b; Sasaki *et al.*, 1999; Phousongphouang *et al.*, 2000) genotoxicity of ambient air. Since PAH-quinones can be produced by atmospheric reactions of PAHs and by photolysis of their nitro-derivatives, it seems likely that atmospheric formation of PAH-quinones may be an important contributor to the PAH-quinone burden of California's air. Therefore, it is imperative to understand the role of atmospheric reactions in the production of PAH-quinones in order to assess the potentially significant consequences for the health of California's residents.

Ambient PAH Concentrations. In the late 1980's we conducted a CARB-funded study of ambient concentrations of selected PAHs at seven locations throughout California impacted by different combustion emissions and observed that at all locations naphthalene was the most abundant PAH (Atkinson *et al.*, 1988). While atmospheric PAH concentrations have decreased

since the 1980's, the PAH profiles, with the most abundant PAHs being the most volatile, remain unchanged. Table 1 shows the ambient concentrations of the 2- to 4-ring PAHs recently measured in Los Angeles near the intersection of two major freeways (samplers located on the roof of the Denney Research Center at the University of Southern California [USC]).

The relative concentrations of the PAHs shown in Table 1 may be considered a typical "traffic PAH profile", with the Σmethylnaphthalenes (MNs) roughly half that of naphthalene and the Σdimethylnaphthalenes (DMNs) roughly 10% of the naphthalene concentration. The relative abundances of the specific DMNs (see Figure 1) is very similar to what we have observed in diesel fuel, with the most abundant isomers being 1,6-, 1,7-, 2,6- and 2,7- DMN and with no 1,8-DMN present.

The PAHs listed in Table 1 are expected to be mainly in the gas-phase or distributed between the gas- and particle-phases (fluoranthene and pyrene). The lifetimes of these PAHs due to gas-phase OH radical-initiated reaction are significantly less than one day and as shown in Table 1 for an OH radical concentrations of 5×10^6 molecule cm^{-3} [a noontime, summer value measured in Los Angeles (George *et al.*, 1999)] could be less than one hour, for example, for the dimethylnaphthalenes. Thus, atmospheric reaction products of naphthalene and alkylnaphthalenes, such as their nitro- or quinone-derivatives, should also be present in California's atmosphere.

As seen in Table 1, phenanthrene is generally in higher concentration in ambient atmospheres than the ≥ 4-ring PAHs. Because of its relatively high abundance and the potentially significant toxicity of 9,10-phenanthrenequinone, in addition to naphthalene and the alkylnaphthalenes, we studied the atmospheric reactions of phenanthrene and their potential to form 9,10-phenanthrenequinone.

Table 1. Average morning (7:30-10:30 PST) PAH concentrations measured in Los Angeles January 13-17, 2003 (data from Reisen and Arey, 2005) and selected calculated lifetimes (τ) for reaction with the OH radical [data from Phousongphouang and Arey (2002) and Arey and Atkinson (2003)].

PAH	ng m^{-3}	τ_{OH}[a]
Naphthalene	1,590	2.3 hr
2-Methylnaphthalene	728	1.1 hr
1-Methylnaphthalene	306	1.4 hr
Σ Methylnaphthalenes	1,034	
2-Ethylnaphthalene	30.2	1.4 hr
1-Ethylnaphthalene	4.5	1.5 hr
Σ Ethylnaphthalenes	34.7	
2,6 + 2,7-Dimethylnaphthalene	40.3	
1,3 + 1,7-Dimethylnaphthalene	40.8	
1,6-Dimethylnaphthalene	19.4	
1,4-Dimethylnaphthalene	3.3	
1,5 + 2,3-Dimethylnaphthalene	9.6	
1,2-Dimethylnaphthalene	6.9	
Σ Dimethylnaphthalenes	120.3	40-60 min
Biphenyl	22.9	7.8 hr
Phenanthrene	17.3	3.1 hr
Anthracene	1.6	
Σ Methylphenanthrenes	8.8	
Fluoranthene	6.0	
Pyrene	6.9	

[a]Lifetimes calculated for an OH radical concentration of 5×10^6 molecule cm^{-3} (George *et al.*, 1999).

Time (min)

Abundance

50   49   48   47   46   45   44

20   40   60   80

1,8-DMN

1,2-DMN

1,5-DMN

1,4-DMN

2,3-DMN

1-EN

2-EN

1,7-DMN

2,6-DMN

2,7-DMN

1,3-DMN
1,6-DMN
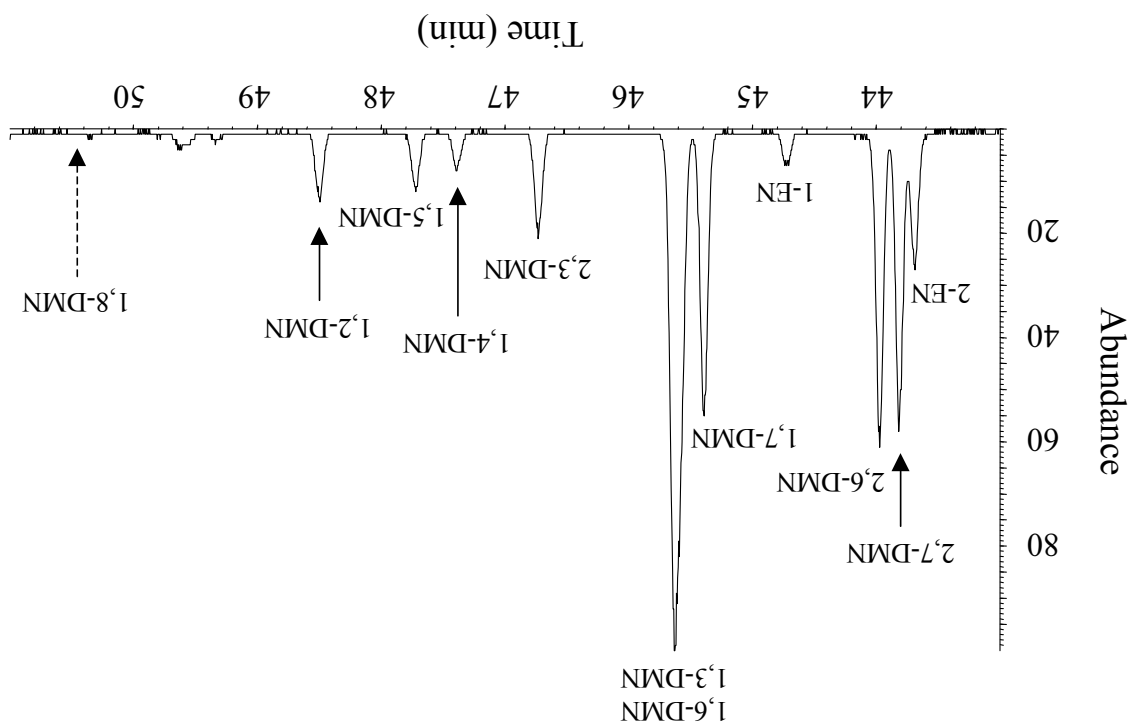
Figure 1. GC/MS SIM analysis of a nighttime sample from Riverside, CA for the molecular ion (m/z 156) of the dimethylnaphthalenes (DMNs) and ethylnaphthalenes (ENs) separated on a DB-17 capillary column. Analysis on a DB-1701 capillary column confirmed the presence of both 1,3- and 1,6-DMN. Note that the dashed arrow shows the retention time for 1,8-DMN, which was not observed in the ambient sample. (Figure from Phousongphouang and Arey, 2003a).

4

II. OVERALL OBJECTIVES AND RESULTS

The objectives of this project were to evaluate the potential for atmospheric reactions to contribute to the atmospheric PAH-quinone burden by:

- Assessing formation of PAH-quinones from atmospheric reactions of naphthalene, alkylnaphthalenes and phenanthrene.

- Identifying the dimethylnitronaphthalenes formed from atmospheric reaction of selected dimethylnaphthalenes and studying their photolysis reaction and products, which were expected to include quinones.

To achieve these objectives, we set out to perform several specific tasks during this contract which have resulted to date in four published (or in press) manuscripts and more are in preparation. For convenience in preparation as well as ease in reading, we will present six sections (A-F) each with its own Introduction, Experimental Methods, Results and Discussion sections. The tasks originally defined and the sections in which our results are reported are as follows:

Task 1.
Atmospheric pressure ionization – mass spectrometry (API-MS) analysis of OH radical-initiated reactions of naphthalene, 1- and 2-methylnaphthalene, 1,2-, 1,3-, 1,4-, 1,5-, 1,6, 1,7-, 1,8-, 2,3-, 2,6-, and 2,7- dimethylnaphthalenes, and 1- and 2-ethylnaphthalene screening for quinone products.

- We conducted OH radical-initiated reactions of the alkylnaphthalenes, monitoring by API-MS, and found quinone products to be minor. The major products observed were two groups of ring-opened dicarbonyl products: in the first, all the carbons of the alkylnaphthalene remained and, in the second, the dicarbonyls resulted from a loss of two β-carbons [and associated alkyl group(s)]. To help us determine whether these smaller carbonyls were secondary products, we conducted reactions on a series of aromatic carbonyl compounds. The results of these investigations are presented below in: **B. Kinetics and Products of Photolysis and Reaction with OH Radicals of a Series of Aromatic Carbonyl Compounds** and **C. Dicarbonyl Products of OH Radical-Initiated Reactions of Naphthalene and Alkylnaphthalenes**.

Task 2.
API-MS analysis of photolysis products of 1- and 2-nitronaphthalene and 2-methyl-1-nitronaphthalene and selected dimethylnitronaphthalenes (see Task 3 below) screening for quinone products.

- During our NO_3 radical-initiated reactions to determine the dimethylnitronaphthalene products from selected dimethylnaphthalenes (see Task 3), we observed quinone formation. The quinone yields from the NO_3 radical-initiated reactions of naphthalene, 1- and 2-methylnaphthalene, and all 12 dimethyl- and ethyl-naphthalenes, as well as results

5

of preliminary photolysis experiments on alkylnitronaphthalenes are presented in: **F. Oxygenated Products, Including Quinones, from NO₃ Radical-Initiated Reactions of PAHs and from Nitro-PAH Photolysis**.

Task 3.
Identification of dimethylnitronaphthalenes from the OH and NO$_3$ radical-initiated reactions of 1,6-, 1,7-, 2,6- and 2,7-dimethylnaphthalenes (the most abundant dimethylnaphthalene isomers observed in ambient air samples).

- We conducted NO$_3$ radical-initiated reactions of all 12 dimethyl- and ethyl-naphthalenes and utilizing the retention indices developed (see Task 4) determined the nitro-products formed. We also conducted an OH radical-initiated reaction of a mixture of the alkylnaphthalenes proportioned to match ambient concentrations. Finally, we have compared the nitro-products produced with those found in ambient air samples. The results of these investigations are presented in: **E. Nitroarene Products of the NO₃ Radical-Initiated Reactions of Naphthalene and the C₁- and C₂-Alkylnaphthalenes and their Occurrence in Ambient Air**.

Task 4.
Conduct synthesis of dimethylnitronaphthalenes in conjunction with Task 3.

- We have synthesized mg or sub-mg amounts of all 56 dimethyl-/ethyl-nitronaphthalenes to obtain gas chromatographic retention index information to allow identification of all isomers formed by atmospheric reactions. The results are presented in: **D. Synthesis of Dimethylnitronaphthalenes/Ethylnitronaphthalenes**.

Task 5.
API-MS analysis of OH, NO$_3$ and O$_3$ reactions of phenanthrene screening for quinone products.

- We have conducted chamber reactions of gas-phase phenanthrene with OH radicals, NO$_3$ radicals and ozone and measured the formation of 9,10-phenanthrene quinone. The results of these investigations are presented in: **A. Formation of 9,10-Phenanthrenequinone by Atmospheric Gas-phase Reactions of Phenanthrene**.

Task 6.
Identification of most abundant compounds tentatively identified as quinones products from the reactions conducted in Tasks 1, 2, and 5.

- We quantified the formation of 9,10-phenanthrenequinone from the gas-phase reactions of phenanthrene and the results are presented in : **A. Formation of 9,10-Phenanthrenequinone by Atmospheric Gas-phase Reactions of Phenanthrene**. The quinone yields from the NO$_3$ radical reactions of the alkylnaphthalenes are presented in: **F. Oxygenated Products, Including Quinones, from NO₃ Radical-Initiated Reactions of PAHs and from Nitro-PAH Photolysis**.

A. Formation of 9,10-Phenanthrenequinone by
Atmospheric Gas-phase Reactions of Phenanthrene

1. Introduction

Phenanthrene, a 3-ring polycyclic aromatic hydrocarbon (PAH) which exists in the atmosphere mainly in the gas-phase (Bidleman, 1988; Coutant et al., 1988; Wania and Mackay, 1996), has been observed in numerous ambient studies at concentrations higher than the $\geq$ 4-ring PAHs with, for example, phenanthrene concentrations measured in Southern California during 2003 ranging from 5-20 ng m^{-3} (see, for example, Atkinson et al., 1988; Arey et al., 1989a; Reisen and Arey, 2005). The atmospheric gas-phase reaction rates of phenanthrene with hydroxyl radicals (OH), nitrate radicals (NO$_3$) and ozone (O$_3$) have been measured (Lorenz and Zellner, 1984; Biermann et al., 1985; Brubaker et al., 1998; Kwok et al., 1994; Lee et al., 2003) and indicate that reactions with OH radicals and NO$_3$ radicals will be the most important daytime and nighttime atmospheric loss processes for phenanthrene, respectively. Nitrophenanthrene products were identified from the gas-phase reactions of phenanthrene with OH radicals and NO$_3$ radicals in the presence of NO$_x$, but only in low yields (Arey et al., 1989b). Helmig and Harger (1994) identified a number of oxygenated products, including 9,10-phenanthrenequinone, from the gas-phase reaction of phenanthrene with OH radicals in the presence of NO$_x$, and nitrodibenzopyranones formed from this reaction were shown to be highly mutagenic in one bacterial assay system (Helmig et al., 1992a,b).

Quinones have been postulated to contribute to the toxicity of diesel exhaust particles and ambient particles. Many of the toxic effects of quinones are attributed to their ability to form reactive oxygen species (ROS) and cause oxidative stress (Bolton et al., 2000). 9,10-Phenanthrenequinone has a favorable reduction potential to undergo redox cycling in biological systems (Rodriguez et al., 2004), and the formation of ROS by 9,10-phenanthrenequinone has been shown to lead to its toxic action in aerobic yeast systems (Rodriguez et al., 2004; 2005). It has also been hypothesized that murine lung inflammation resulting from intratracheal administration of 9,10-phenanthrenequinone may be mediated by enhancement of oxidative stress and that the phenanthrenequinone present in diesel exhaust particles (Schuetzle, 1983; Cho et al., 2004) may play a role in the pulmonary toxicity of diesel exhaust particles (Hiyoshi et al., 2005). The reported concentrations of 9,10-phenanthrenequinone on urban airborne particulates range up to 1 ng m^{-3} (Allen et al., 1997; Cho et al., 2004; Kishikawa et al., 2006; Chung et al., 2006). The majority of ROS generation by extracts from ambient particles collected in Fresno, CA has recently been attributed to 9,10-phenanthrenequinone (Chung et al., 2006).

Although 9,10-phenanthrenequinone has been quantified in ambient air because of its potential toxicity, its sources remain to be elucidated. Cho et al. (2004) found elevated concentrations at receptor sites in the Los Angeles air basin, but Chung et al. (2006) did not find the positive correlation they expected between quinone mass loadings and ozone concentrations in Fresno, CA. As noted, most ambient phenanthrene is present in the gas-phase (Arey et al., 1987; Coutant et al., 1988; Eiguren-Fernandez et al., 2004) and in this work we have studied the products formed from the gas-phase reactions of phenanthrene with OH radicals, NO$_3$ radicals and O$_3$ and measured the yields of 9,10-phenanthrenequinone from these reactions to allow an assessment of its ambient formation.

2. Experimental Methods

All experiments were carried out in a ~7500 liter Teflon chamber, equipped with two parallel banks of blacklamps, at 296 ± 2 K and 735 torr total pressure of purified air at ~5% relative humidity. The chamber is equipped with a Teflon-coated fan to ensure rapid mixing of reactants during their introduction into the chamber. In all experiments to measure product yields, phenanthrene (or phenanthrene-d_{10}) was introduced into the chamber by flushing N_2 through a Pyrex bulb containing 1.0-1.2 mg of the compound while heating the bulb and inlet tube, resulting in an initial phenanthrene concentration in the chamber of ~2.4×10^{11} molecules cm^{-3} (~10 ppbv).

OH radicals were generated by photolysis of methyl nitrite in air at wavelengths >300 nm, and NO was added into the reactant mixtures to suppress the formation of O_3 and hence of NO_3 radicals (Atkinson et al., 1981). NO_3 radicals were generated from the thermal decomposition of N_2O_5, and NO_2 was also included to lengthen the reaction times (Atkinson et al., 1984). Ozone was generated using a Welsbach T-408 ozone generator. Methyl nitrite, NO, NO_2, N_2O_5, and O_3 in O_2 diluent were flushed into the chamber without heating.

Three series of experiments were carried out: (1) product identification using collection onto Solid Phase MicroExtraction (SPME) fibers with subsequent gas-chromatography-mass spectrometry (GC-MS) analyses, (2) product identification using in-situ analysis by atmospheric pressure ionization mass spectrometry (API-MS), and (3) 9,10-phenanthrenequinone quantification from the NO_3 radical-initiated reactions by large volume sample collection. 9,10-Phenanthrenequinone yields from the OH radical, NO_3 radical and O_3 reactions were also determined on a relative basis from the series (1) experiments by GC/MS with selected ion monitoring (GC/MS-SIM) analyses of the SPME fibers for 9,10-phenanthrenequinone, as detailed below. Two experiments were also carried out to investigate the formation of aerosol following the reaction of phenanthrene with NO_3 radicals. The particle size distributions were measured using a Scanning Mobility Particle Sizer (SMPS), consisting of a ^{210}Po bipolar charger, a differential mobility analyzer and a TSI Model 3010 condensation particle counter (CPC), which is described in detail elsewhere (Lim and Ziemann, 2005).

Product Identification by GC-MS. The concentrations of phenanthrene were measured during the experiments (except for measurements after O_3 injection, see below) by gas chromatography with flame ionization detection (GC-FID). Gas samples of 4.5 liter volume were collected from the chamber onto Tenax-TA solid adsorbent cartridges using a pump with mass flow controller (Tylan General) at a flow rate of 0.3 L min^{-1}. The Tenax samples were subsequently thermally desorbed and analyzed by GC-FID.

SPME samples were collected by exposing a 7 μm polydimethylsiloxane (PDMS) fiber to the chamber contents for 30 min with the mixing fan on. The SPME fiber samples were then thermally desorbed in the heated (320 °C) injection port of an Agilent Technologies 6890N GC interfaced to an Agilent Technologies 5975 inert XL mass selective detector (MSD) onto a 30-m HP-5MS capillary column (0.25 mm i.d., 0.25 μm phase) initially at 40 °C. The MS was operated with electron ionization (EI) in the simultaneous scanning (100-250 Da) and SIM mode. The SIM ions monitored were m/z = 152, 180 and 208 (m/z = 160, 188 and 216 for the phenanthrene-d_{10} experiments).

Additional SPME samples were collected for variable times (including overnight) as described above, with subsequent thermal desorption in the heated (320 °C) injection port of an Agilent Technologies 6890N GC interfaced to an Agilent Technologies 5973 MSD, onto a 30-m DB-17 capillary column (0.25 mm i.d., 0.25 μm phase) initially at 40 °C. The MS was operated

in negative chemical ionization (NCI) mode, using methane as the reagent gas.

For the OH radical reactions, the initial reactant concentrations (molecule cm^{-3}) were: CH_3ONO and NO, ~4.8 x 10^{13} each, with three replicate irradiations of phenanthrene-CH_3ONO-NO-air mixtures being carried out. For the NO$_3$ radical reactions, the initial reactant concentrations (molecule cm^{-3}) were: N$_2$O$_5$, ~9.6 x 10^{11} and NO$_2$, ~1.5 x 10^{12}, and two replicate experiments for phenanthrene and one for phenanthrene-d$_{10}$ were conducted. For the ozone reactions, four additions of 5 L of O$_3$/O$_2$ mixtures were made in each experiment, with each addition corresponding to ~4.8 x 10^{14} molecule cm^{-3} of O$_3$ in the chamber, and three experiments were conducted including two replicates with cyclohexane (~6.0 x 10^{13} molecule cm^{-3}) added to scavenge any OH radicals formed.

Product Identification by API-MS. The ~7500 liter Teflon chamber was interfaced to a *PE* SCIEX API III API-MS and the chamber contents sampled through a 25 mm diameter x 75 cm length Pyrex tube at ~20 liter min^{-1} directly into the API-MS source. The operation of the API-MS in the MS (scanning) and MS/MS [with collision-activated dissociation (CAD)] modes has been described elsewhere (Atkinson et al., 1995). The experimental methods and initial concentrations for the OH radical, NO$_3$ radical and O$_3$ reactions were similar to those described above for the SPME/GC-MS analyses.

Yield of 9,10-Phenanthrenequinone. Four NO$_3$ radical-initiated reactions were conducted with large volume sampling to allow quantification of 9,10-phenanthrenequinone. Tenax cartridge samples were collected and analyzed for phenanthrene as described above. After each reaction, a 4000-6000 liter volume gas sample was collected from the chamber, generally at ~1000 liters min^{-1}. Four sampling configurations were used for the NO$_3$ reactions: (1) two Teflon-impregnated glass fiber filters in series, (2) an upstream filter, two polyurethane foam plugs (PUF) and a downstream filter in series, (3) an upstream filter and two PUF in series, (4) two PUF and a downstream filter in series. At the end of each experiment, the chamber was back-filled with purified air to its maximum volume and the sampled volume was calculated from the NO$_x$ concentrations before and after the back-filling with purified air.

The filter and PUF samples were spiked with known amounts of anthraquinone to serve as the internal standard, and then Soxhlet-extracted in dichloromethane. The extracts were then concentrated, filtered (0.2 μm PTFE membrane, Acrodisc, Gelman Laboratory) and fractionated by high-performance liquid chromatography (HPLC) using a method described previously (Arey et al., 1992). Fractions were collected, concentrated and analyzed by GC-MS to quantify phenanthrene and 9,10-phenanthrenequinone. The HPLC instrumentation consisted of a Hewlett-Packard (HP) 1050 HPLC with an HP 1040M Series II HPLC detection system, and an ISCO FOXY 200 fraction collector. The Agilent 5975-MSD was operated in the SIM mode (m/z = 152, 180, 208). Because the calibration for 9,10-phenanthrenequinone was non-linear, quantification of 9,10-phenanthrenequinone was based on a single point calibration using the 208 ion for a phenanthrenequinone and anthraquinone standard solution that was matched to the amounts present in each sample analyzed.

Chemicals. The chemicals used, and their stated purities, were as follows: phenanthrene (97%, with further re-crystallization), 9,10-phenanthrenequinone (99+%), anthraquinone (97%), and 9-fluorenone (98%) Aldrich Chemical Company; phenanthrene-d$_{10}$ (98%), Cambridge Isotope Labtoratories, Inc.; hexane (Optima), dichloromethane (Optima) and acetonitrile (Optima), Fisher Scientific; dibenzopyranone (synthesized by Helmig and Harger, 1994); and NO (≥99.0%), Matheson Gas Products. Methyl nitrite and N$_2$O$_5$ were prepared and stored as described previously (Atkinson et al., 1981, 1984).

3. Results and Discussion

Monitoring of gas-phase phenanthrene concentrations in the chamber in the dark showed the gas-phase concentrations of phenanthrene to decrease with time, with decay rates of (1.5-6.4) × 10^{-3} min^{-1} (average of 2.9 × 10^{-3} min^{-1} from 8 experiments). In 2 of the 3 OH radical-initiated reactions, apparent wall desorption (likely from a temperature increase due to use of the chamber lights) occurred after the reaction. Additionally, SPME sampling/GC-MS analysis of reaction products indicated dark decays.

Product Identification. SPME samples were analyzed by GC-MS after the gas-phase reactions of phenanthrene with OH radicals, NO$_3$ radicals and O$_3$. API-MS analyses were also used to assist in product identification. The identified reaction products (see Figure 2 for suggested structures) are listed in Table 2 together with their GC retention times (HP-5MS capillary column) and methods of detection.

OH Radical Reactions. In agreement with Helmig and Harger (1994), we observed 9-fluorenone, dibenzopyranone, 9,10-phenanthrenequinone, and 2,2'-diformylbiphenyl by GC-MS analyses of SPME samples and also as [M+H]$^+$ ions in the API-MS analyses (see Table 2). The addition of the OH radical to the 9,10-bond of phenanthrene, forming a 9-hydroxyphenanthrene radical, would initiate the formation of the products observed. Helmig and Harger (1994) suggest a reaction scheme which leads to 2,2'-diformylbiphenyl as a primary product whose further reaction produces dibenzopyranone and 9-fluorenone. Their proposed pathway for the formation of 9,10-phenanthrenequinone involved initial formation of a keto-alcohol at the 9,10-bond. In addition, as listed in Table 2, we observed traces of a MW 198 compound with the tentative formula C$_{12}$H$_6$O$_3$, whose major MS fragments (m/z = 126, 154 and 198) matched the unknown MW 198 product (proposed to be 1,2-naphthalic anhydride) in the Helmig and Harger (1994) study.

NO$_3$ Radical Reactions. 9-Fluorenone, dibenzopyranone, 9,10-phenanthrenequinone, 2,2'-diformylbiphenyl and traces of diphenic acid anhydride were identified by SPME sampling/GC-MS analyses of the NO$_3$ radical-initiated reaction products of phenanthrene, and the corresponding phenanthrene-d$_{10}$ reaction products showed the appropriate degree of deuteration (see Table 2). The initial step in the formation of these products is expected to be NO$_3$ radical addition at the 9,10-bond of phenanthrene, which is strongly olefinic in character (Schmitt et al., 1955).

An apparent MW 226 product was observed by SPME sampling/GC-MS analysis. The presence of 10 non-exchangeable deuteriums in the phenanthrene-d$_{10}$ reaction suggests the addition of 3 oxygens to the phenanthrene molecule and the absence of –OH or –C(O)OH groups. API-MS analyses also showed a product with an [M+H]$^+$ ion at m/z = 227, consistent with an empirical formula of C$_{14}$H$_{10}$O$_3$. However, in the phenanthrene-d$_{10}$ reaction the corresponding product had an exchangeable D, such as expected for acids (see Table 3). The MW 226 product observed by GC-MS eluted quite early (see Table 2) and had a sharp symmetrical peak shape, unlike that expected for an acid. Therefore, the MW 226 product observed by GC-MS differs from that observed by API-MS, which is suggested to be 2-(2-carbonylphenyl)benzoic acid (VI, Figure 2). The EI fragmentation of the product seen by GC-MS would be consistent with a secondary ozonide (see Table 3), but SPME sampling and analysis of an ozonide was thought unlikely (Reisen and Arey, 2002). However as discussed below, a compound attributed to the secondary ozonide was seen in the API-MS analysis of the O$_3$ reaction with phenanthrene and a trace amount of a MW 226 product was seen in the SPME sampling/GC-MS analysis of the O$_3$ reaction.

Figure 2. Structures of phenanthrene and suggested reaction products.

Secondary ozonide (VII)

10-(nitrooxy)-10-hydro-
phenanthrene-9-one (VIII)

Diphenic acid anhydride (V)
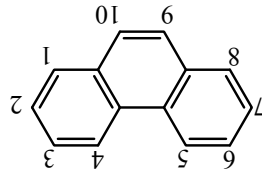
2-(2-carbonylphenyl)benzoic acid (VI)
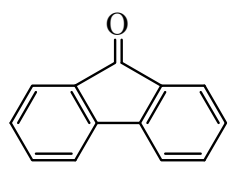
9, 10-Phenanthrenequinone (III)

2, 2'-Diformylbiphenyl (IV)

-Fluorenone (I)

Dibenzopyranone (II)

Table 2. Products observed by GC-MS and API-MS from the gas-phase reactions of phenanthrene (Phen) and phenanthrene-d_{10} (Phen-d_{10}) with OH radicals, NO_3 radicals and O_3.

Product	r.t.[d]	m/z (da) of Products Observed from Gas-phase Reaction with								
		OH		NO_3				O_3		
		GC-MS MW	API-MS [M+H]+	GC-MS MW		API-MS [M+H]+		GC-MS MW	API-MS [M+H]+	
		Phen	Phen	Phen	Phen-d_{10}	Phen	Phen-d_{10}	Phen	Phen	Phen-d_{10}
9-Fluorenone[a] (I)	21.8	180	181[g]	180	188	nd	nd	180	nd	nd
Dibenzopyranone[a] (II)	24.0	196	197[g]	196	204	197	205	196	197	nd
MW 198 ($C_{12}H_6O_3$)	22.9	198 (tr.)[e]	nd	nd	nd	nd	nd	198	nd	nd
9,10-Phenanthrenequinone[a,b] (III)	26.2	208	209[g]	208	216	209	217	208	209	nd
2,2'-Diformylbiphenyl[c] (IV)	23.1	210	211	210[h]	220[h]	211	221	210	211	221
Diphenic acid anhydride[c] (V)	25.2	nd[f]	nd	224 (tr.)	232 (tr.)	nd	nd	224	nd	nd
MW 226 ($C_{14}H_{10}O_3$)	22.6	nd	nd	226[h]	236[h]			226 (tr.)		
MW 226 ($C_{14}H_{10}O_3$) (VI)						227	236			
Monoozonide (MW 226) (VII)									227	237
MW 255 ($C_{14}H_9NO_4$) (VIII)						256[i]	265[j]			

[a]Retention index and EI mass spectrum matched to authentic compound.
[b]MS/MS spectrum matched to authentic compound.
[c]Retention index and EI mass spectrum matched to data of Helmig and Harger (1994).
[d]GC retention time (min) on HP-5 column.
[e](tr.)= trace amount observed.
[f]nd = not detected.
[g]MS/MS spectrum was not taken.
[h]MW confirmed by NCI.
[i]API-MS CAD spectrum fragments: 210 Da = [M+H-NO_2]+, 197 Da = [M+H-NO-HCO]+, 181 Da = [M+H-NO_2-HCO]+.
[j]API-MS CAD spectrum fragments: 219 Da = [M+H-NO_2]+, 205 Da = [M+H-NO-DCO]+, 189 Da = [M+H-NO_2-DCO]+.

12

Table 3. GC-MS and API-MS/MS CAD spectra of the MW 226 and corresponding deuterated species from the phenanthrene (Phen) and phenanthrene-d_{10} (Phen-d_{10}) reactions with the NO_3 radical and with O_3.

GC-MS SPME Product from NO_3 reaction				API-MS Product from NO_3 reaction[a]				Secondary Ozonide from O_3 reaction (VII)			
$C_{14}H_{10}O_3$ from Phen		$C_{14}D_{10}O_3$ from Phen-d_{10}		$_{14}H_{10}O_3$ from Phen		$C_{14}HD_9O_3$ from Phen-d_{10}		$_{14}H_{10}O_3$ from Phen		$C_{14}D_{10}O_3$ from Phen-d_{10}	
m/z	identity	m/z	identity	m/z	identity	m/z	identity	m/z	identity	m/z	identity
226	$[M]^+$	236	$[M]^+$	227	$[M+H]^+$	236	$[M+H]^+$	227	$[M+H]^+$	237	$[M+H]^+$
198	$[M-CO]^+$	208	$[M-CO]^+$	209	$[M+H-H_2O]^+$	218	$[M+H-H_2O]^+$	210	$[M+H-OH]^+$	220	$[M+H-OH]^+$
197	$[M-HCO]^+$	206	$[M-DCO]^+$	181	$[M+H-CH_2O_2]^+$	190	$[M+H-CH_2O_2]^+$	181	$[M+H-CH_2O_2]^+$	190	$[M+H-CHDO_2]^+$
181	$[M-HCO_2]^+$	190	$[M-DCO_2]^+$	153	$[M+H-C_2H_2O_3]^+$	162	$[M+H-C_2H_2O_3]^+$	165	$[M+H-CH_2O_3]^+$	174	$[M+H-CHDO_3]^+$
169	$[M-HC_2O_2]^+$	178	$[M-DC_2O_2]^+$	152	$[M+H-C_2H_3O_3]^+$	160	$[M+H-C_2H_2DO_3]^+$	152	$[M+H-C_2H_3O_3]^+$	160	$[M+H-C_2HD_2O_3]^+$

[a]Tentatively identified as 2-(2-carbonylphenyl)benzoic acid (VI, Figure 2).

API-MS analyses of the phenanthrene-NO$_3$ reaction also showed a MW 255 product attributed to a nitrogen-containing species. The API-MS is generally insensitive to nitrates, but responds to substituted nitrates, such as hydroxynitrates (Arey et al., 2001). Therefore, the MW 255 product is suggested to be 10-(nitrooxy)-10-hydrophenanthrene-9-one (API-MS CAD fragments in Table 2; VIII, Figure 2). It is possible that the apparent MW 226 product observed by GC-MS is due to a compound, such as a dinitrate, not observed by API-MS and degrading to the ozonide during desorption in the GC inlet, but this is speculative at this time.

O$_3$ Reactions. 9-Fluorenone, dibenzopyranone, 9,10-phenanthrenequinone, 2,2'-diformylbiphenyl, and diphenic acid anhydride were observed by SPME sampling/GC-MS analyses from the gas-phase reaction of phenanthrene with O$_3$ (see Table 2). In addition, the MW 198 compound C$_{12}$H$_6$O$_3$ (also observed in the OH radical reaction) and a trace of the MW 226 compound C$_{14}$H$_{10}$O$_3$ (observed in the NO$_3$ radical reaction) were observed by GC-MS. The API-MS spectra of gas-phase reactions of O$_3$ with phenanthrene and phenanthrene-d$_{10}$ showed the presence of a product ion peak [M+H]$^+$ at m/z = 227 and m/z = 237, respectively. Their API-MS CAD fragmentation patterns (see Table 3) are very similar to those of the secondary ozonide identified from the reaction of acenaphthylene and acenaphthylene-d$_8$ with O$_3$ (Reisen and Arey, 2002). Since, as noted above, the 9,10-bond of phenanthrene is olefinic in character (Schmitt et al., 1955), addition of ozone at this bond and rearrangement to a secondary ozonide would be expected. Indeed, Schmitt et al. (1955) suggested exclusive ozonolysis of solution-phase phenanthrene at the 9,10-bond and reported the isolation of the stable monoozonide from this reaction. The monoozonide (VII) was also isolated from the ozonolysis of phenanthrene adsorbed on polyethylene (Huh, 2000).

Relative 9,10-Phenenthrenequinone Yields. Because of its potential toxicological significance, the yields of 9,10-phenanthrenequinone from the gas-phase reactions of phenanthrene with OH radicals, NO$_3$ radicals and O$_3$ were compared on a relative basis during the above product identification experiments. The amounts of phenanthrene reacted in the OH and NO$_3$ radical reactions were determined by Tenax sampling/GC-FID analyses, with correction for wall loss/desorption by extrapolating the concentrations measured from two replicate pre-reaction and two replicate post-reaction analyses to the mid-point of the reaction. The O$_3$ reaction is relatively slow (Kwok et al., 1994) and the 4 large additions of O$_3$ necessary to yield sufficient product precluded Tenax sampling post-reaction for phenanthrene (Cao and Hewitt, 1994). Therefore, the pre-reaction phenanthrene concentration was determined by replicate Tenax sampling/GC-FID analyses and the percent of phenanthrene reacted with O$_3$ was based on the SPME-GC-MS analyses (area counts in TIC mode, pre- and post-reaction, with corrections being made for wall losses).

The amounts of 9,10-phenanthrenequinone formed on a relative basis were obtained by the SPME/GC-MS analyses (area counts of m/z = 208+180+152 in SIM mode). The 30 min SPME sampling collections were started immediately after the reactions were started and no corrections were made for wall losses of 9,10-phenanthrenequinone. The relative 9,10-phenanthrenequinone yields from gas-phase reactions of phenanthrene with OH radicals, NO$_3$ radicals and O$_3$ are given in Table 4. Because the highest yield was observed in the NO$_3$ radical-initiated reaction, it was decided to utilize large volume samples from this reaction to quantify 9,10-phenanthrenequinone and hence place the relative yields on an absolute basis.

It should be noted that two additional NO$_3$ radical reactions were monitored for particle formation using a CPC and it was observed that formation of aerosol (defined as >100 counts cm^{-3}) typically began 4-5 min after the injection of N$_2$O$_5$, and peaked 5-10 min later at ~25,000

Table 4. Yields and formation rates of 9,10-phenanthrenequinone (PQ).

	Gas-phase reaction with		
	OH	NO_3	O_3
Relative Yields[a] of PQ $\pm 2\sigma$	0.10 ± 0.09	1.0	0.056 ± 0.023
Absolute Yield[b] $\pm 2\sigma$		$33 \pm 9\%$	
Yields $\pm 2\sigma$	$3 \pm 3\%$	$33 \pm 9\%$	$2 \pm 1\%$
Reaction rates k (cm^3 molecule^{-1} s^{-1})	3.2×10^{-11} [c]	1.2×10^{-13} [d]	4.0×10^{-19} [d]
Formation rates of phenanthrenequinone (pg m^{-3} h^{-1})[e]	80	800	0.2

[a]The ratio of phenanthrenequinone yields was determined by SPME collection and GC-MS analysis of 9,10-phenanthrenequinone and Tenax/GC-FID analysis of phenanthrene reacted. Three (for OH radical and O_3) or 2 replicate experiments (for NO_3 radical) were conducted. The GC/MS phenanthrenequinone peak area per ppb of phenanthrene reacted with NO_3 radicals was set equal to 1.0.
[b]See Table 5.
[c]Obtained by Lee et al. (2003) from the data of Biermann et al. (1985), Brubaker et al. (1998) and Lee et al. (2003).
[d]From Kwok et al. (1994).
[e]Based on: a constant average 24-hr phenanthrene concentration of 10 ng m^{-3} (Reisen and Arey, 2005), a global-average 12-hr OH radical concentration of 2.0×10^6 molecule cm^{-3} (Prinn et al., 2001), an average 12-hr NO_3 radical concentration of 5×10^8 molecule cm^{-3} (Atkinson, 1991), and a background 24-hr O_3 concentration of 7×10^{11} molecule cm^{-3} (Logan, 1985).

counts cm^{-3}. In one of these experiments particles were also sized with an SMPS and the size distribution was from 20-100 nm with a maximum at ~50 nm and therefore, loss of particles to the walls prior to our sampling for 9,10-phenanthrenequinone should have been minor (McMurry and Rader, 1985). The formation of particles during the reactions may influence to some degree the partitioning of 9,10-phenanthrenequinone to the SPME fiber although apparently particles may also be sampled onto SPME fibers (Koziel et al., 2001).

Quantification of 9,10-Phenanthrenequinone from Large Volume Samples. It was anticipated that, because 9,10-phenanthrenequinone is less volatile than phenanthrene, a single PUF would quantitatively collect 9,10-phenanthrenequinone and it was not anticipated that particles formed during the reaction would penetrate through the PUF. However, a CPC was used to sample room air with and without an 8 cm length PUF in the sampling line, and showed that 50% of the ~12,000 particles cm^{-3} in the room air were transmitted through the PUF.

Shown in Table 5 are the results of four different sampling configurations for the NO$_3$ radical reactions in which large volume samples were collected. It should be noted that sampling of these large-volumes was initiated 38-43 min after addition of N$_2$O$_5$ in these experiments and, therefore, after the maximum number of particles had formed. The total yields of 9,10-phenanthrenequinone from the 4 experiments are listed in Table 5 and result in an average yield of 33 ± 9% (2 standard deviations). GC-MS analyses of extracts of the filter and PUFs indicated that phenanthrene was mainly gas-phase and the majority of 9,10-phenanthrenequinone was particle-associated. Thus, when the sampling configuration started with an upstream filter, ≤20% (and generally <10%) of the phenanthrene was retained on the filter. In contrast, a single PUF was sufficient to retain ~90% of the phenanthrene (see NO$_3$ reaction #4 in Table 4). Yet, while the two PUFs in NO$_3$ reaction #4 collected ~95% of the phenanthrene, 75% of the 9,10-phenanthrenequinone was observed on the filter downstream from the PUFs. While we do not know the efficiency of penetration through the PUF for the particles formed from gas-to-particle conversion in our chamber reactions, we conclude that the 9,10-phenanthrenequinone collected on the filter in NO$_3$ reaction #4 must be particle-associated.

The good agreement in the yield measured for reaction #4, where a PUF was upstream in the sampling configuration, with those of reactions #1-3, where the filter was upstream, suggests that heterogeneous formation of 9,10-phenanthrenequinone on the filter was not occurring. If the 9,10-phenanthrenequinone found on the first filter in reactions #1-3 were formed heterogeneously from phenanthrene on the filter, the amount formed on the filter in reaction #4 would be expected to be greatly reduced since the amount of phenanthrene (and presumably "reactant" species as well) reaching the filter was significantly less than for reaction #1. Note that the sampling system used in reaction #3 is that we have used previously for ambient air sampling (see, for example, Arey et al., 1987; 1989a; Reisen and Arey, 2005).

Combining our absolute yield of 33 ± 9% for 9,10-phenanthrenequinone from the NO$_3$ radical-initiated reaction of phenanthrene with the relative yields in Table 4, the yields from the OH radical and O$_3$ reactions are then ~3% and ~2%, respectively. While there are large uncertainties in these OH radical and O$_3$ reaction yields, they can be used to estimate formation rates for 9,10-phenanthrenequinone under ambient atmospheric conditions.

Table 5. The percent distribution of phenanthrene (Phen) and 9,10-phenanthrenequinone (PQ) and the percent molar yields of 9,10-phenanthrenquinone determined from large volume sample collection.

	$_3$ reaction #1[c]			NO$_3$ reaction #2[e]			NO$_3$ reaction #3[e]			NO$_3$ reaction #4[e]		
Distribution (%)[a]		Phen	PQ		Phen	PQ		Phen	PQ		Phen	PQ
	Filter	$< 10^d$	98	Filter	~20	98	Filter	~8	100	PUF	~87	23
	Filter	$< 5^d$	2	PUF	~75	0	PUF	~92	0	PUF	~9	2
NO				PUF	~2	0	PUF	na[f]	na	Filter	~4	75
				Filter	~1	2						
PQ Yield (%)[b]	38			33			27			34		
avg. $\pm 2\,\sigma$	33 $\pm$ 9%											

[a]The percent distribution was determined based on the GC-MS analysis of the HPLC fractions. For phenanthrene the uncertainty results from a non-exact sample volume.
[b]In determining this yield, the amount of phenanthrene reacted was calculated from the Tenax/GC-FID results because these were judged to be most precise. The PQ was quantified as described in the Experimental Procedures.
[c]Sampled at a flow rate of ~500 L min^{-1}.
[d]The total amount of phenanthrene was assumed to be identical to the total measured from NO$_3$ radical reaction #2.
[e]Sampled at a flow rate of ~1,000 L min^{-1}.
[f]na = not analyzed.

Atmospheric Formation of 9,10-Phenanthrenequinone. Atmospheric formation rates of 9,10-phenanthrenequinone were calculated using our measured yields, rate constants for reaction of phenanthrene with OH radicals, NO_3 radicals and O_3, and assumed ambient gas-phase concentrations for phenanthrene and the reactant species. We used room temperature rate constants for the reactions of phenanthrene with OH radicals of 3.2×10^{-11} cm^3 molecule^{-1} s^{-1} (Lee et al., 2003), with NO_3 radicals of 1.2×10^{-13} cm^3 molecule^{-1} s^{-1} (Kwok et al., 1994) and with O_3 of 4.0×10^{-19} cm^3 molecule^{-1} s^{-1} (Kwok et al., 1994). The formation rates of 9,10-phenanthrenequinone from reactions of phenanthrene with OH radicals, NO_3 radicals and O_3 were calculated to be 80, 800 and 0.2 pg m^{-3} h^{-1}, respectively, assuming a constant gas-phase phenanthrene concentration of 10 ng m^{-3} (Reisen and Arey, 2005) and using the expression [9,10-phenanthrenequinone]$_t$ = $k_x \times$ [X] $\times Y_x \times$ [phenanthrene] $\times t$, where [9,10-phenanthrenequinone]$_t$ is the amount formed after time t, k_x is the rate constant for reaction of phenanthrene with species X, and Y_x is the formation yield of 9,10-phenanthrenequinone from the reaction of phenanthrene with species X.

Both of the OH and NO_3 radical-initiated formation rates of 9,10-phenanthrenequinone are significant in light of its reported ambient concentrations (Allen et al., 1997; Cho et al., 2004; Kishikawa et al., 2006; Chung et al., 2006). The relatively high formation rate from the NO_3 radical reaction suggests that higher 9,10-phenanthrenequinone concentrations may be observed at night. It should be recognized that while OH radicals are ubiquitous under sunlit conditions (Ehhalt et al., 1991), NO_3 radical concentrations are much more variable and the rapid photolysis of NO_3 radicals results in very low daytime concentrations (Atkinson et al., 1986).

The relative importance ascribed here to the NO_3 radical-initiated formation of 9,10-phenanthrenequinone is based on reactions of gas-phase phenanthrene. The gas/particle distribution of phenanthrene is temperature and substrate dependent (Bidleman, 1988). Heterogeneous ozonation kinetics of gas-phase O_3 with PAHs, including phenanthrene, in organic films have recently been measured and the atmospheric lifetime of phenanthrene due to reaction with 50 ppbv of O_3 was calculated to be 44 days (Kahan et al., 2006). Since peak O_3 levels even in very polluted urban areas are unlikely to be more than a factor of 10 higher than the background 30 ppbv used in the calculations given in Table 3, formation of 9,10-phenanthrenequinone from O_3 reactions, either gas-phase or heterogeneous, will not be significant in comparison with homogeneous gas-phase OH or NO_3 radical-initiated formation.

Photooxidation of phenanthrene sorbed on silica gel produced 9,10-phenanthrenequinone in 30% yield (Barbas et al., 1996) and 9,10-phenanthrenequinone was also identified as a major product of photoxidation of phenanthrene in hexane spread as a liquid film on water (Moza et al., 1999). It is difficult to evaluate the potential importance of such heterogeneous reactions occurring on ambient particles, but in warm climates most ambient phenanthrene is in the gas-phase.   A number of nitro-PAHs can serve as markers to distinguish gas-phase OH radical-versus NO_3 radical-initiated chemistry (Gupta et al., 1996; Arey, 1998; Phousongphouang and Arey, 2003c; Reisen and Arey, 2005), and concurrent ambient measurements of diurnal variations in phenanthrene, 9,10-phenethrenequinone and these nitro-PAHs may confirm the importance of nighttime NO_3 radical-initiated formation of 9,10-phenanthrenequinone.

**B. Kinetics and Products of Photolysis and Reaction with OH Radicals
of a Series of Aromatic Carbonyl Compounds**

1. Introduction

In the atmosphere, gaseous PAHs undergo chemical transformations with OH and NO_3 radicals, with the daytime OH radical reaction being estimated to dominate as the atmospheric loss process for most PAHs (Arey and Atkinson, 2003). Naphthalene and the C_1- and C_2-alkylnaphthalenes are the most abundant PAHs observed in ambient air, and rate constants for their OH radical reactions have recently been measured (Phousongphouang and Arey, 2002). The products of the OH radical-initiated reaction of naphthalene include 2-formylcinnamaldehyde and phthaldialdehyde (2-formylbenzaldehyde or 1,2-benzenedicarboxaldehyde) (Sasaki *et al.*, 1997; Bunce *et al.*, 1997). While, as will be discussed in the next each section, alkylnaphthalenes produce unique ring-opened homologs of 2-formylcinnamaldehyde, dicarbonyls formed after loss of ring-carbons, such as phthaldialdehyde, are also formed (see the caption to Figure 3).

These aromatic dicarbonyls are expected to undergo further reaction, including photolysis, in the atmosphere (Atkinson and Arey, 2003) and, indeed, 2-formylcinnamaldehyde has been shown to react with OH radicals and photolyze (Sasaki *et al.*, 1997). In this work the rates and products of photolysis and OH radical reaction of phthaldialdehyde, 2-acetyl-benzaldehyde and 1,2-diacetylbenzene have been studied. The photolysis rates, combined with absorption spectra measured in solution and measured NO_2 photolysis rates at the same light intensity and spectral distribution, allow average quantum yields to be derived for the wavelength region 290-400 nm. Because phthalide was observed as a photolysis product of phthaldialdehyde, its photolysis and OH radical reaction were also investigated. The structures of these aromatic compounds and their reaction products are shown in Figure 3.

2. Experimental Methods

Reactions were carried out in a ~7000 liter Teflon chamber equipped with two parallel banks of blacklamps at 298 ± 2 K and 735 Torr total pressure of purified air at ~5% relative humidity. This chamber is equipped with a Teflon-coated fan to ensure rapid mixing of reactants during their introduction into the chamber. Organic reactants were introduced into the chamber by flushing N_2 through a Pyrex bulb containing a measured amount of the compound while (with the exception of methyl nitrite introduction) heating the bulb and inlet tube.

OH Radical Rate Constants and Photolysis Rates. Rate constants for the reactions of OH radicals with phthaldialdehyde, 2-acetylbenzaldehyde, 1,2-diacetylbenzene and phthalide (hereafter referred to as "aromatic carbonyls") were measured using a relative rate technique in which the concentrations of the aromatic carbonyls and a reference compound (whose OH radical reaction rate constant is reliably known) were measured in the presence of OH radicals (Atkinson *et al.*, 1981). If the only loss process for the aromatic carbonyls and reference compound was by reaction with OH radicals, then

$$\ln \left(\frac{[\text{aromatic carbonyl}]_{to}}{[\text{aromatic carbonyl}]_t} \right) = \frac{k_1}{k_2} \ln \left(\frac{[\text{reference compound}]_{to}}{[\text{reference compound}]_t} \right) \quad \text{(I)}$$
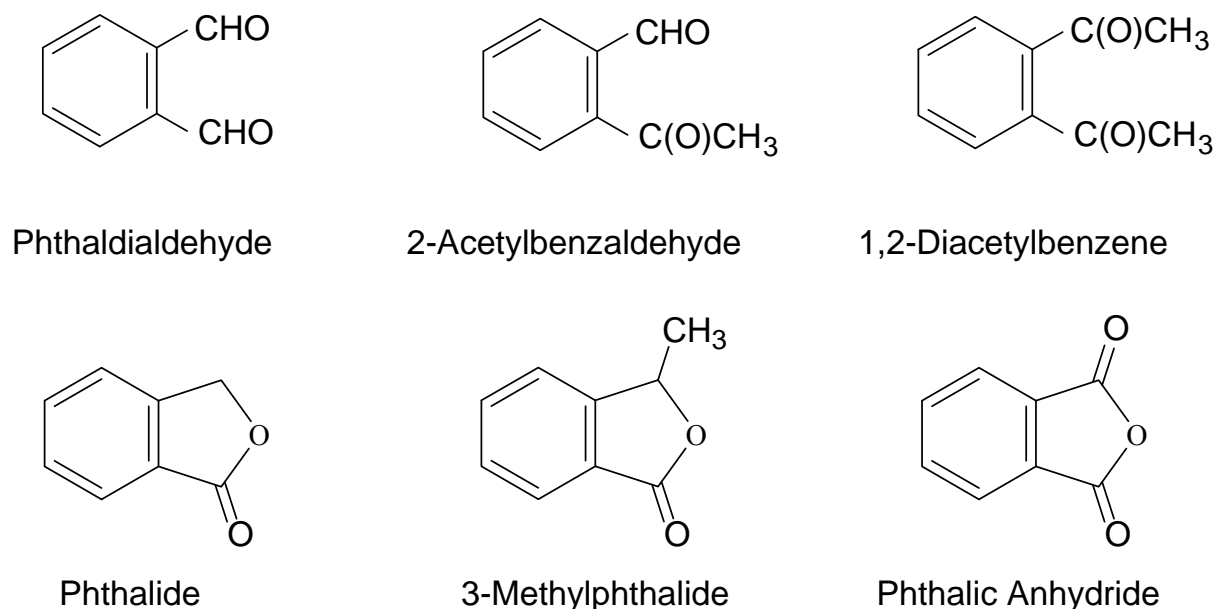
Figure 3. Structures of: (top row) aromatic dicarbonyls studied here; (lower row) ring-closure products of these dicarbonyls. The dicarbonyls are ring-opened products of the OH radical-initiated reactions of naphthalene and alkylnaphthalenes. Phthaldialdehyde has been identified as a product from naphthalene, 2-methylnaphthalene, 2-ethylnaphthalene and 2,3-dimethylnaphthalene; 2-acetylbenzaldehyde has been identified as a product from 1-methylnaphthalene, 1,2-dimethylnaphthalene and 1,3-dimethylnaphthalene; and 1,2-diacetylbenzene has been identified as a product from 1,4-dimethylnaphthalene.

where [aromatic carbonyl]$_{to}$ and [reference compound]$_{to}$ are the concentrations of the aromatic carbonyl and the reference compound, respectively, at time t$_o$, [aromatic carbonyl]$_t$ and [reference compound]$_t$ are the corresponding concentrations at time t, and k$_1$ and k$_2$ are the rate constants for reactions (1) and (2), respectively.

OH + aromatic carbonyl → products   (1)

OH + reference compound → products   (2)

However, the aromatic carbonyls can also undergo photolysis, and wall losses were observed for all four aromatic carbonyls investigated. The data analysis procedures to take these into account are discussed in the results section.

OH radicals were generated by the photolysis of methyl nitrite (CH_3ONO) in air at wavelengths >300 nm, and NO was added to the reactant mixtures to suppress the formation of O_3 and NO_3 radicals (Atkinson *et al.*, 1981). 1,2,4-Trimethylbenzene was used as the reference compound for all four aromatic carbonyls. As expected (Kwok and Atkinson, 1995), 1,2-diacetylbenzene and phthalide were observed to be significantly less reactive than 1,2,4-trimethylbenzene, and hence 2,2,3,3-tetramethylbutane was used as the reference compound for additional experiments with these two aromatic carbonyls. The initial reactant concentrations (molecule cm^{-3}) were: CH_3ONO, ~ 2.4×10^{14}; NO, ~ 2.4×10^{14}; aromatic carbonyl, ~2.4×10^{12} each; and 1,2,4-trimethylbenzene, 2.4×10^{12}, or 2,2,3,3-tetramethylbutane, 4.8×10^{13}. Irradiations of CH_3ONO – NO – phthaldialdehyde – 2-acetylbenzaldehyde – 1,2-diacetylbenzene – 1,2,4-trimethylbenzene – air mixtures and CH_3ONO – NO – phthalide – 1,2,4-trimethylbenzene – air mixtures were carried out at 10% of the maximum light intensity for up to 25-57 min. Additional irradiations of CH_3ONO – NO – phthalide – 1,2-diacetylbenzene – 2,2,3,3-tetramethylbutane – air mixtures were carried out at 30% of the maximum light intensity for up to 35-45 min.

Irradiations of phthaldialdehyde – 2-acetylbenzaldehyde – 1,2-diacetylbenzene – 1,2,4-trimethylbenzene - cyclohexane – air mixtures and phthalide – 1,2,4-trimethylbenzene - cyclohexane – air - mixtures were carried out for up to 60 min at 10% of the maximum light intensity, with 9.6×10^{14} molecule cm^{-3} of cyclohexane being present to scavenge any OH radicals formed. Additional irradiations of phthalide – 1,2-diacetylbenzene – 2,2,3,3-tetramethylbutane – cyclohexane - air mixtures were carried out at 30% of the maximum light intensity for up to 60 min. The chamber was cleaned after each experiment by flushing with purified air for at least 24 hours and with the chamber lights on for at least 8 hr.

The concentrations of phthaldialdehyde, 2-acetylbenzaldehyde, 1,2-diacetylbenzene, phthalide, 1,2,4-trimethylbenzene and 2,2,3,3-tetramethylbutane were measured during the experiments by gas chromatography with flame ionization detection (GC-FID). Samples were collected onto Solid-Phase Micro Extraction (SPME) fibers by exposing a 65 μm polydimethylsiloxane/divinylbenzene (PDMS/DVB) fiber to the chamber contents for 10 min with the mixing fan on, prior to the initial irradiation and after each intermittent irradiation period in the photolysis and OH radical reaction experiments (see Figure 4). The SPME fiber was then thermally desorbed in the injection port of the GC inlet at 250 ^{o}C for 2 min onto a 30-m DB-1 capillary column (0.32 mm i.d., 3 μm phase) held at 40 ^{o}C for 2 min and then temperature programmed to 120 ^{o}C at a rate of 20 ^{o}C min^{-1}, then to 250 ^{o}C at 8 ^{o}C min^{-1} and then held at 280 ^{o}C for 10 min. The NO_2 photolysis rates, $J(NO_2)$, were measured (Zafonte *et al.*, 1977) at the light intensities used and are given in Table 1. The spectral distributions of the blacklights and natural solar radiation were provided by Carter et al. (1995).

Products of the OH Radical Reactions and of Photolysis. The products formed from photolysis and OH radical-initiated reaction of phthaldialdehyde, 2-acetylbenzaldehyde, 1,2-diacetylbenzene and phthalide were identified by combined gas chromatography–mass spectrometry (GC-MS) analyses of irradiated CH_3ONO – NO - aromatic carbonyl – air mixtures and aromatic carbonyl –cyclohexane (in excess) - air mixtures. Samples were collected onto SPME fibers for variable times (including overnight) as described above, with subsequent thermal desorption in the heated (250 ^{o}C) injection port of a Varian 2000 ion trap GC/MS/MS onto a 30-m DB-1 capillary column (.32mm i.d., 3 μm phase) held at 40 ^{o}C for 2 min, then temperature-programmed to 250 ^{o}C at 8 ^{o}C min^{-1} and held at 250 ^{o}C for 30 min. The MS was operated in electron ionization (EI) mode or in chemical ionization (CI) mode using isobutane as

the reagent gas.

Aromatic carbonyl – cyclohexane (in excess) – air and CH_3ONO – NO – aromatic carbonyl – air irradiations were carried out at the maximum light intensity, with sample collection by SPME and analyses by GC-FID as described above. Irradiations of cyclohexane - air mixtures at the maximum light intensity were carried out between each experiment to check that there were no residual products from the previous experiment. GC-FID/SMPE responses for phthaldialdehyde, 2-acetylbenzaldehyde, 1,2-diacetylbenzene, phthalide and phthalic anhydride were determined by introducing known amounts of authentic standards into the chamber with SPME/GC-FID analyses as described above. The GC-FID response for 3-methylphthalide was estimated from the measured response factor for phthalide and their Effective Carbon Numbers (Scanlon and Willis, 1985).

Absorption Spectra. The absorption spectra of phthaldialdehyde, 2-acetylbenzaldehyde, 1,2-diacetylbenzene and phthalide were measured in *n*-hexane solution over the wavelength range 205-500 nm using a Varian CARY 50 Bio UV-Vis spectrophotometer with a 1-cm path length quartz cell. For each aromatic carbonyl, absorption spectra of 4 solutions containing concentrations of the aromatic carbonyl in the range $(1.21-16.7) \times 10^{-5}$ M were measured. The absorption coefficient (ε) at each wavelength was obtained by least-squares analyses of the absorbance, $\log_{10}(I_o/I)$, against concentration using the Beer-Lambert law, $\log_{10}(I_o/I) = (\varepsilon[\text{aromatic carbonyl}]l)$, where l is the pathlength, which was shown to be valid for the wavelength range and concentrations used here.

Chemicals. The chemicals used, and their stated purities, were: phthaldialdehyde (97%), 2-acetylbenzaldehyde (95%), 1,2-diacetylbenzene (99%), phthalide (98%) and phthalic anhydride (99+%), Aldrich Chemical Company; and NO (>99%), Matheson Gas Products. Methyl nitrite was prepared and stored as described previously (Atkinson *et al.*, 1981).

3. Results

GC-FID analyses showed that in all experiments the gas-phase concentrations of phthaldialdehyde, 2-acetylbenzaldehyde, 1,2-diacetylbenzene and phthalide decreased with time in the dark, indicating decays to the chamber walls. For each aromatic carbonyl, the decay rate decreased with time, suggesting an approach to equilibrium at which point the wall adsorption rate would equal the wall desorption rate (although this was not attained in these experiments). The dark decay rates observed in the experiments conducted were (in units of 10^{-4} min^{-1}): phthaldialdehyde, 4-19, average 10 (11 experiments); 2-acetylbenzaldehyde, 7-29, average 16 (10 experiments); 1,2-diacetylbenzene, 11-39, average 22 (14 experiments); and phthalide, 9-41, average 25 (11 experiments). In contrast, $\leq$3% decays of 1,2,4-trimethylbenzene or 2,2,3,3-tetramethylbutane were observed over 4.0 hr.

Photolysis Rates. Irradiations of aromatic carbonyl – cyclohexane (in excess) – air mixtures were carried out at 10%, 30% and 100% of the maximum light intensity. Representative data, in the form of plots of $\ln([\text{aromatic carbonyl}]_{to}/[\text{aromatic carbonyl}]_t)$ against time, are shown for phthaldialdehyde and 1,2-diacetylbenzene in Figure 4 for an experiment with 4 periods of 15 min of photolysis at the maximum light intensity. The concentrations of both aromatic carbonyls decrease before and after the photolysis portion of the experiment, due to wall decay. Phthaldialdehyde clearly undergoes photolysis, while 1,2-diacetylbenzene has a slower decay during the photolysis portion of the experiment. The initial and final decay rates were obtained from least-squares analyses of the first 3 (0-60 min) and last 3 data points (180-240 min), respectively, and the decay rate during the photolysis portion of the experiment was
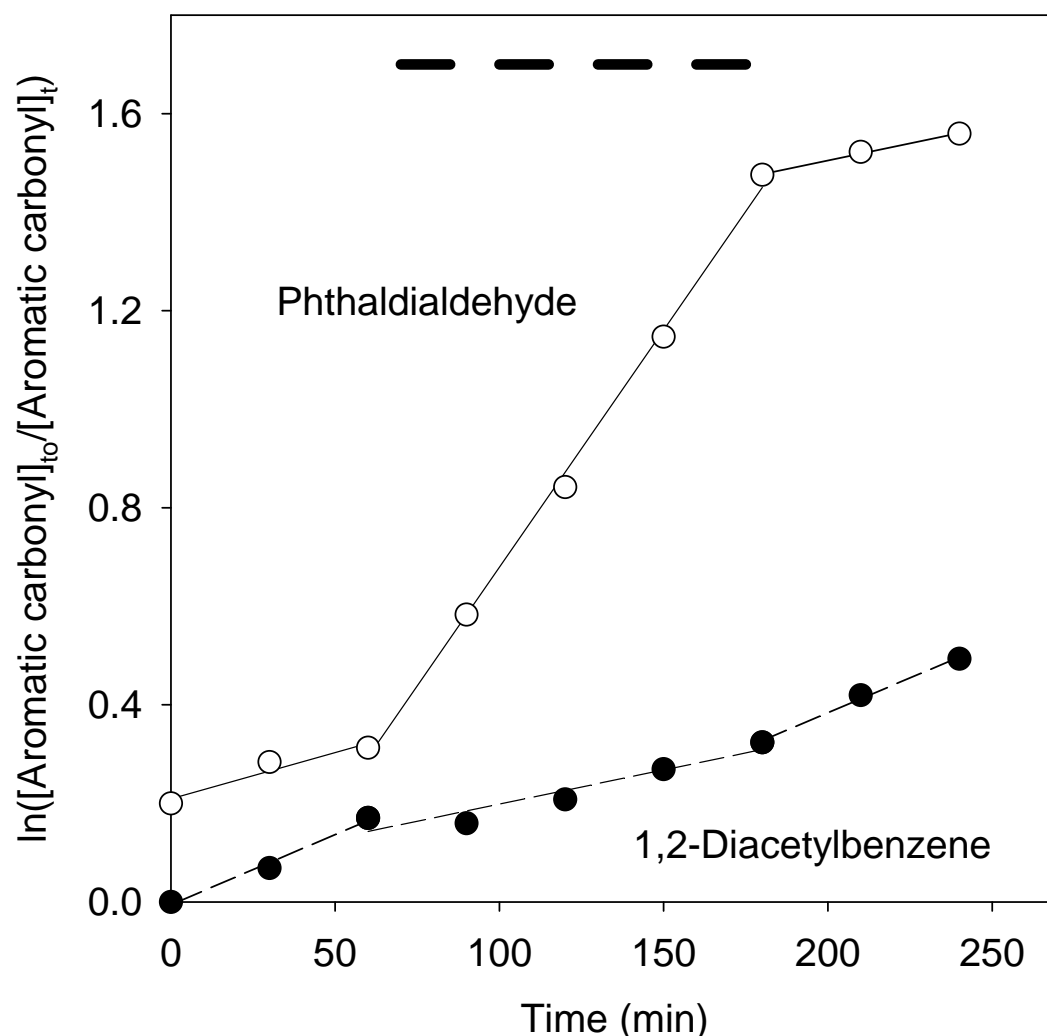
Figure 4. Plots of ln([aromatic carbonyl]$_{to}$/[aromatic carbonyl]$_t$) against time for irradiation of phthaldialdehyde – air and 1,2-diacetylbenzene – air mixtures, with cyclohexane being present to scavenge any OH radicals formed (see text). The four 15-min irradiation periods at the maximum light intensity are noted by the thick solid lines at the top of the figure. The data for the phthaldialdehyde experiment have been displaced vertically by 0.2 units for clarity. The lines are least-squares analyses of the experimental data over the time periods 0-60 min (pre-irradiation), 60-180 min (covering the four irradiation periods) and 180-240 min (post-irradiation period).

obtained from least-squares analyses of data over the time period 60-180 min. After correcting for the wall decay using an average of the initial (0-60 min) and final (180-240 min) decay rates, the photolysis rate was derived. For 1,2-diacetylbenzene this procedure results in a negative photolysis rate, suggesting that wall desorption during the irradiation periods (probably because of slight warming of the chamber walls) overwhelmed any photolysis. Plots of ln([aromatic

carbonyl]$_{to}$/[aromatic carbonyl]$_t$) against time for 2-acetylbenzaldehyde and phthalide were qualitatively similar to those in Figure 4 for phthaldialdehyde and 1,2-diacetylbenzene, respectively, and the photolysis rates obtained at the light intensities used are given in Table 6.

Table 6.   Measured photolysis rates, k$_{phot}$, of phthaldialdehyde, 2-acetylbenzaldehyde, 1,2-diacetylbenzene and phthalide in a ~7000 liter Teflon chamber with blacklamp irradiation

aromatic carbonyl	$10^3 \times$ k$_{phot}$ (min^{-1})^a		
	at 10% lights J(NO$_2$) = 0.061 min^{-1}	at 30% lights J(NO$_2$) = 0.197 min^{-1}	at 100% lights J(NO$_2$) = 0.535 min^{-1}
phthaldialdehyde	2.5 ± 1.8^b		15.9 ± 1.7^c
2-acetylbenzaldehyde	0.9 ± 1.8^b		11.4 ± 1.4^c
1,2-acetylbenzene	-0.8 ± 2.0^{b,d}	-3.4 ± 3.0^{d,e}	-2.9 ± 1.6^{c,d}
phthalide	-1.0 ± 1.0^{b,d}	-4.0 ± 4.0^{d,e}	-4.0 ± 1.8^{c,d}

^{a}The uncertainties in the measured NO$_2$ photolysis rates are estimated to be ~±12%.
^{b}Indicated errors are two standard deviations of the average photolysis rate derived from 3 (phthalide) or 5 (other aromatic carbonyls) replicate experiments.
^{c}Indicated errors are two standard deviations; single experiment.
^{d}Decay rate during photolysis periods less than during pre- and post-photolysis dark periods (see text).
^{e}Indicated errors are two standard deviations associated with a single experiment; photolysis rate is the average of two experiments.

Rate Constants for the OH Radical Reactions. Irradiations of CH$_3$ONO - NO – aromatic carbonyl – reference compound – air mixtures at 10% of the maximum light intensity were carried out with 1,2,4-trimethylbenzene as the reference compound, with additional irradiations at 30% of the maximum light intensity being carried out for 1,2-diacetylbenzene and phthalide with 2,2,3,3-tetramethybutane as the reference compound. The experimental procedures and data analyses were similar to those for the photolysis experiments, except that 3 rather than 4 irradiation periods were employed. The average of the 0-60 min (pre-reaction) and 150-210 min (post-reaction) decay rates was used to correct each of the post irradiation data points (i.e., the data points at 90, 120 and 150 min) for wall decay. The 0-60 min pre-irradiation data were used to obtain the 60 min t$_o$ concentration, and the photolysis rate for the light intensity employed (Table 6) was used to correct each of the 90, 120 and 150 min data points for photolysis, using the negative photolysis rates for 1,2-diacetylbenzene and phthalide to take into account desorption from the walls during the photolysis periods. Photolysis contributed ~10% and ~6% of the total reactive losses for phthaldialdehyde and 2-acetylbenzaldehyde, respectively.

After correction for wall decays and photolysis, the data for phthaldialdehyde and 2-acetylbenzaldehyde are plotted in accordance with Equation (I) in Figure 5. The rate constant ratios obtained are given in Table 7. It should be noted that neglecting wall decays and photolysis (and using the 60 min data point just prior to the first irradiation for the initial
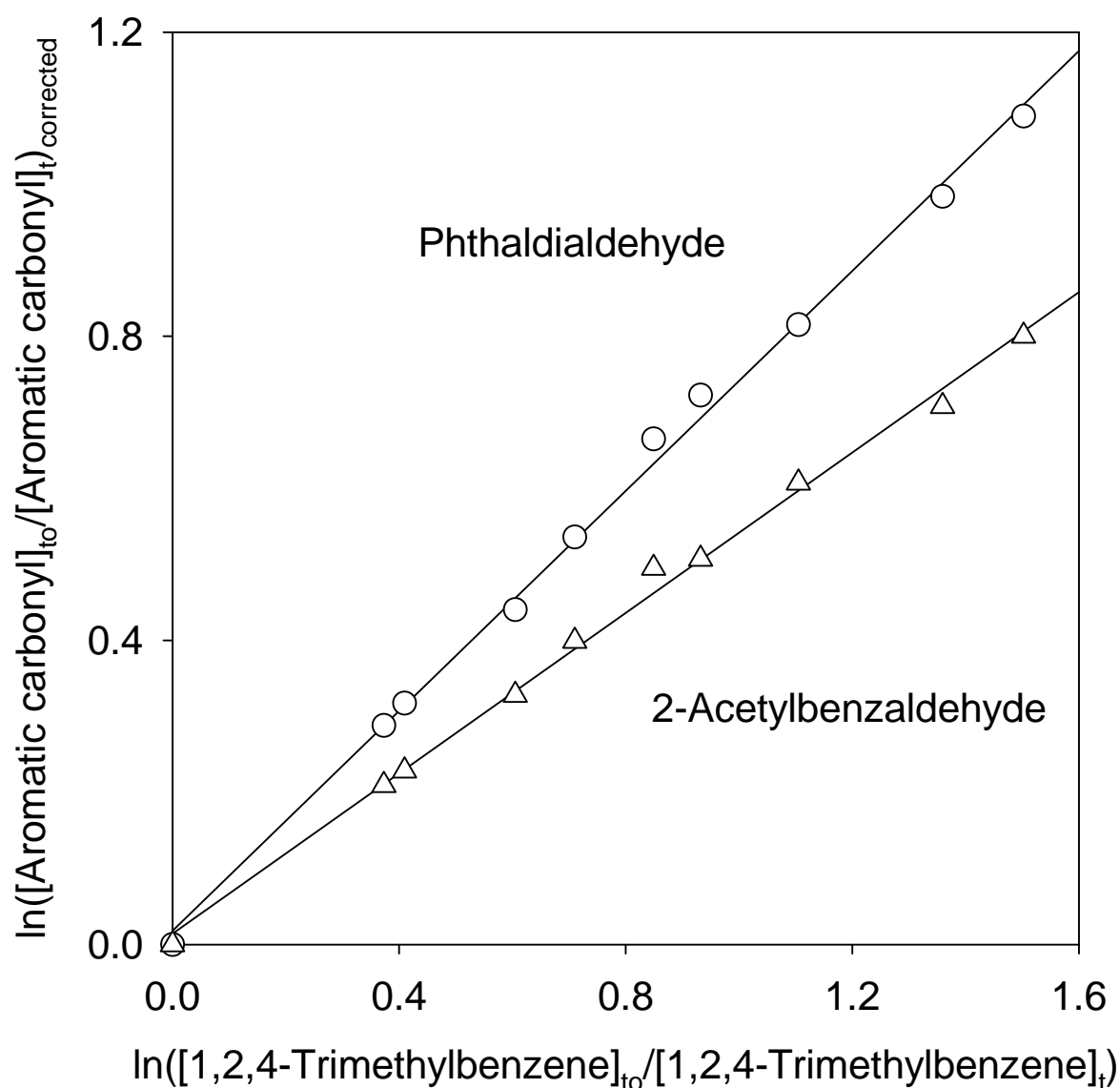
Figure 5. Plots of Equation (I) for the reactions of OH radicals with phthaldialdehyde and 2-acetylbenzaldehyde, with 1,2,4-trimethylbenzene as the reference compound. The experimental data for phthaldialdehyde and 2-acetylbenzaldehyde have been corrected for wall losses and photolysis (see text). Irradiations were at 10% of the maximum light intensity.

Table 7. Rate constant ratios k_1/k_2 and rate constants k_1 for the reactions of OH radicals with phthaldialdehyde, 2-acetylbenzaldehyde, 1,2-diacetylbenzene and phthalide at 298 ± 2 K

aromatic carbonyl	reference compound	k_1/k_2 [a]	$10^{12} \times k_1$ (cm^3 molecule^{-1} s^{-1})[b]
phthaldialdehyde	1,2,4-trimethylbenzene	0.72 ± 0.08	23 ± 3
2-acetylbenzaldehyde	1,2,4-trimethylbenzene	0.53 ± 0.08	17 ± 3
1,2-acetylbenzene	1,2,4-trimethylbenzene	0.12 ± 0.08	4 ± 3
	2,2,3,3-tetramethylbutane	<1.2	<1.2
phthalide	1,2,4-trimethylbenzene	<0.1	<3.3
	2,2,3,3-tetramethylbutane	<0.8	<0.8

[a]Indicated errors are two least-squares standard deviations of the slopes of plots such as those shown in Figure 4, combined with the two standard deviation uncertainties in the corrections for photolysis and dark wall decays.
[b]Placed on an absolute basis using rate constants of k_2(1,2,4-trimethylbenzene) = 3.25×10^{-11} cm^3 molecule^{-1} s^{-1} and k_2(2,2,3,3-tetramethylbutane) = 9.72×10^{-12} cm^3 molecule^{-1} s^{-1} (*10*).

concentration) resulted in equally good straight-line fits as those shown in Figure 5, but with ~20% higher slopes (*i.e.*, rate constant ratios). The rate constant ratios in Table 7 can be placed on an absolute basis using rate constants at 298 K of k_2(1,2,4-trimethylbenzene) = 3.25×10^{-11} cm^3 molecule^{-1} s^{-1} and k_2(2,2,3,3-tetramethylbutane) = 9.72×10^{-12} cm^3 molecule^{-1} s^{-1} (*10*), and the resulting rate constants k_1 are given in Table 7.

Products of Photolysis and OH Radical Reaction. Products of irradiated aromatic carbonyl – cyclohexane (in excess) – air and CH_3ONO – NO – aromatic carbonyl – air mixtures at the maximum light intensity were investigated with GC-MS and GC-FID analyses of SPME fibers exposed to the chamber contents. Products were identified by matching GC retention times and mass spectra with those of authentic standards, and are listed in Table 8. 3-Methylphthalide was first tentatively identified as a photolysis product of 2-acetylbenzaldehyde on the basis of its mass spectrum. Irradiation of 2-acetylbenzaldehyde in *n*-hexane solution yielded the same product, and its identity as 3-methylphthalide was confirmed by ^{1}H NMR. Our ^{1}H NMR data for 3-methylphthalide, which are in agreement with those reported by Kitayama (Kitayama, 1997), and phthalide are given in Table 9, together with MS data.

The experimental procedures and the data analyses were similar to those used in the photolysis rate and kinetic experiments described above. Because the products also decayed to the chamber walls, the product decay rates observed over a 60 min dark period after the irradiations were used to correct the measured product concentrations for wall decay. The products observed are expected to be of low reactivity towards OH radicals (Kwok and Atkinson, 1995) and not undergo photolysis (as shown experimentally for phthalide), and hence no corrections for photolytic or reactive losses were made.

Table 8.   Products of the OH radical reaction and photolysis of phthaldialdehyde, 2-acetylbenzaldehyde, 1,2-diacetylbenzene and phthalide, and their molar formation yields.

aromatic carbonyl	product and % molar yield[a]	
	OH radical reaction	photolysis
phthaldialdehyde	phthalic anhydride (85 ± 20)[b]	phthalic anhydride (35 ± 10) phthalide (53 ± 14)
2-acetylbenzaldehyde	phthalic anhydride (70 ± 25) phthalide (~10)	phthalic anhydride (19 ± 6) 3-methylphthalide (77 ± 20)
1,2-diacetylbenzene	phthalic anhydride (25 ± 15)	no photolysis observed
phthalide	phthalic anhydride (>60)	no photolysis observed

[a]Indicated errors are the estimated overall uncertainties.
[b]Yield is the average of one experiment with 2.4×10^{14} molecule cm^{-3} initial NO and a second experiment with initial NO and NO$_2$ concentrations of 2.4×10^{14} molecule cm^{-3} each.

Photolysis of 1,2-diacetylbenzene – cyclohexane – air and phthalide – cyclohexane – air mixtures showed no evidence for photolytic loss of the aromatic carbonyl nor any evidence for formation of products above the small amounts observed in control cyclohexane – air irradiations. The product formation yields derived from the OH radical-initiated reactions of 1,2-diacetylbenzene and phthalide are subject to large uncertainties because of the small amounts of aromatic carbonyl consumed by OH radical reaction compared to the wall decays and to wall desorption during the irradiations periods (see above). In the OH radical reactions, photolysis of phthaldialdehyde and 2-acetylbenzaldehyde contributed 6-7% of their total reactive losses and was taken into account in the data analysis. The small amounts of phthalide and 3-methylphthalide observed from the OH radical-initiated reactions of phthaldialdehyde and 2-acetylbenzaldehyde were quantitatively accounted for by photolysis and are hence not listed in Table 8. For the OH radical reaction with phthaldialdehyde, an experiment in which the initial NO was replaced by NO + NO$_2$ resulted in a phthalic anhydride yield (90%) which was similar to that (80%) when only NO was initially present in the reactant mixture (see discussion below).

Absorption Spectra. Absorption spectra for the four aromatic carbonyls were measured in solution because their relatively low vapor pressures and rapid dark decays in our 7000 liter Teflon chamber (up to 0.4% min^{-1}) would have made measurement of their absorption spectra and cross-sections in the gas phase subject to great uncertainties. The absorption coefficients obtained for the four aromatic carbonyls in *n*-hexane solution are listed in Appendix A, and are plotted in Figure 6 for the wavelength region 275-400 nm. Our data indicate that in *n*-hexane solution the long-wavelength limits of these absorptions are at 290 nm for phthalide, 370 nm for 1,2-diacetylbenzene and 400 nm for phthaldialdehyde and 2-acetylbenzaldehyde.

Table 9. ^{1}H NMR and MS data for phthalide and 3-methylphthalide

Phthalide

^{1}H NMR data (400 MHz)

proton(s)	chemical shift (ppm)
H(a)	5.33 (s, 2H)
H(b)	7.50 (d, 1H)
H(c)	7.69 (t, 1H)
H(d)	7.54 (t, 1H)
H(e)	7.94 (d, 1H)

Mass Spectral data
(Agilent Technologies 5975 inert XL MSD)

ion (m/z)	relative abundance (%)
134	41
133	15
106	10
105	100
77	47
76	14
51	15
50	13
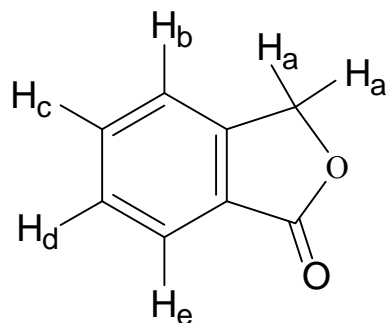
3-Methylphthalide

^{1}H NMR data (400 MHz)

proton(s)	chemical shift (ppm)
H(a)	5.57 (q, 1H)
CH$_3$	1.64 (d, 3H)
H(b)	7.44 (d, 1H)
H(c)	7.68 (t, 1H)
H(d)	7.53 (t, 1H)
H(e)	7.90 (d, 1H)

Mass Spectral data
(Agilent Technologies 5975 inert XL MSD)

ion (m/z)	relative abundance (%)
148	23
133	68
106	10
105	100
77	35
76	12
51	15
50	12
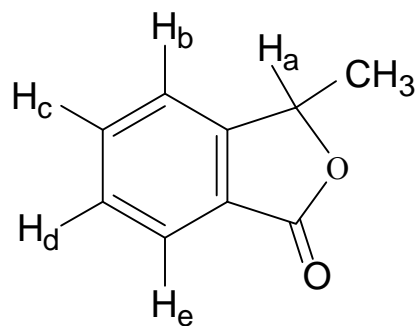
4. Discussion

The rate constants given in Table 7 for the reactions of OH radicals with phthaldialdehyde, 2-acetylbenzaldehyde, 1,2-diacetylbenzene and phthalide are the first reported for these compounds. The empirical structure-reactivity relationship of Kwok and Atkinson (1995) predicts rate constants at 298 K (in units of 10^{-12} cm^3 molecule^{-1} s^{-1}) for H-atom abstraction from the -CHO and -C(O)CH$_3$ substituent groups in phthaldialdehyde, 2-acetylbenzaldehyde, 1,2-diacetylbenzene and from the CH$_2$ group in phthalide of 32.6, 16.4, 0.2 and 1.5, respectively. The aromatic ring is expected to be deactivated with respect to OH radical addition by -CHO, -C(O)CH$_3$ and –C(O)OR groups (Brown and Okamoto, 1958; Zetzsch, 1982) and hence the room temperature rate constants (cm^3 molecule^{-1} s^{-1}) for phthaldialdehyde, 2-acetylbenzaldehyde, 1,2-diacetylbenzene and phthalide are predicted (Kwok and Atkinson, 1995) to be 3.3×10^{-11}, 1.7×10^{-11}, $\leq 1 \times 10^{-12}$ and $\sim 2 \times 10^{-12}$, respectively, reasonably consistent with our measured values (Table 7).

Phthalic anhydride was observed as an OH radical reaction product from all four aromatic carbonyls, being formed from phthaldialdehyde and 2-acetylbenzaldehyde in high yield; the formation yields from 1,2-acetylbenzene and phthalide are highly uncertain because of the small amounts of reaction compared to wall absorption/desorption (see above). The reactions of OH radicals with both phthaldialdehyde and 2-acetylbenzaldehyde are expected to involve initial H-atom abstraction from the CHO group(s) to form an acyl radical. The subsequent steps leading to phthalic anhydride formation are not presently understood, but could involve the pathways shown in Scheme 1. Pathway A1 in Scheme 1 assumes that the RC(O)O$^\bullet$ radical cyclizes rather than decomposing to R$^\bullet$ + CO$_2$ (note that the decomposition C$_6$H$_5$C(O)O$^\bullet$ → C$_6$H$_5$$^\bullet$ + CO$_2$ is calculated (NIST, 1994) to be 2.6 kcal mol^{-1} endothermic assuming an O-H bond dissociation energy in benzoic acid of 104 kcal mol^{-1}). The similar yield of phthalic anhydride from phthaldialdehyde observed on replacing the initial NO by NO + NO$_2$ suggests that pathway A1 is not important because at higher NO$_2$/NO concentration ratios formation of the acyl nitrate would increase while that of phthalic anhydride would decrease. Furthermore, for pathway A2 to be important and unchanged by addition of NO$_2$ would require that the intramolecular isomerization to form the hydroperoxide dominates over reaction of the acyl peroxy radical with NO and NO$_2$. Further theoretical and experimental studies are needed to elucidate the routes to phthalic anhydride formation from these aromatic dicarbonyls. The formation of phthalic anhydride from the OH radical-initiated reaction of phthalide can be readily explained by initial H-atom abstraction from the -CH$_2$- group in the 5-membered ring, followed (*10*) by addition of O$_2$ to form a peroxy (ROO$^\bullet$) radical, reaction of this peroxy radical with NO to form the corresponding alkoxy radical + NO$_2$, and reaction of this alkoxy radical with O$_2$ to form phthalic anhydride + HO$_2$.

The absorption spectra shown in Figure 6 and the absorption coefficients tabulated in Appendix A show that phthalide does not absorb above 290 nm. Hence if the gas-phase spectrum of phthalide is identical in shape to the solution-phase spectrum in Figure 6, then photolysis of phthalide using blacklamps or natural sunlight in the lower troposphere will not occur, in agreement with our observations. However, phthaldialdehyde, 2-acetylbenzaldehyde and 1,2-diacetylbenzene all absorb above 290 nm, and hence absorb in the emission region of blacklamps and in the atmosphere. Our solution-phase spectrum of phthaldialdehyde (Figure 6 and Appendix A) is in good agreement with that in *n*-heptane solution presented in the NIST WebBook (NIST 1975). Our measured photolysis rates of phthaldialdehyde and 2-acetyl-benzaldehyde (Table 6) are only applicable for the light intensity and spectral distribution

Scheme 1. Suggested pathway for the formation of phthalic anhydride from phthaldialdehyde.

Figure 6. Absorption spectra, measured in *n*-hexane solution, of phthaldialdehyde, 2-acetylbenzaldehyde, 1,2-acetylbenzene and phthalide over the wavelength range 275-400 nm.

31

conditions employed. The measured photolysis rates at the maximum light intensity lead to ratios J(aromatic carbonyl)/J(NO$_2$) of 0.030 ± 0.004 for phthaldialdehyde and 0.00215 ± 0.003 for 2-acetylbenzaldehyde. From our measured photolysis rates of phthaldialdehyde, 2-acetylbenzaldehyde and NO$_2$ (J(aromatic carbonyl) and J(NO$_2$), respectively), the blacklamp flux (I$_\lambda$) and the NO$_2$ photolysis quantum yield as a function of wavelength, Φ_λ(NO$_2$) (20), average photolysis quantum yields for phthaldialdehyde and 2-acetylbenzaldehyde, Φ_{av}(aromatic carbonyl), can be derived from Equation (II),

$$\frac{J(\text{aromatic carbonyl})}{J(\text{NO}_2)} = \frac{\Phi_{av}(\text{aromatic carbonyl}) \times \Sigma\{\sigma_\lambda(\text{aromatic carbonyl}) \times I_\lambda\}}{\Sigma\{\Phi_\lambda(\text{NO}_2) \times \sigma_\lambda(\text{NO}_2) \times I_\lambda\}} \quad \text{(II)}$$
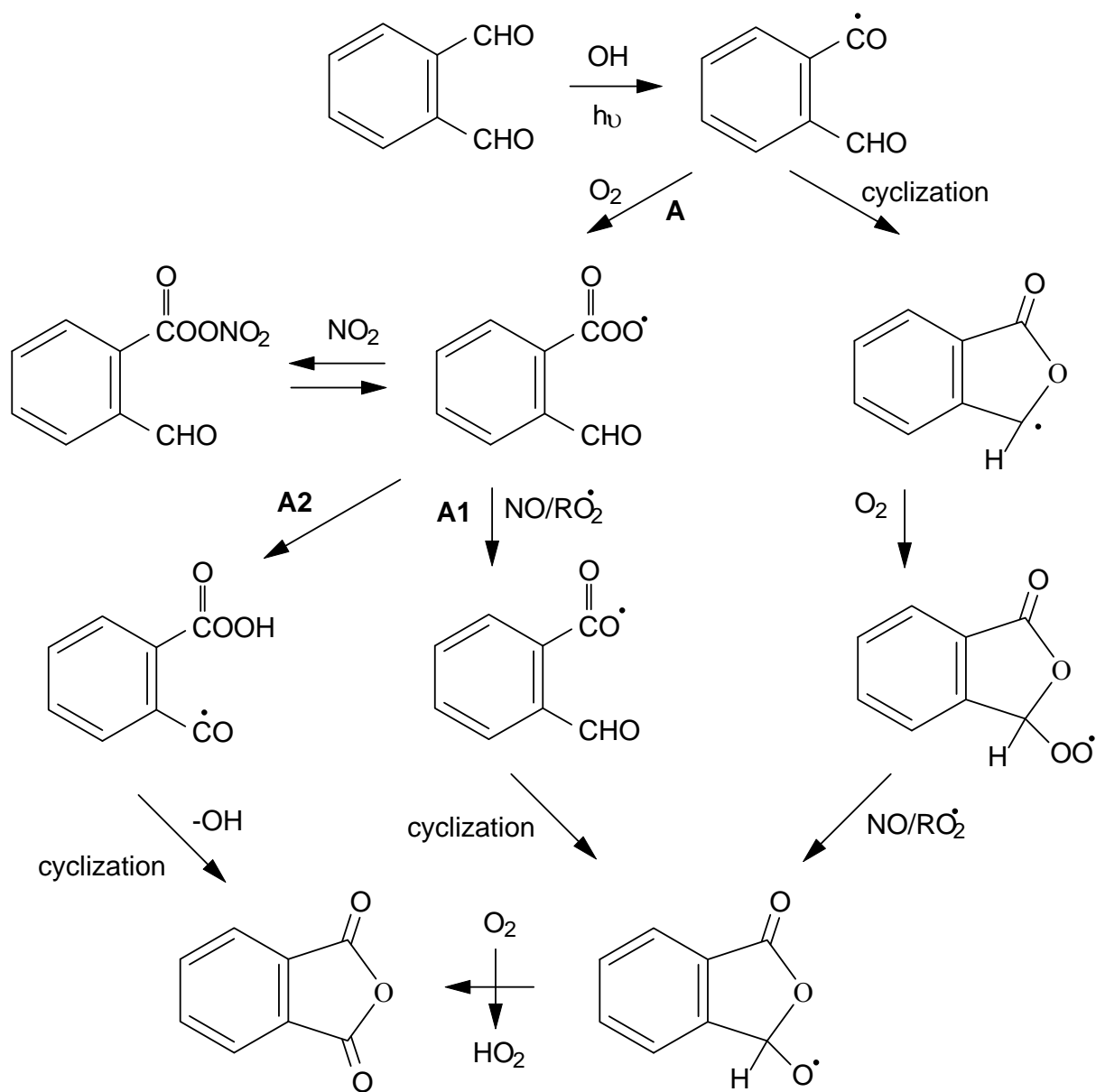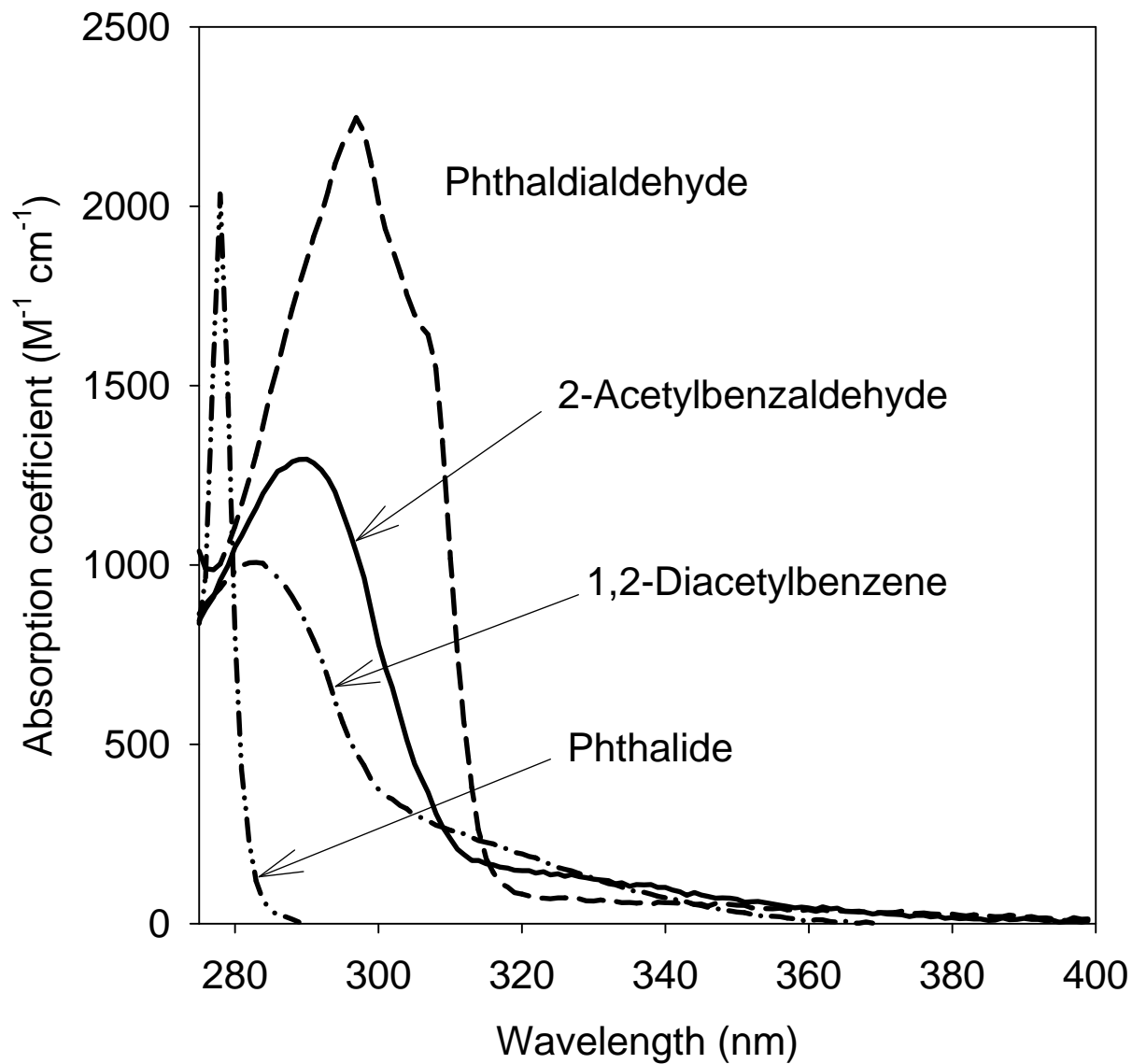
where σ_λ(aromatic carbonyl) and σ_λ(NO$_2$) are the absorption cross-sections of the aromatic carbonyl and NO$_2$, respectively. Using the literature values of σ_λ(NO$_2$) and Φ_λ(NO$_2$) (IUPAC, 2006) and assuming that the gas-phase absorption spectra of phthaldialdehyde and 2-acetylbenzaldehyde are identical to their solution-phase spectra measured here, then average quantum yields of Φ_{av}(aromatic carbonyl) = 0.19 for phthaldialdehyde and 0.21 for 2-acetylbenzaldehyde are derived (290-400 nm). These are only valid for the blacklamp spectral distribution.

Although a minor pathway for photodissociation of aliphatic aldehydes (IUPAC, 2006), one of the photolysis pathways of phthaldialdehyde and 2-acetylbenzaldehyde may involve C-H bond breakage in the –CHO group(s) (Zhu and Cronin, 2000), leading to formation of the same initial radical as from the corresponding OH radical reaction. The formation of phthalide from phthaldialdehyde and of 3-methylphthalide from 2-acetylbenzaldehyde is ascribed to a photoisomerization pathway, and this is also observed in solution (see above). Consistent with our data (Table 8), the formation of phthalic anhydride from the photolysis of phthaldialdehyde and 2-acetylbenzaldehyde is expected in lower yield than from the corresponding OH radical reactions, because C-H bond breakage in the –CHO group is only one of the photolysis pathways and ROO$^\bullet$ to RO$^\bullet$ conversion is less efficient in the absence of NO than in the presence of NO (Atkinson and Arey, 2003).

Atmospheric Lifetimes. The data obtained in this work can be used to estimate the atmospheric lifetimes of the four aromatic carbonyls studied here with respect to photolysis and OH radical reaction. Lifetimes were calculated using a 12-hr average OH radical concentration of 2.0×10^6 molecule cm^{-3} (Krol *et al.*, 2000; Prinn *et al.*, 2001) and by combining the average quantum yields derived above with the solar spectral distribution and the NO$_2$ absorption cross-sections and photolysis quantum yields, using Equation (II). The resulting calculated lifetimes of phthaldialdehyde, 2-acetylbenzaldehyde, 1,2-diacetylbenzene and phthalide with respect to reaction with OH radicals are 6.0 hr, 8.2 hr, >9 day and >14 day, respectively, and with respect to photolysis are 1.4-1.5 hr for both phthaldialdehyde and 2-acetylbenzaldehyde for a 12-hr average NO$_2$ photolysis rate of 0.312 min^{-1} (Atkinson *et al.*, 1989). For the same average NO$_2$ photolysis rate, our measured photolysis rates of NO$_2$, phthaldialdehyde and 2-acetylbenzaldehyde with blacklamp irradiation at the maximum light intensity (Table 6) lead to calculated lifetimes of phthaldialdehyde and 2-acetylbenzaldehyde of 1.8 hr and 2.5 hr, respectively. These differing calculated photolysis lifetimes arise because of differences in the solar and blacklamp spectral distributions. Clearly, however, photolysis is predicted to be the

dominant atmospheric transformation process for phthaldialdehyde and 2-acetylbenzaldehyde, and this may also be the case for 1,2-diacetylbenzene. Our data for phthaldialdehyde and 2-acetylbenzaldehyde and those presented by Thiault et al. (2004) for benzaldehyde and the tolualdehydes suggest that photolysis is the major atmospheric loss process for aromatic aldehydes.

Phthalic acid (1,2-benzenedicarboxylic acid) identified in ambient particles has been suggested as a marker of secondary organic aerosol (SOA) formation (Zheng *et al.*, 2002; Schauer *et al.*, 2002; Fraser *et al.*, 2003; Fine *et al.*, 2004). 4-Methylphthalic acid has also been observed in particles and was found to be highly correlated with phthalic acid (Fraser *et al.*, 2003; Fine *et al.*, 2004). We have shown that gas-phase OH radical-initiated reactions of naphthalene and certain alkylnaphthalenes will produce dicarbonyls which react further in the atmosphere to ultimately yield phthalic anhydride. Hydrolysis of phthalic anhydride, possibly in the particle-phase, may be the source of the phthalic acid found to correlate with SOA. By analogy, 4-methylphthalic acid could be formed from the anhydride atmospheric reaction product of 2-methylnaphthalene and several C_2-naphthalenes substituted on both rings (see Section C).

C. Dicarbonyl Products of OH Radical-Initiated Reactions of Naphthalene and the C_1- and C_2- Alkylnaphthalenes

1. Introduction

Naphthalene and the C_1- and C_2-alkylnaphthalenes are emitted by vehicle traffic and are the most abundant polycyclic aromatic hydrocarbons (PAHs) in urban atmospheres. For example, for a 5-day period in January 2003 at a heavily traffic-impacted site in Los Angeles, CA the average morning concentrations for naphthalene, the sum of the methylnaphthalenes, and the sum of the dimethyl- and ethyl-naphthalenes were ~1600 ng m^{-3}, ~1000 ng m^{-3}, and ~160 ng m^{-3}, respectively (Reisen and Arey, 2005), while co-located particle-associated benzo[*ghi*]perylene concentrations were ~ 2 ng m^{-3} (Fine *et al.*, 2004). Naphthalene and the alkylnaphthalenes are mainly in the gas-phase under typical ambient conditions (Bidleman, 1998; Wania and Mackay, 1996) and their atmospheric lifetimes are controlled by their reaction with the hydroxyl (OH) radical, with estimated lifetimes of ~6 h for naphthalene and ~2-4 h for the alkylnaphthalenes (Phousongphouang and Arey, 2002).

Previous studies of the OH radical-initiated reaction of naphthalene have identified numerous products, including 2-formylcinnamaldehyde and nitronaphthalenes (Sasaki *et al.*, 1997a; Bunce *et al.*, 1997). Nitronaphthalenes and alkylnitronaphthalenes have received much attention because they are mutagenic in bacterial (Gupta *et al.*, 1996) and human cells (Sasaki *et al.*, 1997b) and their presence in ambient air has been attributed to atmospheric formation (Gupta *et al.*, 1996; Arey, 1998; Cecinato, 2003; Reisen *et al.*, 2003; Arey and Atkinson, 2003). While a more polar chromatographic fraction of naphthalene reaction products than that containing the nitronaphthalenes was found to induce micronuclei in human cells (Sasaki *et al.*, 1997b), very little is known about the identity and possible health implications of the polar atmospheric reaction products of alkylnaphthalenes.

We report here on the most abundant products formed from the OH radical-initiated reactions of naphthalene, naphthalene-d$_8$, 1- and 2-methylnaphthalene (MN), 1- and 2-MN-d$_{10}$, 1- and 2-ethylnaphthalene (EN), and the 10 isomeric dimethylnaphthalenes (DMNs).

2. Experimental Methods

Experiments were carried out in a ~7500 liter Teflon chamber, equipped with two parallel banks of blacklamps, at 296 ± 2 K and 735 Torr total pressure of purified air at ~5% relative humidity. The chamber is also equipped with a Teflon-coated fan to ensure rapid mixing of reactants during their introduction into the chamber. Reactants were introduced into the chamber by flowing nitrogen gas through a Pyrex bulb containing a measured amount of the compound while (with the exception of methyl nitrite and NO) heating the bulb and inlet tube. OH radicals were generated by the photolysis of the methyl nitrite (CH$_3$ONO) in air at wavelengths > 300 nm, and NO was added to the reactant mixtures to suppress the formation of O$_3$ and hence of NO$_3$ radicals (Atkinson *et al.*, 1981). The chamber was cleaned after each experiment by flushing with purified air for at least 20 hours, with the chamber lights on for at least 6 hours.

Products of irradiated CH$_3$ONO-NO-naphthalene/alkylnaphthalene-air mixtures were analyzed by direct air sampling atmospheric pressure ionization tandem mass spectrometry (API-MS) and by gas chromatography (GC). Initial reactant concentrations were (in units of molecule cm^{-3}): naphthalene, naphthalene-d$_8$, alkylnaphthalenes, 1-MN-d$_{10}$, or 2-MN-d$_{10}$, 2.4 x 10^{12}; CH$_3$ONO, ~ 4.8 x 10^{13}; and NO, ~ 4.8 x 10^{13}. Two series of irradiations were carried out at 10% of the maximum light intensity corresponding to an NO$_2$ photolysis rate of 0.061 min^{-1} (Wang *et*

al., 2006) for 2-6 min resulting in 20-30% reaction of the initial alkylnaphthalene, and for 6-30 min resulting in 60-70% reaction.

Real-time Product Monitoring with API-MS Analysis. Analysis of irradiated naphthalene/alkylnaphthalene-CH$_3$ONO-NO-air mixtures were carried out using a *PE* SCIEX API III MS/MS (API-MS) interfaced to the ~7500 liter Teflon chamber, with operation of the API-MS in the MS (scanning) and MS/MS [with collision-activated dissociation (CAD)] modes as described elsewhere (Aschmann *et al.*, 1997). The MS mode was used in a time-resolved manner (MRM mode) by monitoring the intensities of selected ion peaks continuously before, during and after each irradiation. After the irradiation, the MS/MS mode with CAD was used to collect the product ion or precursor ion spectra of peaks which were observed in the MS mode.

The concentrations of naphthalene and alkylnaphthalenes were measured before and after irradiation by GC with flame ionization detection (GC-FID). Gas samples of 1 liter volume were collected from the chamber onto Tenax-TA solid adsorbent cartridges with subsequent thermal desorption in the injection port of the GC inlet at 250 $^\circ$C onto a 30-m DB-1701 widebore column held at 40 $^\circ$C for 10 min and then temperature-programmed.

Authentic standards of phthaldialdehyde, 2-acetylbenzaldehyde, 1,2-diacetylbenzene, phthalic anhydride, 4-methylphthalic anhydride, phthalide, phthalic acid and 4-methylphthalic acid were analyzed by API-MS/MS with CAD by sampling pure air from the chamber passing over a small vial containing the pure standard placed in the Pyrex sampling tube.

Product Studies Using Gas Chromatography/Mass Spectrometry. Solid-Phase Micro Extraction (SPME) samples of the irradiated naphthalene/alkylnaphthalene-CH$_3$ONO-NO-air mixtures were collected for variable times (including overnight sample collections) by exposing a 65 μm polydimethylsiloxane/divinylbenzene (PDMS/DVB) fiber to the chamber contents. The SPME fiber samples were thermally desorbed in the heated (250 $^\circ$C) GC injection port in a Varian model 2000 GC/MS/MS ion trap system onto a 30-m DB-1 widebore column held at 40 $^\circ$C for 2 min, then temperature-programmed. The ion trap was operated in the Electron Ionization (EI) mode or Chemical Ionization (CI) mode with isobutane as the reagent gas. Authentic standards of phthaldialdehyde, 2-acetylbenzaldehyde, 1,2-diacetylbenzene, phthalide, phthalic anhydride, *E*-cinnamaldehyde, and 4-methylphthalic anhydride were also analyzed by SPME-GC/MS in the EI and CI modes.

Chemicals. The chemicals used, and their stated purities, were: naphthalene (98%), 1-MN (99%), 2-MN (98%), 2-MN-d$_{10}$ (98%D), 1-EN (98+%), 2-EN (99+%), 1,2-DMN (98%), 1,3-DMN (96%), 1,4-DMN (95%), 1,5-DMN (98%), 1,6-DMN (99%), 1,7-DMN (99%), 1,8-DMN (95%), 2,3-DMN (98%), 2,6-DMN (99%), 2,7-DMN (99%), phthaldialdehyde (97%), phthalide (98%), 2-acetylbenzaldehyde (95%), 1,2-diacetylbenzene (99%), phthalic anhydride (99+%), phthalic acid (99.5+%), 4-methylphthalic anhydride (95%), 4-methylphthalic acid (99%), *E*-cinnamaldehyde (99+%), Aldrich Chemical Company; naphthalene-d$_8$ (99% D), 1-MN-d$_{10}$ (98% D), Cambridge Isotope Laboratories; and NO (>99%), Matheson Gas Products. Methyl nitrite was prepared and stored as described previously (Taylor *et al.*, 1980; Atkinson *et al.*, 1981).

3. Results and Discussion

API-MS Time-Resolved Analysis of OH + Naphthalene Reaction. The major challenge to identifying the OH radical reaction products of naphthalene and alkylnaphthalenes is the scarcity of commercially available standards. 2-Formylcinnamaldehyde was previously synthesized and identified in two independent laboratories as the most abundant of the numerous

products formed from the OH radical-initiated reaction of naphthalene (Sasaki *et al.*, 1997; Bunce *et al.*, 1997). In addition to 2-formylcinnamaldehyde, reported to be formed in 35% molar yield (*Z* + *E* isomers) and a product of molecular weight (m.w.) 176 with a 13% yield, phthaldialdehyde and phthalic anhydride were also prominent in the API-MS analysis of the naphthalene reaction (Sasaki *et al.*, 1997). It was noted that phthaldialdehyde could be a secondary product from reaction of OH radicals with 2-formylcinnamaldehyde and phthalic anhydride was also suggested to be a secondary product (Sasaki *et al.*, 1997). More recent work shows glyoxal to be a primary product on the OH + naphthalene reaction (Atkinson and Arey, 2006) and, because phthaldialdehyde is the presumed co-product of glyoxal, this suggests that phthaldialdehyde is also, at least in part, a primary product.

Shown in Figure 7 are the MRM data points monitoring the $[M+H]^+$ ions of 2-formylcinnamaldehyde and isomers (m/z 161 da), phthaldialdehyde (m/z 135 da) and phthalic anhydride [m/z 149 + 167 (water cluster) da] from a naphthalene reaction. At the later extents of reaction, phthaldialdehyde is more abundant than 2-formylcinnamaldehyde, which could either mean that phthaldialdehyde is a secondary product or that it is less reactive than 2-formylcinnamaldehyde. Also shown in Figure 7 are curves calculated using the FACSIMILE program. The rates of photolysis and OH radical reaction of phthaldialdehyde, and their phthalic anhydride product formation yields, have recently been studied (Wang *et al.*, 2006) and the loss processes of 2-formylcinnamaldehyde were estimated (Kwok and Atkinson, 1995; Baker *et al.*, 2004) [see caption to Figure 7 and Table 10 for more details and a complete list of reactions used]. Curves for phthaldialdehyde and phthalic anhydride are calculated assuming them to be either a first-generation or second-generation (phthaldialdehyde from 2-formylcinnamaldehyde and phthalic anhydride from 1st generation phthaldialdehyde) products. The API-MS data and the calculated curves in Figure 7 suggest that phthaldialdehyde is likely a primary product (but do not exclude some secondary formation from 2-formylcinnamaldehyde) and that phthalic anhydride is a secondary product from phthaldialdehyde.

API-MS Analyses of Naphthalene and Alkylnaphthalenes. Table 11 shows the dominant protonated molecular ions from the API-MS analyses of naphthalene, 1-MN, 2-MN, and their fully deuterated analogues, showing that the $[M+H]^+$ ions observed for the deuterated species are consistent with the proposed structures. Analogous to the naphthalene reaction, the most abundant products from 1- and 2-MN were dicarbonyls of molecular weight 174, and these ring-opened products without loss of carbon (which we will refer to as C_{all}-dicarbonyls) were also the most abundant products from the ethylnaphthalenes (ENs) and dimethylnaphthalenes (DMNs) [see Table 12]. As seen in Table 11, the corresponding C_{11}-dicarbonyl products from 1- and 2-MN-d_{10} retain all the deuterium atoms of the parent compounds, i.e., $[M+H]^+ = 185$ da.

The proposed structure of the m.w. 176 product from the naphthalene reaction (Sasaki *et al.*, 1997) is shown in Table 11 ([M+H] = 177), with corresponding proposed structures for the 1-MN and 2-MN products. The presence of 7 and 9 non-exchangeable hydrogens in the naphthalene and MN products, respectively, is consistent with rapid –OD to –OH exchange noted previously for the hydroxyl group (Atkinson *et al.*, 1995).

Phthaldialdehyde was confirmed as a product of the naphthalene and 2-MN reactions by comparison of the MS/MS spectra with that of an authentic standard. The lack of phthaldialdehyde in the 1-MN reaction and the presence of molecular weight 148 product(s) suggests that only β-carbons are lost to produce the lower molecular weight dicarbonyl products (which we will refer to as $C_{2\beta\text{-loss}}$-dicarbonyls [see Figure 8]).
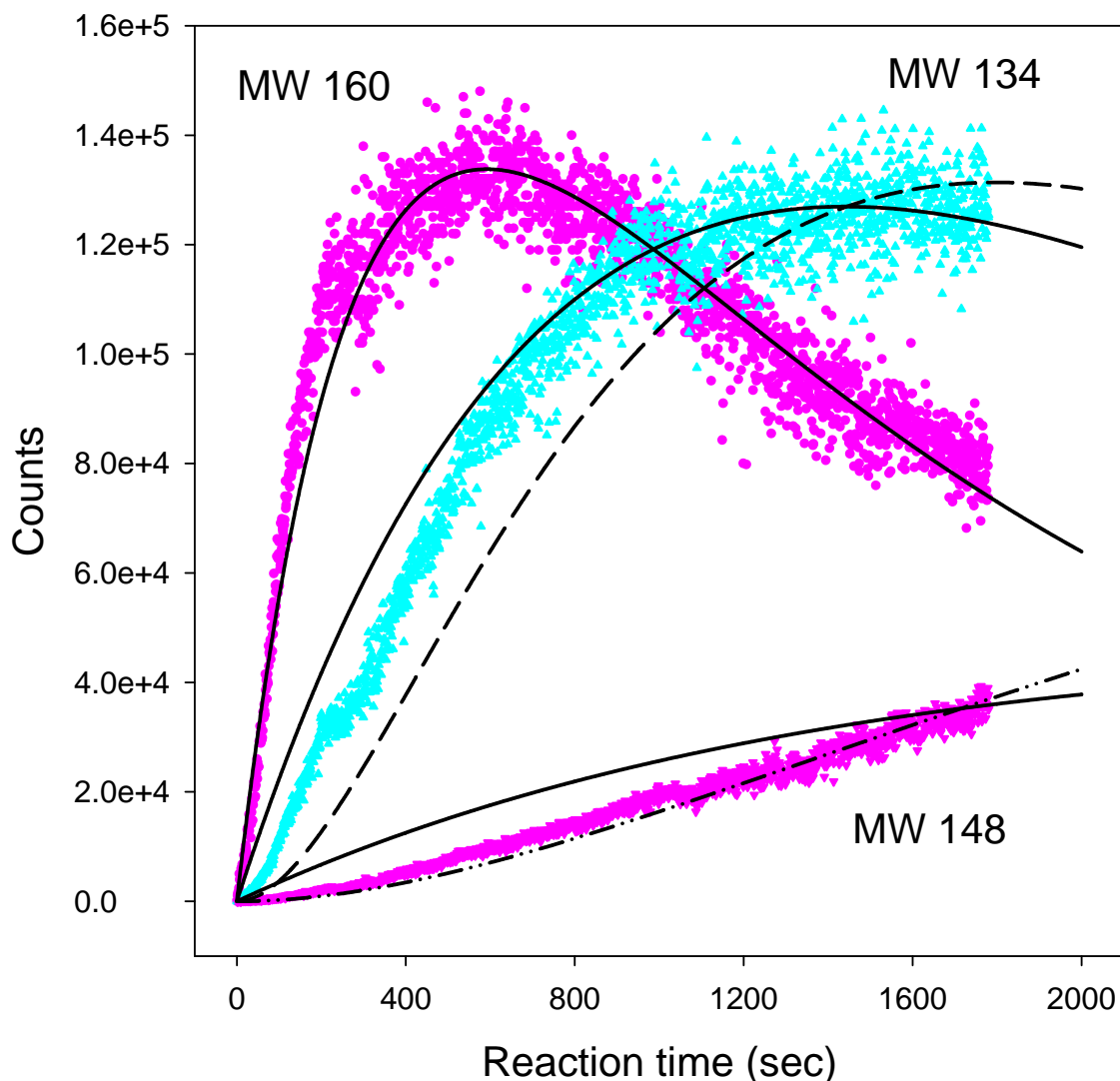
Figure 7. Plots of the API-MS MRM signals during an irradiated $CH_3ONO - NO -$ naphthalene
– air mixture for the molecular weight 160 (mainly 2-formylcinnamaldehyde), 134
(phthaldialdehyde) and 148 (phthalic anhydride) products. The calculated lines are:
solid lines for formation of the m.w. 160, 134 and 148 species as solely first-
generation products of the OH + naphthalene reaction. The dashed line for the m.w.
134 product is for second-generation formation from OH + 2-formylcinnamaldehyde,
and the dash-dot-dot line for the m.w. 148 product is for second-generation formation
from first-generation phthaldialdehyde. Rate constants used were: for the OH radical
reactions, naphthalene, 2.39×10^{-11} cm^3 molecule^{-1} s^{-1}; 2-formylcinnamaldehyde, $5.3 \times$
10^{-11} cm^3 molecule^{-1} s^{-1}; phthaldialdehyde, 2.3×10^{-11} cm^3 molecule^{-1} s^{-1}. Photolysis
rates used were: 2-formylcinnamaldehyde, 0.11 min^{-1}; phthaldialdehyde, 0.0025
min^{-1}. Wall loss rates used were: 2-formylcinnamaldehyde, 0.003 min^{-1};
phthaldialdehyde, 0.001 min^{-1}; phthalic anhydride, 0.002 min^{-1}. An average OH
radical concentration of 2.85×10^7 molecule cm^{-3} was used, based on the measured
pre- and post-irradiation naphthalene concentrations, with
$[OH] = \{\ln([naphthalene]_{to}/[naphthalene]_t)/k_{(OH + naphthalene)} \times t\}$.

Table 10. Reactions Used for Kinetic Simulations of the OH + Naphthalene Reaction

	reaction[a]	rate constant (cm^3 molecule^{-1} s^{-1})	reference or note
1	OH + naphthalene → α(160) + β(134) + γ(148)	2.39×10^{-11}	Phousongphouang and Arey, 2002
1a	OH + naphthalene → α(160)	2.39×10^{-11}	Phousongphouang and Arey, 2002
1b	OH + naphthalene → α(160) + β(134)	2.39×10^{-11}	Phousongphouang and Arey, 2002
2	OH + (160) → products	5.3×10^{-11}	estimated[b]
2a	OH + (160) → δ(134)	5.3×10^{-11}	estimated[b]
3	(160) + hν → products	0.11 min^{-1}	fitted[c]
4	(160) → wall	0.003 min^{-1}	assumed
5	OH + (134) → products	2.3×10^{-11}	Wang *et al.*, 2006
5a	OH + (134) → 0.85(148)	2.3×10^{-11}	Wang *et al.*, 2006
6	(134) + hν → products	0.0025 min^{-1}	Wang *et al.*, 2006
6a	(134) + hν → 0.35(148)	0.0025 min^{-1}	Wang *et al.*, 2006
7	(134) → wall	0.001 min^{-1}	Wang *et al.*, 2006
8	(148) → wall	0.002 min^{-1}	Wang *et al.*, 2006
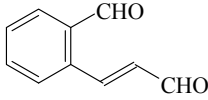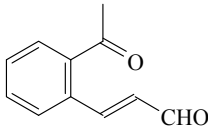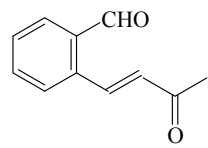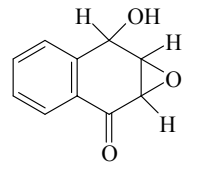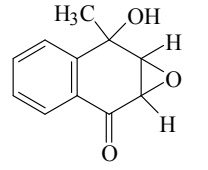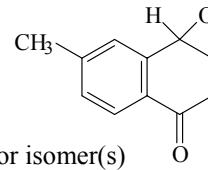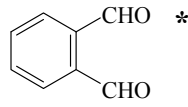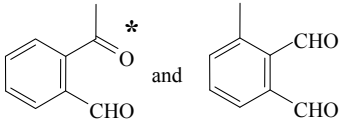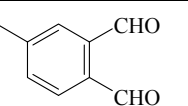
[a]The symbols α, β, γ, and δ in these reactions are molar formation yields. Since the fits used the API-MS counts for the specific product ions monitored and not concentrations, the fitted values are in arbitrary units.
[b]Estimated using the method of Kwok and Atkinson (1995).
[c]Value leading to good fit of experimental and calculated time-concentration profiles, especially the timing of the maximum m.w. 160 counts (Baker *et al.*, 2004).

An average OH radical concentration of 2.85 x 10^7 molecule cm^{-3} was used, based on the measured pre- and post-irradiation naphthalene concentrations. Photolysis rates are those measured or derived for the light intensity employed, corresponding to an NO_2 photolysis rate of 0.061 min^{-1} (Wang *et al.*, 2006). Reactions used to generate the calculated curves in Figure 1: solid lines for m.w. 160, 134, and 148 products, reactions 1, 2, 3, 4, 5, 6, 7, and 8; dashed line for m.w. 134 product, reactions 1a, 2a, 3, 4, 5, 6, and 7; dash-dot-dot line for m.w. 148 product, reactions 1b, 2, 3, 4, 5a, 6a, 7, and 8.

Table 11. Products and their $[M+H]^+$ ions (da) Observed by API-MS from the Gas-phase OH Radical-Initiated Reactions of Naphthalene, 1-Methylnaphthalene, 2-Methyl-naphthalene and their Deuterated Analogues

Parent compound	Product		$[M+H]^+$ observed by API-MS[a]	
	Formula	Structure	(da)	deuterated (da)
Naphthalene	$C_{10}H_8O_2$	CHO / CHO and isomers[b]	161	169
1-MN	$C_{11}H_{10}O_2$	O / CHO and isomers	175	185
2-MN	$C_{11}H_{10}O_2$	CHO / O and isomers	175	185
Naphthalene	$C_{10}H_8O_3$	H OH H O H O or isomer(s)	177	184
1-MN	$C_{11}H_{10}O_3$	H_3C OH H O H O or isomer(s)	191	200
2-MN	$C_{11}H_{10}O_3$	CH_3 H OH H O H O or isomer(s)	191	200
Naphthalene 2-MN	$C_8H_6O_2$	CHO * CHO	135	141
1-MN	$C_9H_8O_2$	O * CHO and CHO CHO	149	157
2-MN	$C_9H_8O_2$	CHO CHO	149	157

[a]Water adducts also occasionally seen and identified by MS/MS analysis.
[b]Structure was confirmed by comparison of MS/MS spectra with spectrum from the literature (Sasaki *et al.*, 1997).
*Structure was confirmed by comparison of MS/MS spectra with that of an authentic standard.

Table 12. Relative Abundances of API-MS Dicarbonyl Products from MRM Analyses of the OH Radical-Initiated Reactions of Naphthalene and Alkylnaphthalenes[a]

Parent Compound	k_1/k_{naph}[b]	C_{all}-Dicarbonyls			$C_{2\beta\text{-loss}}$-Dicarbonyls		
		C_{10}-dicarbonyl m.w. 160	C_{11}-dicarbonyl m.w. 174	C_{12}-dicarbonyl m.w. 188	C_8-dicarbonyl m.w. 134	C_9-dicarbonyl m.w. 148	C_{10}-dicarbonyl m.w. 162
Naphthalene	1.0	1.0			0.24	e	
Naph-d8[c]		1.0					
1-MN	1.71				e	0.29	
1-MN-d10[d]					e	0.07	
2-MN	2.03				0.33	0.05	
2-MN-d10[d]					0.14	0.01	
1-EN	1.52			1.0 / 0.19	e		0.09
2-EN	1.68			1.0	0.11		0.03
1,2-DMN	2.49	1.0				0.11	0.006
1,3-DMN	3.13	1.0				0.08	0.002
1,4-DMN	2.42	1.0		1.0	e		0.08
1,5-DMN	2.51	1.0				e	0.16
1,6-DMN	2.65					0.02	0.02
1,7-DMN	2.84		1.0			0.03	0.04
1,8-DMN	2.62		1.0			e	0.05
2,3-DMN	2.57			1.0	0.39		0.02
2,6-DMN	2.78		1.0			0.14	e
2,7-DMN	2.87		1.0			0.06	e

[a]Blanks indicate the ions were not monitored because these ions were not observed during the API-MS analyses of the reaction products.

[b]Data were collected after 200 s (naphthalene), 100 s (MNs) and 50 s (ENs and DMNs) of irradiation corresponding to ~10% reaction; rate constant ratios from Phousongphouang and Arey (2002).

[c]Corresponding molecular weights of deuterated species for C_{10}- and C_8- dicarbonyls were 168 and 140, respectively.

[d]Corresponding molecular weights of deuterated species for C_{11}-; C_8-; and C_9-dicarbonyls were 184, 140, and 156, respectively.

[e]Abundance <0.6% of the most abundant peak in the reaction.

40

R_1

+ OH

R_2

naphthalene: $R_1, R_2 = H$
2-MN: $R_1 = CH_3$; $R_2 = H$
2-EN: $R_1 = CH_3CH_2$; $R_2 = H$
2,3-DMN: $R_1, R_2 = CH_3$

CHO O
R_1
R_2

CHO
CHO
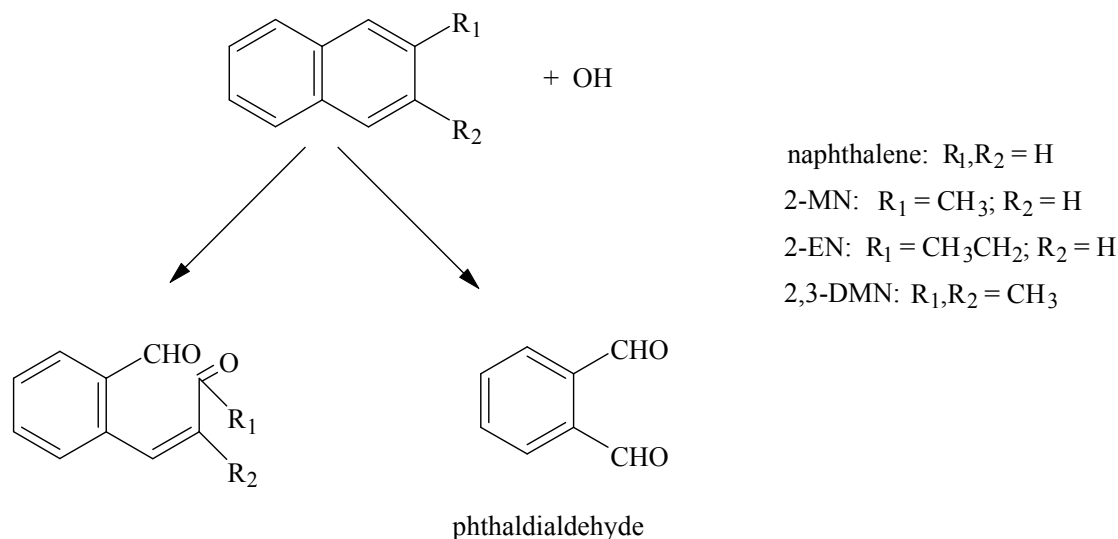
phthaldialdehyde

Figure 8. In naphthalene the α-carbons are C_1, C_4, C_5 and C_8 and the β-carbons are C_2, C_3, C_6 and C_7. Formation of phthaldialdehyde occurs by loss of two β-carbons and their associated alkyl groups and is observed as a product from naphthalene, 2-MN, 2-EN and 2,3-DMN. Note that the presumed co-products would be glyoxal from naphthalene, methylglyoxal from 2-MN, ethylglyoxal from 2-EN and biacetyl from 2,3-DMN. Recently SPME analysis with on-fiber derivatization has been used to identify glyoxal from naphthalene (Atkinson and Arey, 2006).

API-MS analyses of reaction products of each of the ten DMNs and the two ENs showed the major product always was 32 mass units above the parent compound and was presumably one or more C_{12}-ring-opened dicarbonyl(s). Additionally, mass peaks analogous to the multifunctional m.w. 176 product from naphthalene (see Table 11) at 205 da $[M+H]^+$ and products of m.w. 162, 148 and 134 were observed. Table 12 shows the ions attributed to dicarbonyls observed in the API-MS analyses of naphthalene, the MNs, ENs and DMNs with the ion abundances normalized to the most abundant peak for each reaction (the C_{all}-dicarbonyls). The abundances of the carbonyls were determined during MRM monitoring experiments and, to minimize the effect of secondary reactions, the values reported in Table 12 were determined from data at ~10% reaction of the naphthalene/alkylnaphthalene.

The observation that only β-carbons (and their associated alkyl groups) are lost after ring-cleavage and that the OH reaction occurs predominantly on the alkyl-substituted ring can be seen from Table 12 and Figures 8 and 9. In addition to being formed from reaction of naphthalene, phthaldialdehyde is formed only from those alkylnaphthalenes with only β-alkyl-substitution and substitution on a single ring, i.e., 2-MN, 2-EN and 2,3-DMN (Figure 8). When the parent C_2-alkylnaphthalene is substituted only on the α-carbon(s), loss of two β-carbons results only in carbonyl products of m.w. 162, as seen for 1,4-; 1,5- and 1,8-DMN and 1-EN (Figure 9), and no products of m.w. 134 or 148 are observed.

R₄   R₁

+ OH

1,4-DMN: $R_1,R_2 = CH_3$; $R_3,R_4 = H$

1,5-DMN: $R_1,R_3 = CH_3$; $R_2,R_4 = H$

1,8-DMN: $R_1,R_4 = CH_3$; $R_2,R_3 = H$

1-EN: $R_1 = CH_3CH_2$; $R_2,R_3,R_4 = H$
(or $R_4 = CH_3CH_2$; $R_1,R_2,R_3 = H$)

M.W. = 188 da   M.W. = 162 da
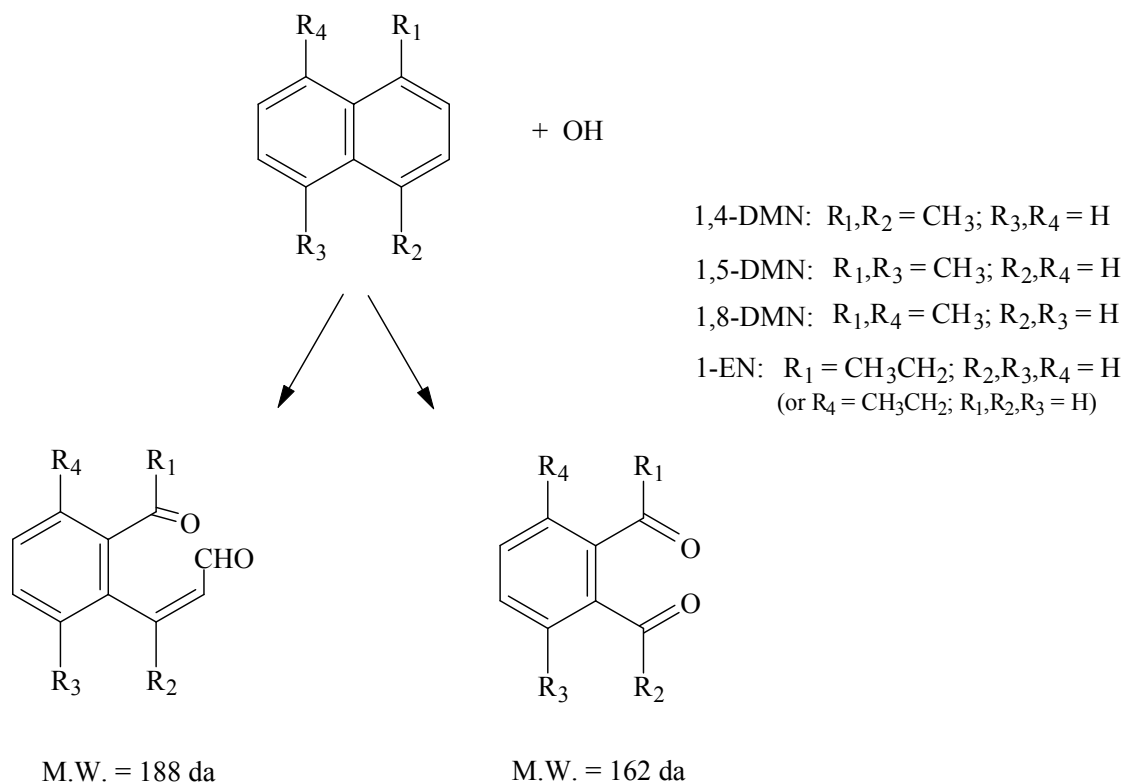
Figure 9. Loss of two β-carbons from C_2-alkylnaphthalenes with substitution only on α-carbon(s) results in a m.w. 162 dicarbonyl. Note that the co-product to the m.w. 162 dicarbonyl is expected to be glyoxal.

OH radical addition on the unsubstituted ring is less favored, but still occurs to some extent as seen by the low abundance of the m.w. 148 product in the 2-MN reaction (see Table 11 for the proposed structure), which would result from loss of the two β-carbons from the unsubstituted ring (Figure 10). This preference for the substituted ring is further confirmed by the low abundance of m.w. 162 products in the 2-EN and 2,3-DMN reactions (see Table 12). Where methyl substitution was on an α-carbon in one ring and on a β-carbon on the second ring, namely 1,6- and 1,7-DMN, the nearly 1:1 ratio of m.w. 148/162 products (see Table 12) suggests that OH addition was equally likely on either ring, as expected.

GC/MS Analyses of C_{all}-Dicarbonyls. The API-MS analyses do not distinguish among isomers, and GC/MS analyses were also performed on samples collected post-reaction by SPME. 10-min samples were analyzed by isobutane CI to determine isomer distributions, and samples collected overnight were analyzed in the EI mode to obtain characteristic mass spectra. As noted previously, *Z*- and *E*-2-formylcinnamaldehyde were observed as the major products from the naphthalene reaction, presumably after OH radical addition to the 1- or 2-position of naphthalene and breaking of the C_1-C_2 bond (Sasaki *et al.*, 1997; Bunce *et al.*, 1997). Two additional m.w. 160 products, in lower abundance, were reported by Sasaki et al. (1997). GC/MS analyses of the MN, EN and DMN products revealed that, analogous to the naphthalene reaction products, the most abundant ring-opened dicarbonyl product from the alkylnaphthalenes always had an EI

42
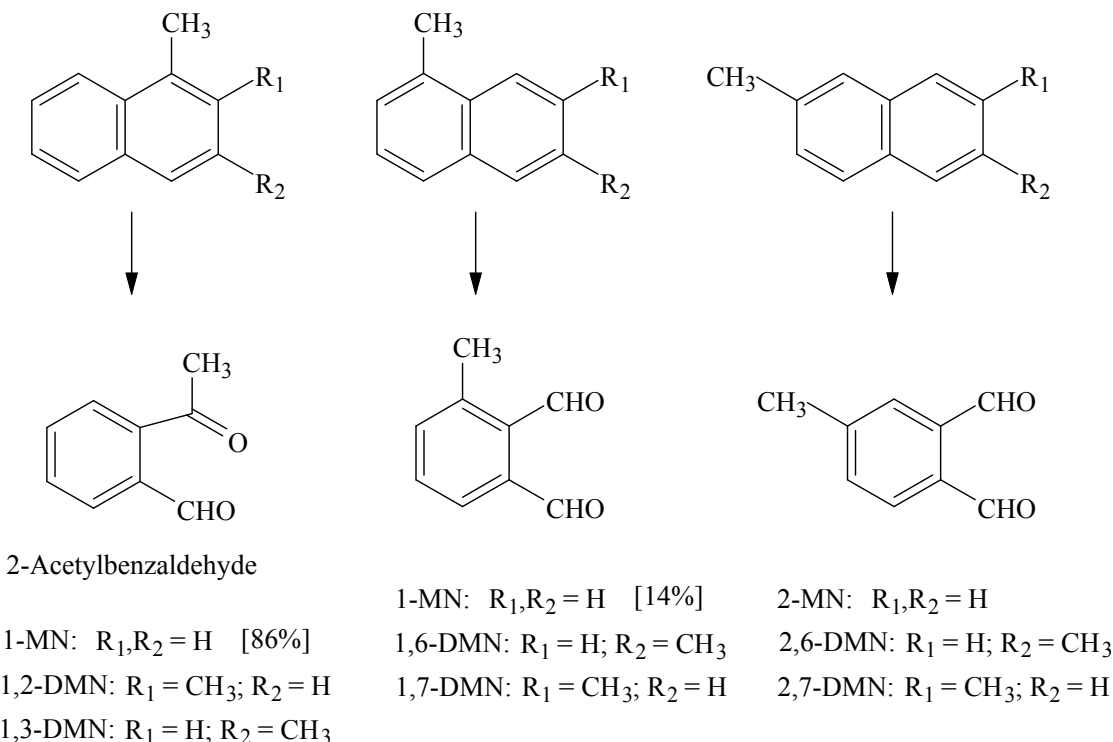
Figure 10. Molecular weight 148 species, resulting from the loss of two β-carbons from the MNs and two β-carbons and an associated methyl group from the DMNs. 2-Acetylbenzaldehyde was confirmed by matching EI/CI spectra and retention times with those of an authentic standard. Values in brackets give an estimated percentage of each isomer formed from 1-MN based on GC/MS CI peak areas.

spectrum consistent with a product formed by breaking the C_1-C_2 bond (see Table 13 and Tables 14a-c). For toluene, addition of the OH radical to the aromatic ring at the position *ortho* to the methyl group is slightly thermodynamically favored over addition at the other positions (Calvert *et al.*, 2002) and occurs ~80% of the time, based on the *o*-cresol vs *m*- + *p*-cresol yields (Atkinson *et al.*, 1989 and references therein). Addition *ortho* to the alkyl group is shown in Table 13 for all alkylnaphthalenes with the exception of 1,2-DMN, where addition *ipso* is shown. The rationale for proposing *ipso* addition will be discussed below.

The characteristic EI fragmentation used to support the structural assignments of the ring-cleavage dicarbonyls shown in Table 13 are given in Table 14a for naphthalene, the MNs and the ENs, and in Tables 14b and 14c for the DMNs. As is the case for the naphthalene reaction, these products may occur as *Z*- and *E*- isomers [potentially at least in part the result of photoisomerization and isomerization during analysis (Sasaki *et al.*, 1997)]. The estimated percent of OH radical addition at the suggested position listed in Table 13 is the result of taking the area of the [M+H]$^+$ ion peaks in the SPME–GC/MS-CI analysis attributed to the structures shown (*Z* + *E* isomers where observed) and dividing by the sum of all the isomers, i.e., all the isomer peaks corresponding to m.w. 160 for naphthalene, 174 for the MNs and 188 for the ENs and DMNs. The MNs and ENs, which have less symmetry than the DMNs, had the highest

number of observable C_{all}-dicarbonyl isomer peaks. For example, for 2-EN the area of the peaks attributed to the $Z + E$ isomers of the structure shown in Table 13 represented only 36% of the total peak area with 10 additional smaller apparent isomer peaks being observed. Because the CI response may vary somewhat among isomers, the percentages of OH addition/bond breakage as shown in Table 13 are only approximate. For example, based on the yield data of Sasaki et al. (1997), the addition of OH at C_1 (or C_2) of naphthalene followed by breakage of the C_1-C_2 bond results in 92% of the m.w. 160 products, compared to the 68% derived here.

      The identifications of the C_{all}-dicarbonyls given in Tables 13 and 14a-c must be viewed as tentative due to a lack of authentic standards. Structural assignments were made on the basis of the EI fragmentation (McLafferty and Turecek, 1993). 2-Acetylbenzaldehyde (Figure 10) has $[M-COCH_3]^+$ as the base peak in its EI spectrum (see Table 15a) and an abundant fragment ion in E-cinnamaldehyde is from loss of the aldehyde $[M-HCO]^+$ adjacent to the double bond. The structure proposed for the m.w. 188 product from 1,4-DMN is consistent with these fragmentation patterns as well as with the confirmed 1,2-diacetylbenzene product (see Figure 11 and Table 15b); both result from breaking the ring in 1,4-DMN between C_1-C_2: So the fragmentation is assigned as:
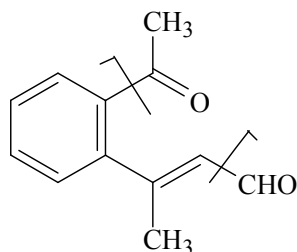
m/z 159 da = $[M-HCO]^+$ base peak

m/z 145 da = $[M-COCH_3]^+$

      Analogous base peaks from the loss of an aldehyde next to a double bond $[M-HCO]^+$ and a smaller fragment from loss of an acetyl group $[M-COCH_3]^+$ are consistent with the proposed structures for the most abundant product from 1-MN and 1,3-; 1,5-; 1,6-; 1,7-; and 1,8-DMNs (see Tables 14a and 14b). Analogous losses of 29 da, $[M-HCO]^+$, and 57 da, $[M-COC_2H_5]^+$, occur from the major product of the 1-EN + OH reaction (Table 14a).

      For 1,2-DMN, 2-acetylbenzaldehyde was a confirmed $C_{2\beta\text{-loss}}$-dicarbonyl product (see Figure 10 and Table 15a) and this product is ~20-fold more abundant than the m.w. 162 $C_{2\beta\text{-loss}}$-dicarbonyl formed from OH radical addition to the unsubstituted ring (see Table 12). The structure shown in Tables 13 and 14b for the only m.w. 188 product observed from reaction of 1,2-DMN is consistent with OH radical addition to the substituted ring and with the large $[M-COCH_3]^+$ fragment observed (presumably from loss of either acetyl group) in the EI mass spectrum. Both addition of the OH radical to C_3 of the substituted ring (i.e., *ortho* to the methyl group) followed by breakage of the C_3-C_4 bond and addition on the unsubstituted ring followed by breakage of the C_7-C_8 or C_5-C_6 bonds would be expected to result in structures that would give an $[M-HCO]^+$ fragment in their EI mass spectra. For 1,2-DMN, $[M-43]^+$ is the dominant fragment in the spectrum with no $[M-29]^+$ fragment observed, suggesting *ipso* addition of the OH radical on C_1 or C_2 followed by breakage of the C_1-C_2 bond. Formation of 2-acetyl-benzaldehyde ($C_{2\beta\text{-loss}}$-dicarbonyl) noted above argues against the remaining possibility, namely of addition on C_3 and breakage of the C_2-C_3 bond. *Ipso* addition of OH radicals, rather than H-atom abstraction from the methyl groups, has been reported for hexamethylbenzene (Koch *et al.*, 2006) and a recent theoretical study of the mechanism of the *p*-xylene reaction predicts

Table 13. Position(s) for OH Radical Addition on Naphthalene and Alkylnaphthalenes, Resulting C_{all}-Dicarbonyl Product(s) and Estimated Occurrence
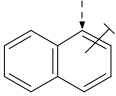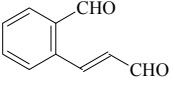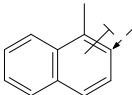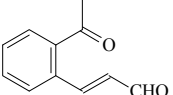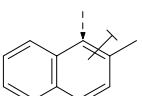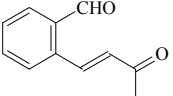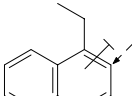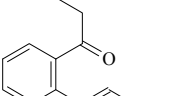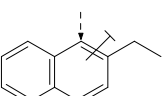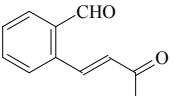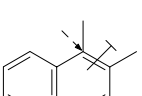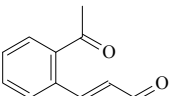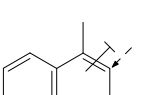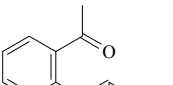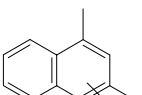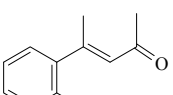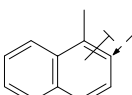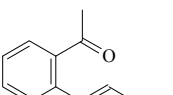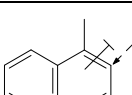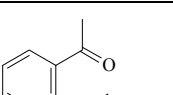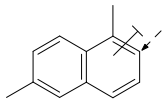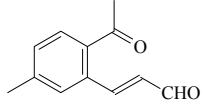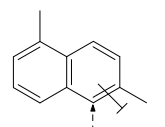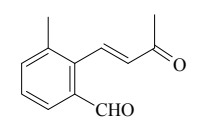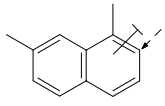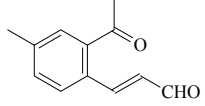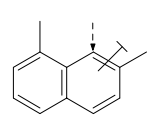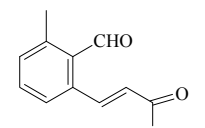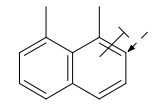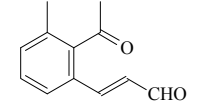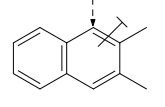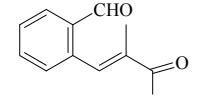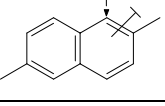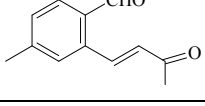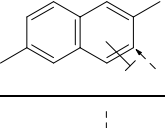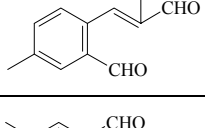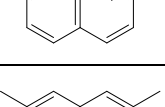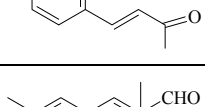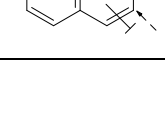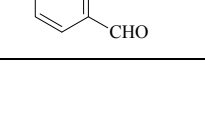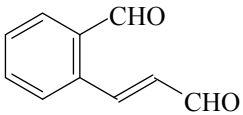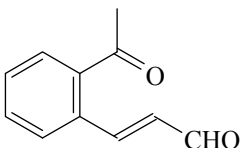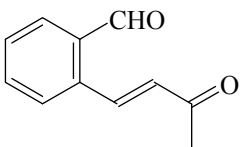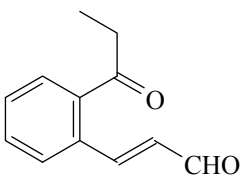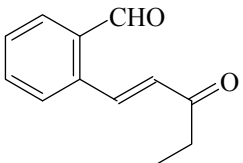
Parent	Position of OH addition	C_{all}-ring-cleavage Product	Estimated % of OH addition[a]
Naphthalene		CHO / CHO	68
1-MN		O / CHO	48
2-MN		CHO / O	53
1-EN		O / CHO	68
2-EN		CHO / O	36
1,2-DMN		O / O	100
1,3-DMN		O / CHO	64
		O / CHO	13
1,4-DMN		O / CHO	94
1,5-DMN		O / CHO	98

45

Table 13 (cont.). Position(s) for OH Radical Addition on Naphthalene and Alkylnaphthalenes, Resulting C_{all}-Dicarbonyl Product(s) and Estimated Occurrence

Parent	Position of OH addition	Ring-cleavage Product	Estimated % of OH addition[a]
1,6-DMN	*(structure)*	*(structure)*	62
	(structure)	*(structure)*	28
1,7-DMN	*(structure)*	*(structure)*	46
	(structure)	*(structure)*	19
1,8-DMN	*(structure)*	*(structure)*	90
2,3-DMN	*(structure)*	*(structure)*	96
2,6-DMN	*(structure)*	*(structure)*	76
	(structure)	*(structure)*	24
2,7-DMN	*(structure)*	*(structure)*	67
	(structure)	*(structure)*	29

[a]See text for details.

Table 14a. Suggested Structures and Characteristic Fragmentation for the Most Abundant Isomers of the C_{all}-Dicarbonyls from the OH Radical-Initiated Reactions of the Naphthalene, the Methylnaphthalenes and the Ethylnaphthalenes

Parent	Structure	M.W.[a] (da)	% of dicarbonyl isomers[b]	Base peak in the mass spectrum for the most abundant isomer			Second characteristic fragment		
				$[M-HCO]^+$	$[M-COCH_3]^+$	$[M-COC_2H_5]^+$	$[M-HCO]^+$	$[M-COCH_3]^+$	$[M-COC_2H_5]^+$
Naphthalene[c]	(structure)	160	68 (Z + E)	X					
1-MN	(structure)	174	48	X				X	
2-MN	(structure)	174	53 (Z + E)				X		
1-EN	(structure)	188	68	XX					X
2-EN	(structure)	188	36 (Z + E)			X	X		

[a]Molecular weights were confirmed by GC/MS with isobutane CI analyses.
[b]The area of all dicarbonyl isomers without loss of carbons observed in the CI analyses for each reaction were summed. The percent area of the isomer peak(s) attributed to the structure shown is given.
[c]Second characteristic fragment was $[M-HCO-CO]^+$.

Table 14b. Suggested Structures and Characteristic Fragmentation for the Most Abundant Isomers of the C_{all}-Dicarbonyls from the OH Radical-Initiated Reactions of the 1,2-; 1,3-; 1,4-; 1,5-; 1,6-; 1,7-; and 1,8-Dimethylnaphthalenes
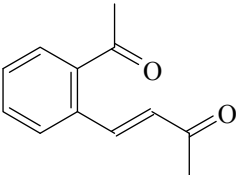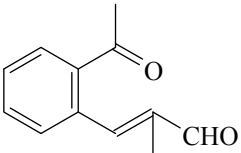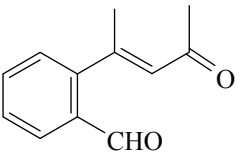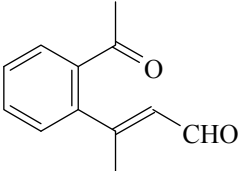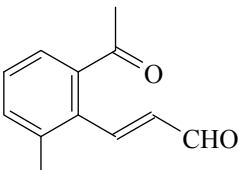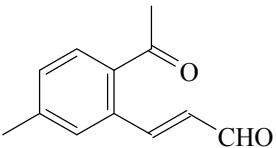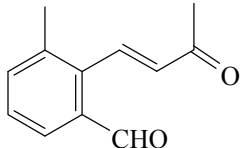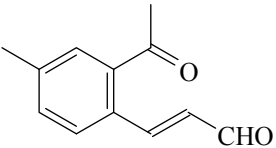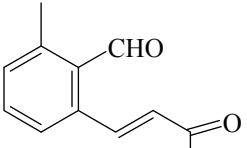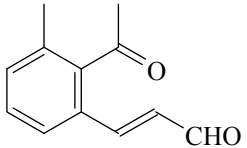
Parent	Structure	M.W.[a] (da)	% of dicarbonyl isomers[b]	Base peak in the mass spectrum for the most abundant isomer		Second characteristic fragment	
				$[M\text{-}HCO]^+$	$[M\text{-}COCH_3]^+$	$[M\text{-}HCO]^+$	$[M\text{-}COCH_3]^+$
1,2-DMN		188	100				
1,3-DMN		188	64	X X			X
		188	13			X	
1,4-DMN		188	94	X X			X
1,5-DMN		188	98 (Z + E)	X			X

Table 14b (cont.). Suggested Structures and Characteristic Fragmentation for the Most Abundant Isomers of the C_{all}-Dicarbonyls from the OH Radical-Initiated Reactions of the 1,2-; 1,3-; 1,4-; 1,5-; 1,6-; 1,7-; and 1,8-Dimethylnaphthalenes

Parent	Structure	M.W.[a] (da)	% of dicarbonyl isomers[b]	Base peak in the mass spectrum for the most abundant isomer		Second characteristic fragment	
				$[\text{M-HCO}]^+$	$[\text{M-COCH}_3]^+$	$[\text{M-HCO}]^+$	$[\text{M-COCH}_3]^+$
1,6-DMN		188	62 (Z + E)	X			
		188	28 (Z + E)			X	X
1,7-DMN		188	46 (Z + E)	X X			
		188	19			X X	
1,8-DMN		188	90	X X			

[a]Molecular weights were confirmed by GC/MS with isobutane CI analyses.
[b]The area of all dicarbonyl isomers without loss of carbons observed in the CI analyses for each reaction were summed. The percent area of the isomer peak(s) attributed to the structure shown is given.

X
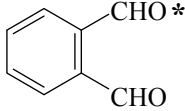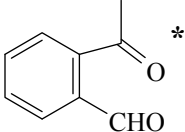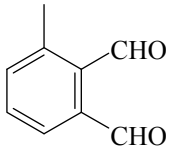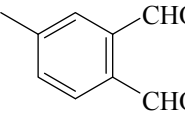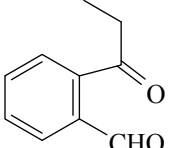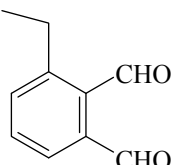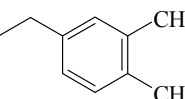
Table 14c. Suggested Structures and Characteristic Fragmentation for the Most Abundant Isomers of the C_{all}-Dicarbonyls from the OH Radical-Initiated Reactions of the 2,3-; 2,6-; and 2,7-Dimethylnaphthalenes

Parent	Structure	M.W.[a] (da)	% of dicarbonyl isomers[b]	Base peak in the mass spectrum for the most abundant isomer [M-HCO]+	Base peak [M-COCH₃]+	Second characteristic fragment [M-HCO]+	Second characteristic fragment [M-HCO-CO]+
2,3-DMN	(structure: CHO, =O)	188	96 (Z + E)			X	
2,6-DMN	(structure: CHO, O)	188	76 (Z + E)	X		X	
2,6-DMN	(structure: CHO, CHO)	188	24 (Z + E)	X	X		
2,7-DMN	(structure: CHO, O)	188	67 (Z + E)	X		X	
2,7-DMN	(structure: CHO, CHO)	188	29 (Z + E)	X	X		X

[a]Molecular weights were confirmed by GC/MS with isobutane CI analyses.

[b]The area of all dicarbonyl isomers without loss of carbons observed in the CI analyses for each reaction were summed. The percent area of the isomer peak(s) attributed to the structure shown is given.

50

CH$_2$CH$_3$

CH$_2$CH$_3$ O
CHO [80%]

CH$_2$CH$_3$
CHO
CHO [20%]

+

1,2-Diacetylbenzene

CH$_3$ CH$_3$

CH$_3$ O
O CH$_3$

R$_4$ CH$_3$
R$_3$ R$_1$
R$_2$

CH$_3$ O
R$_4$ CHO
R$_3$ R$_1$
R$_2$

1,5-DMN: R$_1$ = CH$_3$; R$_2$,R$_3$,R$_4$ = H
1,6-DMN: R$_2$ = CH$_3$; R$_1$,R$_3$,R$_4$ = H
1,7-DMN: R$_3$ = CH$_3$; R$_1$,R$_2$,R$_4$ = H
1,8-DMN: R$_4$ = CH$_3$; R$_1$,R$_2$,R$_3$ = H

CH$_2$CH$_3$

CH$_2$CH$_3$
CHO
CHO

R$_1$
R$_2$
R$_3$

R$_1$
R$_2$
CHO
CHO
R$_3$

1,2-DMN:
1,3-DMN:
2,3-DMN:

R$_1$, R$_2$ = CH$_3$; R$_3$ = H
R$_1$,R$_3$ = CH$_3$; R$_2$ = H
R$_2$,R$_3$ = CH$_3$; R$_1$ = H

Figure 11. Molecular weight 162 da species, resulting from the loss of two β-carbons. 1,2-Diacetylbenzene formed from 1,4-DMN was confirmed by matching EI/CI spectra and retention times with those of an authentic standard. Values in brackets give an estimated percentage of each isomer formed from 1-EN based on GC/MS CI peak areas. Note that no m.w. 162 product was observed from 2,6-DMN nor 2,7-DMN.

51

Table 15a. Suggested Structures of $C_{2\beta\text{-loss}}$-Dicarbonyl Products and the Specific Alkylnaphthalene OH Radical-initiated Reactions in which Observed.
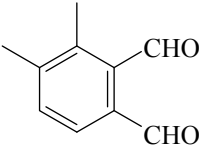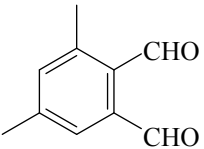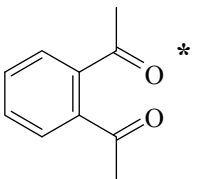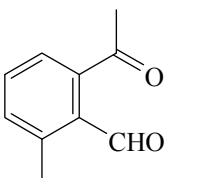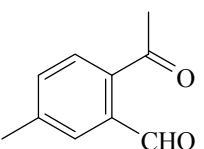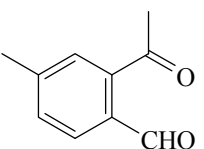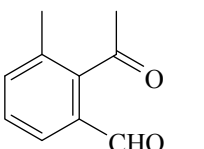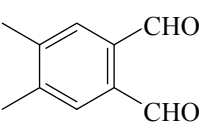
Structure	M.W.[a]	Base peak[b] and characteristic losses or ions	Naph	1MN	2MN	1EN	2EN	Dimethylnaphthalenes 1,2-	1,3-	1,4-	1,5-	1,6-	1,7-	1,8-	2,3-	2,6-	2,7-
(CHO, CHO)*	134	$[M-HCO]^+$ $[M-HC_2O_2]^+$	X		X		X								X		
(COCH₃, CHO)*	148	$[M-COCH_3]^+$ $[M-CH_3]^+$		X				X	X								
(CH₃, CHO, CHO)	148	$[M-HCO]^+$ m/z 91 da		X								X	X				
(CH₃, CHO, CHO)	148	$[M-HCO]^+$ m/z 91 da			X											X	X
(COC₂H₅, CHO)	162	$[M-HCO]^+$ $[M-COC_2H_5]^+$				X											
(C₂H₅, CHO, CHO)	162	$[M-C_2H_5]^+$ $[M-HCO]^+$ m/z 91 da				X											
(C₂H₅, CHO, CHO)	162	$[M-HCO]^+$ m/z 91 da					X										

*Structure was confirmed by comparison of GC/MS retention time and EI mass spectrum with those of an authentic standard.

[a] Molecular weights were confirmed by GC/MS with isobutane CI analyses.

[b] The first ion listed in each case was the base peak in the EI mass spectrum.

52

Table 15b. Suggested Structures of $C_{2\beta\text{-loss}}$-Dicarbonyl Products of M.W. 162 Formed from OH Radical-initiated Reactions of Dimethylnaphthalenes.

Structure	M.W.[a]	Base peak[b] and characteristic losses or ions	Dimethylnaphthalenes									
			1,2-	1,3-	1,4-	1,5-	1,6-	1,7-	1,8-	2,3-	2,6-	2,7-
dimethyl-benzene with CHO, CHO	162	$[M-HCO]^+$ m/z 91 da	X									
dimethyl-benzene with CHO, CHO	162	$[M-HCO]^+$ m/z 91 da		X								
benzene with two COCH₃ (C(=O)CH₃) groups *	162	$[M-CH_3]^+$			X							
benzene with COCH₃, CHO, methyl	162	$[M-COCH_3]^+$ m/z 91 da				X						
benzene with COCH₃, CHO, methyl	162	$[M-COCH_3]^+$ m/z 91 da					X					
benzene with COCH₃, CHO, methyl	162	$[M-COCH_3]^+$ m/z 91 da						X				
benzene with methyl, COCH₃, CHO	162	$[M-COCH_3]^+$ $[M-CH_3]^+$ m/z 91 da							X			
dimethyl-benzene with CHO, CHO	162	$[M-HCO]^+$ m/z 91 da								X		

*Structure was confirmed by comparison of GC/MS retention time and EI mass spectrum with those of an authentic standard.

[a]Molecular weights were confirmed by GC/MS with isobutane CI analyses.

[b]The first ion listed in each case was the base peak in the EI mass spectrum.

branching ratios of 0.8 for *ortho* OH radical addition and 0.2 for *ipso* addition (Fan and Zhang, 2006).

Loss of the acetyl fragment next to the double bond gives the base peak, $[M-COCH_3]^+$ in the proposed structures for 2-MN, the smaller product shown from 1,3-; 1,6-; and 1,7- DMNs, and from 2,3-; 2,6- (largest product); and 2,7-DMN (largest product). Each of these spectra also shows an $[M-HCO]^+$ ion consistent with an aldehyde group directly attached to the ring. The major 2-EN product shows a corresponding base ion, $[M-COC_2H_5]^+$, and $[M-HCO]^+$ fragment ions.

The minor product from 1,3-DMN is attributed to OH addition *ortho* to the methyl on C_3 and again breakage of a C_α-C_β carbon bond (see Table 13). For 2,6- and 2,7-DMN, four significant m.w. 188 isomer peaks were observed from each reaction. The most abundant peaks are attributed to the *Z-* and *E-* isomers of the structure resulting from breaking the C_1-C_2 bond (see Table 13) and the two smaller peaks to the *Z- + E-* isomers from breaking the C_3-C_4 bond (after OH addition at C_3). Assuming no breakage of the C_2-C_3 bond is consistent with the m.w. 148 $C_{2\beta-loss}$-dicarbonyl products observed and the lack of m.w. 162 $C_{2\beta-loss}$-dicarbonyl products for 2,6- and 2,7-DMN (see Table 15b). The fragmentation observed for the smaller products from 2,6- and 2,7-DMN is consistent with that seen for 2-formylcinnamaldehyde (see Tables 14a and 14c). These products suggest that if there is a methyl group on a β-carbon the OH radical adds preferentially to the *ortho* position which is an α-carbon over the *ortho* position which is a β-carbon (see 2,6- and 2,7-DMN in Table 13).

GC/MS Analyses of $C_{2\beta-loss}$-Dicarbonyls. The lower m.w. dicarbonyl products whose relative abundances are given in Table 12 are shown in Figures 8, 10, and 11, and Tables 15a and 15b list their structures, molecular weights and diagnostic EI fragmentations. These $C_{2\beta-loss}$-dicarbonyl products and their relative abundances can be rationalized based on OH radical addition occurring preferentially on the substituted ring and only loss of β-carbons (and their attached alkyl substituents). GC/MS analyses matching the retention times and mass spectra with those of authentic standards confirmed the formation of phthaldialdehyde from naphthalene, 2-MN, 2-EN and 2,3-DMN (see Figure 8 and Table 15a), 2-acetylbenzaldehyde as the m.w. 148 species from 1,2- and 1,3-DMN and as the most abundant of two m.w. 148 species from 1-MN (see Figure 10), and 1,2-diacetylbenzene from 1,4-DMN (see Figure 11). The base peak in the EI mass spectrum of 2-acetylbenzaldehyde at m/z 105 da results from characteristic fragmentation by loss of the acetyl group, $[M-COCH_3]^+$.

The smaller m.w. 148 product from 1-MN matched in retention time and spectrum with the m.w. 148 species from 1,6-DMN and 1,7-DMN and is attributed to 3-methylphthal-dialdehyde (2-formyl-3-methylbenzaldehyde) (see Figure 10). The EI spectrum of a phthaldialdehyde (2-formylbenzaldehyde) standard showed a loss of the aldehyde group, $[M-HCO]^+$, and this fragmentation, taken to be characteristic of an aldehyde group attached to the aromatic ring, is observed in the smaller m.w. 148 product from 1-MN, as well as many other decomposition products (see Tables 15a and 15b). A characteristic m/z 91 da ion fragment in this product is consistent with the presence of a methyl group on the aromatic ring (McLafferty and Turecek, 1993). Analogous fragmentation was seen for the m.w. 148 compound formed from 2-MN, 2,6-DMN and 2,7-DMN, which as shown on Figure 10 is attributed to 4-methylphthaldialdehyde (2-formyl-4-methylbenzaldehyde).

As noted above, 1,2-diacetylbenzene was confirmed as a product from 1,4-DMN and consistent with breakage of the C_1-C_2 bond and formation of an acetyl group and loss of two β-carbons, spectra of the m.w. 162 species from 1,5-; 1,6;, 1,7; and 1,8-DMN have base peaks at

m/z 119 da, $[M\text{-}COCH_3]^+$ (see Figure 11 and Table 15b). Analogous to the m.w. 148 products from 1-MN, 1-EN gave two products resulting from the loss of the β-carbons from each ring, with the most abundant isomer showing a characteristic ion, $[M\text{-}COC_2H_5]^+$, attributed to 1-(2-carbonylphenyl)propan-1-one formed from the substituted ring (see Figure 11). For 2-EN and 1,2-; 1,3-; and 2,3-DMN, where the small yield of m.w. 162 products must result from reaction on the unsubstituted ring (see lower part of Figure 11), the base peak in the spectra is at m/z 133 da resulting from the loss of the formyl group (see Tables 15a and 15b). Consistent with only β-carbons and their associated alkylsubstituents being lost, no m.w. 162 dicarbonyl products were observed from 2,6- and 2,7-DMN.

     Other Products. In addition to the three main classes of products discussed above, namely C_{all}- and $C_{2\beta\text{-loss}}$-dicarbonyls and the tentatively identified epoxy-carbonyls, the SPME-GC/MS analyses showed spectra consistent with carboxaldehydes, such as 3-methyl-2-naphthalenecarboxaldehyde from 2,3-DMN, presumably the result of H-atom abstraction from an alkyl group on the parent compounds. Consistent with the expectation that the OH radical reaction will occur mainly by addition to the ring (Calvert *et al.*, 2002), these products were in low abundance, in agreement with the reported <5% yield of carboxaldehydes from the 1-MN and 2-MN reactions (Atkinson *et al.*, 1997). Consistent with reported naphthalene products (Sasaki *et al.*, 1997), small amounts of quinones were observed in the SPME-GC/MS analyses and large-volume samples analyzed by negative ion CI-GC/MS (unpublished data from this laboratory) have confirmed that dimethyl- and ethyl-nitronaphthalenes and hydroxyalkylnitronaphthalenes are also formed in low yields in these reactions.

     Anhydride Secondary Products. Another class of compound readily observed in the SPME-GC/MS analyses were anhydrides. Analogous to the naphthalene reaction, we assume the anhydrides are second-generation products. The identified, or tentatively identified, anhydride products are given in Table 16 together with their presumed precursors. Standards are available for phthalic anhydride and 4-methylphthalic anhydride and both gave a diagnostic fragment ion, $[M\text{-}CO_2]^+$, in their EI mass spectra which was used to identify other anhydrides. Our recent studies of the OH radical-initiated and photolysis reactions of phthaldialdehyde, 2-acetylbenzaldehyde and 1,2-diacetylbenzene show that these produce phthalic anhydride, phthalide and 3-methylphthalide (Wang *et al.*, 2006). Under our experimental conditions it is calculated that OH radical reaction of these carbonyls dominated over their photolysis (see Figure 7 and Table 10) giving phthalic anhydride, and this is consistent with phthalide and 3-methylphthalide [which are formed only from photolysis (Wang *et al.*, 2006)] not being observed. As seen from Table 16, phthalic anhydride is observed from the reaction of naphthalene, 2-MN, 2-EN and 2,3-DMN, with phthaldialdehyde the presumed precursor, and from the reaction of 1-MN, 1,2-DMN and 1,3-DMN, with 2-acetylbenzaldehyde the presumed precursor. Additionally, the phthalic anhydride observed from 1-EN suggests that 2-(propan-1-one)benzaldehyde also reacts with the OH radical to yield phthalic anhydride. The only alkylnaphthalene for which an anhydride could not be identified was 1,4-DMN where the precursor would be 1,2-diacetylbenzene, which has a rate constant for reaction with the OH radical at least an order of magnitude lower than phthaldialdehyde and 2-acetylbenzaldehyde (Wang *et al.*, 2006). As seen from Table 16, the corresponding methylphthalic anhydrides were observed from the methyl-substituted phthaldialdehydes and acetylbenzaldehydes. From 1- and 2-ethylphthaldialdehyde and 1,2- and 2,3-dimethylphthaldialdehyde, m.w. 176 anhydrides were formed from precursors resulting from the less-favored OH radical addition on the unsubstituted ring.

Table 16. Anhydride Secondary Products and Suggested Precursors in the OH Radical-Initiated Reactions of Naphthalene and Alkylnaphthalenes
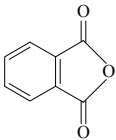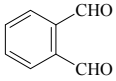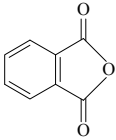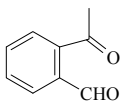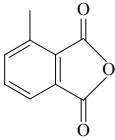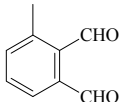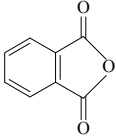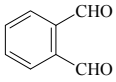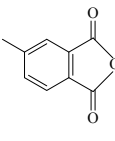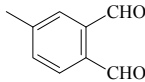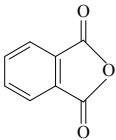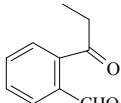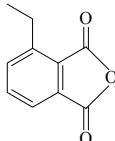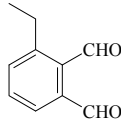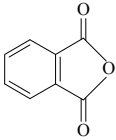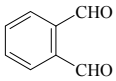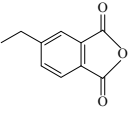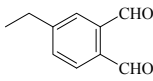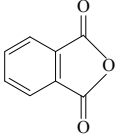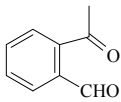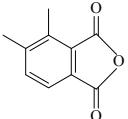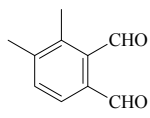
Parent	Phthalic Anhydride[a,b]	Precursor	Methyl-phthalic Anhydride[b,c]	Precursor	M.W. 176 Andydride[b]	Precursor
naphthalene						
1-MN	(1.0)		(0.5)			
2-MN	(1.0)		(0.3)			
1-EN	(1.0)				(0.4)	
2-EN	(1.0)				(0.3)	
1,2-DMN	(1.0)				(0.2)	

Table 16. (cont.) Anhydride Secondary Products and Suggested Precursors in the OH Radical-
Initiated Reactions of Naphthalene and Alkylnaphthalenes
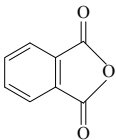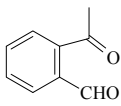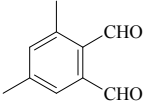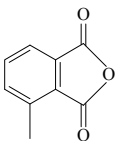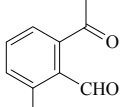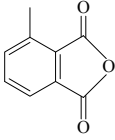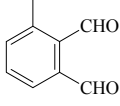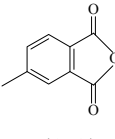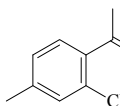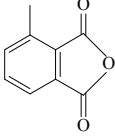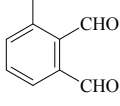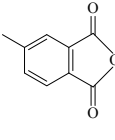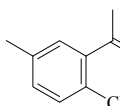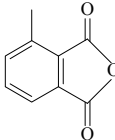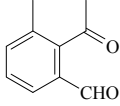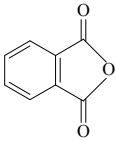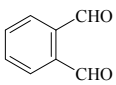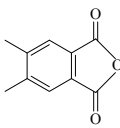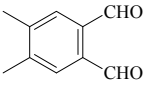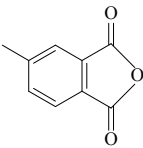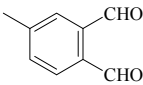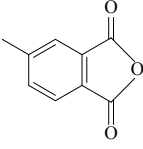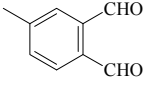
Parent	Phthalic Anhydride[a,b]	Precursor	Methyl-phthalic Anhydride[b,c]	Precursor	M.W. 176 Andydride[b]	Precursor
1,3-DMN	[structure]	[structure]			isomer not detected[d]	[structure]
1,5-DMN			[structure]	[structure]		
1,6-DMN			[structure] (1.0)	[structure]		
			[structure] (0.3)	[structure]		
1,7-DMN			[structure] (1.0)	[structure]		
			[structure] (0.4)	[structure]		
1,8-DMN			[structure]	[structure]		
2,3-DMN	[structure]	[structure] (1.0)			[structure] (0.1)	[structure]

57

Table 16. (cont.) Anhydride Secondary Products and Suggested Precursors in the OH Radical-Initiated Reactions of Naphthalene and Alkylnaphthalenes

Parent	Phthalic Anhydride[a,b]	Precursor	Methyl-phthalic Anhydride[b,c]	Precursor	M.W. 176 Andydride[b]	Precursor
2,6-DMN						
2,7-DMN						

[a]An authentic standard available for matching mass spectra and retention times.
[b]Numbers in parenthesis show relative amounts of the anhydrides for each reaction.
[c]An authentic standard of 4-methylphthalic anhydride (CH_3 group on an α-carbon) was available for matching mass spectra and retention times.
[d]No anhydride other than phthalic anhydride was detected.

Implications for Ambient Analyses. In the API-MS analyses we looked for phthalic acid formation since this compound has been proposed as a particle-associated marker for atmospheric reactions (Fine *et al.*, 2004). However, no evidence for phthalic acid formation was observed and, as we have suggested previously (Wang *et al.*, 2006), it is possible that hydrolysis on particles of phthalic anhydride and 4-methylphthalic anhydride may lead to the corresponding acids which have been observed in ambient particles and found to correlate with secondary organic aerosols (Fine *et al.*, 2004). If this is the case, our data suggest that other alkyl-substituted phthalic acids would also be present in ambient particle samples, and studies are needed which analyze both the anhydrides and the corresponding acids in ambient samples.

Clearly, further research is needed to unequivocally identify the ring-opened dicarbonyls formed from the alkylnaphthalenes and to confirm the postulated *ipso* addition of the OH radical on 1,2-DMN. Considering the relatively high ambient concentrations of naphthalene and the alkylnaphthalenes, the potential health risks of the polar oxygenated products from their OH radical-initiated reactions should be investigated.

D. Synthesis of Dimethylnitronaphthalenes/Ethylnitronaphthalenes

1. Introduction

Nitrated polycyclic aromatic hydrocarbons (nitro-PAHs) in ambient atmospheres are of concern because nitro-PAHs have been found to be mutagenic and carcinogenic (IARC, 1984; Tokiwa and Ohnishi, 1986; Gupta *et al.*, 1996; Durant *et al.*, 1996; Sasaki *et al.*, 1997; IPCS, 2003). Naphthalene and alkylnaphthalenes are generally the most abundant PAHs in ambient atmospheres (Arey *et al.*, 1987; Atkinson *et al.*, 1988; Arey *et al.*, 1989a; Arey *et al.*, 2004; Reisen and Arey, 2005) and their nitrated derivatives have been found to be the most abundant nitro-PAHs (Arey *et al.*, 1987; Atkinson *et al.*, 1988; Arey *et al.*, 1989a; Wilson *et al.*, 1995; Arey *et al.*, 2004; Reisen and Arey, 2005; Cecinato, 2003). Isomer-specific nitro-PAH analyses are required to assess ambient air toxicity (Gupta *et al.*, 1996) and knowledge of the specific nitro-isomers present in ambient samples can also provide information on their sources (Arey, 1998; Arey and Atkinson, 2003; Zielinska and Samy, 2006). Like PAHs, nitro-PAHs may be emitted from combustion sources (Paputa-Peck *et al.*, 1983), but the nitronaphthalenes and alkylnitronaphthalenes present in ambient air have been attributed largely to *in situ* atmospheric formation from gas-phase reaction of naphthalene and the alkylnaphthalenes with hydroxyl (OH) radicals and nitrate (NO_3) radicals (Zielinska *et al.*, 1989; Gupta *et al.*, 1996, Arey, 1998; Arey and Atkinson, 2003; Reisen *et al.*, 2003; Arey *et al.*, 2004; Reisen and Arey, 2005; Atkinson and Arey, 2007). The nitronaphthalenes (NNs) and methylnitronaphthalenes (MNNs) formed from these radical-initiated reactions have been identified (Zielinska *et al.*, 1989, Gupta, 1995; Bunce *et al.*, 1997; Sasaki *et al.*, 1997) and certain isomer profiles have been suggested as markers of daytime OH radical or nighttime NO_3 radical formation (Arey, 1998; Arey and Atkinson, 2003; Atkinson and Arey, 2007).

While the rate constants for the reactions of the dimethylnaphthalenes (DMNs) and ethylnaphthalenes (ENs) with OH and NO_3 radicals have been measured (Phousongphouang and Arey, 2002; 2003), isomer-specific dimethylnitronaphthalene (DMNN) and ethylnitronaphthalene (ENN) formation has not been reported, in part because of a lack of standards. Identification of nitro-PAHs in ambient samples generally relies on gas chromatography/mass spectrometry (GC/MS) analysis (Arey and Zielinska, 1989; Bamford *et al.*, 2003; Crimmins and Baker, 2006; Zielinska and Samy, 2006), most recently using negative ion chemical ionization where the lack of characteristic fragmentation makes reliance on GC retention information especially important (Bamford *et al.*, 2003; Reisen and Arey, 2005; Crimmins and Baker, 2006; Zielinska and Samy, 2006). To begin to address the lack of standards, we report here on the synthesis of mg, or sub-mg amounts, of the 42 DMNN and 14 ENN isomers, their electron impact (EI) mass spectra and their GC elution characteristics on a 5% phenylmethylpolysiloxane column.

2. Experimental Methods

N_2O_5 Nitration. Nitration with dinitrogen pentoxide (N_2O_5) in CCl_4 solution (Zielinska *et al.*, 1986; Gupta, 1995; Gallagher, 2006) was performed by adding dropwise ~150 mg N_2O_5 in 20 ml CCl_4 to a stirred solution of ~250 mg of parent alkylnaphthalene in 40 ml CCl_4. After 10 min stirring at room temperature, the reaction was considered complete. A small aliquot of the reaction mixture, eluted through a silica-containing Pasteur pipette to remove polar impurities

such as nitric acid, was analyzed by GC with flame ionization detection (FID) to monitor the extent of the nitration.

Fractionation and Identification. The reaction mixtures were concentrated by rotary-evaporation and placed on 10 gram Solid-Phase Extraction silica columns (SPE-Si; Supelco) pre-wetted with hexane. These columns readily separated the unreacted parent compound which eluted with 100 ml hexane and also provided some separation of the nitro-isomers. The 50-100 ml fractions were analyzed by GC-FID, combined where appropriate, and fractions containing isomer products ~70% or greater in purity were further purified by micro-scale recrystallization from reagent alcohol using a Craig tube.

^{1}H NMR and 2D gCOSY spectra were obtained from 1-3 mg solutions in CDCl$_3$ analyzed on a Varian Inova 400 MHz NMR instrument using the GLIDE program. NMR analyses were performed using the crystals obtained, SPE-Si fractions and in some cases the mother liquors from the recrystallizations. Spectra of each precursor alkylnaphthalene were also taken for reference.

Retention Indices. Linear retention indices were calculated using 1-nitronaphthalene and 9-nitrophenanthrene as the bracketing standards (Arey and Zielinska, 1989) and for chromatographic separation an HP-5ms capillary column (30 m x 0.25 mm; 0.25 μm phase) in an Agilent Technologies 6890N GC System interfaced to a 5975 inert XL Mass Selective Detector. The GC inlet temperature was 250 °C and the initial oven temperature was 40 °C, followed by ramping at 4 °C min^{-1}.

Ambient Analyses. Ambient air sampling was conducted at an Agricultural Operations site on the University of California, Riverside campus with a high-volume sampler modified with polyurethane foam (PUF) plugs beneath the filter. Sampling was conducted between 6 pm and 6 am local time at a flow rate of 0.56 m^3 min^{-1} yielding a ~400 m^3 sample. The sample was spiked with 1-nitronaphthalene-d$_7$, Soxhlet extracted and fractionated by high performance liquid chromatography (HPLC) as described previously (Reisen and Arey, 2005). The ambient sample was analyzed by GC/MS with negative ion methane chemical ionization (NCI) using the instrument and GC temperature program noted above for the RI measurements.

1-Nitronaphthalene was present in the ambient sample and 9-nitrophenanthrene was co-injected with the sample to allow the RI values of the ENNs and DMNNs in the ambient sample to be calculated.

Chemicals. The alkylnaphthalenes were purchased from Aldrich Chemical Company and their stated purities were: 1-EN (98+%), 2-EN (99+%), 1,2-DMN (98%), 1,3-DMN (96%), 1,4-DMN (95%), 1,5-DMN (98%), 1,6-DMN (99%), 1,7-DMN (99%), 1,8-DMN (95%), 2,3-DMN (98%), 2,6-DMN (99%) and 2,7-DMN (99%). The sources of other chemicals were: 1-nitronaphthalene, 1-nitronaphthalene-d$_7$, chloroform-d (99.8 atom % D), and CCl$_4$, Aldrich Chemical Company; 9-nitrophenanthrene (>99%), AccuStandard. N$_2$O$_5$ was prepared and stored under vacuum at liquid nitrogen temperatures as described previously (Atkinson *et al.*, 1984).

3. Results and Discussion

From a single parent DMN, ring nitration gives three or six DMNN isomers, and 7 ENN isomers can be formed from each ethylnaphthalene. For each alkylnaphthalene, all isomers were formed by the N$_2$O$_5$ nitration, although with widely differing yields. The HP-5ms capillary GC column used was able to resolve all the isomers from a single parent and, therefore, mass spectra and GC retention times of each isomer could readily be obtained. The electron impact (EI) mass

spectra of the 42 DMNN isomers are shown in Figures 12-19 and the EI spectra of the 14 ENN isomers in Figures 20 and 21. Their retention indices (RI) on the HP-5 column are listed in Table 17 and, estimating that a difference in RI value of 0.5 results in resolved peaks, almost half of the DMNN and ENN isomers cannot be resolved on this single GC column.

On non-polar columns such as the 5% phenylmethylpolysiloxane columns, 2-methylnaphthalene elutes before 1-methylnaphthalene and it was observed here that, with the exception of *ortho* or *peri* substituted DMNs, 2-alkyl-substituted isomers eluted before those with 1-alkyl-substitution and the elution order of the DMNs and ENs was: 2-EN, 1-EN, 2,6-DMN, 2,7-DMN, 1,7-DMN, 1,3-DMN, 1,6-DMN, 2,3-DMN, 1,4-DMN, 1,5-DMN, 1,2-DMN and 1,8-DMN. 1-Nitronaphthalene elutes before 2-nitronaphthalene, so in general, nitrating on an α-carbon increases the retention time less than nitration on a β-carbon. The steric interaction between nitro- and methyl- groups when they are *ortho* or *peri* to one another on the naphthalene ring influences their GC elution, their MS fragmentation and the NMR chemical shifts of the protons influenced by the NO_2 group. As a result, the 42 DMNN isomers can be discussed as six different isomer groups: DMNN isomers with NO_2 substitution on an α-carbon and no steric interaction with the methyl substituents (Figures 12 and 13), DMNN isomers with NO_2 and CH_3 substituents in *peri* positions (Figure 14), DMNN isomers with NO_2 substitution on an α-carbon and with an *ortho* CH_3 group (Figure 15), DMNN isomers with NO_2 substitution on a β-carbon and no steric interaction with the methyl substituents (Figures 16 and 17), DMNN isomers with NO_2 substitution on a β-carbon and with an *ortho* CH_3 group also on a β-carbon (Figure 18), and DMNN isomers with NO_2 substitution on a β-carbon and with an *ortho* CH_3 group on an α-carbon (Figure 19).

Dimethylnitronaphthalenes. Crystals of 14 DMNN isomers were obtained and NMR analyses of mixtures containing different proportions of the isomers (fractions from the SPE-Si column or in some cases the mother liquors from the microcrystallizations) allowed NMR identification of 32 of 42 DMNN isomers. As noted in Table 17, in many cases a single isomer from nitration of a given parent was formed in too low an amount to obtain an NMR and, therefore, was identified by elimination. It should be noted that it was important to take the presence of isomeric DMN and/or EN impurities in the starting materials into account when identifying the minor isomers formed. As noted, the location of the nitro group on either an α- or β-carbon and whether there is steric interaction with an *ortho* or *peri* alkyl group determines both the elution behavior and fragmentation pattern of the DMNNs and these were used to determine identification in those cases in which two isomer possibilities remained (see Table 17). The EI mass spectra and retention indices (Arey and Zielinska, 1989) and ^{1}H NMR spectra (Wells and Alcorn, 1963) have been reported for the 14 methylnitronaphthalenes and these were very informative in the identifications of the DMNNs and ENNs.

NO_2 Substitution on an α-Carbon and No Steric Interaction. The 10 DMNN isomers shown in Figures 12 and 13 have NO_2 substitution on an α-carbon and there is no steric interaction between the NO_2 and methyl groups. NMR spectra were obtained for all 10 of these isomers, which were formed in relatively high abundance. The addition of a methyl group to naphthalene causes a slight upfield shift of the protons in the position *ortho* to the methyl group (Gupta, 1995; Wells and Alcorn, 1963), while a proton in the *peri* position to a CH_3 group is shifted slightly downfield (Wells and Alcorn, 1963). Identification of the *peri* protons in 1,4-DMN was unambiguous and the downfield shift relative to naphthalene was 0.07 ppm for H-5 and H-8.
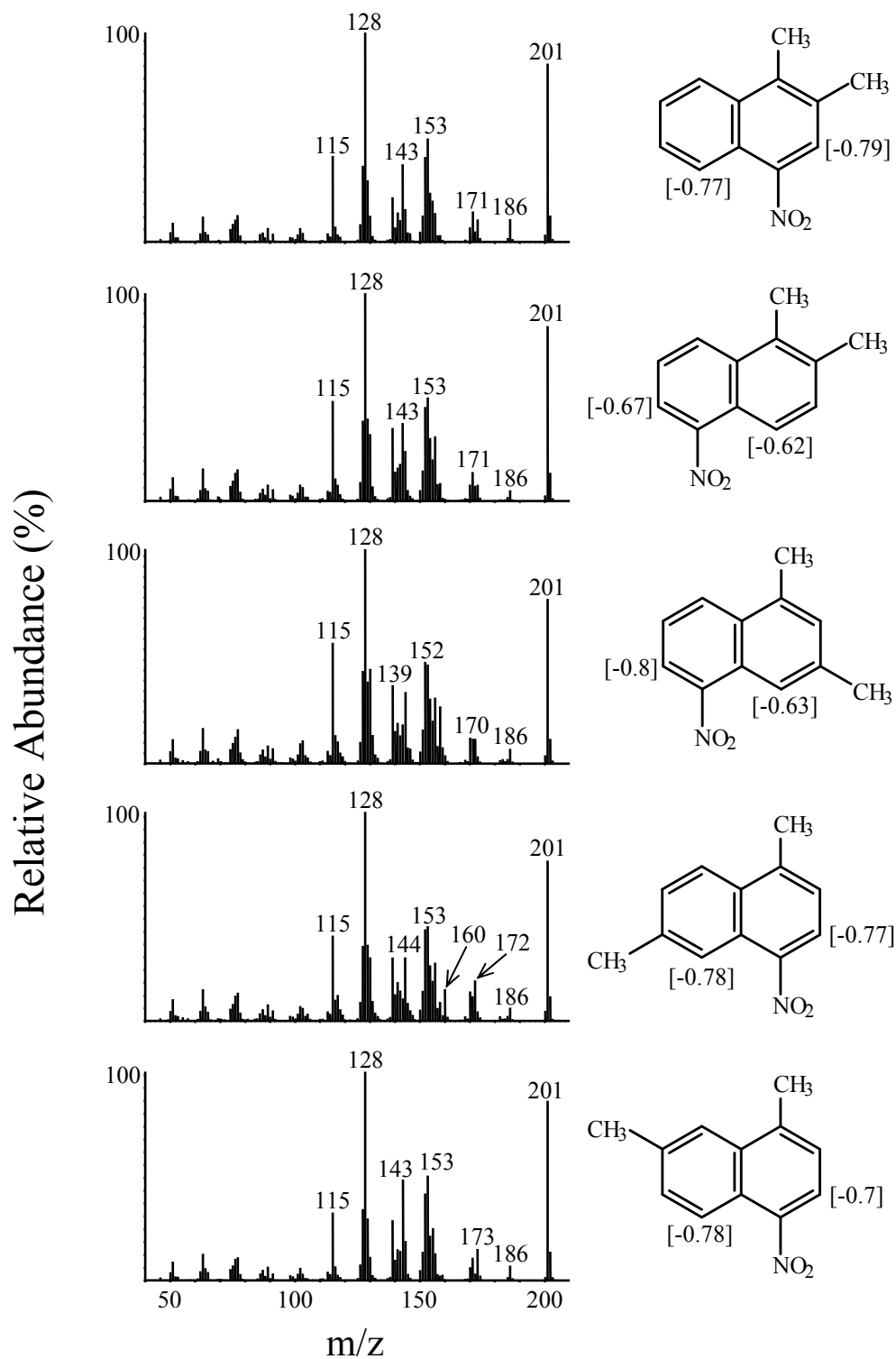
Figure 12. EI mass spectra of DMNN isomers with NO_2 substitution on an α-carbon and no steric interaction with the methyl substitutents (1,2-DM-4NN; 1,2-DM-5NN; 1,3-DM-5NN; 1,6-DM-4NN and 1,7-DM-4NN). The chemical shifts (relative to the parent DMN) of the protons adjacent to the NO_2 group are given in brackets.
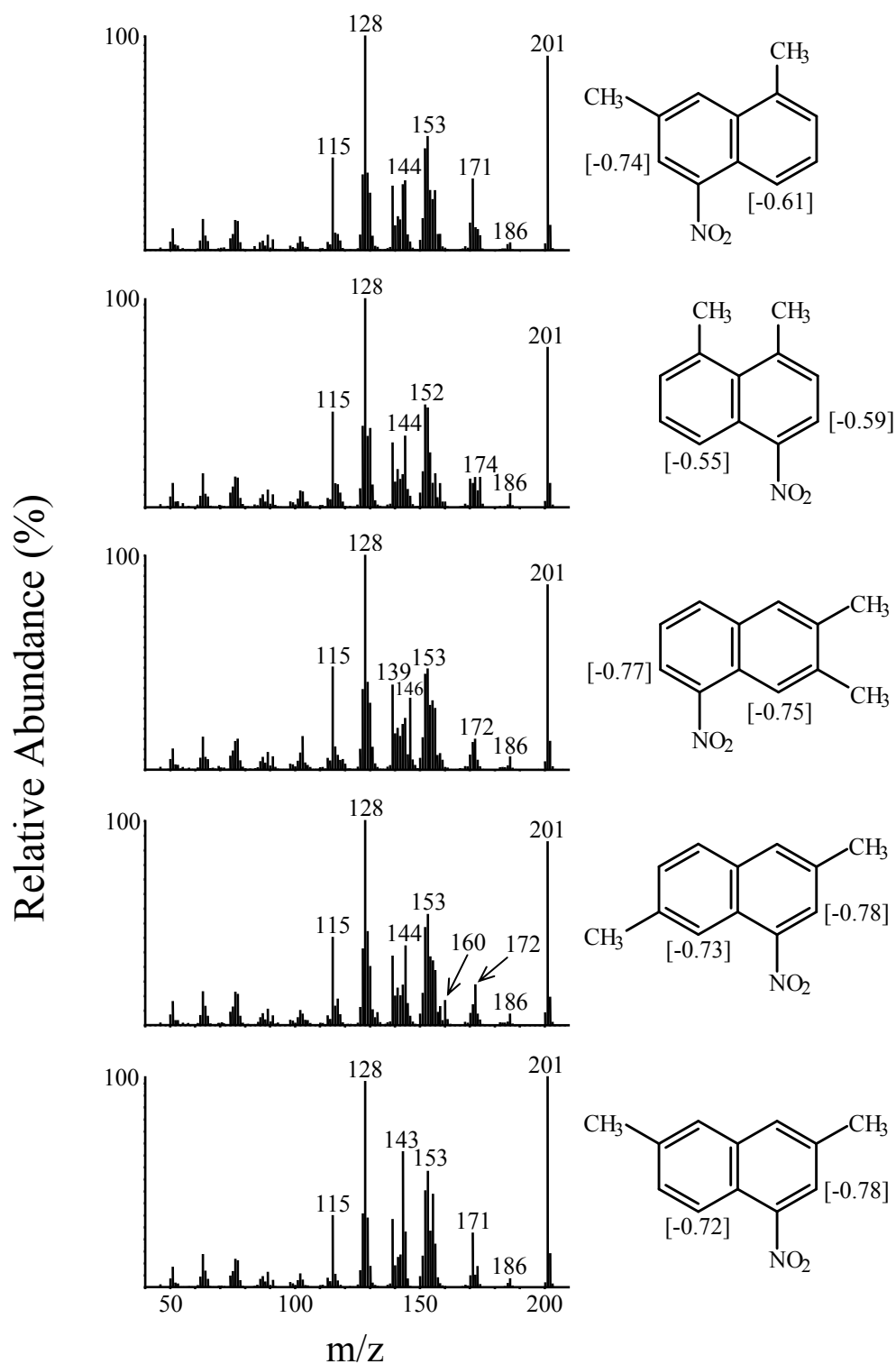
Figure 13. EI mass spectra of DMNN isomers with NO_2 on an α-carbon and no steric interaction with the methyl substitutents - continued (1,7-DM-5NN; 1,8-DM-4NN; 2,3-DM-5NN; 2,6-DM-4NN and 2,7-DM-4NN).
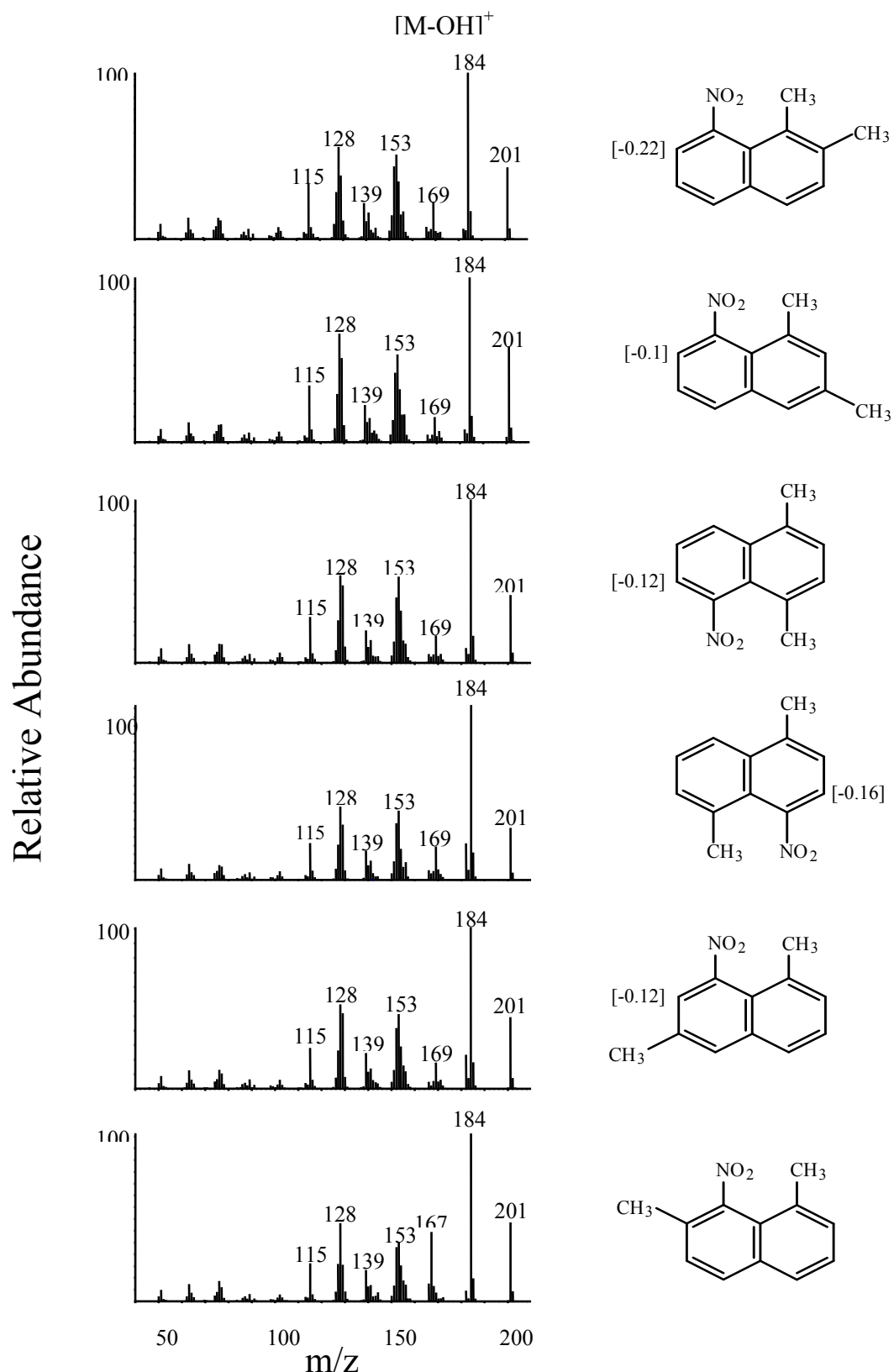
Figure 14.   EI mass spectra of DMNN isomers with NO$_2$ and CH$_3$ substituents in *peri* positions (1,2-DM-8NN; 1,3-DM-8NN; 1,4-DM-5NN; 1,5-DM-4NN; 1,6-DM-8NN and 1,7-DM-8NN), analogous to 1-M-8NN and 1-E-8NN. Note that 1,2-DM-8NN elutes 1st of the six 1,2-DMNN isomers; 1,3-DM-8NN elutes 3rd of the six 1,3-DMNN isomers after 1,3-DM-2NN (Figure 18) and 1,3-DM-4NN (Figure 15); 1,4-DM-5NN elutes 1st of the three 1,4-DMNN isomers; 1,5-DM-4NN elutes 1st of the three 1,5-DMNN isomers; 1,6-DM-8NN elutes 2nd of the six 1,6-DMNN isomers after 1,6-DM-5NN (Figure 15) and 1,7-DM-8NN elutes 1st of the six 1,7-DMNN isomers. The chemical shift (relative to the parent DMN) of the proton adjacent to the NO$_2$ group is given in brackets.

64
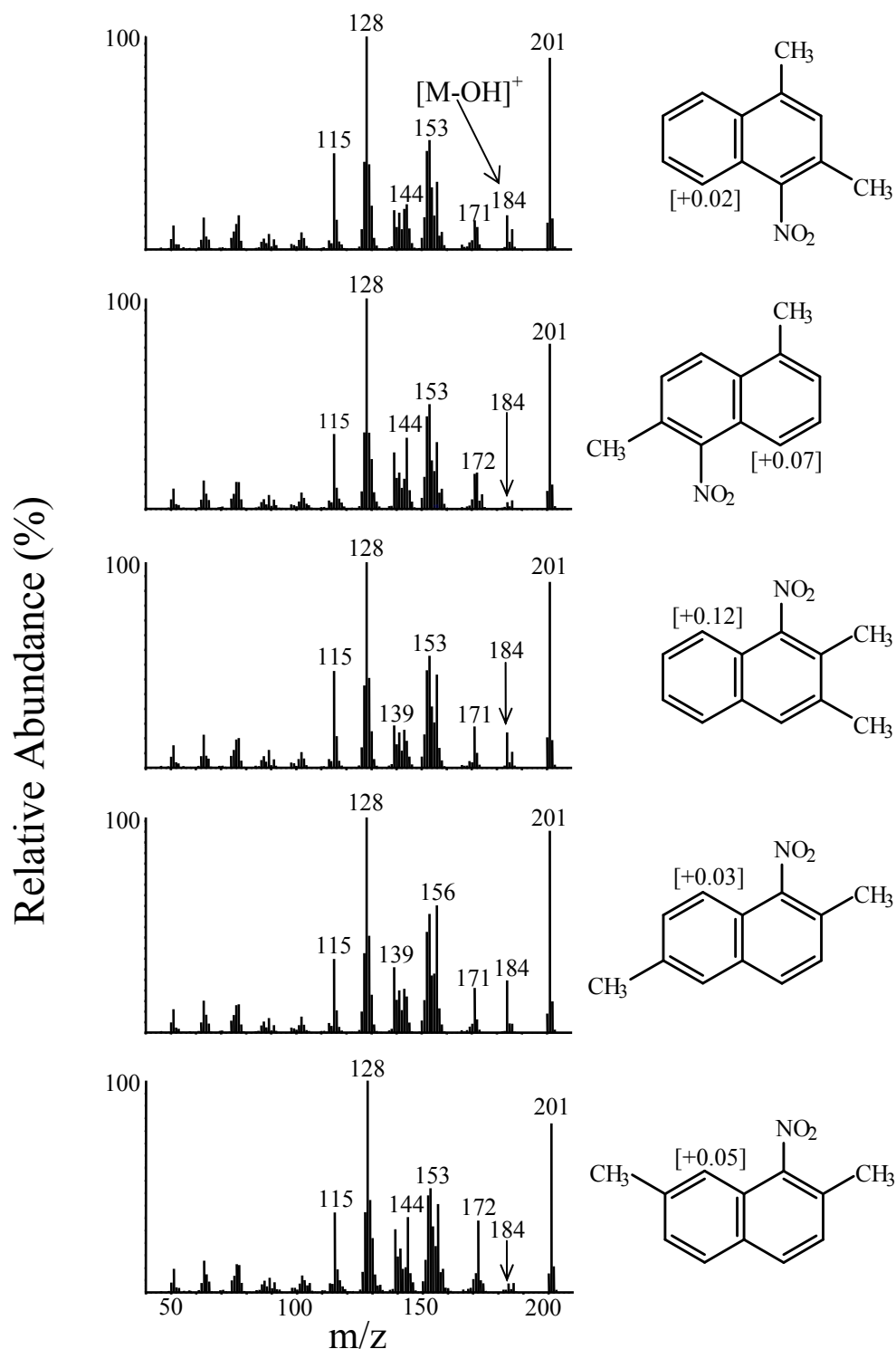
Figure 15. EI mass spectra of DMNN isomers with NO_2 substitution on an α-carbon and with an *ortho* CH_3 group (1,3-DM-4NN; 1,6-DM-5NN; 2,3-DM-1NN; 2,6-DM-1NN and 2,7-DM-1NN), analogous to 2-M-1NN and 2-E-1NN. Note that 1,3-DM-4NN elutes 2nd of the six 1,3-DMNN isomers after 1,3-DM-2NN (Figure 18); 1,6-DM-5NN elutes 1st of the six 1,6-DMNN isomers; 2,3-DM-1NN elutes 1st of the three 2,3-DMNN isomers; 2,6-DM-1NN elutes 1st of the three 2,6-DMNN isomers and 2,7-DM-1NN elutes 1st of the three 2,7-DMNN isomers. The upfield chemical shift (relative to the parent DMN) of the proton *peri* to the NO_2 group is given in brackets.
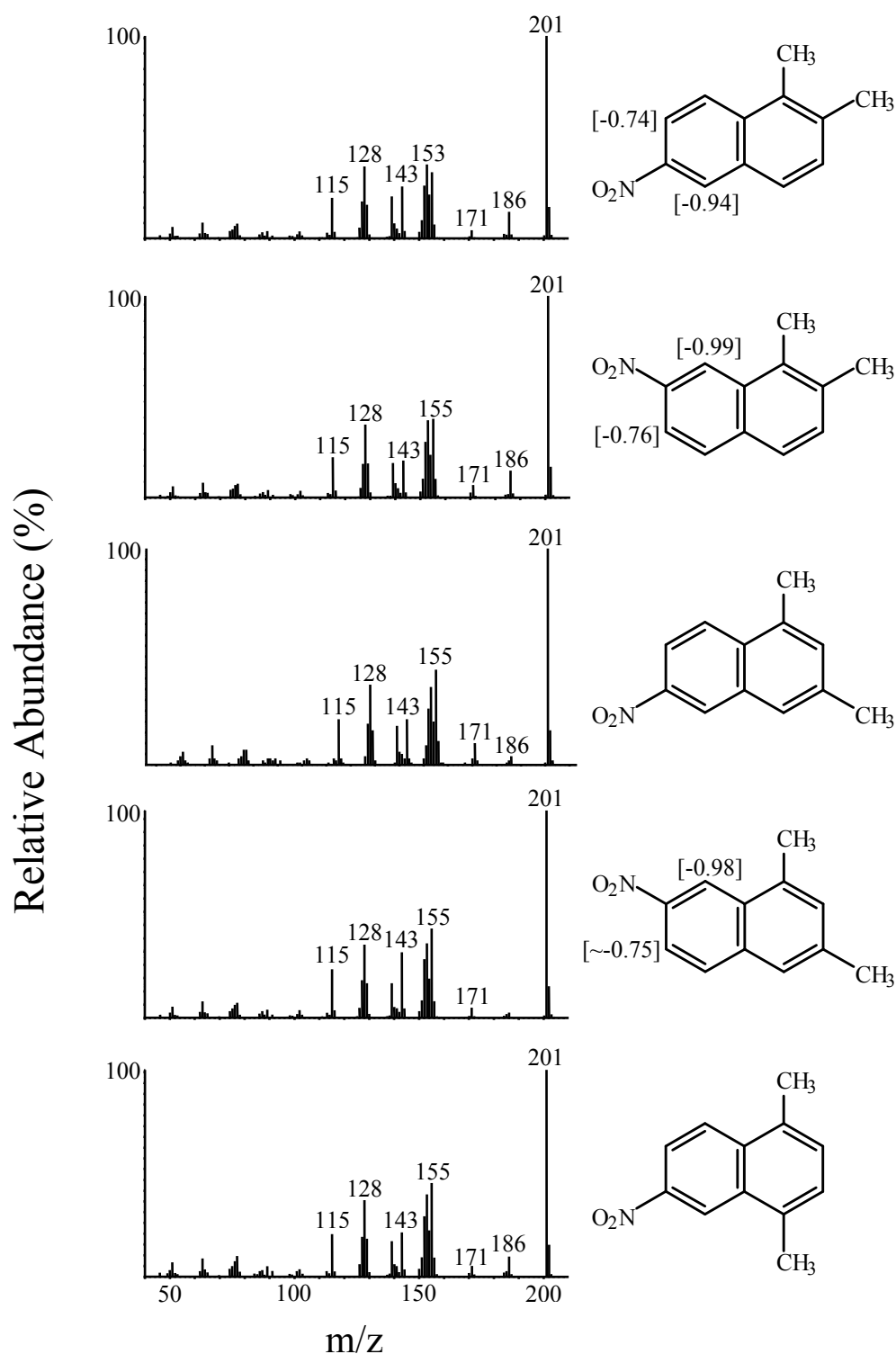
Figure 16. EI mass spectra of DMNN isomers with NO_2 substitution on a β-carbon and no steric interaction with the methyl substitutents (1,2-DM-6NN; 1,2-DM-7NN; 1,3-DM-6NN; 1,3-DM-7NN and 1,4-DM-6NN). Note that 1,2-DM-6NN and 1,2-DM-7NN elute 6th and 5th, respectively, of the six 1,2-DMNN isomers; 1,3-DM-6NN and 1,3-DM-7NN elute 6th and 5th, respectively, of the six 1,3-DMNN isomers and 1,4-DM-6NN elutes last of the three 1,4-DMNN isomers. The chemical shifts (relative to the parent DMN) of the protons adjacent to the NO_2 group are given in brackets.
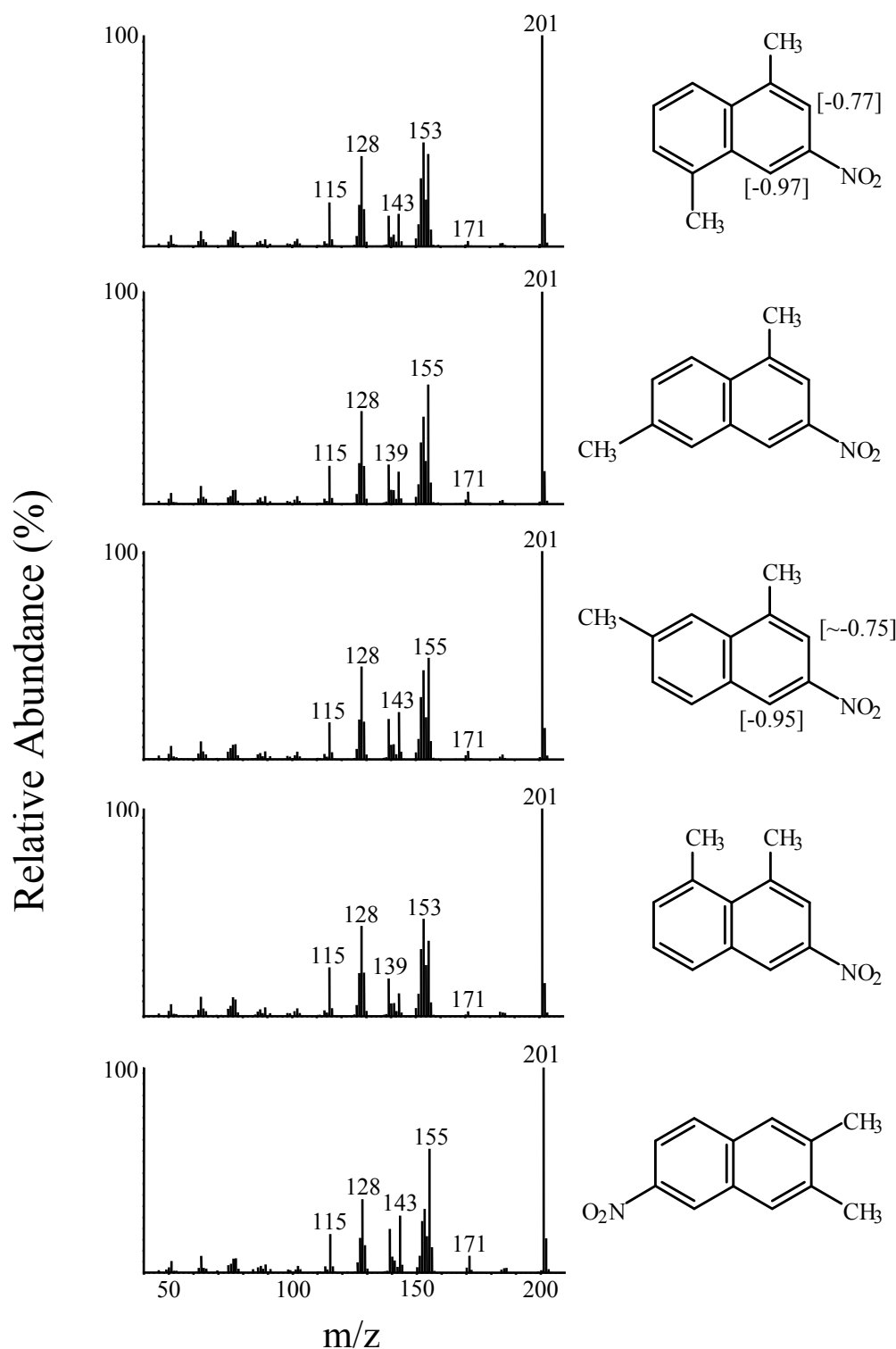
Figure 17. EI mass spectra of DMNN isomers with NO_2 substitution on a β-carbon and no steric interaction with the methyl substitutents – continued (1,5-DM-3NN; 1,6-DM-3NN; 1,7-DM-3NN; 1,8-DM-3NN and 2,3-DM-6NN). Note that 1,5-DM-3NN elutes last of the three 1,5-DMNN isomers; 1,6-DM-3NN elutes last of the six 1,6-DMNN isomers; 1,7-DM-3NN elutes last of the six 1,7-DMNN isomers; 1,8-DM-3NN elutes last of the three 1,8-DMNN isomers and 2,3-DM-6NN elutes last of the three 2,3-DMNN isomers.

67
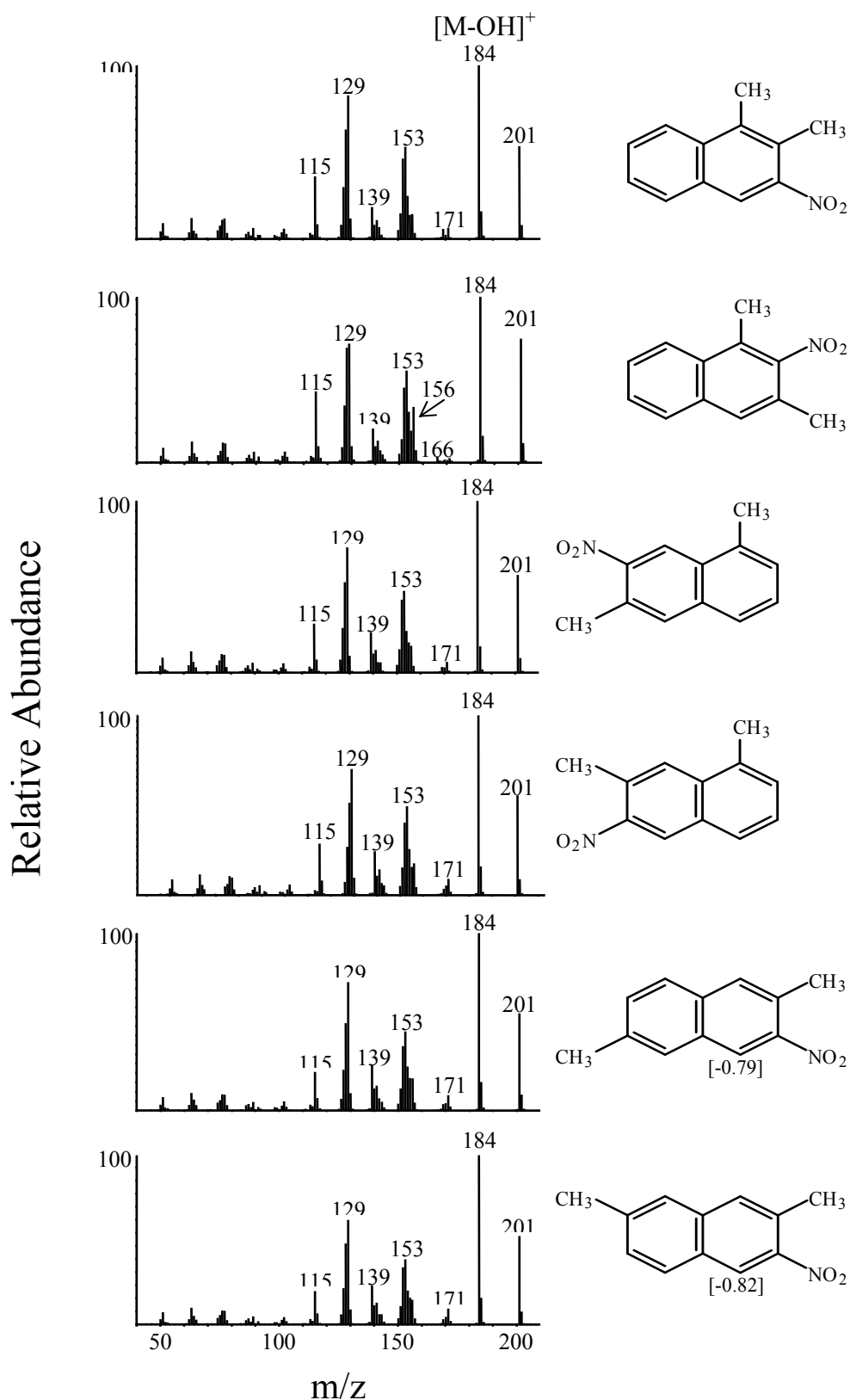
Figure 18. EI mass spectra of DMNN isomers with NO$_2$ substitution on a β-carbon and with an *ortho* CH$_3$ group also on a β-carbon (1,2-DM-3NN; 1,3-DM-2NN; 1,6-DM-7NN; 1,7-DM-6NN; 2,6-DM-3NN and 2,7-DM-3NN), analogous to 2-M-3NN and 2-E-3NN. Note that 1,3-DM-2NN elutes 1st of the six 1,3-DMNN isomers. The chemical shift (relative to the parent DMN) of the proton adjacent to the NO$_2$ group is given in brackets

68
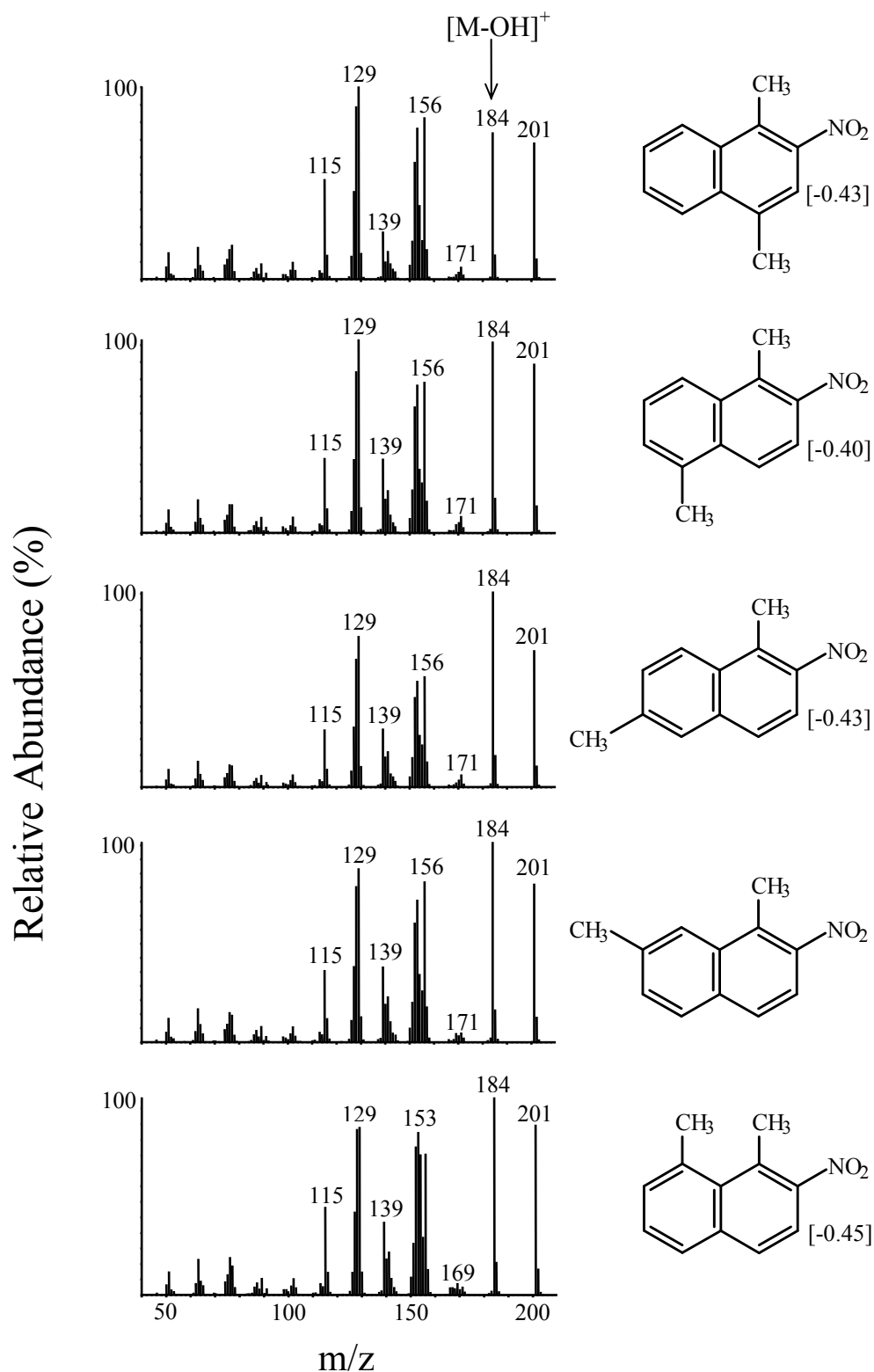
Figure 19. EI mass spectra of DMNN isomers with NO_2 substitution on a β-carbon and with an *ortho* CH_3 group on an α-carbon (1,4-DM-2NN; 1,5-DM-2NN; 1,6-DM-2NN; 1,7-DM-2NN and 1,8-DM-2NN), analogous to 1-M-2NN and 1-E-2NN. The chemical shift (relative to the parent DMN) of the proton adjacent to the NO_2 group is given in brackets.

69
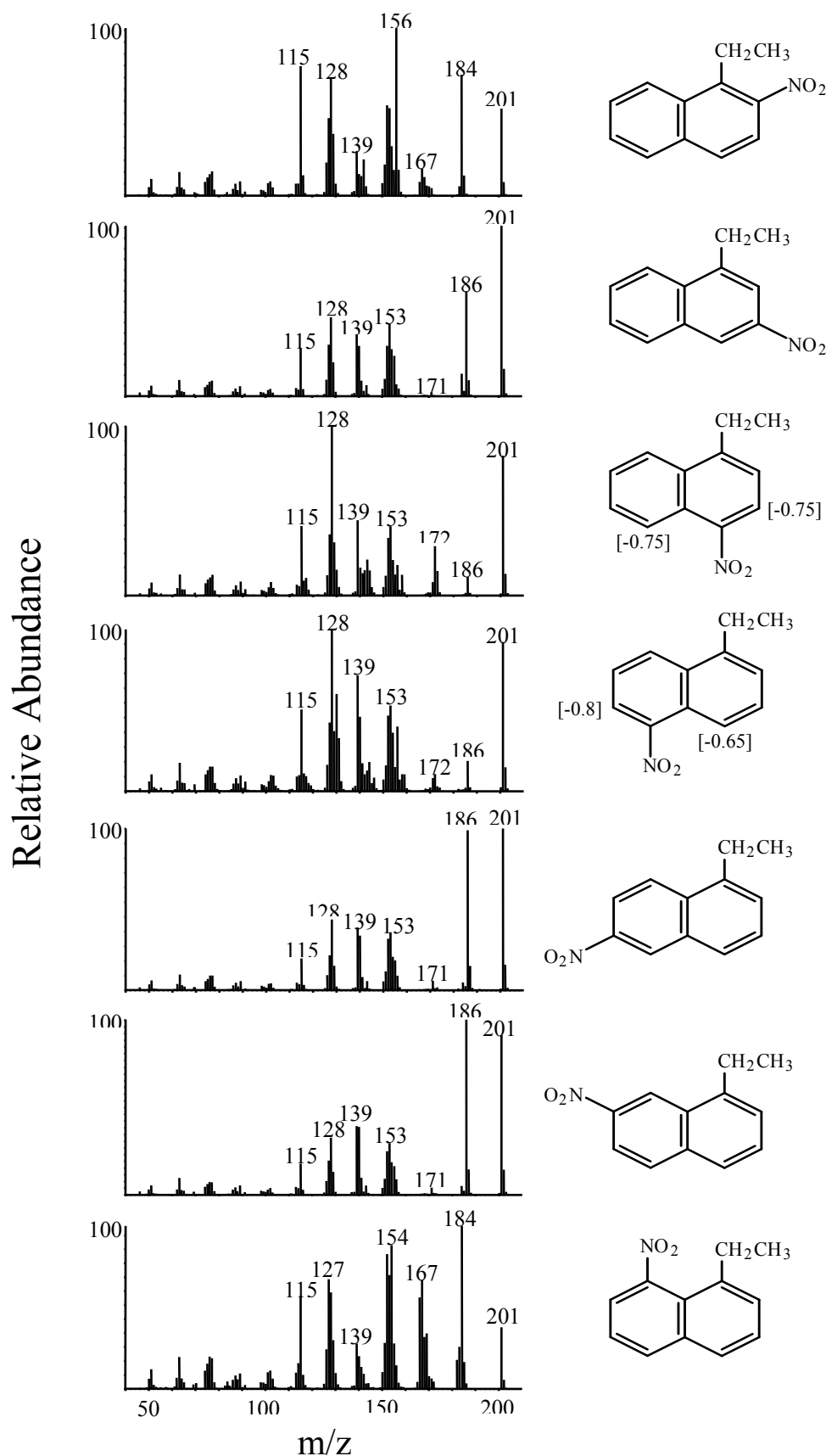
Figure 20. EI mass spectra of the seven 1-ethylnitronaphthalene isomers (1-E-2NN; 1-E-3NN; 1-E-4NN; 1-E-5NN; 1-E-6NN, 1-E-7NN and 1-E-8NN). Note the [M-OH]⁺ fragments in 1-E-2NN and 1-E-8NN. The assignments among the 1-E-3NN, 1-E-6NN and 1-E-7NN isomers should be viewed as tentative. The chemical shifts relative to 1-ethyl-naphthalene are given in brackets.
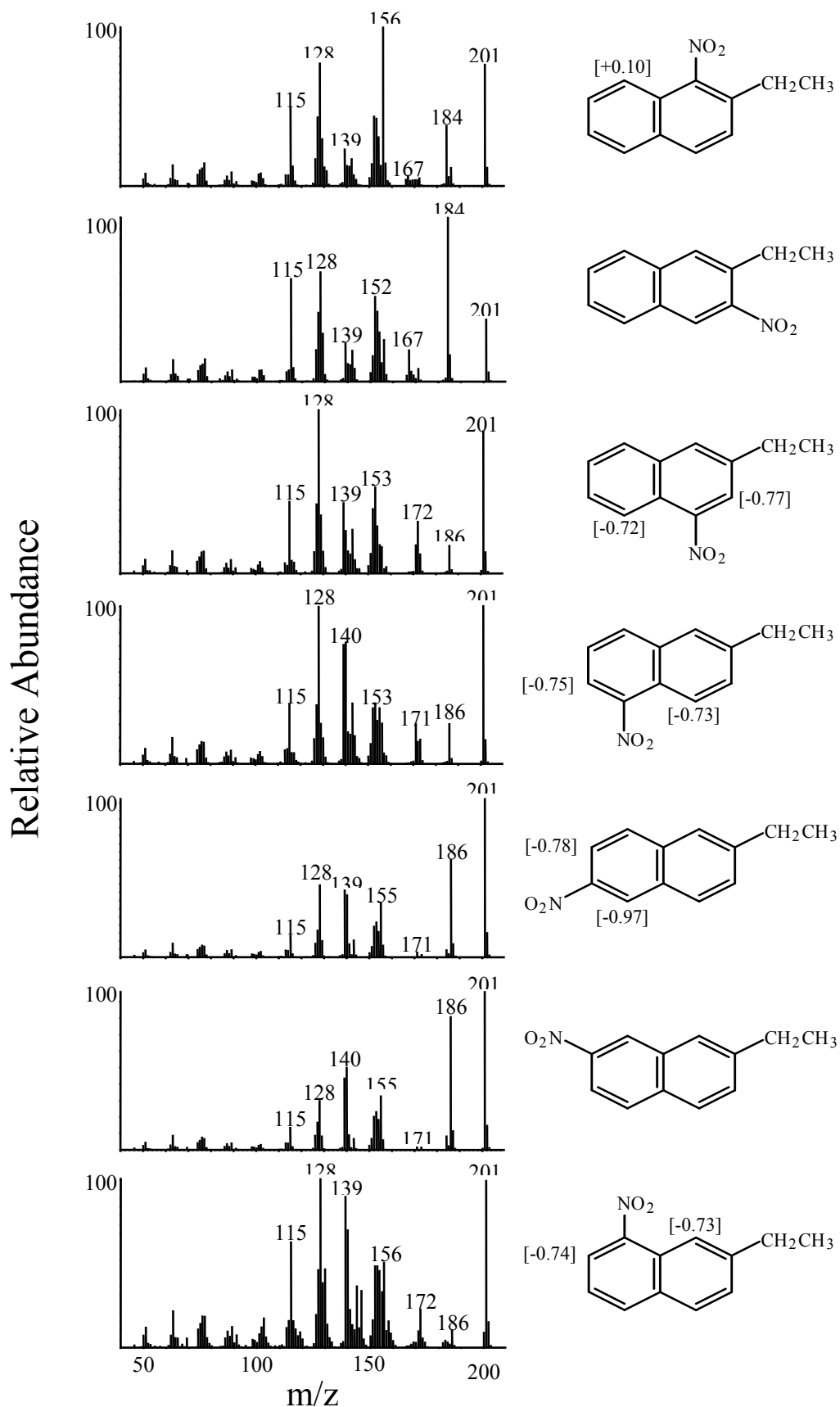
Figure 21. EI mass spectra of the seven 2-ethylnitronaphthalene isomers (2-E-1NN; 2-E-3NN; 2-E-4NN; 2-E-5NN; 2-E-6NN; 2-E-7NN and 2-E-8NN). Note the $[M-OH]^+$ fragments in 2-E-1NN and 2-E-3NN. The chemical shifts relative to 2-ethyl-naphthalene are given in brackets.

Table 17. Linear Retention Indices (RI) for Ethylnitronaphthalenes and
Dimethylnitronaphthalenes on a (5% Phenyl)-methylpolysiloxane (HP-5ms) Capillary
Column and Basis for Isomer Identification.

Compound	RI[a]	Identification Method
1-Nitronaphthalene	200.0	Standard
2-E-1NN	219.3	^{1}H NMR
1,7-DM-8NN	223.2	^{1}H NMR
2,7-DM-1NN	224.4	^{1}H NMR
1-E-8NN	226.2	2 out of 7 identified by NMR[b]
2,6-DM-1NN	226.4	^{1}H NMR
1,3-DM-2NN	226.9	4 out of 6 identified by NMR[c]
1-E-2NN	229.4	2 out of 7 identified by NMR[b]
1,6-DM-5NN	230.1	^{1}H NMR
1,3-DM-4NN	231.2	^{1}H NMR
1,6-DM-8NN	231.9	^{1}H NMR
2,3-DM-1NN	232.1	^{1}H NMR
2-E-3NN	232.2	5 out of 7 identified by NMR[d]
1,3-DM-8NN	232.3	^{1}H NMR
2-E-8NN	235.2	^{1}H NMR
2-E-4NN	237.0	^{1}H NMR
1,4-DM-5NN	237.0	^{1}H NMR
1,2-DM-8NN	239.0	^{1}H NMR
2,6-DM-4NN	239.1	^{1}H NMR
1,5-DM-4NN	239.3	^{1}H NMR
2-E-5NN	239.4	^{1}H NMR
1-E-5NN	239.6	^{1}H NMR
1,6-DM-7NN	239.8	4 out of 6 identified by NMR[e]
1-E-6NN	240.5	tentative[b,f]
2,6-DM-3NN	240.6	^{1}H NMR
2,7-DM-4NN	241.2	^{1}H NMR
1,7-DM-2NN	241.2	4 out of 6 identified by NMR[g]
2,7-DM-3NN	241.8	^{1}H NMR
1,7-DM-6NN	242.0	4 out of 6 identified by NMR[g]
1,3-DM-5NN	242.8	^{1}H NMR
1-E-4NN	242.8	^{1}H NMR
1,7-DM-5NN	243.0	^{1}H NMR
1,6-DM-2NN	243.5	^{1}H NMR
1,4-DM-2NN	245.1	^{1}H NMR
1,5-DM-2NN	245.4	^{1}H NMR
1-E-3NN	245.9	tentative[b,f]
1,6-DM-4NN	246.4	^{1}H NMR
2-E-7NN	246.5	5 out of 7 identified by NMR[d]
1-E-7NN	246.5	tentative[b,f]
2,3-DM-5NN	246.7	^{1}H NMR
1,7-DM-4NN	247.3	^{1}H NMR
1,2-DM-3NN	247.4	5 out of 6 identified by NMR[h]
1,8-DM-2NN	247.5	^{1}H NMR

2-E-6NN	248.1	^{1}H NMR
1,3-DM-7NN	249.2	^{1}H NMR
1,4-DM-6NN	250.7	2 out of 3 identified by NMR[i]
1,2-DM-5NN	251.5	^{1}H NMR
1,3-DM-6NN	251.6	4 out of 6 identified by NMR[c]
1,5-DM-3NN	251.9	^{1}H NMR
1,6-DM-3NN	252.6	4 out of 6 identified by NMR[e]
1,7-DM-3NN	253.2	^{1}H NMR
1,2-DM-4NN	253.7	^{1}H NMR
1,2-DM-7NN	254.7	^{1}H NMR
1,8-DM-4NN	256.2	^{1}H NMR
2,3-DM-6NN	257.5	2 out of 3 identified by NMR[J]
1,2-DM-6NN	259.9	^{1}H NMR
1,8-DM-3NN	261.9	2 out of 3 identified by NMR[k]
9-Nitrophenanthrene	300.0	Standard

[a]RI measured on a 30 m HP-5ms column (0.25 mm i.d., 0.25 μm phase) using a linear temperature program (26). RI = 200.0 for 1-nitronaphthalene; RI = 300.0 for 9-nitrophenanthrene. For each isomer: RI = 200 + [100 (retention time of compound – retention time of 1-NN)/(retention time of 9-nitrophenanthrene – retention time of 1-NN)].

[b]NMR spectra were obtained only for 1-E-4NN and 1-E-5NN. 1-E-2NN and 1-E-8NN show the characteristic [M-OH]$^+$ fragment of *ortho* and *peri* substituted NO_2 and alkyl groups. By analogy with the 1-MNN isomers (Arey and Zielinska, 1989), 1-E-8NN was assigned as the 1st eluting and 1-E-2NN as the 2nd eluting of the 1-ENN isomers.

[c]After NMR identification of four 1,3-DMN isomers, 1,3-DM-2NN and 1,3-DM-6NN remained. The identity of 1,3-DM-2NN was confirmed by its early elution and its large [M-OH]$^+$ fragment ion characteristic of DMNN isomers with NO_2 substitution on a β-carbon and with an *ortho* CH_3 group also on a β-carbon (see Figure 18). This isomer can also be considered as a DMNN with NO_2 substitution on a β-carbon and with an *ortho* CH_3 group on an α-carbon as in Figure 19. Note that it has a more abundant m/z 156 fragment than the other spectra in Figure 18, but less than those in Figure 19. The identity of 1,3-DM-6NN was confirmed by its elution last of the 6 isomers and its EI spectrum characteristic of NO_2 substitution on a β-carbon with no steric interaction (see Figure 16). Distinguishing the NMR of 1,3-DM-6NN (which was too weak to find most protons with the exception of the most downfield proton) from the more abundant isomer identified as 1,3-DM-7NN was based on assuming that H8 in 1,3-DM-7NN will be more downfield than H5 in 1,3-DM-6NN because H8 is more downfield in 1,3-DMN (Gallagher, 2006).

[d]After NMR identification of five 2-ENN isomers, 2-E-3NN and 2-E-7NN remained. 2-E-3NN was confirmed by its large [M-OH]$^+$ fragment ion characteristic of isomers with NO_2 substitution on a β-carbon and with an *ortho* alkyl group also on a β-carbon (see Figure 21). 2-E-7NN (with NO_2 substitution of a β-carbon and no steric interaction) was confirmed by its molecular ion base peak (analogous to the DMNNs in Figures 16 and 17). Distinguishing the NMR of 2-E-7NN

(which was too weak to find most protons with the exception of the most downfield proton) from the more abundant isomer identified as 2-E-6NN was based on analogy with 2-M-6NN and 2-M-7NN (23) and, therefore, assuming that H5 in 2-E-6NN is downfield of H8 in 2-E-7NN.

[e]After NMR identification of four 1,6-DMN isomers, 1,6-DM-7NN and 1,6-DM-3NN remained. The identity of 1,6-DM-7NN was confirmed by its large $[M-OH]^+$ fragment ion characteristic of DMNN isomers with NO_2 substitution on a β-carbon and with an *ortho* CH_3 group also on a β-carbon (see Figure 18). The identity of 1,6-DM-3NN was confirmed by its elution last of the 6 isomers and its EI spectrum characteristic of NO_2 substitution on a β-carbon with no steric interaction (see Figure 17).

[f]The isomers identified as 1-E-6NN, 1-E-3-NN and 1-E-7NN could not be unequivocally distinguished. It is also possible that the isomers previously identified as 1-M-6NN and 1-M-7NN (Zielinska *et al.*, 1989; Arey and Zielinska, 1989; Gupta, 1995) are in fact reversed.

[g]After NMR identification of four 1,7-DMN isomers, 1,7-DM-2NN and 1,7-DM-6NN remained. Both have base peaks of $[M-OH]^+$. The isomers were assigned on the basis of the $[M-NO-CH_3]^+$ fragment ion at m/z 156 in 1,7-DM-2NN; this fragment is characteristic of DMNN isomers with NO_2 substitution on a β-carbon and with an *ortho* CH_3 group on an α-carbon (see Figure 19). The spectrum identified as 1,7-DM-6NN matches closely those of DMNN isomers with NO_2 substitution on a β-carbon and with an *ortho* CH_3 group also on a β-carbon (see Figure 18).

[h]1,2-DM-3NN was the remaining 1,2-DMN isomer; its identity was confirmed by its elution after 1,2-DM-8NN and its large $[M-OH]^+$ fragment ion characteristic of DMNN isomers with NO_2 substitution on a β-carbon and with an *ortho* CH_3 group also on a β-carbon (see Figure 18).

[i]1,4-DM-6NN was the remaining 1,4-DMN isomer; its identity was confirmed by its elution last of the 3 isomers and its EI spectrum characteristic of NO_2 substitution on a β-carbon with no steric interaction (see Figure 16).

[j]2,3-DM-6NN was the remaining 2,3-DMN isomer; its identity was confirmed by its elution last of the 3 isomers and its EI spectrum characteristic of NO_2 substitution on a β-carbon with no steric interaction (see Figure 17).

[k]1,8-DM-3NN was the remaining 1,8-DMN isomer; its identity was confirmed by its elution last of the 3 isomers and its EI spectrum characteristic of NO_2 substitution on a β-carbon with no steric interaction (see Figure 17).

Nitro-substitution generally results in large downfield shifts of the *ortho* and *peri* protons if the NO_2 group is in the plane of the aromatic ring (Wells and Alcorn, 1963; Miller *et al.*. 1985), but the anisotropy of the NO_2 group means that as it is shifted out of the plane by steric interactions a shielding effect occurs, and decreased downfield or even upfield shifts can occur (Wells and Alcorn, 1963; Miller *et al.*, 1985).

The NMR shifts in the DMNNs shown in Figures 12 and 13 were consistent with those observed for 1-nitronaphthalene (1-NN) where the proton *ortho* to the NO_2 group was shifted 0.6 ppm downfield and the proton *peri* to the NO_2 was shifted 0.58 ppm downfield from their positions in naphthalene (Gupta, 1995). As seen from Figures 12 and 13, the downfield shifts of the protons relative to their position in the parent DMN range from 0.59 to 0.8 ppm for the protons *ortho* to the NO_2 group and from 0.55-0.78 ppm for the protons *peri* to the NO_2 group and, as in 1-NN, the *peri*-shifts are generally slightly lower than the *ortho*-shifts on a given molecule.

The EI spectra of the DMNNs are consistent with those of other nitroarenes (Schuetzle and Jensen, 1985; Arey and Zielinska, 1989) with strong molecular ions, m/z 201, and fragment ions of $[M-NO]^+$ at m/z 171 (presumably after nitro to nitrite rearrangement), $[M-NO_2]^+$ at m/z 155, $[M-HNO_2]^+$ at m/z 154, $[M-H_2NO_2]^+$ at m/z 153, $[M-NO-CO]^+$ at m/z 143. Unlike the methylnaphthalenes which have only small $[M-CH_3]^+$ fragment ions, the dimethylnaphthalenes and ethylnaphthalenes have strong fragments from loss of a methyl radical (which is sometimes the base peak), as well as indenyl ions at m/z 115 and naphthalene ions at m/z 128 (Gallagher, 2006). The DMNNs also show loss of a methyl radical at m/z 186 and have stable naphthalene ions (m/z 128 may be the base peak, see for example Figures 12, 13 and 15) and indenyl ions.

It has been reported (Arey and Zielinska, 1989) for the MNNs that a fragment ion due to loss of CO from the molecular ion occurs in spectra of isomers where a hydrogen is *peri* to the NO_2 group (1-M-4NN, 1-M-5NN, 2-M-4NN and 2-M-5NN) and that a unique $[M-HCO]^+$ fragment ion occurs in 2-M-8NN. Small ion fragments at m/z 173, $[M-CO]^+$ occur in the spectra shown in Figures 12 and 13 where a hydrogen is *peri* to the NO_2 group and a fragment ion at m/z 172, $[M-HCO]^+$ occurs in the spectra of 1,3-DM-5NN, 1,6-DM-4NN, 2,3-DM-5NN, and 2,6-DM-4NN , which are analogous to 2-M-8NN.

NO$_2$ and CH$_3$ Substituents in Peri Positions. As reported for 1-M-8NN (Arey and Zielinska, 1989), a very characteristic fragmentation, loss of a hydroxyl, $[M-OH]^+$, occurs when the nitro and methyl groups are *peri* to one another. Figure 14 shows the EI spectra of the 6 DMNN isomers with a *peri* configuration. The spectra are very similar to one another and in each case the base peak is the m/z 184 fragment. The steric interaction between the nitro- and methyl- groups causes early GC elution (see Figure 14 caption) and is also evident in the resulting NMR shifts. The anisotropic NO_2 group is twisted out of the plane of the naphthalene ring by the *peri* CH_3 group, lessening the deshielding effect of the NO_2 group and the downfield shift of the proton *ortho* to the NO_2 is only 0.1-0.2 ppm.

NO$_2$ Substitution on an α-Carbon and with an Ortho CH$_3$ Group. 2-M-1NN elutes first of all the MNN isomers (Arey and Zielinska, 1989) and, as noted in the caption to Figure 15, four out of the five isomers with NO_2 substitution on an α-carbon and a CH_3 group adjacent on a β-carbon elute first of the isomers from the individual parent DMNs. The sole exception is 1,3-DM-4NN which elutes after 1,3-DM-2NN, in which there are two *ortho* methyl groups crowding the NO_2 group. A characteristic $[M-OH]^+$ fragment is seen in each spectrum, but it is generally small [as is the case for 2-M-1NN (Arey and Zielinska, 1989)] and the m/z 128 ion is the base peak in the spectra. As noted above, the shifts of the *peri* protons in the DMNN isomers in

Figures 12 and 13 where there are no steric interactions with a CH_3 group is 0.55-0.78 ppm downfield. For NO_2 substitution on an α-carbon with an *ortho* CH_3 group, the shifts of the *peri* protons are slightly upfield (Figure 15). An upfield shift of the *peri* proton for a sterically crowded NO_2 has previously been described for NO_2 groups between two *peri* hydrogens, such as in 9-nitroanthracene (Miller *et al.*, 1985), for the *peri* proton in 2-M-1NN (Wells and Alcorn, 1963; Gupta, 1995) and for the *peri* proton, H4, in 2,3-dinitrofluoranthene (Zielinska *et al.*, 1988).

As noted above, an unusual $[M-HCO]^+$ fragment ion occurs in 2-M-8NN and this fragment is seen at m/z 172 in 2,7-DM-1NN. Another characteristic fragment presumably resulting from the adjacent *ortho* CH_3 and NO_2 groups is at m/z 156 $[M-CH_3-NO]^+$. The corresponding fragment at m/z 142 is observed in 2-M-1NN and, as noted below, this fragmentation also occurs when the NO_2 is on a β-carbon and the CH_3 on an α-carbon (see Figure 19).

1,7-DM-8NN (see Figure 14) also has NO_2 substitution on an α-carbon with an *ortho* CH_3 group, but it was classified with the isomers with the NO_2 and CH_3 substituents *peri* to one another because its EI spectrum with the $[M-OH]^+$ fragment ion as its base peak suggests that the *peri* substituents dominate the fragmentation.

NO_2 Substitution on a β-Carbon and No Steric Interaction. The EI mass spectra of the 10 DMNN isomers with NO_2 substitution on a β-carbon and no steric interaction (Figures 16 and 17) are all very similar, with the molecular ion as the base peak and low abundances of the fragment ions. As noted on the figure captions, these isomers elute last. Consistent with the NO_2 group being in the plane of the naphthalene ring, the downfield shifts of the *ortho* protons are large, ranging from 0.74-0.77 ppm for the *ortho* protons on β-carbons and from 0.94-0.99 ppm for *ortho* protons on α-carbons, consistent with analogous shifts of 0.6 (for proton H3) and 0.8 ppm (for proton H1) in 2-NN. These isomers were generally formed in low abundance and, for several of them, their identities were confirmed on the basis of their late GC elution and characteristic mass spectra.

NO_2 Substitution on a β-Carbon and with an Ortho CH_3 Group also on a β-Carbon. As reported for 2-M-3NN (Arey and Zielinska, 1989), a $[M-OH]^+$ fragment ion is abundant in these DMNNs, as seen in Figure 18. Note that while the downfield shifts of the protons *ortho* to the NO_2 and on an α-carbon (-0.79 ppm in 2,6-DM-3NN and -0.82 ppm in 2,7-DM-3NN) are less than the corresponding proton shifts for the NO_2 on β-carbons with no steric interactions which range from -0.94 to -0.99 ppm (see Figures 16 and 17), they are still large and suggest that the NO_2 group is mainly in the plane of the naphthalene ring.

1,3-DM-2NN has two methyl groups *ortho* to the NO_2 group and could also be considered a member of the next group discussed.

NO_2 Substitution on a β-Carbon and with an Ortho CH_3 Group on an α-Carbon. As reported for 1-M-2NN (Arey and Zielinska, 1989), a $[M-OH]^+$ fragment ion is abundant in these DMNNs, as seen in Figure 19. A characteristic fragment ion at m/z 156, $[M-CH_3-NO]^+$, is prominent in each of these spectra [a corresponding ion at m/z 142 is prominent in the spectrum of 1-M-2NN (Arey and Zielinska, 1989)]. As noted above, this m/z 156 fragment was also seen for *ortho* substitution when the NO_2 was on the α-carbon and the CH_3 on the β-carbon (see Figure 15). Interestingly, 1,3-DM-2NN has an m/z 156 fragment more prominent than the other isomers shown on Figure 18, but smaller than those in this group (Figure 19).

Ethylnitronaphthalenes. Previously the EI mass spectra and RI values of the 14 methylnitronaphthalenes (MNNs) have been published (Arey and Zielinska, 1989) and Gupta (1995) has shown their NMR spectra. For those ENNs for which NMR data could be generated, the appearance of the aromatic portions of the ENN spectra closely matched those of the corresponding MNN spectra. The appearance of the EI spectra of the ENNs (Figures 20 and 21) is different from both the DMNN spectra and the MNN spectra in that fragments from the loss of a methyl radical at m/z 186 are more prominent in many of the ENN spectra.

1-Ethylnitronaphthalenes. NMR spectra were obtained for only two of the seven 1-ENN isomers, 1-E-4NN and 1-E-5NN (see Figure 20). 1-M-8NN elutes first and 1-M-2NN elutes second of the 1-MNN isomers and the isomers assigned as 1-E-8NN and 1-E-2NN eluted first and second, respectively, of the 1-ENN isomers. Both isomers show prominent [M-OH]$^+$ fragments and, comparing the spectra of 1-E-2NN with the DMNN spectra in Figure 19 and that of 1-E-8NN with DMNNs with *peri* NO$_2$ and CH$_3$ groups (Figure 14), it is clear that the EI spectra are consistent with these assignments.

The remaining 3 isomers, 1E-3NN, 1E-6NN, and 1E-7NN, have generally similar EI spectra. Although their assignments must be considered as tentative at this time, they have been assigned as 1-E-6NN eluting earliest of the three, consistent with the elution order reported for the 1MNN isomers (Arey and Zielinska, 1989), and 1-E-3NN eluting just prior to 1-E-7NN. The latter is the reverse of the 1-MNN isomers, but is based on the assumption that the relative yields of the 1-ENN isomers formed from the gas-phase reaction of 1-ethylnaphthalene with the NO$_3$ radical will be the same as for the NO$_3$ reaction of 1-methylnaphthalene (Wang, 2006).

2-Ethylnitronaphthalenes. Complete NMR spectra of five 2-ENN isomers were obtained and the most downfield proton in 2-E-7NN (proton H8) was located in the spectra of a mixture containing both 2-E-6NN and 2-E-7NN, thereby, allowing the protons in 2-E-6NN to be unambiguously assigned (Gallagher, 2006). The only remaining 2-ENN isomer, 2-E-3NN, shows a characteristic [M-OH]$^+$ fragment at m/z 184 (see Figure 21). The NMR chemical shifts and EI spectra of the seven 2-ENN isomers are consistent with those obtained for the DMNNs. 2-E-1NN has a [M-OH]$^+$ fragment with <50% abundance, consistent with the corresponding DMNN isomers shown on Figure 15. 2-E-3NN has m/z 184 as the base peak, as do the corresponding DMNNs shown in Figure 18. 2-E-4NN and 2-E-5NN have NMRs shifts consistent with NO$_2$ substitution on an α-carbon and no steric interaction with an alkyl substituent (see Figures 12 and 13 for corresponding DMNNs). The EI spectra of 2-E-6NN and 2-E-7NN are consistent with those of the DMNN isomers with NO$_2$ substitution on a β-carbon and no steric interaction with the methyl substituents (Figures 16 and 17), with low abundances of the fragments below 180 da. They differ from the spectra seen in Figures 16 and 17 in that the [M-CH$_3$]$^+$ fragments are higher for the ENNs than for the DMNNs.

2-E-8NN has an m/z 172 fragment, which corresponds to the [M-HCO]$^+$ occurring in the spectra of 1,3-DM-5NN, 1,6-DM 4NN, 2,3-DM-5NN, 2,6-DM-4NN and analogous to 2-M-8NN (Arey and Zielinska, 1989). Additionally, the GC elution order of the 2-ENN isomers parallels that of the 2-MNN isomers, except that 2-E-3NN elutes before 2-E-8NN while 2-M-8NN and 2-M-3NN co-eluted (Arey and Zielinska, 1989).

Ambient Sample. Shown in Figure 22 is the GC/MS-NCI analysis for m/z 201, the molecular ion of the DMNNs and ENNs, in the nitro-PAH containing HPLC fraction from a nighttime ambient sample collected on a PUF plug in Riverside, CA on July 14, 2006. It should be noted that NNs and MNNs were also present in this ambient sample at higher abundances than the DMNNs and ENNs. The ozone reached a maximum of 121 ppbv in late afternoon on
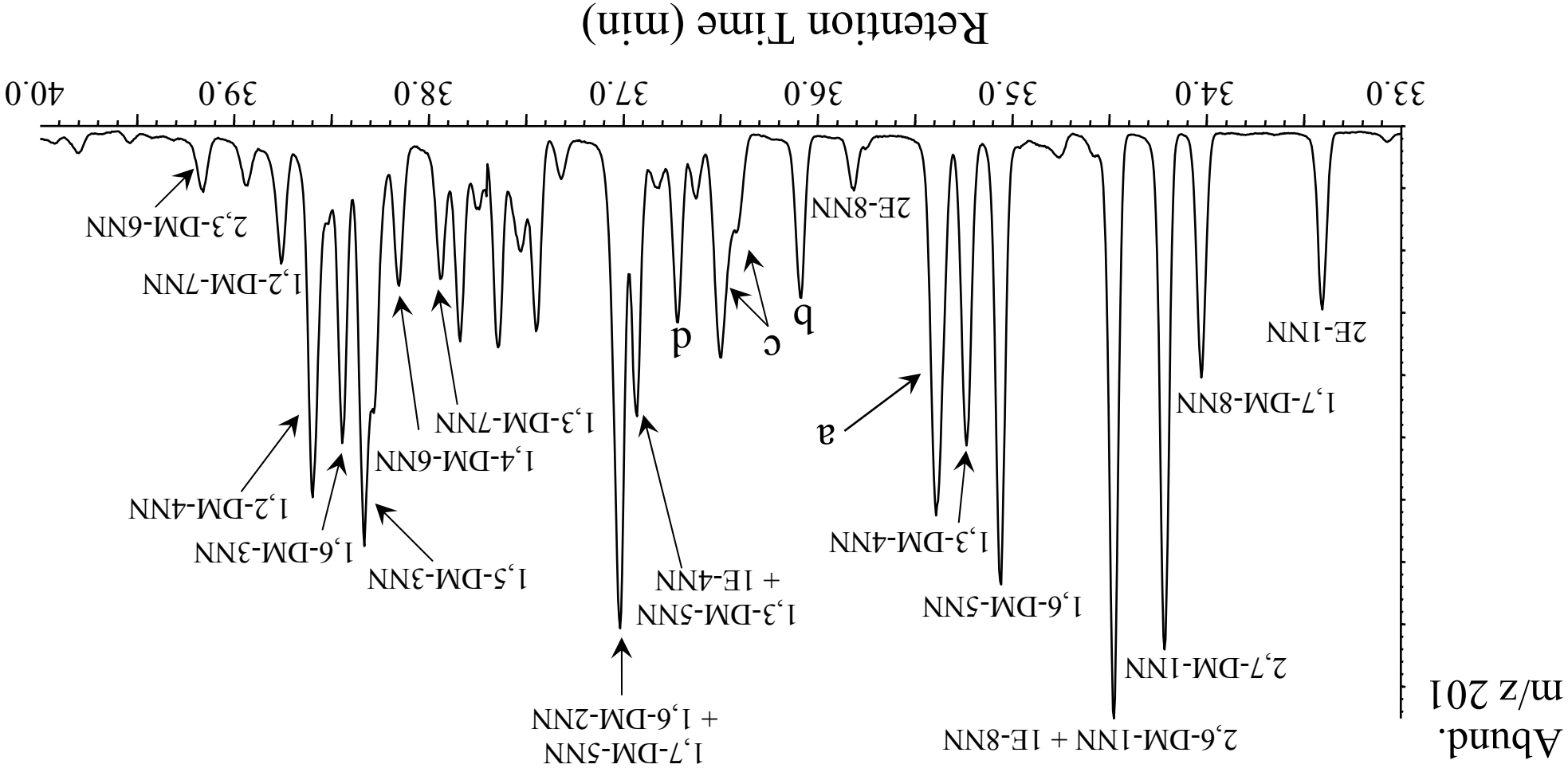
Figure 22. NCI-GC/MS analysis of the nitro-PAH containing HPLC fraction of an extract from a nighttime ambient air sample collected on PUF plugs in Riverside, CA, July 14, 2006. The peak labeled "a", RI = 232.32 includes 1,6-DM-8NN, 2,3-DM-1NN, 2-E-3NN and 1,3-DM-8NN; the peak labeled "b", RI = 236.97 includes 2-E-4NN and 1,4-DM-5NN, the peaks labeled "c", RI = 238.99 and 239.71 include 1,2-DM-8NN, 2,6-DM-4NN, 1,5-DM-4NN, 2-E-5NN, 1-E-5NN, 1,6-DM-7NN and the peak labeled "d", RI = 241.19 includes 2,7-DM-4NN and 1,7-DM-2NN.

Retention Time (min)

40.0   39.0   38.0   37.0   36.0   35.0   34.0   33.0

Ambient Sample
GC/MS – NCI

Abund.
m/z 201

2,3-DM-6NN
1,2-DM-7NN
1,2-DM-4NN
1,6-DM-3NN
1,5-DM-3NN
1,4-DM-6NN
1,3-DM-7NN
1,7-DM-5NN + 1,6-DM-2NN
1,3-DM-5NN + 1E-4NN
d
c
b
2E-8NN
a
1,3-DM-4NN
1,6-DM-5NN
2,6-DM-1NN + 1E-8NN
2,7-DM-1NN
1,7-DM-8NN
2E-1NN

this date (CARB data for Riverside-Rubidoux) and it is anticipated that in late afternoon and early evening, NO_3 radical reactions forming nitro-PAH products may have occurred. Indeed the five early peaks in Figure 22 from *ortho* and *peri* substituted DMNNs and ENNs have recently been suggested as markers of NO_3 radical-initiated reactions (Wang, 2006). So, although many DMNNs and ENNs co-elute on the HP-5 column, certain isomers may still provide clues to the DMNN and ENN formation mechanisms. Previously, Gupta and co-workers (1996) noted that NNs and MNNs contributed significantly to the gas-phase mutagencity of ambient samples measured using a bacterial reversion assay. It seems likely that a significant fraction of the "unaccounted for" mutagenicity in the nitro-PAH containing fraction of those samples may have been due to the presence of DMNNs and ENNs. Additional separation strategies, including, for example, the use of liquid crystalline stationary phases which separate isomers on the basis of "length-to-breath" ratio (Poster *et al.*, 1998) and GC X GC analyses (Panic and Gorecki, 2006) should prove useful in uniquely identifying DMNNs and ENNs in ambient samples and elucidating their formation pathways.

E. Nitroarene Products of the NO$_3$ Radical-Initiated Reactions of Naphthalene and the C$_1$- and C$_2$-Alkylnaphthalenes and their Occurrence in Ambient Air

1. Introduction

Naphthalene and its C$_1$- and C$_2$-alkyl derivatives, which are present in the atmosphere predominantly in the gas phase (Bidleman, 1988; Wania and Mackay, 1996), are the most abundant semi-volatile polycyclic aromatic hydrocarbons (PAHs) in ambient air (Arey *et al.*, 1989; Reisen and Arey, 2005). An important source of these compounds in urban areas is vehicle exhaust, especially from diesel-fueled vehicles (Fraser *et al.*, 1998; Zielinska *et al.,* 2004). In the atmosphere, naphthalene and its C$_1$- and C$_2$-alkyl derivatives undergo chemical transformations with OH radicals, NO$_3$ radicals and Cl atoms (Phousongphouang and Arey, 2002; 2003; Wang *et al.*, 2005), with the daytime OH radical reaction being estimated to dominate as their atmospheric loss process (Arey, 1998). Both the OH radical- and NO$_3$ radical-initiated reactions have been shown to produce nitrated products from naphthalene and the methylnaphthalenes (MNs) (Pitts *et al.*, 1985; Zielinska *et al.*, 1989; Sasaki *et al.*, 1997; Arey, 1998) and ambient measurements suggest that the higher nitro-yields from the NO$_3$ radical *versus* OH radical reactions can result in significant nighttime formation of nitronaphthalenes (NNs) and methylnitronaphthalenes (MNNs) (Gupta *et al.*, 1996; Reisen and Arey, 2005). Nitro-PAHs are of concern because they are mutagens and animal carcinogens (IARC, 1984; IPCS, 2003) and the NNs and MNNs have been shown to contribute to the vapor-phase mutagenicity of ambient air samples as measured with one bacterial reversion assay (Gupta *et al.*, 1996).

Recently dimethyl-/ethyl-nitronaphthalenes (DMNNs/ENNs) have been observed from ambient air samples collected in Southern California (Reisen *et al.*, 2003), although the identities of individual isomers could not be obtained because of the lack of authentic standards. The synthesis of all 56 DMNN/ENN isomers (Section D above and Gallagher, 2006) makes possible a further investigation of their formation and occurrence in the atmosphere. In this work, we measured the formation yields of nitroarenes from the NO$_3$ radical-initiated reactions of naphthalene and its C$_1$- and C$_2$-alkyl derivatives. Profiles of DMNNs/ENNs from environmental chamber reactions and ambient samples were obtained and several specific isomers have been proposed to be markers of either NO$_3$ radical reaction or OH radical reaction.

2. Experimental Methods

Experiments were carried out in a ~7500 liter Teflon chamber, equipped with two parallel banks of blacklamps, at 296 ± 2 K and 735 Torr total pressure of purified air at ~5% relative humidity. The chamber is also equipped with a Teflon-coated fan to ensure rapid mixing of reactants during their introduction into the chamber. Naphthalene and alkylnaphthalenes were introduced into the chamber by flowing nitrogen gas through a Pyrex bulb containing a measured amount of the liquid or solid compound while heating the bulb and inlet tube.

NO$_3$ radicals were generated from the thermal decomposition of N$_2$O$_5$, and NO$_2$ was also included to lengthen the reaction times (Atkinson *et al.*, 1984). For certain experiments (see below), OH radicals were generated by photolysis of methyl nitrite in air at wavelengths >300 nm, and NO was added into the reactant mixtures to suppress the formation of O$_3$ and hence of NO$_3$ radicals (Atkinson *et al.*. 1981). Methyl nitrite, NO, NO$_2$ and N$_2$O$_5$ were flushed into the chamber without heating. The NO and NO$_2$ concentrations during the experiments were monitored using a NO-NO$_2$ chemiluminescence analyzer. The chamber was cleaned after each

experiment by flushing with purified air for at least 20 hours, with the chamber lights on for at least 6 hours.

Identification and yields of (alkyl-)nitronaphthalenes formed from the NO₃ radical-initiated reactions. The initial reactant concentrations (molecule cm^{-3}) were: naphthalene or alkylnaphthalenes, ~7.2 x 10^{12}; N_2O_5, ~2.4 x 10^{13} and NO_2, ~2.4 x 10^{13}. An excess of NO was added to the reaction mixture to quench the NO_3 radical prior to carrying out post-reaction analyses. The NO was added between 4-24 min after the N_2O_5, resulting in 17-55% consumption of the initial naphthalene (5 replicate experiments) or 40-50% consumption of the initial alkylnaphthalenes (2 replicate experiments for each of 1-MN and 1,6-DMN;1 experiment for each of the other isomers).

The concentrations of naphthalene, alkylnaphthalenes and alkylnitronaphthalenes were measured during the experiments by gas chromatography with flame ionization detection (GC-FID). 6.0 liter volume gas samples were collected from the chamber onto Tenax-TA solid adsorbent cartridges using a pump with mass flow controller (Tylan General) at a flow rate of 400 cm^3 min^{-1} to quantify naphthalene, alkylnaphthalenes and alkylnitronaphthalenes. In addition, a gas-tight all-glass syringe was used to collect 100 cm^3 volume gas samples onto a Tenax-TA solid adsorbent cartridge to quantify naphthalene and alkylnaphthalenes. The Tenax solid adsorbent samples were thermally desorbed in the injection port of a Hewlett-Packard (HP) 5890 series II GC at 270 ^{o}C onto a 30-m DB-5MS capillary column (0.53 mm i.d., 1.5 μm phase) held at 40 ^{o}C for 10 min and then temperature programmed to 140 ^{o}C at 20 ^{o}C min^{-1}, then to 280 ^{o}C at 5 ^{o}C min^{-1} and held at 280 ^{o}C for 10 min..

Solid Phase MicroExtraction (SPME) samples were collected by exposing a 65 μm polydimethylsiloxane/divinylbenzene (PDMS/DVB) fiber to the chamber contents for 5 min with the mixing fan on. The SPME fiber samples were then thermally desorbed in the heated (270 ^{o}C) injection port of an Agilent Technologies 6890N GC interfaced to an Agilent Technologies 5975 inert XL mass selective detector (MSD), onto a 30-m HP-5MS capillary column (0.25 mm i.d., 0.25 μm phase) held at 40 ^{o}C and then temperature programmed to 250 ^{o}C at 4 ^{o}C min^{-1}. The mass spectrometery (MS) was conducted in the negative chemical ionization (NCI) mode, using methane as the reagent gas.

Additional SPME samples were collected for variable times and in addition to the GC-MSD-NCI analyses described above, the GC-MSD was operated in the positive chemical ionization (PCI) mode using methane as the reagent gas. Selected samples were also analyzed with a HP 5890 GC with a 60-m DB-5MS capillary column (0.25 mm i.d., 0.25 μm phase), interfaced to a HP 5971 MSD operated in electron ionization (EI) mode; or a Varian 2000 GC/MS/MS ion trap system with a 30-m DB-1 capillary column (0.32 mm i.d., 3.0 μm phase) operated in EI mode.

GC-FID responses for naphthalene, alkylnaphthalenes and nitronaphthalenes (NNs) were determined by spiking a methanol solution of authentic standards onto Tenax-TA solid adsorbent cartridges with GC-FID analyses as described above. Assuming that isomers will have identical GC-FID responses (Scanlon and Willis, 1985), the measured response factor for 2-methyl-1-nitronaphthalene (2-M-1NN) was used for all MNNs and the measured response factor for 2,6-dimethyl-1-nitronaphthalene (2,6-DM-1NN) was used for all DMNN/ENN isomers.

DMNN/ENN profiles from chamber reactions. A methanol solution of dimethylnaphthalenes (DMNs) and ethylnaphthalenes (ENs), including 1-EN, 2-EN, 1,2-DMN, 1,3-DMN, 1,4-DMN, 1,5-DMN, 1,6-DMN, 1,7-DMN, 2,3-DMN, 2,6-DMN and 2,7-DMN was made. The ratios of isomers in the solution were chosen to mimic those obtained from previous

ambient measurements (Phousongphouang and Arey, 2003; Reisen and Arey, 2005), and it should be noted that 1,8-DMN was not found in these ambient samples. Both NO_3 radical and OH radical reactions were carried out using this "ambient concentration profile" solution of DMNs/ENs as the initial reactant.

For the NO_3 radical reaction, the initial reactant concentrations (molecule cm^{-3}) were: $\sum$DMNs + ENs, ~7.2 x 10^{12}; N_2O_5, ~2.4 x 10^{13} and NO_2, ~2.4 x 10^{13}. An excess amount of NO was subsequently added into the reaction mixture to quench the NO_3 radical reaction, resulting in ~40% consumption of the initial alkylnaphthalenes. SPME samples were collected by exposing a PDMS/DVB fiber to the chamber contents for 15 min with the mixing fan on and analyzed by the GC-MSD-NCI method described above.

For the OH radical reaction, the initial reactant concentrations (molecule cm^{-3}) were: $\sum$DMNs + ENs, ~1.4 x 10^{13}; CH_3ONO, ~4.8 x 10^{13}; NO, ~4.8 x 10^{13}. Irradiation was carried out at 20% of the maximum light intensity for 4 min, resulting in ~50% consumption of the initial alkylnaphthalenes. The lower yields of the DMNNs/EMMs in the OH radical reaction precluded the use of SPME sampling for convenient product analysis. Therefore, the post-reaction chamber contents was sampled onto a Teflon-impregnated glass fiber filter (20 cm x 25 cm) and two polyurethane foam plugs (PUFs) in series beneath the filter at a flow rate of ~1.0 m^3 min^{-1}, followed by Soxhlet extraction in dichloromethane. The extracts were then concentrated, filtered (0.2 μm PTFE membrane, Acrodisc, Gelman Laboratory) and fractionated by high-performance liquid chromatography (HPLC) using a method described previously (Arey *et al.*, 1992). Fractions were collected, concentrated and analyzed by GC-MS. The HPLC instrumentation consisted of a HP 1050 HPLC with an HP 1040M Series II HPLC detection system, and an ISCO FOXY 200 fraction collector. The Agilent 5975-MSD was operated in the NCI mode with selected ion monitoring (SIM) (m/z = 201 and 217 da).

DMNN/ENN profiles from ambient samples. Archived ambient samples collected in Redlands, CA on October 18-29, 1994 (Gupta *et al.*, 1996) and in Mexico City on April 27-30, 2003 (Marr *et al.*, 2006) were re-analyzed by GC-MS-NCI. Ambient sample collection was also carried out during July 14-15, 2006 in Riverside, CA. The sampling site was located at an agricultural operation site on the University of California, Riverside (UCR) campus. A high-volume (Hi-vol) air sampler equipped with a Teflon-impregnated glass fiber filter (20 cm x 25 cm) and two PUFs in series beneath the filter and without a size-selective inlet was used to collect semi-volatile and particle-associated nitro-PAHs at a flow rate of ~0.6 m^3 min^{-1}. Samples were collected from 18:00-06:00 (PDT). The filter and PUF samples were Soxhlet-extracted, fractionated by HPLC and analyzed by GC-MS as described above.

Chemicals. The chemicals used, and their stated purities, were as follows: naphthalene (98%), 1-MN (99%), 2-MN (98%), 1-EN (98+%), 2-EN (99+%), 1,2-DMN (98%), 1,3-DMN (96%), 1,4-DMN (95%), 1,5-DMN (98%), 1,6-DMN (99%), 1,7-DMN (99%), 1,8-DMN (95%), 2,3-DMN (98%), 2,6-DMN (99%), 2,7-DMN (99%), 1-NN (99%), 2-NN (98%), 2-M-1-NN (99%), Aldrich Chemical Company; 2,6-dimethyl-1-nitronaphthalene, synthesized as described in Section D; hexane (Optima), dichloromethane (Optima) and acetonitrile (Optima), Fisher Scientific; and NO (≥99.0%), Matheson Gas Products. Methyl nitrite and N_2O_5 were prepared and stored as described previously (Atkinson *et al.*, 1981; 1984).

3. Results and Discussion

Yields of (alkyl-)nitronaphthalenes. The concentrations of naphthalene and alkylnaphthalenes monitored in the dark showed generally small decreases, attributed to wall losses, which were not taken into account when calculating the yields of alkylnitronaphthalenes. In contrast, ~20% decays of (alkyl-)nitronaphthalenes were observed over 1.0 hr. Thus the amounts of (alkyl-)nitronaphthalenes formed were quantified using a 15 min Tenax sample immediately after the addition of NO to quench the NO_3 radical-initiated reaction and the yields should be viewed as lower limits since wall losses were almost certainly occurring during the sampling period.

Using the retention indices of alkylnitronaphthalenes measured in this laboratory (Arey and Zielinska, 1989; Gallagher, 2006, see also Section D), individual (alkyl-)nitronaphthalene isomers formed from the NO_3 radical-initiated reactions were first identified by GC/MS-NCI. Subsequently, alkylnitronaphthalene isomers were identified from GC-FID chromatograms with the assistantance of the GC/MS-PCI and GC/MS-EI analyses. The yields obtained for the nitronaphthalenes (NNs) and methylnitronaphthalenes (MNNs) are tabulated in Table 18. The yields of dimethylnitronaphthalenes (DMNNs) and ethylnitronaphthalenes (ENNs), together with estimated ambient formation rates from the NO_3 radical reactions, are tabulated in Table 19.

Our yields of 1-nitronaphthalene (19.6 ± 1.3 %) and 2-nitronaphthalene (6.4 ± 0.6 %) [note that the errors given reflect precision only] are in good agreement with three previous measurements made in this laboratory (Pitts *et al*., 1985; Atkinson *et al*., 1987; Sasaki *et al*., 1997). The total yields of MNNs from the NO_3 radical-initiated reactions of 1-MN and 2-MN, respectively, were estimated as ~30% in a previous study (Zielinska *et al.*, 1989). In contrast, the nitroarene yields from 1-MN and 2-MN, respectively, were measured to be 12 ± 2 % and 21% in this work. In the earlier study, large volume sample collection followed by Soxhlet-extraction and HPLC fractionation prior to GC-FID analysis was utilized, in contrast to the Tenax cartridge sampling used here. The discrepancy between the two results is presently not understood and should be investigated further. The isomer distributions and yields of DMNNs/ENNs from the NO_3 radical-initiated reactions of DMNs/ENs are being reported for the first time.

The reactions of alkylnaphthalenes with NO_3 radicals are proposed to occur by initial addition of the NO_3 radical to the aromatic ring to form an NO_3-PAH adduct which then either decomposes back to reactants, reacts with NO_2, reacts with O_2, or possibly decomposes unimolecularly (see Atkinson and Arey, 2007 and Scheme 2). The measured rate constants k_{obs} (Phousongphouang and Arey, 2002) for the gas-phase reaction of NO_3 radicals with 1-MN, 2-MN, 1-EN and 2-EN indicate that methyl- and ethyl-substitution are almost equivalent in terms of reactivity enhancement. Furthermore, our nitroarene yields for 1-MN and 2-MN (12% and 21%, respectively) are close to those obtained for 1-EN and 2-EN (12% and 19%, respectively). Note that the MNN isomer distributions from the reactions of 1-MN and 2-MN with NO_3 radicals in this study are only partly available because of the poor resolution of the GC-FID chromatogram. Our ENN isomer distribution from the reaction of 2-EN with NO_3 radicals was 2-E-4NN > 2-E-1NN > 2-E-5NN > 2-E-8NN > 2-E-3NN ~ 2-E-7NN ~ 2-E-6NN, which parallels, in terms of the position of nitration, the MNN isomer distribution from the reaction of 2-MN with NO_3 radicals from previous studies (Zielinska *et al.*, 1989; Gupta, 1995). Our ENN isomer distribution from the reaction of 1-EN with NO_3 radicals was 1-E-4NN > 1-E-3NN > 1-E-5NN > 1-E-8NN > 1-E-6NN > 1-E-7NN > 1-E-2NN, and is generally similar to the MNN isomer distribution from the reaction of 1-MN with NO_3 radicals previously reported (Zielinska *et al.*, 1989) except that 1-E-4NN is somewhat more abundant.

Table 18. Nitroarene products formed from the NO_3 radical reactions of naphthalene, 1-methylnaphthalene and 2-methylnaphthalene, and their molar formation yields.

parent compound	products	% molar yield[a]	literature
naphthalene	1-NN	19.6 ± 1.3	17.2 ± 3.4 (Pitts *et al.*, 1985)
			15.3 ± 2.2 (Atkinson *et al.*, 1987)
			24.4 ± 6.5 (Sasaki *et al*, 1997)
	2-NN	6.4 ± 0.6	7.5 ± 1.2 (Pitts *et al.*, 1985)
			6.9 ± 2.1 (Atkinson *et al.*, 1987)
			11.0 ± 3.6 (Sasaki *et al*, 1997)
1-MN	1-M-2NN	0.6 ± 0.4	
	1-M-3NN/1-M-7NN[b]	2.9 ± 0.6	
	1-M-4NN/1-M-6NN[c]	3.6 ± 0.4	
	1-M-5NN	2.7 ± 0.4	
	1-M-8NN	1.7 ± 0.6	
	Σ isomers	**12 ± 2**	~ 30[e]
2-MN	2-M-1NN	4.9; 4.8	
	2-M-3NN/2-M-4NN /2-M-8NN[d]	12.2; 11.9	
	2-M-5NN	2.3; 2.3	
	2-M-6NN	0.6; 0.6	
	2-M-7NN	0.6; 0.6	
	Σ isomers	**21**	~ 30[f]

[a]Yields are lower limits (see text) and indicated errors are two standard deviations derived from 5 (naphthalene), or 2 (1-MN) replicate experiments. The listed nitroarene yields from 2-MN are two measurements in one experiment.

[b]Mainly 1-M-3NN.

[c]Mainly 1-M-4NN.

[d]Mainly 2-M-4NN.

[e]Reported results for replicate experiments were 37% and 23% (Zielinska *et al.*, 1989).

[f]Reported results for replicate experiments were 31% and 29% (Zielinska *et al.*, 1989).

Table 19. Nitroarene products formed from the NO_3 radical reactions of dimethylnaphthalenes and ethylnaphthalenes, their molar formation yields and formation rates.

parent compound	reaction rates k_{obs} x 10^{28} (cm^6 molecule^{-2} s^{-1})[a]	products	% molar yields[b]	formation rates (fg m^{-3} h^{-1})[c]
1-EN	9.82	1-E-2NN	0.4; 0.4	2.3
		1-E-3NN	2.3; 2.2	13.3
		1-E-4NN	4.5; 4.3	25.9
		1-E-5NN	1.7; 1.6	9.9
		1-E-6NN	1.2; 1.1	6.8
		1-E-7NN	0.9; 0.8	4.9
		1-E-8NN	1.3; 1.3	7.8
		Σ isomers	**12**	
2-EN	7.99	2-E-1NN	4.5; 4.1	47.4
		2-E-3NN	1.2; 1.1	12.6
		2-E-4NN	7.1; 6.4	74.4
		2-E-5NN	2.7; 2.4	28.1
		2-E-6NN	0.7; 0.6	7.5
		2-E-7NN	1.0; 0.9	10.2
		2-E-8NN	2.3; 2.1	23.8
		Σ isomers	**19**	
1,2-DMN	64.0	1,2-DM-3NN	1.0; 0.9	21.2
		1,2-DM-4NN	9.9; 8.6	205
		1,2-DM-5NN	0.7; 0.6	14.7
		1,2-DM-6NN	tr.[d]	-[e]
		1,2-DM-7NN	0.4; 0.3	8.3
		1,2-DM-8NN	0.8; 0.7	17.4
		Σ isomers	**12**	
1,3-DMN	21.3	1,3-DM-2NN	0.6; 0.6	11.1
		1,3-DM-4NN	1.5; 1.5	29.4
		1,3-DM-5NN	1.1; 1.1	21.5
		1,3-DM-6NN	0.2; 0.2	4.3
		1,3-DM-7NN	0.4; 0.4	8.0
		1,3-DM-8NN	0.5; 0.5	11.3
		Σ isomers	**4**	

Table 19 (cont.). Nitroarene products formed from the NO$_3$ radical reactions of dimethylnaphthalenes and ethylnaphthalenes, their molar formation yields and formation rates.

parent compound	reaction rates k_{obs} x 10^{28} (cm^6 molecule^{-2} s^{-1})[a]	products	% molar yields[b]	formation rates (fg m^{-3} h^{-1})[c]
1,4-DMN	13.0	1,4-DM-2NN	1.2; 1.0	6.1
		1,4-DM-5NN	2.9; 2.3	14.7
		1,4-DM-6NN	1.4; 1.2	7.2
		Σ isomers	5	
1,5-DMN	14.1	1,5-DM-2NN	0.6; 0.6	2.9
		1,5-DM-3NN	6.3; 5.8	29.5
		1,5-DM-4NN	2.8; 2.5	12.9
		Σ isomers	9	
1,6-DMN	16.5	1,6-DM-2NN	0.7 ± 0.2	18.2
		1,6-DM-3NN	2.9 ± 0.6	74.2
		1,6-DM-4NN	0.9 ± 0.2	24.1
		1,6-DM-5NN	3.1 ± 0.6	78.6
		1,6-DM-7NN	1.6 ± 0.3	41.1
		1,6-DM-8NN	5.7 ± 1.0	145
		Σ isomers	15 ± 2	
1,7-DMN	13.5	1,7-DM-2NN	0.3; 0.3	3.5
		1,7-DM-3NN	3.0; 2.6	35.5
		1,7-DM-4NN	1.8; 1.5	21.1
		1,7-DM-5NN/ 1,7-DM-6NN	5.0; 4.4	60.2[f]
		1,7-DM-8NN	3.7; 3.2	44.4
		Σ isomers	13	
1,8-DMN	212	1,8-DM-2NN	5.3; 4.3	--[g]
		1,8-DM-3NN	0.2; 0.2	--[g]
		1,8-DM-4NN	14.1; 11.4	--[g]
		Σ isomers	18	
2,3-DMN	15.2	2,3-DM-1NN	13.5; 10.5	63.1
		2,3-DM-5NN	2.3; 1.8	10.7
		2,3-DM-6NN	0.5; 0.3	2.1
		Σ isomers	14	

Table 19 (cont.). Nitroarene products formed from the NO_3 radical reactions of dimethylnaphthalenes and ethylnaphthalenes, their molar formation yields and formation rates.

parent compound	reaction rates k_{obs} x 10^{28} (cm^6 molecule^{-2} s^{-1})[a]	products	% molar yields[b]	formation rates (fg m^{-3} h^{-1})[c]
2,6-DMN	21.2	2,6-DM-1NN	6.3; 5.4	150
		2,6-DM-3NN	0.9; 0.8	22.5
		2,6-DM-4NN	7.9; 6.7	188
		Σ isomers	**14**	
2,7-DMN	21.0	2,7-DM-1NN	5.4; 5.0	131
		2,7-DM-3NN/ 2,7-DM-4NN[h]	16.7; 15.5	410
		Σ isomers	**21**	

[a] Obtained from Phousongphouang and Arey (2003).

[b] Listed yields are lower limits (see text) and are from two measurements in one experiment. There were two replicate experiments for 1,6-DMN and indicated errors are two standard deviations.

[c] The formation rates of nitroarene products from reactions of alkylnaphthalene with NO_3 radicals were calculated, using the expression

$$[\text{Nitroarene}]_t = k_{obs} \times [NO_3] \times [NO_2] \times Y \times [\text{alkylnaphthalene}] \times t,$$

where [Nitroarene]$_t$ is the amount formed after time t, k_{obs} is the rate constant for reaction of alkylnaphthalene with NO_3 radicals, and Y is the formation yield of nitroarenes from the reaction of alkylnaphthalene with NO_3 radicals. An average 12-hr NO_3 radical concentration of 5×10^8 molecule cm^{-3} (Atkinson, 1991) and a background 12-hr NO_2 concentration of 4.8×10^{11} molecule cm^{-3} during sample collection (California Air Resources Board) were assumed. The concentrations of alkylnaphthalenes used were those measured from 19:00-06:30 during Aug. 26-30, 2002, in Riverside, CA (Reisen and Arey, 2005) (ng m^{-3}): 1-EN, 0.7; 2-EN, 1.6; 1,2-DMN, 0.4; 1,3-DMN, 1.1; 1,4-DMN, 0.5; 1,5-DMN, 0.4; 1,6-DMN, 1.8; 1,7-DMN, 1.1; 2,3-DMN, 0.4; 2,6- DMN, 1.4; 2,7-DMN, 1.4.

[d] tr.= trace amount observed by GC-MS/NCI.

[e] The formation rate is very small since the yield is below detection limit.

[f] Mainly 1,7-DM-5NN; 1,7-DM-6NN is estimated to be <6% of total.

[g] Note that 1,8-DMN was not observed from the ambient sample (Phousongphouang and Arey, 2003; Reisen and Arey, 2005).

[h] Mainly 2,7-DM-4NN.
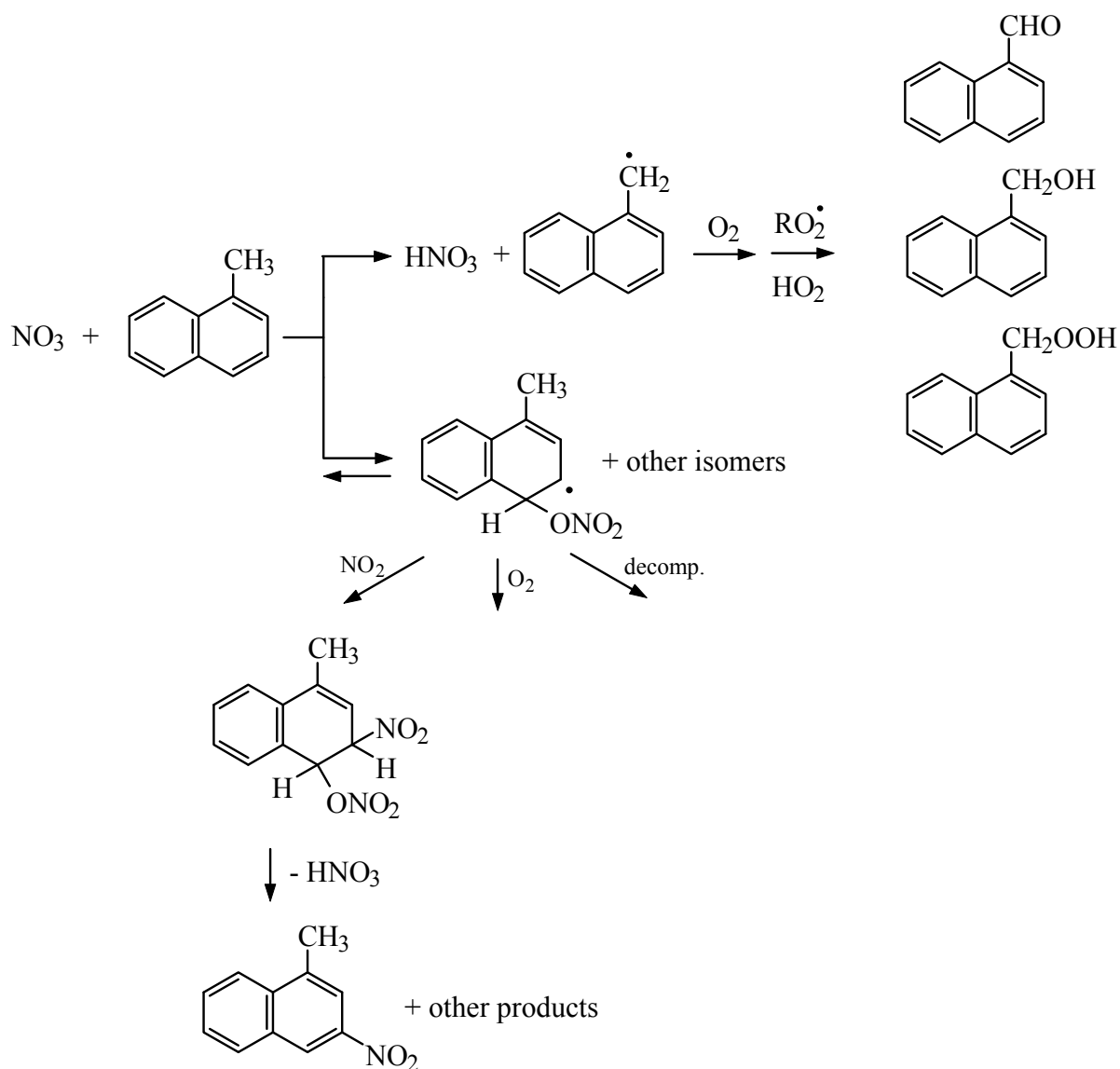
Scheme 2. Suggested reaction pathway for the reaction of alkylnaphthalenes (1-methylnaphthalene shown) with the NO_3 radical.

Keeping in mind that MS-NCI responses of isomers may vary with the position of the substituents on the naphthalene ring and that, therefore, the GC-FID pattern used for quantification may look different from the GC-MS/NCI pattern of peaks, it can be seen from Figure 23 that the profile obtained here for the 2-MNN isomers formed from NO_3 radical reaction with 2-MN closely matches the profile of the 2-ENN isomers formed from 2-EN (both analyzed by GC-MS/NCI). The similarity of the profiles suggests that the relative abundance of the nitration product at a given position on 2-MN and 2-EN are the same. Figure 24 gives the corresponding profiles for 1-M-NN and 1-E-NN isomers. Previous work synthesizing and identifying the DMNN/ENN isomers unambiguously identified retention indices for all isomers except 1-E-3NN, 1-E-6NN and 1-E-7NN (Gallagher, 2006). The assignment of 1-E-3NN as the more abundant isomer eluting just before 1-E-7NN (see Figure 23) is based on the assumption that, as observed for reactions of 2-MN and 2-EN, the relative abundance of the various nitro-isomers from 1-MN and 1-EN will be very similar.

It is interesting to note that 1-E-4NN was also formed in the highest abundance from the solution phase reactions with N_2O_5 in CCl_4 (Gallagher, 2006). However, 1-M-4NN, a nitroarene isomer of highest yield in electrophilic nitration (Alcorn and Wells, 1965; Eaborn *et al.*, 1968), was not observed to be the most abundant isomer either from the gas-phase reaction of 1-MN with NO_3 radicals, or from the solution phase reactions with N_2O_5 in CCl_4 (Zielinska *et al.*, 1989; Gupta, 1995). It should be noted that the identification of 1-E-4NN as the most abundant nitroarene isomer from the gas-phase reaction of 1-EN with NO_3 radicals is based on matching the RI with an isomer unambiguously identified by NMR (Gallagher, 2006).

The nitroarene yields from the gas phase reactions of dimethylnaphthalenes with NO_3 radicals are in the range of 4-21% (Table 19). In the past, the nitroarenes formed from radical-initiated reactions have been explained by suggesting that the radical adds to the most electron-dense site (i.e., the site where electrophilic nitration will occur) followed by NO_2 adding to the *ortho* position and then loss of water, in the case of the OH radical reactions, or loss of nitric acid, in the case of NO_3 radical reactions, leading to the nitro-PAH. This is consistent, for example, with the formation of 2-nitrofluoranthene (2-NF) from both the OH radical- and NO_3 radical-initiated reactions of fluoranthene, where 3-NF is the electrophilic nitration product of fluoranthene (Arey, 1998). Furthermore, the formation of 2-NF as the sole NF from the NO_3 radical reaction, while small amounts of 7-NF and 8-NF are also formed from the OH radical reaction suggests higher selectivity for the NO_3 radical reaction(Arey, 1998).

For naphthalene, 1-NN and 2-NN are formed in ratios of approximately 1:1 from the OH radical reaction (Sasaki *et al.*, 1997) and >2:1 from the NO_3 radical reaction (see Table 18). Based on addition of NO_3 to the most electron dense position followed by *ortho* addition of NO_2, it would be expected that 2-NN would be formed in higher yield than 1-NN. Shown in Scheme 3 is a mechanism that would explain the higher yield of 1-NN from the NO_3 radical reaction with naphthalene. The NO_3 radical is shown adding at the 1-position and the NO_2 adds either to the *para* position or *ortho* position with subsequent loss of nitric acid to form 1-NN or 2-NN, respectively. [Note that no comparable *para* position exists in fluoranthene, where the NO_2 adds, as noted above, *ortho* to the NO_3 group.]

The most abundant nitro-isomer from both of the methylnaphthalenes and the majority of the dimethylnaphthalenes can be explained by this mechanism. Shown in Table 20 are the most abundant nitro-isomers from electrophilic nitration of the MNs (Alcorn and Wells, 1966) and eight of the DMNs (Davies and Warren, 1969). For 2-MN, 2,3-; 2,6-; and 2,7-DMN,
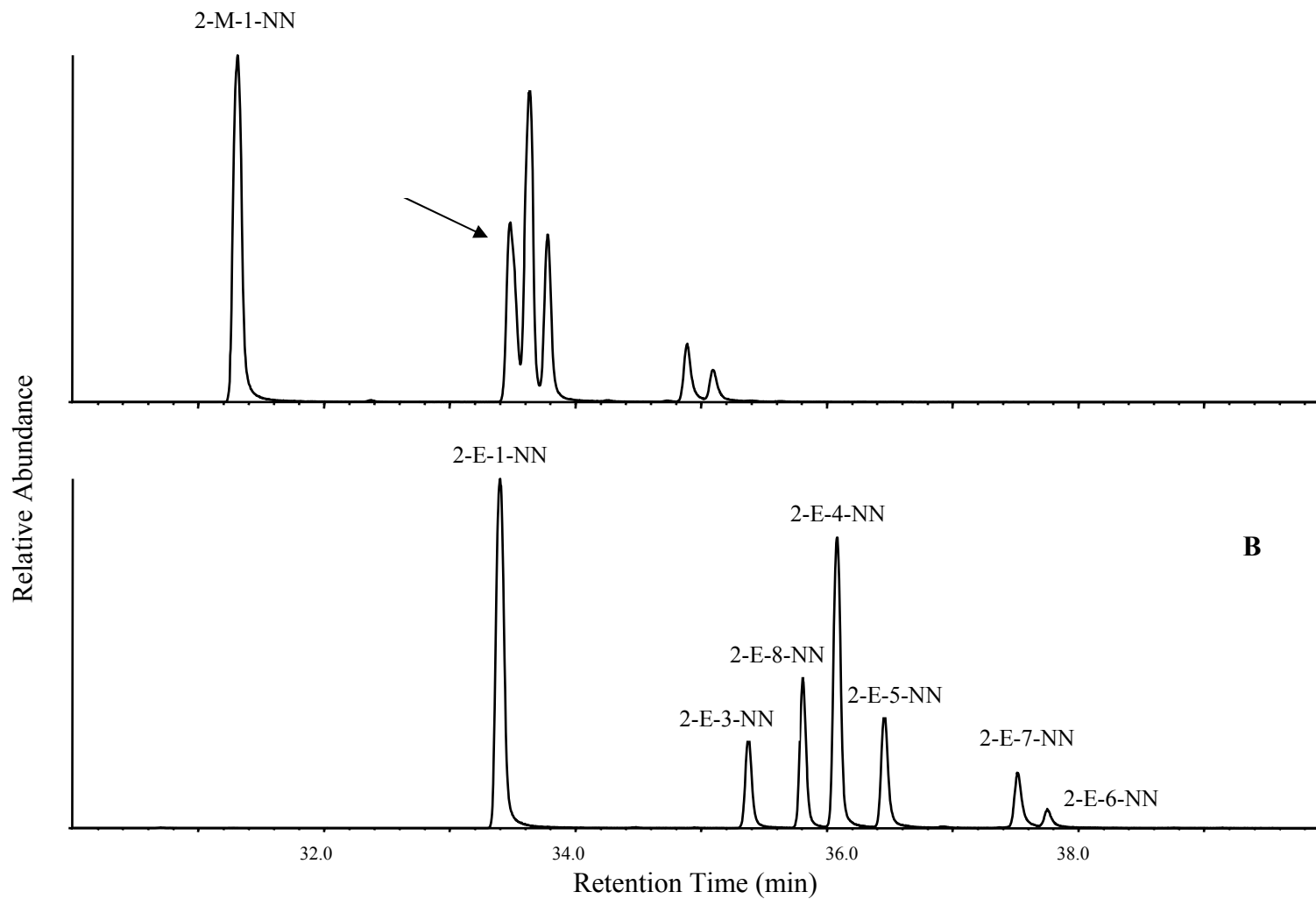
Figure 23. GC-MS/NCI profiles of the 2-M-NNs (A) and 2-E-NNs (B) formed from NO_3 radical-initiated reaction of 2-MN and 2-EN, respectively.
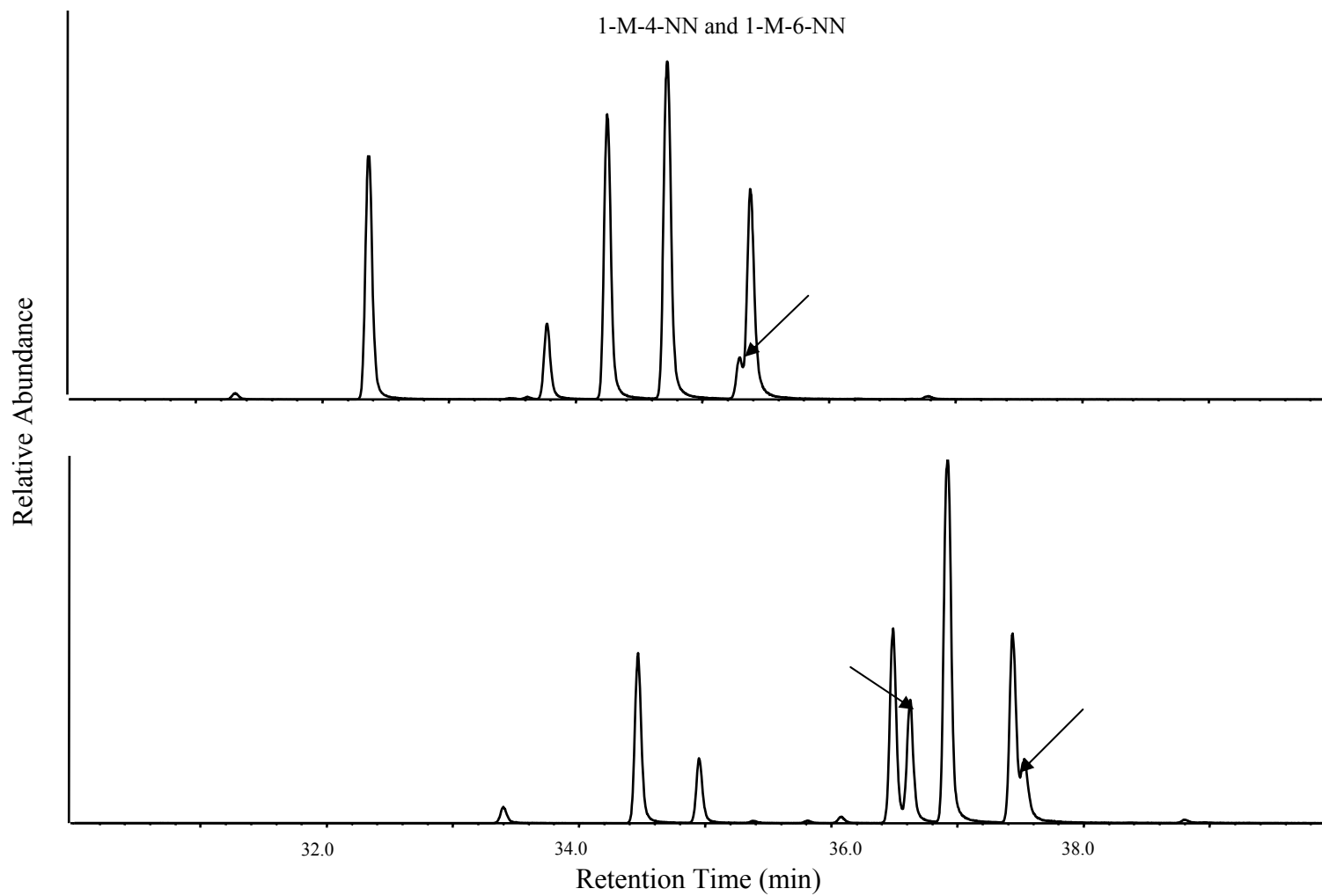
Figure 24. GC-MS/NCI profiles of the 1-M-NNs (A) and 1-E-NNs (B) formed from NO_3 radical-initiated reaction of 1-MN and 1-EN, respectively.
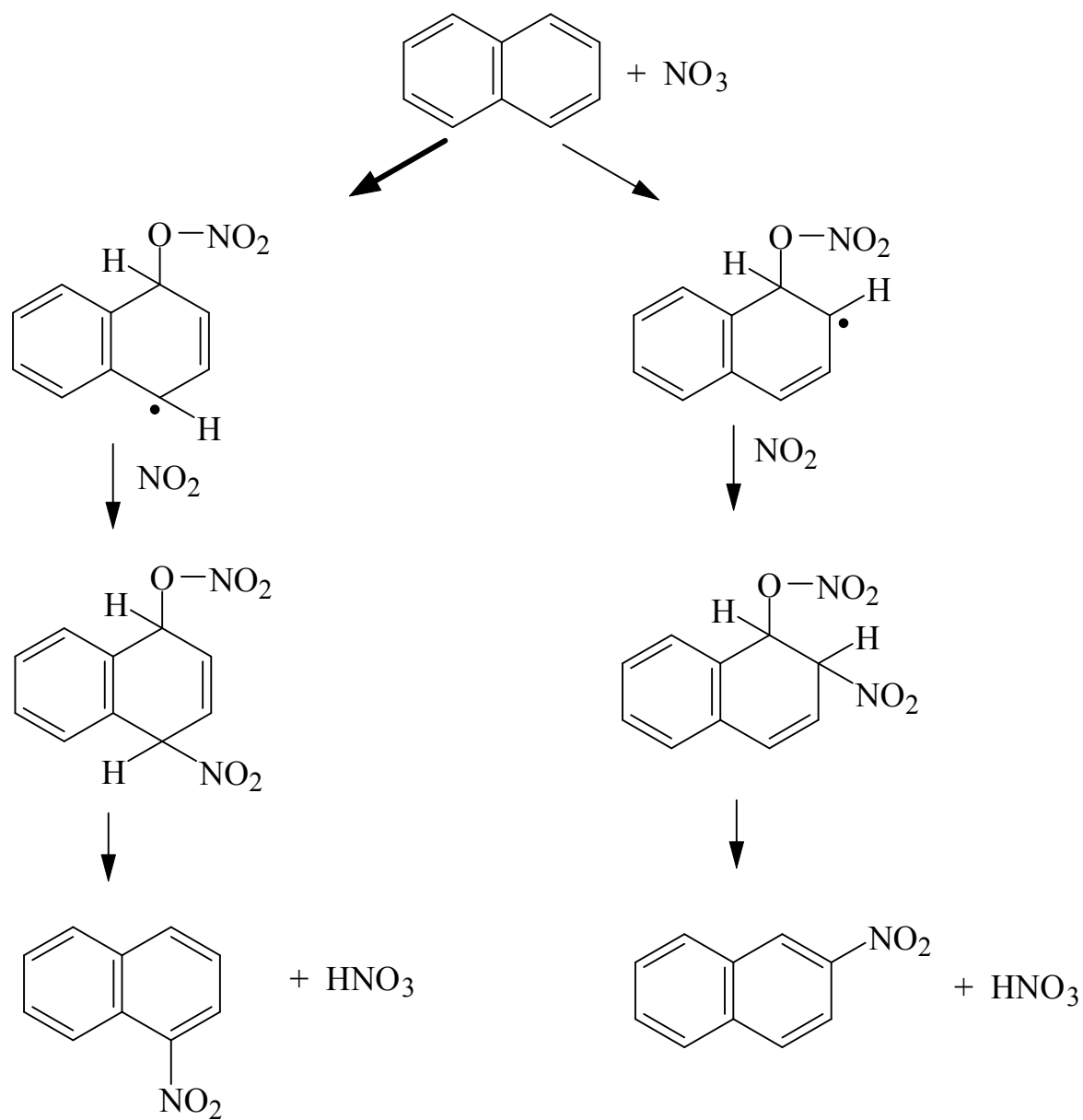
Scheme 3. Postulated mechanism for the reaction of naphthalene with the NO_3 radical showing addition at the 1-position with preferred addition of the NO_2 in the 4-position resulting in the formation of 1-NN > 2-NN.

Table 20. Solution-phase major electrophilic nitration products (Alcorn and Wells, 1965; Davies and Warren, 1969), suggested position for addition of NO_3 radical, and isomer predicted to form from naphthalene and alkylnaphthalenes.

electrophilic product	position to add NO_3	position to add NO_2	gas-phase isomer formed
1-NN	1-	*para*	1-NN
1-M-4NN	4-	*ortho*	1-M-3NN
2-M-1NN	1-	*para*	2-M-4NN
1,2-DM-4NN	*ipso*[a]	*para*	1,2-DM-4NN
1,3-DM-4NN	*ipso*[a]	*para*	1,3-DM-4NN
1,4-DM-5NN	5-	*para*	1,4-DM-5NN
1,5-DM-4NN	4-	*ortho*	1,5-DM-3NN
1,6-[b]	5-	*para*	1,6-DM-8NN
1,7-[b]	8-	*para*	1,7-DM-5NN
1,8-DM-2NN	*ipso*[a]	*para*	1,8-DM-4NN
2,3-DM-1NN	1-	*para*	2,3-DM-1NN
2,6-DM-1NN	1-	*para*	2,6-DM-4NN
2,7-DM-1NN	1-	*para*	2,7-DM-4NN

[a] Addition at the 4-position for 1,2-DMN and 1,3-DMN or at the 2-position for 1,8-DMN will not result in the correct isomer. See text for justification of assuming *ipso* addition.
[b] Electrophilic nitration product not available, assumed to be analogous to 2-MN with most electron dense site the α-carbon *ortho* to the methyl group on a β-carbon.

electrophilic nitration occurs at the 1-position. As shown in Scheme 4 addition of the NO_3 radical at the 1-position, followed by addition of NO_2 at the *para*- position and subsequent loss of nitric acid will give the most abundant nitration products observed in the gas-phase NO_3 reactions, namely, 2-M-4NN, 2,3-DM-1NN, 2,6-DM-4NN, and 2,7-DM-4NN, respectively. For 1-MN, if the NO_3 radical adds at the 4-position (note that 1-M-4NN is the electrophilic nitration product) and NO_2 adds *ortho*, loss of HNO_3 gives 1-M-3NN (see Scheme 5). Analogously, 1,5-DMN will form 1,5-DM-3NN. For 1,4-DMN, electrophilic nitration occurs at the 5-position and adding the NO_2 in the *para* position will, because of the molecule's symmetry, also form 1,4-DM-5NN. To our knowledge, the electrophilic nitration of 1,6- and 1,7-DMN have not been studied, but assuming the NO_3 will add to the α-position *ortho* to the β-methyl (i.e., analogous to the 1-position in 2-MN in Scheme 4), reaction analogous to that shown in Scheme 4 will give the major products observed, namely, 1,6-DM-8NN from 1,6-DMN and 1,7-DM-5NN from 1,7-DMN.
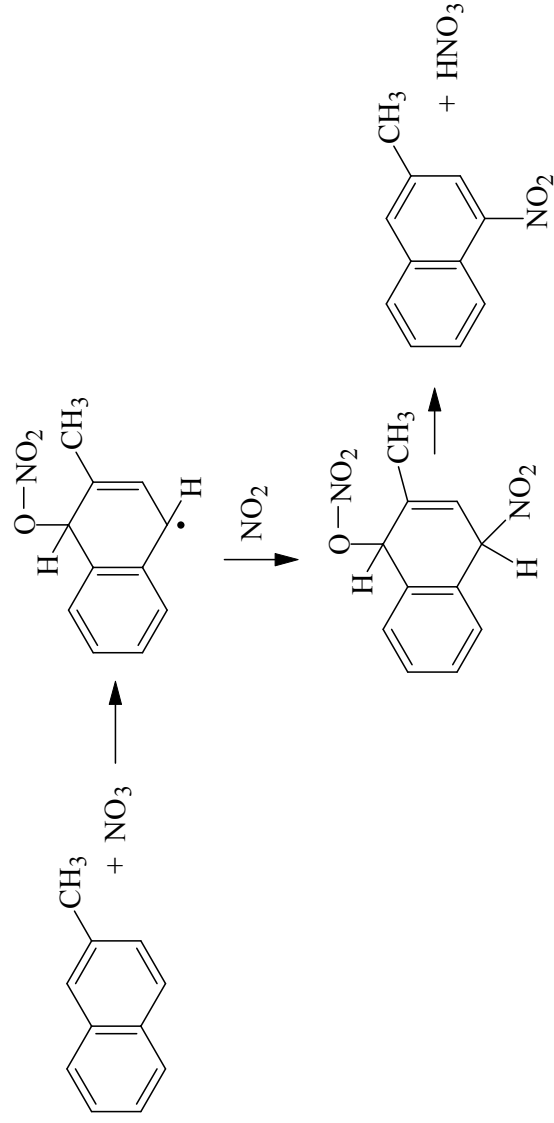
Scheme 4. Postulated mechanism of reaction of 2-MN with the NO₃ radical showing addition at the 1-position (where electrophilic reaction occurs) and NO₂ adding *para*, resulting in the formation of the most abundant isomer formed, 2-M-4NN.
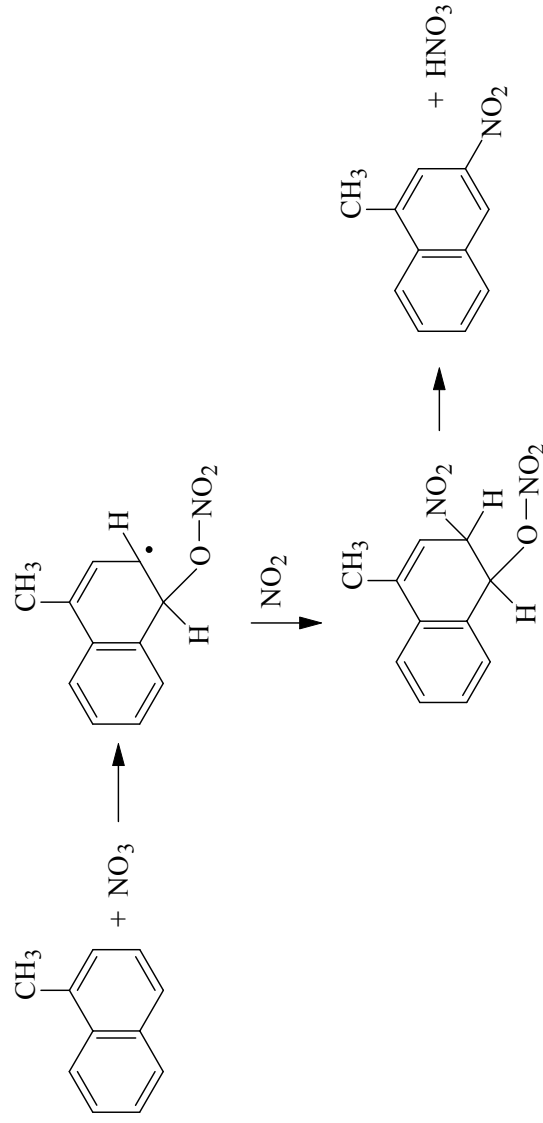
Scheme 5. Postulated mechanism of reaction of 1-MN with the NO₃ radical showing addition at the 4-position (where electrophilic reaction occurs) and NO₂ adding *ortho*, resulting in the most abundant isomer formed, 1-M-3NN. Note that 1-M-3NN would also result from addition of the NO₃ radical *ortho* to the methyl group (position 2), followed by *ortho* addition of NO₂.

94

The three remaining DMNs, 1,2-DMN; 1,3-DMN and 1,8-DMN give major nitro-products with the NO_2 group *para* to the 1-methyl. These three DMNs have the fastest rate constants for NO_3 radical reaction (Phousongphouang and Arey, 2003) with the rate constants being approximately 9, 3, and 30-fold higher, respectively, than the rate constant for 1-MN. In the earlier study of Phousongphouang and Arey (2003), it was initially speculated that the very high rate constant for 1,8-DMN might result from "overall H-atom abstraction after *ipso* addition of the NO_3 radical". However, enhanced methylnaphthalenecarboxaldehyde products which would support the importance of *ipso* addition in 1,8- and 1,2-DMN were not observed in the API-MS analyses (Phousongphouang and Arey, 2003). In this work, products were observed from the SPME analysis which eluted with retention times comparable to the nitro-products and showed only an NO_2 fragment ion at m/z 46 da in GC-MS/NCI analysis. Subsequent EI analysis of the "unidentified" product collected from a 1,2-DMN reaction showed a very small ion peak at m/z 201 and a base peak of m/z 155. We originally speculated that these products were nitrates, but the apparent small molecular ion peak at m/z 201 and recent NMR data on the product from the 1,2-DMN reaction suggests side-chain nitration forming nitro-products (see structure for example) and not nitrooxy-products:
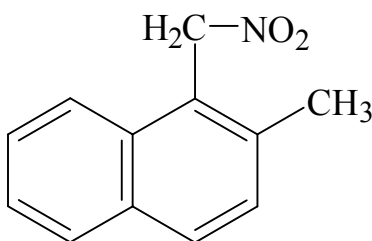
Side-chain nitration has been reported for solution phase nitrations of 1,4-DMN (Fischer and Wilkinson, 1972; Eberson and Radner, 1986; Sankararaman and Kochi, 1991; Suzuki and Mori, 1996).

The largest apparent side-chain nitration peak was seen in the 1,2-DMN reaction, followed by the 1,4-DMN, 1,8-DMN and 1,3-DMN reactions. *Ipso* addition of the OH radical to 1,2-DMN has been suggested based on the single m.w. 188 dicarbonyl observed in the 1,2-DMN + OH radical reaction (see Section C). A reaction mechanism involving *ipso* addition to the methyl group on C_1 is shown in Scheme 6 and would give the observed major nitro-products, namely, 1,2-DM-4NN, 1,3-DM-4NN and 1,8-DM-4NN from 1,2-; 1,3- and 1,8-DMN, respectively. It is unclear what the gas-phase products from *ipso* addition of 1,4-DMN would be. The possibility of heterogeneous reaction on the chamber walls during our "gas-phase" reactions of DMNs with the NO_3 radical cannot be ruled out at this time.

Shown in Table 19 are formation rates of the nitroarene products from reactions of dimethyl-/ethyl-lnaphthalenes with NO_3 radicals calculated using the expression $[\text{Nitroarene}]_t = k_{obs} \times [NO_3] \times [NO_2] \times Y \times [\text{alkylnaphthalene}] \times t$, where $[\text{Nitroarene}]_t$ is the amount formed after time t, k_{obs} is the rate constant for reaction of alkylnaphthalene with NO_3 radicals, and Y is the formation yield of nitroarenes from the reaction of alkylnaphthalene with NO_3 radicals. An average 12-hr NO_3 radical concentration of 5×10^8 molecule cm^{-3} (Atkinson, 1991) and a background 12-hr NO_2 concentration of 4.8×10^{11} molecule cm^{-3} (20 ppbv) during sample

collection (CARB) were assumed. The concentrations of alkylnaphthalenes used were those measured from 19:00-06:30 during Aug. 26-30, 2002, in Riverside, CA (Reisen and Arey, 2005). The isomers with the highest mass formation rates from the NO_3 radical initiated reactions with dimethyl-/ethyl-naphthalenes are 2,7-DM-4NN, 1,2-DM-4NN, 2,6-DM-4NN, 2,6-DM-1NN, 1,6-DM-8NN and 2,7-DM-1NN.
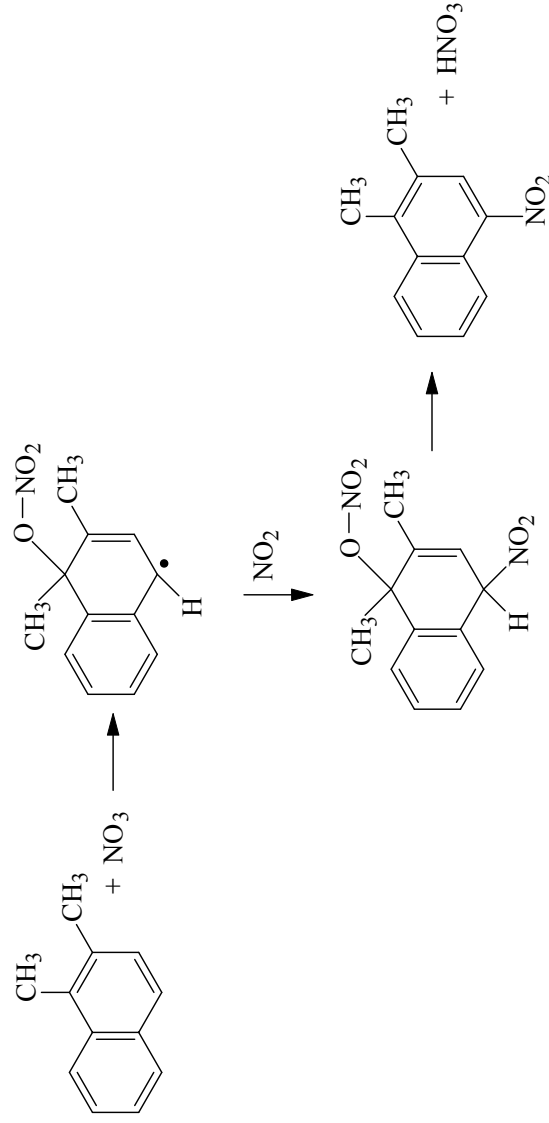
Scheme 6. Postulated mechanism of reaction of 1,2-DMN with the NO_3 radical showing *ipso* addition.

Profiles of alkylnitronaphthalenes. Figure 25 shows GC-MS/NCI profiles of the dimethyl-/ethyl-nitronaphthalene molecular ions obtained from the reaction of NO_3 radicals with a mixture of dimethyl/ethyl-naphthalenes in the chamber (Figure 25-A); from nighttime ambient air samples collected in Riverside, CA on Jul. 15, 2006 (Figure 25-B); and from nighttime ambient air samples collected in Redlands, CA on Oct. 27, 1994 (Figure 25-C). Figure 26 shows GC-MS/NCI profiles of the dimethyl-/ethyl-nitronaphthalene molecular ions obtained from the reaction of OH radicals with a mixture of dimethyl/ethyl-naphthalenes in the chamber (Figure 26-A); from morning ambient air samples collected in Mexico City on Apr. 25, 2003 (Figure 26-B); and from nighttime ambient air samples collected in Mexico City on Apr. 23, 2003 (Figure 26-C). [The numbered peaks are identified on Table 21.]

The ambient samples were extracted from PUF plugs which were located beneath a filter in the Hi-Vol sampler. The PUF plugs collected, therefore, both the gas-phase DMNNs/ENNs and any of these compounds that were "blown-off" from the particles on the filter during the sampling. The majority of DMNNs/ENNs were observed in the PUF plug extracts rather in the filter extracts (Reisen *et al.*, 2003). The profile of DMNNs/ENNs from the NO_3 radical-initiated chamber reaction was obtained using the SPME collection method for convenience.
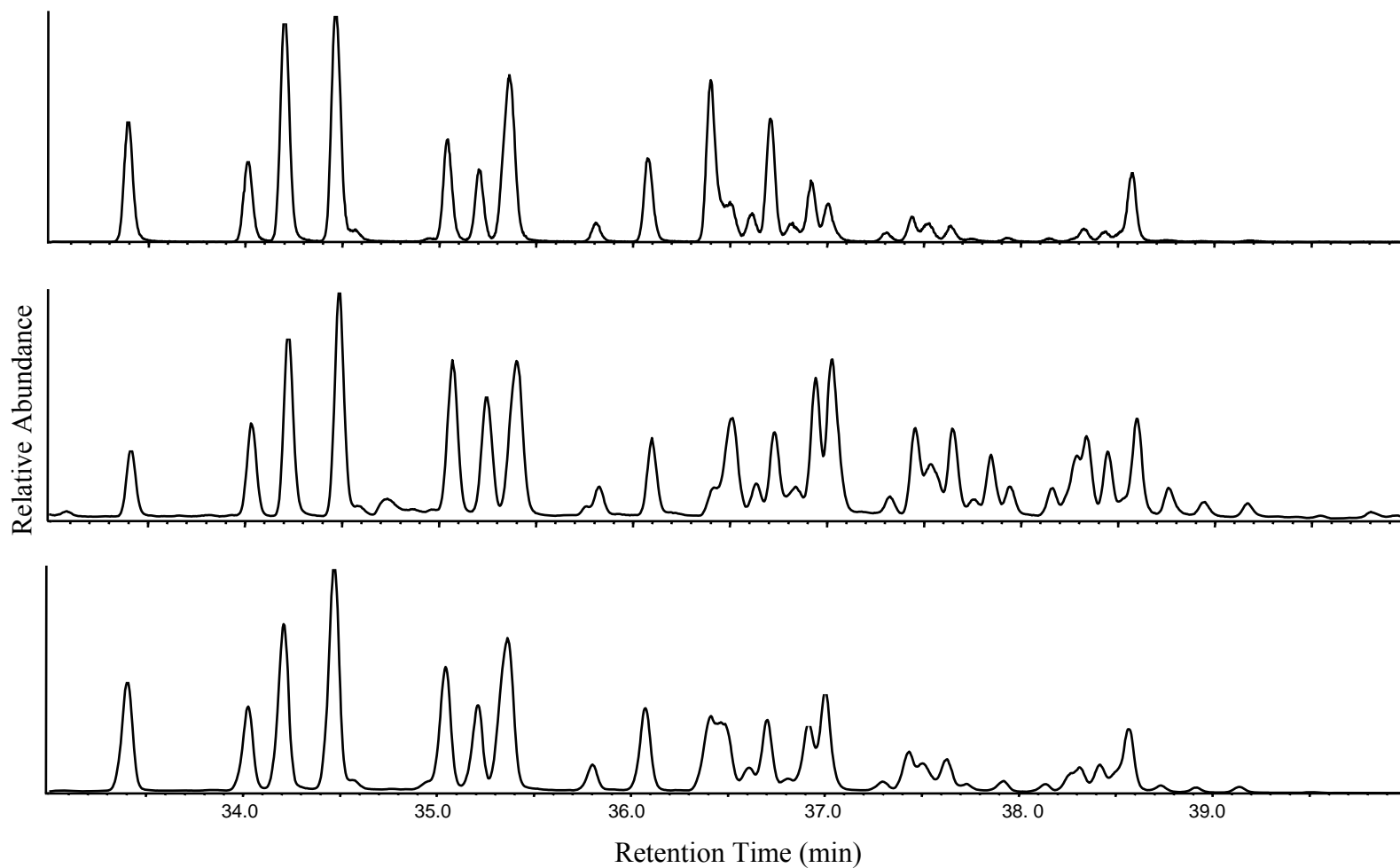
Figure 25 . GC-MS/NCI profiles of the dimethyl-/ethyl-nitronaphthalene molecular ions obtained from: (A) the reaction of NO_3 radicals with a mixture of dimethyl/ethyl-naphthalenes in the chamber; (B) nighttime ambient air samples collected in Riverside, CA on July 15, 2006; (C) nighttime ambient air samples collected in Redlands, CA on Oct. 27, 1994. The peak numbers correspond to identities of the DMNN/ENN isomers in Table 21.
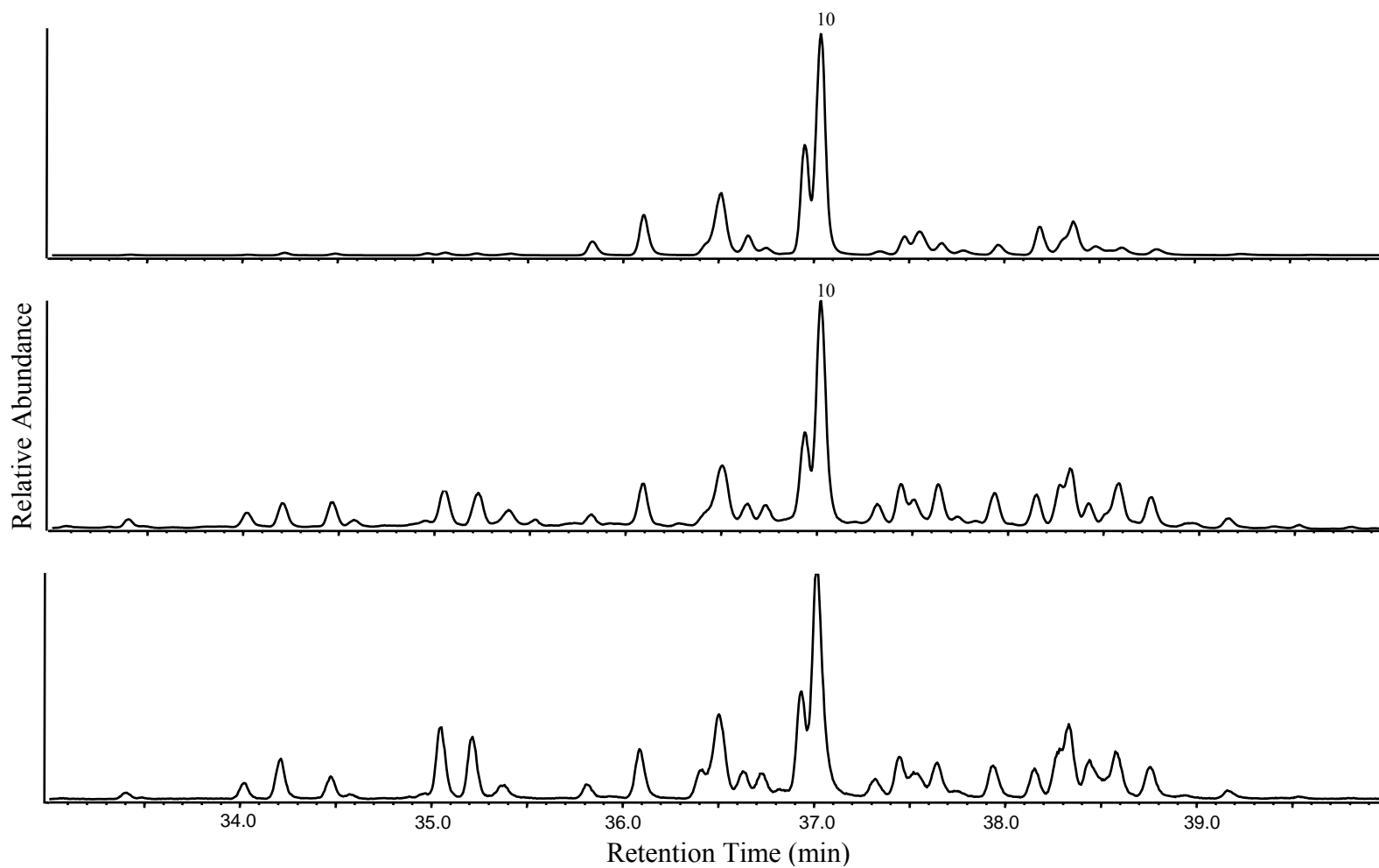
Figure 26. GC-MS/NCI profiles of the dimethyl-/ethyl-nitronaphthalene molecular ions obtained from: (A) the reaction of OH radicals with a mixture of dimethyl/ethyl-naphthalenes in the chamber; (B) morning ambient air samples collected in Mexico City on Apr. 25, 2003; (C) nighttime ambient air samples collected in Mexico City on Apr. 23, 2003. The peak numbers correspond to identities of the DMNN/ENN isomers in Table 21.

Table 21. Dimethyl-/ethyl-nitronaphthalene isomers that are suggested as markers for gas-phase reactions of dimethyl-/ethyl-naphthalenes with OH radicals and NO_3 radicals, and the retention time and retention indices (RIs) of standards.

gas-phase reaction with							
NO_3 radicals				OH radicals			
peak #[a]	name of isomer	retention time (min)	RIs	peak #[a]	name of isomer	retention time (min)	RIs
1	2-E-1NN	33.525	219.3	9	1,3-DM-5NN	37.036	242.8
2	1,7-DM-8NN	34.102	223.2		1-E-4NN	37.050	242.8
3	2,7-DM-1NN	34.328	224.4	10	1,7-DM-5NN	37.088	243.0
4	2,6-DM-1NN[b]	34.597	226.4		1,6-DM-2NN	37.162	243.5
	1-E-8NN[b]	34.552	226.2				
5	1,6-DM-5NN	35.137	230.1				
6	1,3-DM-4NN	35.303	231.2				
7	1,6-DM-8NN	35.415	231.9				
	2,3-DM-1NN	35.452	232.1				
	2-E-3NN	35.452	232.2				
	1,3-DM-8NN	35.465	232.3				
8	2,7-DM-4NN[c]	36.847	241.2				
	1,7-DM-2NN[c]	36.817	241.2				
11	1,2-DM-4NN[d]	38.677	253.7				
	1,7-DM-3NN[d]	38.608	253.2				

[a]Peak numbers are from Figures 25 and 26.

[b]Based on Table 19, this peak is expected to be mainly 2,6-DM-1NN.

[c]Based on Table 19, this peak is expected to be mainly 2,7-DM-4NN.

[d]Based on Table 19, this peak is expected to be mainly 1,2-DM-4NN.

For the OH radical-initiated chamber reaction, a filter/PUFs sample collection with Soxhlet extraction and HPLC fractionation was used. The sample fractionation was required to separate dimethyl-/ethyl-hydroxynitronaphthalenes (m/z = 217 da), which are formed in higher yields, from the DMNNs/ENNs. The GC elution of the hydroxynitro-species overlapped with the DMNNs/ENNs and the abundance of a small fragment due to loss of oxygen (m/z 201 da = [M-O]$^-$) overwhelmed the [M]$^-$ molecular ion signals from the DMNNs/ENNs. Since the hydroxynitro-species elute later from the HPLC than the DMNNs/ENNS, HPLC fractionation removed their interference. The PUF plug extracts and the filter extracts were combined together before HPLC fractionation, as DMNNs/ENNs could be trapped on the filter during the large volume sample collection after the OH radical-initiated chamber reaction.

Clearly the profiles of dimethyl-/ethyl-nitronaphthalenes from gas-phase reactions with NO$_3$ radicals (Figure 25-A) and OH radicals (Figure 26-A) show distinct patterns. Using the retention indices (Gallagher, 2006; Section D) and the calculated formation rates, 2-E-1NN, 1,7-DM-8NN, 2,7-DM-1NN, 2,6-DM-1NN, 1,6-DM-5NN, 2,7-DM-4NN and 1,2-DM-4NN, which correspond to Peak #'s 1, 2, 3, 4, 5, 8 and 11 in Figure 25 and Figure 26, are proposed to be DMNN/ENN isomer markers from NO$_3$ radical initiated reactions. Note that there are small amounts of co-eluting isomers in addition to the main DMNN/ENN noted above in Peak #'s 4, 8 and 11 (Table 21). For OH radical-initiated reactions, 1,3-DM-5NN/1-E-4NN and 1,7-DM-5NN/1,6-DM-2NN are proposed as potential markers of OH radical reaction because of their relatively high abundance.

There are tens of DMNN/ENN isomers in the ambient samples and their possible identities have been discussed elsewhere (Gallagher, 2006 and Section D). The isomer profiles from a Riverside nighttime sample (Figure 25-B) and an archived Redlands nighttime sample (Figure 25-C) are characterized by high abundances of Peak #'s 1, 2, 3, 4, 5, suggesting an important contribution from NO$_3$ radical chemistry to the DMNNs/ENNs observed. In contrast, the ion profiles from Mexico City (Figure 26-B and -C) are dominated by peaks #'s 9 and 10, which suggest their formation from OH radical-initiated reaction. Using the ratio of 2-E-1NN to 1,7-DM-5NN/1,6-DM-2NN (peak #1/peak #10), it is concluded that NO$_3$ radical chemistry is relatively more important in the Redlands sample than in the Riverside sample. Redlands is a receptor site further downwind than Riverside and the Redlands sample was collected during an ozone episode in 1994 and, therefore, higher levels of the NO$_3$ radical than occurred in Riverside in 2003 were likely to be present. Using the same ratio, Mexico City morning and nighttime samples indicate that daytime formation of DMNNs/ENNs dominates over nighttime formation. It should be noted that the Mexico nighttime sample had a relatively higher abundance of 2,7-DM-1NN, 1,6-DM-5NN and 1,6-DM-8NN (Peak #'s 3, 5 and 6) than that from the chamber OH reaction, suggesting some formation through NO$_3$ reaction. This is in contrast to the MNN profiles obtained from the same sample, which suggests no occurrence of NO$_3$ chemistry (Atkinson and Arey, 2007). However, the change to the nitro-isomer profile from DMN/EN reactions with NO$_3$ radicals may be more obvious than for MN reactions where only 2-M-1NN and 2-M-4NN are significantly elevated relative to the OH reaction products. Since the early peaks which are suggested as markers of NO$_3$ reaction all have the NO$_2$ groups *ortho* or *peri* to a methyl group, they would be expected to rapidly photolyze [Phousongphouang and Arey, 2003 and Section F). Further research on the OH radical-initiated products of the DMNs/ENs and their photolysis is required before it can definitely be stated that NO$_3$ radical-initiated reactions contributed to the DMNNs/ENNs in Mexico City.

The presence of DMNNs/ENNs in ambient samples will undoubtedly contribute to the vapor-phase mutagenic activity. It is possible that nitronaphthalenes, methylnitronaphthalenes, dimethynitronaphthalenes and ethylnitronaphthalenes might account for most of the mutagenicity, measured by Gupta *et al*. for ambient gas-phase samples from Redlands, CA (Gupta *et al.*, 1996). Clearly, isomer-specific genotoxicity tests of DMNNs/ENNs are needed to evaluate the potential health effect of these compounds.

F. Oxygenated Products, Including Quinones, from NO$_3$ Radical-Initiated Reactions of PAHs and from Nitro-PAH Photolysis

1. Introduction

Naphthalene and its C$_1$- and C$_2$-alkyl derivatives, which are present in the atmosphere predominantly in the gas phase (Bidleman, 1988; Wania and Mackay, 1996), have been observed to be the most abundant semi-volatile polycyclic aromatic hydrocarbons (PAHs) in ambient air (Arey *et al.*, 1989; Reisen and Arey, 2005). An important source of these compounds in urban areas is vehicle exhaust, especially from diesel-fueled vehicles (Fraser *et al.*, 1998; Zielinska *et al.*, 2004). In the atmosphere, naphthalene and its C$_1$- and C$_2$-alkyl derivatives undergo chemical transformations with OH and NO$_3$ radicals (Phousongphouang and Arey, 2002; 2003), with the daytime OH radical reaction being estimated to dominate as the atmospheric loss process (Arey, 1998). The products identified from the OH radical-initiated reactions of naphthalene and its C$_1$- and C$_2$-alkyl derivatives include a wide range of compound classes including dicarbonyls, alcohols, epoxides, nitro- and hydroxynitro-derivatives, and quinones (Atkinson *et al.*, 1987; Zielinska *et al.*, 1989; Sasaki *et al.*, 1997; Bunce *et al.*, 1997; Wang, 2006; Wang *et al.*, 2007a,b; see Sections B and C). In contrast, product studies of the NO$_3$ radical-initiated reactions of PAHs, including the C$_1$- and C$_2$-alkylnaphthalenes, have generally concentrated on nitroarene formation. (Pitts *et al.*, 1985; Atkinson *et al.*, 1987; Zielinska *et al.*, 1989; Sasaki *et al.*, 1997; see also Section E).

The toxicity of aldehydes (O'Brien *et al.*, 2005) has recently been reviewed and various diseases, particularly those associated with aging, have been associated with the accumulation of aldehydes (O'Brien *et al.*, 2005). There are numerous studies on the formation of smaller aldehydes by atmospheric gas-phase reactions (Atkinson and Arey, 2003 and references therein), but PAH-aldehydes have received little attention.

Quinones are able to create a variety of hazardous effects *in vivo*, including acute cytotoxicity, immunotoxicity, and carcinogenesis, with many of these toxic effects being attributed to their ability to form reactive oxygen species (ROS) and cause oxidative stress (Bolton *et al.*, 2000). It has been hypothesized that 9,10-phenanthrenequinone may play a role in the pulmonary toxicity of diesel exhaust particles (Hiyoshi *et al.*. 2005) and the majority of ROS generation by extracts from ambient particles collected in Fresno, CA has been attributed to 9,10-phenanthrenequinone (Chung *et al.*, 2006). Our recent work has shown that gas-phase NO$_3$ radical-initiated reaction of phenanthrene may be an important source of ambient 9,10-phenanthrenequinone (Section A and Wang *et al.*, 2007a).

In this work, we measured the yields of oxygenated products formed from the NO$_3$ radical-initiated reactions of naphthalene and its C$_1$- and C$_2$-alkyl derivatives. Because the photolysis of 1-nitronaphthalene and 2-methyl-1-nitronaphthalene have been reported to yield quinones (Atkinson *et al.*, 1989; Arey *et al.*, 1990), the photolysis of selected alkyl-nitronaphthalenes was also conducted to evaluate the potential for atmospheric alkylnaphthoquinone formation through this route.

2. Experimental Methods

Experiments were carried out in a ~7500 liter Teflon chamber, equipped with two parallel banks of blacklamps, at 296 ± 2 K and 735 Torr total pressure of purified air at ~5% relative humidity. The chamber is also equipped with a Teflon-coated fan to ensure rapid mixing of reactants during their introduction into the chamber. Naphthalene, alkylnaphthalenes and

alkylnitronaphthalenes were introduced into the chamber by flowing nitrogen gas through a Pyrex bulb containing a measured amount of the liquid or solid compound while heating the bulb and inlet tube.

NO$_3$ radicals were generated from the thermal decomposition of N$_2$O$_5$, and NO$_2$ was also included to lengthen the reaction times (Atkinson *et al.*, 1984). NO, NO$_2$ and N$_2$O$_5$ were flushed into the chamber without heating. The NO and NO$_2$ concentrations during the experiments were monitored using a NO-NO$_2$ chemiluminescene analyzer. The chamber was cleaned after each experiment by flushing with pure air for at least 24 hours and with the chamber lights on for at least 8 hours.

Oxygenated products formed from the NO$_3$ radical-initiated reactions. The initial reactant concentrations (molecule cm^{-3}) were: naphthalene or alkylnaphthalene, ~7.2 x 10^{12}; N$_2$O$_5$, ~2.4 x 10^{13} and NO$_2$, ~2.4 x 10^{13}. An excess of NO was added to the reaction mixture to quench the NO$_3$ radical prior to carrying out post-reaction analyses. The NO was added 4-24 min after the N$_2$O$_5$, resulting in 17-55% consumption of the initial naphthalene (5 replicate experiments) or 40-50% consumption of the initial alkylnaphthalenes (2 replicate experiments for each of 1-MN and 1,6-DMN;1 experiment for each of the other isomers).

The concentrations of naphthalene, alkylnaphthalenes, and their oxygenated and nitroarene products were measured during the experiments by gas chromatography with flame ionization detection (GC-FID). 6.0 Liter volume gas samples were collected from the chamber onto Tenax-TA solid adsorbent cartridges using a pump with mass flow controller (Tylan General) at a flow rate of 400 cm^3 min^{-1} to quantify naphthalene, alkylnaphtahlenes, and their oxygenated and nitroarene products. In addition, a gas-tight all-glass syringe was used to pull 100 cm^3 volume gas samples onto a Tenax-TA solid adsorbent cartridge to quantify naphthalene and alkylnaphthalenes. The Tenax solid adsorbent samples were thermally desorbed in the injection port (270 ^{o}C) of a Hewlett-Packard (HP) 5890 series II GC onto a 30-m DB-5MS capillary column (0.53 mm i.d., 1.5 μm phase) held at 40 ^{o}C for 10 min and then temperature programmed to 140 ^{o}C at 20 ^{o}C min^{-1}, then to 280 ^{o}C at 5 ^{o}C min^{-1} and held at 280 ^{o}C for 10 min.

Solid Phase MicroExtraction (SPME) samples were collected by exposing a 65 μm polydimethylsiloxane/divinylbenzene (PDMS/DVB) fiber to the chamber contents for 5 min with the mixing fan on. The SPME fiber samples were then thermally desorbed in the heated (270 ^{o}C) injection port of an Agilent Technologies 6890N GC interfaced to an Agilent Technologies 5975 inert XL mass selective detector (MSD), onto a 30-m HP-5MS capillary column (0.25 mm i.d., 0.25 μm phase) held at 40 ^{o}C and then temperature programmed to 250 ^{o}C at 4 ^{o}C min^{-1}. The mass spectrometry (MS) was conducted in the negative chemical ionization (NCI) mode, using methane as the reagent gas.

Additional SPME samples were collected for variable times as described above. The SPME fiber samples were then analyzed by (1) the above Agilent Technologies 6890N GC interfaced to the Agilent Technologies 5975 inert XL MSD, operated in positive chemical ionization (PCI) mode using methane as the reagent gas; (2) a HP 5890 GC with a 60-m DB-5MS capillary column (0.25 mm i.d., 0.25 μm phase), interfaced to a HP 5971 MSD operated in electron ionization (EI) mode; or (3) a Varian 2000 GC/MS/MS ion trap system with 30-m DB-1 capillary column (0.32 mm i.d., 3.0 μm phase) operated in EI mode.

GC-FID responses for naphthalene, alkylnaphthalenes, 2-methyl-1-nitronaphthalene (2-M-1-NN), 2,6-dimethyl-1-nitronaphthalene (2,6-DM-1-NN), 1- and 2-naphthaldehyde, 1,4-naphthoquinone (1,4-NQ) and 2-methyl-1,4-naphthoquinone (2-M-1,4-NQ) were determined by spiking methanol solutions of authentic standards onto Tenax-TA solid adsorbent cartridges with

GC-FID analyses as described above. The GC-FID responses for methylnaphthaldehydes, acetylnaphthalenes and dimethyl-/ethyl-naphthoquinones (DMNQs/ENQs) were estimated from the measured response factors for naphthaldehydes and 2-methyl-1,4-naphthoquinone, and their Effective Carbon Numbers (Scanlon and Willis, 1985).

DMNQ/ENQ profiles from chamber reaction. A methanol solution of dimethylnaphthalenes (DMNs) and ethylnaphthalenes (ENs), including 1-EN, 2-EN, 1,2-DMN, 1,3-DMN, 1,4-DMN, 1,5-DMN, 1,6-DMN, 1,7-DMN, 2,3-DMN, 2,6-DMN and 2,7-DMN, was made. The ratios of isomers in the solution were chosen to mimic those obtained from previous ambient measurements (Phousongphouang and Arey, 2003; Reisen and Arey, 2005), and it should be noted that 1,8-DMN was not found in these ambient samples.

For the NO_3 radical reaction, the initial reactant concentrations (molecule cm^{-3}) were: $\sum DMNs + ENs$, $\sim$7.2 x 10^{12}; N_2O_5, $\sim$2.4 x 10^{13} and NO_2, $\sim$2.4 x 10^{13}. An excess amount of NO was subsequently added into the reaction mixture to quench the NO_3 radical reaction, resulting in $\sim$40% consumption of the initial alkylnaphthalenes. SPME samples were collected by exposing a PDMS/DVB fiber to the chamber contents for 15 min with the mixing fan on and analyzed by the GC-MS/NCI method as described above.

Photolysis of 2-M-1NN and 2,6-DM-1NN. The initial reactant concentrations (molecule cm^{-3}) were: alkylnitronaphthalene, $\sim$3.6 x 10^{11}; CH_3OH (used as a solvent for the alkylnitro-naphthalene mixture), $\sim$2.4 x 10^{14}; NO or NO_2, 0-2.4 x 10^{14}; and cyclohexane (added to scavenge any OH radicals formed), $\sim$7.2 x 10^{14}. Irradiations were carried out at 50% of the maximum light intensity for 9-11 min. The concentrations of alkylnitronaphthalenes and aklylnaphthoquinones were measured using Tenax cartridges (6.0 liter volume gas samples) and SPME, respectively, followed by GC-FID and GC-MS/NCI analyses as described above.

Chemicals. The chemicals used, and their stated purities, were as follows: naphthalene (98%), 1-MN (99%), 2-MN (98%), 1-EN (98+%), 2-EN (99+%), 1,2-DMN (98%), 1,3-DMN (96%), 1,4-DMN (95%), 1,5-DMN (98%), 1,6-DMN (99%), 1,7-DMN (99%), 1,8-DMN (95%), 2,3-DMN (98%), 2,6-DMN (99%), 2,7-DMN (99%), 2-methyl-1-nitronaphthalene (99%), 1-naphthaldehyde (97%), 2-naphthaldehyde (98%), 1,4-naphthoquinone (97%), 2-methyl-1,4-naphthoquinone (98%), Aldrich Chemical Company; 2,6-dimethyl-1-nitronaphthalene, synthesized by Gallagher and Arey (see Section D); and NO ($\geq$99.0%), Matheson Gas Products. N_2O_5 was prepared and stored as described previously (Atkinson *et al.*, 1984).

3. Results and Discussion

Yields of oxygenated products. The concentrations of naphthalene and alkylnaphthalenes monitored in the dark showed generally small decreases, attributed to wall losses, which were not taken into account when calculating the yields of alkylnitronaphthalenes. In contrast, $\sim$20% decays of oxygenated products were observed over 1.0 hr. Thus the amounts of oxygenated products formed were quantified using a 15 min Tenax sample immediately after the NO_3 radical-initiated reaction. The yields should be viewed as lower limits since wall losses are likely to occur during the sampling.

Oxygenated product peaks were identified on the GC-FID chromatograms by comparing these with the GC-MS total ion current (TIC) analysis and using (alkyl)-nitronaphthalenes formed from the same reactions as retention time references. The yields obtained for the oxygenated products, together with the nitroarene yields (see Section E), are tabulated in Table 22, and Table 23 shows a comparison with the available literature values.

Table 22. Oxygenated and nitroarene products formed from the NO_3 radical-initiated reactions of naphthalene, methylnaphthalenes (MNs), ethylnaphthalenes (ENs) and dimethylnaphthalenes (DMNs), and their molar formation yields.

parent	products					
	aldehydes/ketones	% yields[a]	quinones	% yields[a]	Σ nitroarenes	% yields[a]
naphthalene			1,4-NQ[b]	3.6 ± 0.5	Σ NN[b]	26.0 ± 1.4
1-MN	1-naphthaldehyde[b]	5.9 ± 1.0	1-M-5,8-NQ	0.7 ± 0.5	Σ1-M-NN[b]	12 ± 2
2-MN	2- naphthaldehyde[b]	2.1; 2.1	2-M-1,4-NQ[b]	3.4; 3.3	Σ 2-M-NN[b]	21
			2-M-5,8-NQ	0.6; 0.6		
1-EN	1-acetylnaphthalene	3.4; 3.3[c]	1-E-5,8-NQ	0.3; 0.2[c]	Σ 1-E-NN[b]	12
2-EN	2-acetylnaphthalene	3.9; 3.5	2-E-1,4-NQ	1.8; 1.6	Σ 2-E-NN[b]	19
			2-E-5,8-NQ	0.4; 0.4		
1,2-DMN	1-methyl-2- naphthaldehyde	observed[d]			Σ 1,2-DM-NN[b]	12
	2-methyl-1- naphthaldehyde	observed[d]				
1,3-DMN	1-methyl-3- naphthaldehyde	observed[d]	1,3-DM-5,8-NQ	observed[d]	Σ1,3- DM-NN[b]	4
	3-methyl-1- naphthaldehyde	observed[d]				
1,4-DMN	4-methyl-1-naphthaldehyde	7.3; 5.9			Σ 1,4-DM-NN[b]	5
1,5-DMN	5-methyl-1-naphthaldehyde	2.7; 2.5			Σ 1,5-DM-NN[b]	9
1,6-DMN	methyl- naphthaldehyde[e]	1.7 ± 0.5	1,6-DM-5,8-NQ	1.8 ± 0.3	Σ 1,6-DM-NN[b]	15 ± 2
1,7-DMN	methyl- naphthaldehyde[f]	1.8; 1.6[g]	1,7-DM-5,8-NQ	0.8; 0.7[g]	Σ 1,7-DM-NN[b]	13
1,8-DMN	8-methyl-1-naphthaldehyde	4.2; 3.4			Σ 1,8-DM-NN[b]	18
2,3-DMN	3-methyl-2-naphthaldehyde	1.5; 1.2	2,3-DM-1,4-NQ	4.1; 3.2	Σ 2,3-DM-NN[b]	14
2,6-DMN	6-methyl-2-naphthaldehyde	1.3; 1.1	2,6-DM-1,4-NQ	2.2; 1.8	Σ 2,6-DM-NN[b]	14
2,7-DMN	7-methyl-2-naphthaldehyde	0.7; 0.6	2,7-DM-1,4-NQ	3.9; 3.6	Σ 2,7-DM-NN[b]	21

Table 23 Oxygenated and nitroarene products formed from the NO_3 radical-initiated reactions of naphthalene and methylnaphthalenes (MNs), and their molar formation yields with comparison to literature data.

parent	products					
	aldehydes	% yields[a]	quinones	% yields[a]	Σ nitros	% yields[a]
naphthalene			1,4-NQ[b]	3.6 ± 0.5	Σ NNs[b]	26.0 ± 1.4
				1.9 ± 1.1[c]		35.4 ± 7.5[c]
						24.7 ± 3.6[d]
						22.2 ± 3.1[e]
1-MN	1-naphthaldehyde[b]	5.9 ± 1.0	1-M-5,8-NQ	0.7 ± 0.5	Σ 1-M-NNs[b]	12 ± 2
						~30[f]
2-MN	2- naphthaldehyde[b]	2.1; 2.1	2-M-1,4-NQ[b]	3.4; 3.3	Σ 2-M-NNs[b]	21
			2-M-5,8-NQ	0.6; 0.6		~30[f]

[a] Yields are lower limits (see text) and indicated errors are two standard deviations derived from 5 (naphthalene), or 2 (1-MN and 1,6-DMN) replicate experiments. The listed yields from 2-MN are two measurements in one experiment.

[b] Authentic standards available.

[c] Sasaki *et al*. (1997).

[d] Pitts *et al*. (1985).

[e] Atkinson *et al*. (1987).

[f] Zielinska *et al*. (1989).

Our measured yields of 1,4-naphthoquinone and nitronaphthalenes formed from the reaction of naphthalene with NO_3 radicals are in good agreement with those previously reported (Pitts *et al.*, 1985; Atkinson *et al.*, 1987; Sasaki *et al.*, 1997). Our yield value, ($\sum$ 2-M-NNs = 21%), is close to the approximate value, ($\sum$ 2-M-NNs ~30%), given by Zielinska *et al.* (1989), but our yield value for ($\sum$ 1-M-NNs) is significantly lower than that of Zielinska *et al.* (1989). The pattern of nitration, i.e., the isomer distribution of the 2-E-NNs, we observed for 2-EN was very similar to the 2-M-NNs we observed from 2-MN (see Figure 23 in Section E). Similarly, the relative yields for the various positions of nitration for 1-EN and 1-MN appeared very similar (see Figure 24 in Section E). We also observed in each case lower yields of nitration for the α-alkyl-substituted naphthalene relative to the β-alkyl-substituted naphthalene, *i.e.*, both 1-MN and 1-EN gave a 12% yield of nitration products while 2-MN and 2-EN gave 21% and 19%, respectively. The nitroarene yields from the gas phase reactions of (alkyl-)naphthalenes with NO_3 radicals are in the range of 4-26%. Both (alkyl-)naphthoquinones and (alkyl-) nitronaphthalenes are formed from NO_3 radical addition to the aromatic ring.

Our measured yields of (methyl-)naphthaldehydes and acetylnaphthalenes are less than 8%. Note that an aldehyde peak was observed by GC-MS/NCI to be formed from every methyl group, i.e., 2 isomers were observed for 1,2-; 1,3-; 1,6-; and 1,7-DMN. For the ethylnaphthalenes, only acetylnaphthalenes formed after H-atom abstraction from the –CH_2- group were observed, consistent with the expected higher reactivity of the –CH_2- hydrogens compared to those of the CH_3 group (Atkinson, 1991). Note that the acetylnaphthalenes were confirmed by the presence of a characteristic $[M-CH_3]^+$ ion in the GC-MS/EI analyses.

Our measured yields of (alkyl-)naphthoquinones are generally less than 4%. Alkyl-naphthalenes with an alkyl-substitution on a β-carbon (2-, 3-, 6- or 7-carbon) generally give higher yields of quinone products. EI mass spectra consistent with that of a standard of 2-M-1,4-NQ confirmed that the products listed in Table 22 were quinones. The isomer identities given for the quinones listed in Table 22 assume that quinones with dione-substitution on the same ring as alkyl-substitution have higher yields than those on the opposite ring. Also, two quinones each were observed to be formed from 1,6-DMN and 1,7-DMN and it was assumed that the quinone formed on the ring with the β-methyl substituent will be the more abundant isomer.

Scheme 2 in Section E., taking 1-MN for example, is proposed to describe the reaction pathway. For the methyl-, ethyl-, and dimethylnaphthalenes, H-atom abstraction from the substituent alkyl groups by NO_3 radicals is minor, as expected (Atkinson, 1991). We estimate that H-atom abstraction under our experimental conditions is less than 10% (allowing for our measured yields as lower limits). The reactions of alkylnaphthalenes with NO_3 radicals mainly occur by initial addition of the NO_3 radical to the aromatic ring to form a NO_3-PAH adduct which then either decomposes back to reactants, reacts with NO_2 to form nitroarenes, reacts with O_2, or possibly decomposes unimolecularly (Phousongphouang and Arey, 2003).

Profiles of dimethyl-/ethyl-nitronaphthoquinones. The retention indices (RIs) and formation rates of dimethyl-/ethyl-naphthoquinones, tabulated in Table 24, were calculated to assist identification of dimethyl-/ethyl-naphthoquinones formed from the reaction of the dimethyl-/ethyl-naphthalene mixture with NO_3 radicals. 1-Nitronaphthalene (1-NN) and 9-nitrophenanthrene (9-NPhen) were chosen as the reference standards for RI calculation with the RI (1-NN) assigned as 200 and RI (9-NPhen) assigned as 300. The retention indices were then calculated, using the expression RI (Quinone) = 200 + {100 x [(retention time of the quinone of interest) – (retention time of 1-NN)] / [(retention time of 9-NPhen) – (retention time of 1-NN)]}, where the retention time of 1-NN is 30.632 min and that of 9-NPhen is 45.661 min.

Table 24. Retention time and retention indices (RIs) of dimethyl-/ethyl-naphthoquinones formed
from the NO_3 radical-nitiated reactions, and their formation rates.

name	retention time	retention indices[a]	formation rates $(fg\ m^{-3}\ h^{-1})$[b]
1-E-5,8-NQ	29.832	194.7	1.5
1,6-DM-5,8-NQ	30.704	200.5	46.4
2-E-1,4-NQ	30.811	201.2	18.7
1,7-DM-5,8-NQ	30.906	201.8	9.6
2-E-5,8-NQ	31.379	205.0	4.5
2,3-DM-1,4-NQ	31.434	205.3	19.3
1,3-DM-5,8-NQ	31.447	205.4	-[c]
2,6-DM-1,4-NQ	31.654	206.8	50.9
2,7-DM-1,4-NQ	31.713	207.2	96.0

[a] 1-Nitronaphthalene (1-NN) and 9-nitrophenanthrene (9-NPhen) were chosen as the reference
standards for RI calculation with the RI (1-NN) assigned as 200 and RI (9-NPhen) assigned as
300. The retention indices were calculated, using the expression
RI = 200 + {100 × [(retention time of the quinone of interest) – (retention time of 1-NN)] /
[(retention time of 9-NPhen) – (retention time of 1-NN)]},
where the retention time of 1-NN is 30.632 min and that of 9-NPhen is 45.661 min.

[b] The formation rates of dimethyl-/ethyl-naphthoquinones from reactions of alkylnaphthalene
with NO_3 radicals were calculated, using the expression

$[Quinone]_t = k_{obs} \times [NO_3] \times [NO_2] \times Y \times [alkylnaphthalene] \times t$

where $[Quinone]_t$ is the amount formed after time t, k_{obs} is the rate constant for reaction of
alkylnaphthalene with NO_3 radicals, and Y is the formation yield of dimethyl-/ethyl-
naphthoquinones from the reaction of alkylnaphthalene with NO_3 radicals. An average 12-hr
NO_3 radical concentration of 5×10^8 molecule cm^{-3} (Atkinson, 1991) and a background 12-hr
NO_2 concentration of 4.8×10^{11} molecule cm^{-3} during sample collection (CARB) were assumed.
The concentrations of alkylnaphthalenes used were those measured from 19:00-06:30 during
Aug. 26-30, 2002, in Riverside, CA (Reisen and Arey, 2005) (ng m^{-3}): 1-EN, 0.7; 2-EN, 1.6;
1,3-DMN, 1.1; 1,6-DMN, 1.8; 1,7-DMN, 1.1; 2,3-DMN, 0.4; 2,6-DMN, 1.4; 2,7-DMN, 1.4.

[c] The formation rate is very small since the yield (see Table 22) is below detection limit.

The formation rates of dimethyl-/ethyl-naphthoquinones from reactions of
alkylnaphthalene with NO_3 radicals were calculated, using the expression $[Quinone]_t = k_{obs}$ x
$[NO_3]$ x $[NO_2]$ x Y x [alkylnaphthalene] x t, where $[Quinone]_t$ is the amount formed after time t,
k_{obs} is the rate constant for reaction of alkylnaphthalene with NO_3 radicals, and Y is the
formation yield of dimethyl-/ethyl-naphthoquinones from the reaction of alkylnaphthalene with

NO$_3$ radicals. An average 12-hr NO$_3$ radical concentration of 5 x 10^8 molecule cm^{-3} (Atkinson, 1991) and a background 12-hr NO$_2$ concentration of 4.8 x 10^{11} molecule cm^{-3} (CARB) were assumed. The concentrations of alkylnaphthalenes used were those measured from 19:00-06:30 during Aug. 26-30, 2002, in Riverside, CA (Reisen and Arey, 2005) (ng m^{-3}): 1-EN, 0.7; 2-EN, 1.6; 1,3-DMN, 1.1; 1,6-DMN, 1.8; 1,7-DMN, 1.1; 2,3-DMN, 0.4; 2,6-DMN, 1.4; 2,7-DMN, 1.4. The isomers with the highest mass formation rates from the NO$_3$ radical initiated-reactions with dimethyl-/ethyl-naphthalenes are 2,7-DM-1,4-NQ and 2,6-DM-1,4-NQ (Table 24).

Using the calculated retention indices and formation rates, isomers were identified from the GC-MS/NCI profile of the dimethyl-/ethyl-naphthoquinone molecular ions obtained from the reaction of NO$_3$ radicals with a mixture of dimethyl/ethyl-naphthalenes in the chamber (Figure 27). Note that there might be a small amount of 1,3-DM-5,8-NQ co-eluting with 2,3-DM-1,4-NQ. Clearly, the presence of these quinones in ambient air should be investigated. Additionally, the isomer-specific toxicity and the potential of these DMNQs/ENQs to form ROS needs to be examined in order to evaluate the potential health effect of those compounds.

Photolysis of 2-M-1NN and 2,6-DM-1NN. Photolysis of 1-nitronaphthalene has been shown to be an atmospheric formation source of 1,4-naphthoquinone (Atkinson *et al.*, 1989) and 2-methyl-1,4-naphthoquinone has been observed as the photolysis product of 2-M-1NN (Arey *et al.*, 1990). In this study, we conducted preliminary experiments to measure the yields of 2-methyl-1,4-naphthoquinone formed from the photolysis of 2-M-1NN under varying initial NO$_x$ concentrations. Figure 28 shows plots of 2-methyl-1,4-naphthoquinone formed against 2-methyl-1-nitronaphthalene photolyzed.

Our initial measurement of the yield of 2-M-1,4-NQ from 2-M-1NN without added NO was significantly below the reported value of 18% in the presence of 10 ppm NO (Arey *et al.*, 1990). Subsequently an experiment with 10 ppm added NO was conducted and the yield (18±1 % using least-squares analyses, see Figure 28) agreed with the literature value (Arey *et al.*, 1990). Together with experiments with 9 ppb initial NO and 9 ppb initial NO$_2$, our data suggest that the yield of 2-methyl-1,4-naphthoquinone increases as the initial NO$_x$ concentration increases, although this may be an artifact due to wall effects.

A photolysis experiment of 2,6-dimethyl-1-nitronaphthalene was also conducted, with 9 ppb of initial NO$_2$ (a realistic level for an urban atmosphere) and 2,6-dimethyl-1,4-naphthoquinone was observed.

Our results suggest that photolysis of (alkyl-)nitronaphthalenes may lead to formation of (alkyl-)naphthoquinones in the atmosphere, but the apparent involvement of NO$_x$ needs to be verified and understood before the importance of this formation pathway can be assessed. Based on the yields of DMNNs/ENNs from the NO$_3$ radical-initiated reactions of the DMNs/ENs and the less than unity yields of quinones by photolysis, it appears that direct formation of quinones from NO$_3$ radical reaction of, in particular, the β-alkyl-substituted naphthalenes will be the dominant atmospheric formation mechanism. For naphthalene, formation of 1,4-naphthoquinone from the OH radical-initiated reaction of naphthalene (Sasaki *et al.*, 1997) could also be a significant atmospheric source and OH radical-initiated formation of alkylnaphthoquinones should also be considered. Clearly, further work remains to understand the importance of atmospheric formation of alkylnaphthoquinones. The data provided here will be useful for conducting ambient measurements of alkylnaphthoquinones, which will help determine the relative importance of atmospheric formation sources of these potentially cytotoxic, immunotoxic and carcinogenic (alkyl-)naphthoquinones.
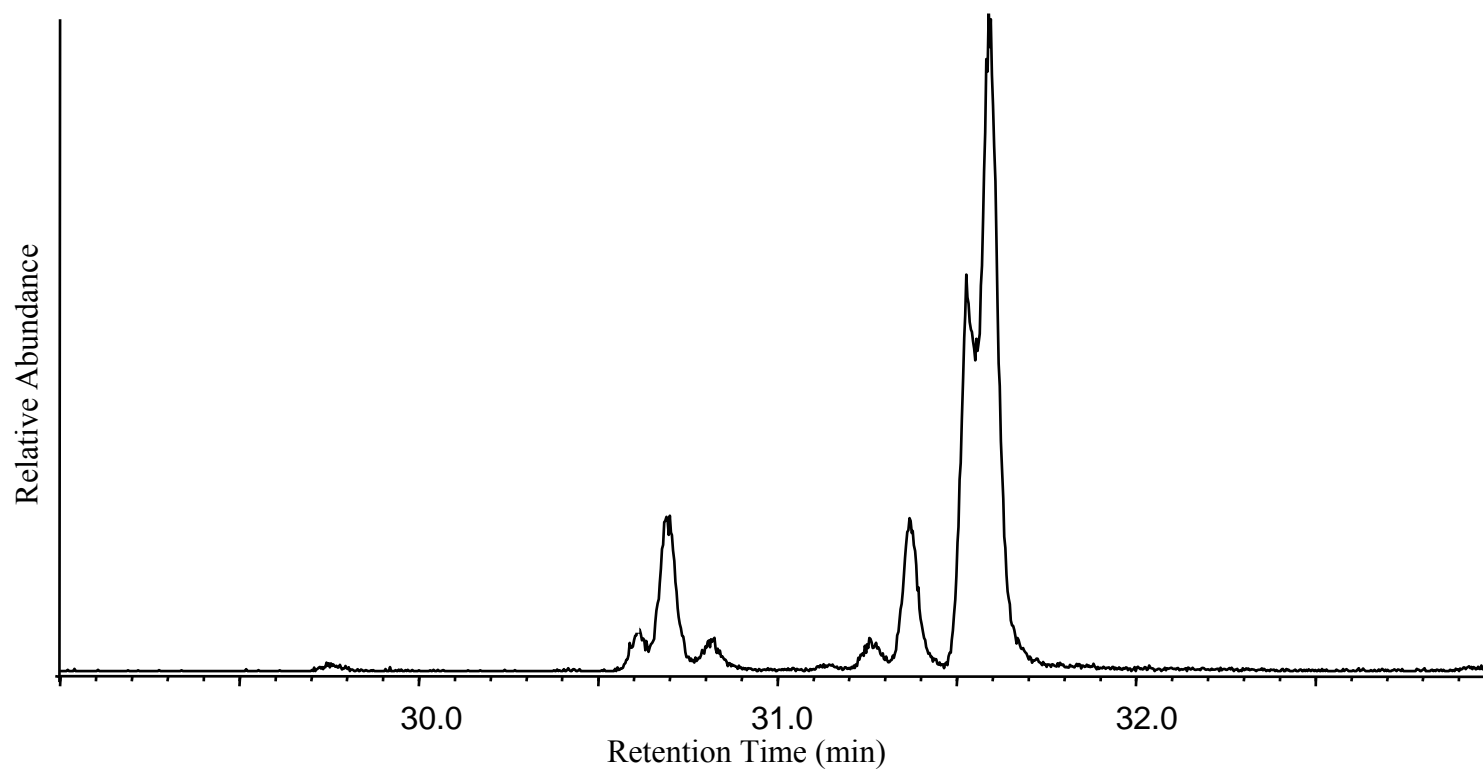
Figure 27. GC-MS/NCI profile of the dimethyl-/ethyl-nitronaphthoquinone molecular ions obtained from the reaction of NO_3 radicals with a mixture of dimethyl/ethyl-naphthalenes in the chamber.
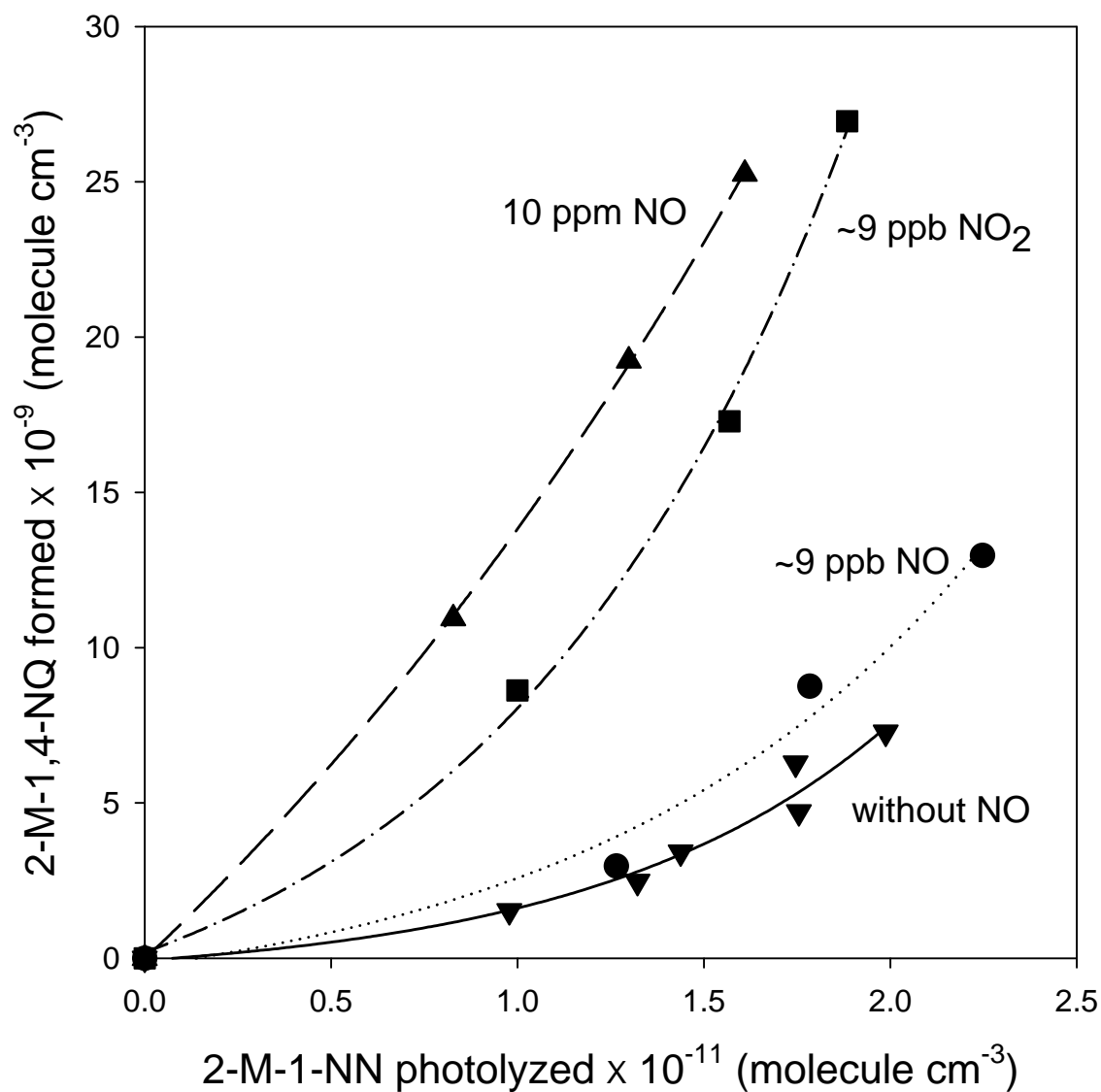
Figure 28. Formation of 2-methyl-1,4-naphthoquinone (2-M-1,4-NQ) from photolysis of 2-methyl-2-nitronaphthalene (2-M-1NN) under varied starting NO_x concentrations. The lines are for illustrative purposes only.

III. RECOMMENDATIONS FOR FUTURE RESEARCH

Our research suggests that nighttime NO_3 chemistry can be a significant source of nitro-PAHs and PAH-quinones in ambient atmospheres. Our previous measurements of DMNNs suggest that in Southern California, NO_3 radical chemistry will be important.

- Ambient measurements of 9,10-phenanthrenequinone and alkylnitronaphthalenes should be made to assess the importance of the NO_3 radical-initiated formation pathways.

- Health effects studies designed to specifically address the importance of nighttime NO_3 chemistry should be initiated. An optimum study would have measurements of the NO_3 radical, measurements of important PAH products such as 9,10-phenanthrene quinone and nitro-PAHs, and an appropriate bioassay and/or biological exposure.

Several surprising findings in this work need to be confirmed and understood. These uncertainties include:

- The apparent importance of *ipso* addition of the OH radical to 1,2-DMN, and of the *ipso* addition of NO_3 radical to several DMNs should be explored.

- The carboxaldehyde formation from NO_3 radical reactions of alkylnaphthalenes needs to be understood as part of a comprehensive mechanism for the NO_3 reactions.

- The apparent NO_x dependence of the quinone yields from the photolysis of alkylnitronaphthalenes must be evaluated.

- Side-chain nitration in the NO_3 reactions of alkylnaphthalenes cannot be explained based on known gas-phase NO_3 reaction mechanisms. The possibility of heterogeneous (i.e., wall) reactions causing this unusual nitration should be examined.

- Most importantly, the mechanisms after the initial step of the reactions of OH and NO_3 radicals with naphthalene and alkylnaphthalenes need to be elucidated.

We have identified a suite of oxygenated products from the OH radical-initiated reaction of the alkylnaphthalenes and the health effects of these polar products should be studied. Also, we have identified, many for the first time, specific isomers of alkylnitronaphthalenes in ambient samples and their contribution to the genotoxicity of ambient air should be assessed.

IV. REFERENCES

Alcorn, P. G. E., Wells, P. R. 1965. Nitration of the methylnaphthalenes. Aust. J. Chem., 18, 1377-1389.

Allen, J.O., Dookeran, N.M., Taghizadeh, K., Lafleur, A.L., Smith, K.A., Sarofim, A.F., 1997. Measurement of oxygenated polycyclic hydrocarbons associated with a size-segregated urban aerosol. Environmental Science and Technology, 31, 2064-2070.

Arey, J., Zielinska, B., Atkinson, R., Winer, A.M., 1987. Polycyclic aromatic hydrocarbon and nitroarene concentrations in ambient air during a wintertime high-NO_x episode in the Los Angeles basin. Atmospheric Environment, 21, 1437-1444.

Arey, J., Zielinska, B., Harger,W.P., Atkinson, R., Winer, A.M., 1988. The contribution of nitrofluoranthenes and nitropyrenes to the mutagenic activity of ambient particulate organic matter collected in southern California. Mutat. Res., 207, 45-51.

Arey, J., Zielinska, B. 1989. High resolution gas chromatography/mass spectrometry analysis of the environmental pollutants methylnitronaphthalenes. J. High Res. Chrom., 12, 101-105.

Arey, J., Harger, W. P., Helmig, D., Atkinson, R. 1992. Bioassay-directed fractionation of mutagenic PAH atmospheric photooxidation products and ambient particle extracts. Mutat. Res., 281, 67-76.

Arey, J., 1998. Atmospheric reaction of PAHs including formation of nitroarenes. In: Nielson, A.H. (Ed.) The Handbook of Environmental Chemistry, Vol. 3: Anthropogenic Compounds, Part I: PAHs and Related Compounds., pp. 347-385 (Chapter 9).

Arey, J., Atkinson, R., Zielinska, B., McElroy, P.A., 1989a. Diurnal concentrations of volatile polycyclic aromatic hydrocarbons and nitroarenes during a photochemical air pollution episode in Glendora, California. Environmental Science and Technology, 23, 321-327.

Arey, J., Zielinska, B., Atkinson, R., Aschmann, S.M., 1989b. Nitroarene products from the gas-phase reactions of volatile polycyclic aromatic hydrocarbons with the OH radical and N_2O_5. International Journal of Chemical Kinetics, 21, 775-799.

Arey, J., Atkinson, R., Aschmann, S.M., Schuetzle, D., 1990. Experimental investigation of the atmospheric chemistry of 2-methyl-1-nitronaphthalene and a comparison of predicted nitroarene concentrations with ambient air data. Polycyclic Aromatic Compounds, 1, 33-50.

Arey, J., Harger, W.P., Helmig, D., Atkinson, R., 1992. Bioassay-directed fractionation of mutagenic PAH atmospheric photooxidation products and ambient particle extracts. Mutation Research, 281, 67-76.

Arey, J., Aschmann, S.M., Kwok, E.S.C., Atkinson, R., 2001. Alkyl nitrate, hydroxyalkyl nitrate, and hydroxycarbonyl formation from the NO_x – air photooxidations of $C_5 - C_8$ *n*-alkanes. Journal of Physical Chemistry A., 105, 1020-1027.

Arey, J., Atkinson, R., 2003. Photochemical reactions of PAHs in the atmosphere. In: PAHs: An Ecotoxicological Perspective, P.E.T. Douben, Ed., pp. 47-63. John Wiley & Sons Ltd., West Sussex, England.

Arey, J., Bethel, H. L., Reisen, F., Brune, W. H. 2004. Nitro-PAHs in Mexico City: can their presence by attributed to hydroxyl radical reactions? Megacity Impacts on Air Quality, AGU Fall Meeting, San Francisco, CA, December 13-15.

Aschmann, S. M., Chew, A. A., Arey, J., Atkinson, R. 1997. Products of the gas-phase reaction of OH radicals with cyclohexane: reactions of the cyclyhexoxy radical. J. Phys. Chem. A, 101, 8042-8048.

Atkinson, R., Carter, W.P.L., Winer, A.M., Pitts, J.N.Jr., 1981. An experimental protocol for the determination of OH radical rate constants with organics using methyl nitrite photolysis as an OH radical source. Journal of the Air Pollution Control Association, 31, 1090-1092.

Atkinson, R., Plum, C.N., Carter, W.P.L., Winer, A.M., Pitts, J.N.Jr., 1984. Rate constants for the gas-phase reactions of nitrate radicals with a series of organics in air at 298 ± 1 K. Journal of Physical Chemistry, 88, 1210-1215.

Atkinson, R., Winer, A.M., Pitts, J.N., Jr., 1986. Estimation of night-time N_2O_5 concentrations from ambient NO_2 and NO_3 radical concentrations and the role of N_2O_5 in night-time chemistry. Atmospheric Environment, 20, 331-339.

Atkinson, R., Arey, J., Zielinska, B., Aschmann, S. M. 1987. Kinetics and products of the gas-phase reactions of OH radicals and N_2O_5 with naphthalene and biphenyl. Environ. Sci. Technol., 21, 1014-1022.

Atkinson, R., Arey, J., Winer, A.M., Zielinska, B., Dinoff, T.M., Harger, W.P., McElroy, P.A., 1988. A Survey of Ambient Concentrations of Selected Polycyclic Aromatic Hydrocarbons (PAH) at Various Locations in California, Final Report to the California Air Resources Board, Contract No. A5-185-32, Sacramento.

Atkinson, R., Aschmann, S. M., Arey, J., Zielinska, B., Schuetzle, D. 1989. Gas-phase atmospheric chemistry of 1- and 2-nitronaphthalene and 1,4-naphthoquinone, Atmos. Environ., 23, 2679-2690.

Atkinson, R., Aschmann, S. M., Arey, J., Carter, W. P. L. 1989. Formation of ring-retaining products from the OH radical-initiated reactions of benzene and toluene. Int. J. Chem. Kinet., 21, 801-827.

Atkinson, R., 1991. Kinetics and mechanisns of the gas-phase reactions of the NO_3 radical with organic compounds. Journal of Physical and Chemical Reference Data, 20, 459-507.

Atkinson, R., Kwok, E.S.C., Arey, J., Aschmann, S.M., 1995. Reactions of alkoxy radicals in the atmosphere. Faraday Discussions ,100, 23-37.

Atkinson, R., Arey, J., Tuazon, E. C., Aschmann, S. M., Sasaki, J., Chew, A. A. 1997. *Product Studies of the Atmospherically-Important Reactions of Selected VOCs.* Final Report to CRC-APRC Contract No. AQ-1-1-94, Coordinating Research Council, Atlanta, GA.

Atkinson, R., Arey, J. 2003. Atmospheric degradation of volatile organic compounds. Chem. Rev., 103, 4605-4638.

Atkinson, R., Arey, J. 2006. Identification and Atmospheric Reactions of Polar Products of Selected Aromatic Compounds; Contract No. 03-319; Final Report to the Calfornia Air Resources Board.

Atkinson, R., Arey, J. 2007. Mechanisms of the gas-phase reactions of aromatic hydrocarbons and PAHs with OH and NO_3 radicals. Polycyclic Aromatic Compounds, in press.

Baker, J., Arey, J., Atkinson, R. 2004. Rate constants for the gas-phase reactions of OH radicals with a series of hydroxyaldehydes at 296 ± 2 K. J. Phys. Chem. A, 108, 7032-7037.

Bamford, H. A., Bezabeh, D. Z., Schantz, M. M., Wise, S. A., Baker, J. E.. 2003. Determination and comparison of nitrated-polycyciic aromatic hydrocarbons measured in air and diesel particulate reference materials. Chemosphere, 50, 575-587.

Barbas, J.T., Sigman, M.E., Dabestani, R., 1996. Photochemical oxidation of phenanthrene sorbed on silica gel. Environmental Science and Technology, 30, 1776-1780.

Biermann, H.W., Mac Leod, H., Atkinson, R., Winer, A.M., Pitts, J.N.Jr., 1985. Kinetics of the gas-phase reactions of the hydroxyl radical with naphthalene, phenanthrene, and anthracene. Environmental Science and Technology, 19, 244-248.

Bidleman, T.F., 1988. Atmospheric processes, Environmental Science and Technology, 22, 361-367.

Bolton, J.L., Trush, M.A., Penning, T., Dryhurst, G., Monks, T.J., 2000. Role of quinones in toxicology. Chemical Research in Toxicology, 13, 135-160.

Brown, H. C., Okamoto, Y. 1958. Electrophilic substituent constants, J. Am. Chem. Soc., 80, 4979-4987.

Brubaker, W.W.Jr., Hites, R.A., 1998. OH reaction kinetics of polycyclic aromatic hydrocarbons and polychlorinated dibenzo-*p*-dioxins and dibenzofurans. Journal of Physical Chemistry A, 102, 915-921.

Bunce, N. J., Liu, L., Zhu, J., Lane, D. A. 1997. Reaction of naphthalene and its derivatives with hydroxyl radicals in the gas phase. Environ. Sci. Technol., 31, 2252-2259.

California Air Resources Board, data for Riverside-Rubidoux, www.arb.ca.gov.

California Air Resources Board, Air Quality and Emissions, Air Quality Data, Historical Air Quality, www.arb.ca.gov.

Calvert, J. G., Atkinson, R., Becker, K. H., Kamens, R. M., Seinfeld, J. H., Wallington, T. J., Yarwood, G. 2002. The Mechanisms of Atmospheric Oxidation of Aromatic Hydrocarbons; Oxford University Press: New York.

Cao, X.-L., Hewitt, C.N., 1994. Study of the degradation by ozone of adsorbents and of hydrocarbons adsorbed during the passive sampling of air. Environmental Science and Technology, 28, 757-762.

Carter, W. P. L., Luo, D. M., Malkina, I. L., Pierce, J. A. 1995. Environmental chamber studies of atmospheric activities of volatile organic compounds, effects of varying chamber and light source. Final Report to National Renewable Energy Laboratory, Contact XZ-2-12075.

Cecinato, A. 2003. Nitrated polynuclear aromatic hydrocarbons in ambient air in Italy. A brief overview. J. Sep. Sci., 26, 402-408.

Chung, M.Y., Lazaro, R.A., Lim, D., Jackson, J., Lyon, J., Rendulic, D., Hasson, A.S., 2006. Aerosol-borne quinones and reactive oxygen species generation by particulate matter extracts. Environmental Science and Technology, 40, 4880-4886.

Cho, A.K., Di Stefano, E., You, Y., Rodriguez, C.E., Schmitz, D.A., Kumagai, Y., Miguel, A.H., Eiguren-Fernandez, A., Kobayashi, T., Avol, E., Froines, J.R., 2004. Determination of four quinones in diesel exhaust particles, SRM 1649a, and atmospheric PM2.5. Aerosol Science and Technology, 38 S1, 68-81.

Choudhury, D.R., 1982. Characterization of polycyclic ketones and quinones in diesel emission particulates by gas chromatography/mass spectrometry. Environ. Sci. Technol., 16, 102-106.

Coutant, R.W., Brown, L., Chuang, J.C., Riggin, R.M., Lewis, R.G., 1988. Phase distribution and artifact formation in ambient air sampling for polynuclear aromatic hydrocarbons. Atmospheric Environment, 22, 403-409.

Crimmins, B. S., Baker, J.E. 2006. Improved GC/MS methods for measuring hourly PAH and nitro-PAH concentrations in urban particulate matter. Atmos. Environ., 40, 6764-6779.

Davies, A., Warren, K. D. 1969. Nitration of dimethylnaphthalenes in acetic anhydride. J. Chem. Soc. (B), 873-878.

Durant, J. L., Busby, W. F., Jr., Lafleur, A. L., Penman, B. W., Crespi, C. L. 1996. Human cell mutagenicity of oxygenated, nitrated and unsubstituted polycyclic aromatic hydrocarbons associated with urban aerosols. Mutat. Res., 371, 123-157.

Eaborn, C., Golborn, R., Spillett, R. E., Taylor, R. 1968. Aromatic reactivity. Part XXXVII. detritiation of substituted 1- and 2-tritionaphthalenes. J. Chem. Soc. B, 1112-1123.

Eberson, L., Radner, F. 1986. Nitration of reactive aromatics *via* electron transfer. V. on the reaction between nitrogen dioxide and the radical cation hexafluorophosphates of some methyl-substituted naphthalenes. Acta Chem. Scan. B, 40, 71-78.

Ehhalt, D.H., Dorn, H.-P., Poppe, D., 1991. The chemistry of the hydroxyl radical in the troposphere. Proceedings of the Royal Society of Edinburgh, 97B, 17-34.

Eiguren-Fernandez, A., Miguel, A.H., Froines, J.R., Thurairatnam, S., Avol, E.L., 2004. Seasonal and special variation of polycylic aromatic hydrocarbons in vapor-phase and $PM_{2.5}$ in southern California urban and rural communities. Aerosol Science and Technology, 38, 447-455.

Fan, J.; Zhang, R. 2006. Atmospheric oxidation mechanism of *p*-xylene: a density functional theory study. J. Phys. Chem., 110, 7728-7737.

Fine, P. M., Chakrabarti, B., Krudysz, M., Schauer, J. J., Sioutas, C. 2004. Diurnal variations of individual organic compound constituents of ultrafine and accumulation mode particulate matter in the Los Angeles basin. Environ. Sci. Technol., 38, 1296-1304.

Fischer, A., Wilkinson, A. L. 1972. Adduct intermediates in the side-chain nitration of 1,4-dimethylnaphthalene. Canadian J. Chem., 50, 3988-3992.

Fraser, M. P., Cass, G. R., Simoneit, B. R. T. 1998. Gas-phase and particle-phase organic compounds emitted from motor vehicle traffic in a Los Angeles roadway tunnel. Environ. Sci. Technol., 32, 2051-2060.

Fraser, M. P., Cass, G. R., Simoneit, B. R. T. 2003. Air quality model evaluation data for organics. 6. C_3-C_{24} organic acids. Environ. Sci. Technol., 37, 446-453.

Froines, J., 2003. Director's dialogue by John Froines, Newsletter of the Southern California Occupational and Environmental Health Centers, p. 6, Summer.

Gallagher, K. A. Master of Science Thesis in Environmental Toxicology, *The Synthesis of Dimethylnitronaphthalenes and Ethylnitronaphthalenes as an Aid to Their Identification in Ambient Air.* University of California, Riverside, 2006.

George, L.A., Hard, T.M., O'Brien, R.J., 1999. Measurements of free radicals OH and HO_2 in Los Angeles smog. Journal of Geophysical Research, 104, 11643-11655.

Gupta, P., 1995. The Contribution of Methylnitronaphthalenes to the Vapor-Phase Mutagenicity Observed in Ambient Air Samples Collected at Redlands, Califo*rnia.* Thesis in Environmental Toxicology, March 1995, University of California, Riverside.

Gupta, P., Harger, W.P., Arey, J., 1996. The contribution of nitro- and methylnitro-naphthalenes to the vapor-phase mutagenicity of ambient air samples. Atmospheric Environment, 30, 3157-3166.

Helmig, D., Arey, J., Harger, W.P., Atkinson, R., Lopez-Cancio, J., 1992a. Formation of mutagenic nitrodibenzopyranones and their occurrence in ambient air. Environmental Science and Technology, 26, 622-624.

Helmig, D., Lopez-Cancio, J., Arey, J., Harger, W.P., Atkinson, R., 1992b. Quantification of ambient nitrodibenzopyranones: further evidence for atmospheric mutagen formation. Environmental Science and Technology, 26, 2207-2213.

Helmig, D., Harger, W.P., 1994. OH radical-initiated gas-phase reaction products of phenanthrene. Science of the Total Environment, 148, 11-21.

Hiyoshi, K., Takano, H., Inoue, K., Ichinose, T., Yanagisawa, R., Tomura, S., Cho, A.K., Froines, J.R., Kumagai, Y., 2005. Effects of a single intratracheal administration of phenanthraquinone on murine lung. Journal of Applied Toxicolology, 25, 47-51.

Huh, T.S., 2000. Ozonolysis of phenanthrene adsorbed on polyethylene. Bulletin of the Korean Chemical Society, 21, 365-452.

IARC Monographs on the Evaluation of the Carcinogenic Risk of Chemicals to Humans. 1984. *Polynuclear Aromatic Compounds, Part 2, Carbon Blacks, Mineral Oils and Some Nitroarenes*, Vol. 33, Lyon: World Health Organization, International Agency for Research on Cancer.

IPCS Environmental Health Criteria 229. 2003. *Selected Nitro- and Nitro-oxy-polycyclic Aromatic Hydrocarbons,* Geneva: World Health Organization, International Programme on Chemical Safety.

IUPAC, http://www.iupac-kinetic.ch.cam.ac.uk/ (2006).

Kahan, T.F., Kwamena, N.-O.A., Donaldson, D.J., 2006. Heterogeneous ozonation kinetics of polycyclic aromatic hydrocarbons on organic films. Atmospheric Environment, 40, 3448-3459.

Kishikawa, N., Nakao, M., Ohba, Y., Nakashima, K., Kuroda, N., 2006. Concentration and trend of 9,10-phenanthrenequinone in airborne particulates collected in Nagasaki city, Japan. Chemosphere, 64, 834-838.

Kitayama, T. 1997. Microbial asymmetric syntheses of 3-alkylphthalide derivatives. Tetrahedron: Asymmetry, 8, 3765-3774.

Koch, R., Knispel, R., Elend, M., Siese, M., Zetzsch, C. 2006. Consecutive reactions of aromatic-OH adducts with NO, NO_2 and O_2: benzene, toluene, m- and p-xylene, hexamethylbenzene, phenol, m-cresol and aniline. Atmos. Chem. Phys. Discuss., 6, 7623-7656.

Koziel, J.A., Odziemkowski, M., Pawliszyn, J., 2001. Sampling and analysis of airborne particulate matter and aerosols using in-needle trap and SPME fiber devices. Analytical Chemistry, 73, 47-54.

Krol, M., van Leeuwen, P. J., Lelieveld, J. 1998. Global OH trend inferred from methylchloroform measurements, J. Geophy. Res., 103, 10697-10711.

Kumagai, Y., Nakajima, H., Midorikawa, K., Homma-Takeda, S., Shimojo, N., 1998. Inhibition of nitric oxide formation by neuronal nitric oxide synthase by quinones: nitric oxide synthase as a quinone reductase. Chem. Res. Toxicol., 11, 608-613.

Kumagai, Y., Hayashi, T. Miyauchi, T., Endo, A., Iguchi, A., Kiriya-sakai, M., Sakai, S., Yuki, K., Kikushima, M., Shimojo, N., 2001. Phenanthraquinone inhibits eNOS activity and suppresses vasorelaxation. Am. J. Physiol. Regulatory Integrative Comp. Physiol., 281, R25-R30.

Kumagai, Y., Koide, S., Taguchi, K., Endo, A., Nakai, Y., Yoshikawa, T., Shimojo, N., 2002. Oxidation of proximal protein sulfhydryls by phenanthraquinone, a component of diesel exhaust particles. Chem. Res. Toxicol., 15, 483-489.

Kwok, E.S.C., Harger, W.P., Arey, J., Atkinson, R., 1994. Reactions of gas-phase phenanthrene under simulated atmospheric conditions. Environmental Science and Technology, 28, 521-527.

Kwok, E. S. C., Atkinson, R. 1995. Estimation of hydroxyl radical reaction rate constants for gas-phase organic compounds using a structure-reactivity relationship: an update. Atmos. Environ., 29, 1685-1695.

Lame, M.W., Jones, A.D., Wilson, D.W., Segall, H.J., 2003. Protein targets of 1,4-benzoquinone and 1,4-naphthoquinone in human bronchial epithelial cells. Proteomics, 3, 479-495.

Lee, W., Stevens, P.S., Hites, R.A., 2003. Rate constants for the gas-phase reactions of methylphenanthrenes with OH as a function of temperature. Journal of Physical Chemistry A, 107, 6603-6608.

Lim, Y.B., Ziemann, P.J., 2005. Products and mechanism of secondary organic aerosol formation from reactions of n-alkanes with OH radicals in the presence of NO_x. Environmental Science and Technology, 39, 9229-9236.

Logan, J.A., 1985. Tropospheric ozone: seasonal behavior, trends, and anthropogenic influence. Journal of Geophysical Research, 90, 10463-10482.

Lorenz, K., Zellner, R., 1984. 8th International symposium on gas kinetics. University of Nottingham, U.K.. Cited in: Atkinson, R., 1989. Kinetics and mechanisms of the gas-phase reactions of the hydroxyl radical with organic compounds. Journal of Physical and Chemical Reference Data Monograph, 1, 1-246.

Marr, L. C., Dzepina, K., Jimenez, J. L., Reisen, F., Bethel, H. L., Arey, J., Gaffney, J. S., Marley, N. A., Molina, L. T., Molina, M. J. 2006. Sources and transformations of particle-bound polycyclic aromatic hydrocarbons in Mexico City. Atmos. Chem. Phys., 6, 1733-1745.

McLafferty, F.W., Turecek, F. 1993. Interpretation of Mass Spectra; University Science Books: Mill Valley, CA.

McMurry, P.H., Rader, D.J., 1985. Aerosol wall losses in electrically charged chambers. Aerosol Science and Technology, 4, 249-268.

Miller, D. W., Evans, F. F., Fu, P. P. 1985. Effect of a nitro group geometry on the proton NMR chemical shifts of nitro aromatics. Spectros. Int. J., 4, 91-94.

Moza, P.N., Hustert, K., Kettrup, A., 1999. Photooxidation of naphthalene and phenanthrene in hexane as an oil film on water. Chemosphere, 39, 569-574.

NIST Structures and Properties, Standard Reference Database 25, Version 2.0, Stein, S. E. (Ed.), Chemical Kinetics and Thermodynamics Division, National Institute of Standards and Technology, Gaithersburg, MD, January 1994.

NIST Chemistry WebBook, http://webbook.nist.gov/chemistry (2006); Láng, L. (ed), Absorption Spectra in the Ultraviolet and Visible Region, Academic Press, 1975, Vol. 20, p. 27.

O'Brien, P. J., Siraki, A. G., Shangari, N. 2005. Aldehyde sources, metabolism, molecular toxicity mechanisms, and possible effects on human health. Crit. Rev. Tocicol., 35, 609-662.

Panic, O., Gorecki, T. 2006. Comprehensive two-dimensional gas chromatography (GC X GC) in environmental analysis and monitoring. Anal. Bioanal. Chem., 386, 1013-1023.

Paputa-Peck, M.C., Marano, R.S., Schuetzle, D., Riley, T.L., Hampton, C., Prater, T.J., Skewes, L.M., Jensen, T.E., Ruehle, P.H., Bosch, L.C., Duncan, W.P. 1983. Determination of nitrated polynuclear aromatic hydrocarbons in particulate extracts by capillary column gas chromatography with nitrogen selective detection. Anal. Chem., 55, 1946-1954.

Phousongphouang, P.T., Grosovsky, A.J., Eastmond, D.A., Covarrubia, M., Arey, J., 2000. The genotoxicity of 3-nitrobenzanthrone and the nitropyrene lactones in human lymphoblasts. Environ. Mutagenesis, 472, 93-103.

Phousongphouang, P.T., Arey, J., 2002. Rate constants for the gas-phase reactions of a series of alkylnaphthalenes with the OH radical. Environmental Science & Technology, 36, 1947-1952.

Phousongphouang, P.T., Arey, J., 2003a. Rate constants for the gas-phase reactions of a series of alkylnaphthalenes with the nitrate radical. Environmental Science & Technology, 37, 308-313.

Phousongphouang, P.T., Arey, J., 2003b. Rate constants for the photolysis of the nitronaphthalenes and methylnitronaphthalenes. Journal of Photochemistry and Photobiology A., 157, 301-309.

Phousongphouang, P.T., Arey, J., 2003c. Sources of the atmospheric contaminants, 2-nitrobenzanthrone and 3-nitrobenzanthrone. Atmospheric Environment, 37, 3189-3199.

Pitts, J. N. Jr., Atkinson, R., Sweetman, J. A., Ziekinska, B. 1985. The gas-phase reaction of naphthalene with N_2O_5 to form nitronaphthalenes. Atmos. Environ., 19, 701-705.

Poster, D.L., Sander, L.C., Wise, S.A. 1998. Chromatographic methods of analysis for the determination of PAHs in environmental samples. In *PAHs and Related Compounds*, A. H. Neilson, Ed. The Handbook of Environmental Chemistry, Volume 3, Part I, O. Hutzinger, Series Ed., Berlin: Springer-Verlag, pp. 77-135.

Prinn, R.G., Huang, J., Weiss, R.F., Cunnold, D.M., Fraser, P.J., Simmonds, P.G., McCulloch, A., Harth, C., Salameh, P., O'Doherty, S., Wang, R.H.J., Porter, L., Miller, B.R., 2001. Evidence for substantial variations of atmospheric hydroxyl radicals in the past two decades. Science, 292, 1882-1888.

Reisen, F., Arey, J., 2002. Reactions of hydroxyl radicals and ozone with acenaphthene and acenaphthylene. Environmental Science and Technology, 36, 4302-4311.

Reisen, F., Wheeler, S., Arey, J., 2003. Methyl- and dimethyl-/ethyl-nitronaphthalenes measured in ambient air in Southern California. Atmos. Environ., 37, 3653-3657.

Reisen, F., Arey, J., 2005. Atmospheric reactions influence seasonal PAH and nitro-PAH concentrations in the Los Angeles Basin. Environmental Science and Technology, 39, 64-73.

Rodriguez, C.E., Shinyashiki, M., Froines, J., Yu, R.C., Fukuto, J.M., Cho, A.K., 2004. An examination of quinine toxicity using the yeast *Saccharomyces cerevisiae* model system. Toxicology, 201, 185-196.

Rodriguez, C.E., Fukuto, J.M., Taguchi, K., Froines, J., Cho, A.K., 2005. The interactions of 9,10-phenanthrenequinone with glyceraldehyde-3-phosphate dehydrogenase (GAPDH) a potential site for toxic actions. Chemical-Biological Interactions, 155, 97-110.

Sankararaman, S., Kochi, J. K. 1991. Kinetics and mechanisms of charge-transfer nitration. part 2. time-resolved spectral evolution of the *ipso* adducts from 1,4-dimethylnaphthalene cation radical. J. Chem. Sco. Perkin Trans. 2, 165-174.

Sasaki, J., Arey, J., Harger, W.P., 1995. Formation of mutagens from the photooxidations of 2 - 4-ring PAH. Environmental Science & Technology, 29, 1324-1335.

Sasaki, J., Aschmann, S.M., Kwok, E.S.C., Atkinson, R. Arey, J., 1997a. Products of the gas-phase OH and NO_3 radical-initiated reaction of naphthalene. Environ. Sci. Technol., 31, 3173-3179.

Sasaki, J.C., Arey, J., Eastmond, D.A., Parks, K.K., Grosovsky, A.J., 1997b. Genotoxicity induced in human lymphoblasts by atmospheric reaction products of naphthalene and phenanthrene. Mutation Research, 393, 23-35.

Sasaki, J.C., Arey, J., Eastmond, D.A., Parks, K.K., Phousongphouang, P.T., Grosovsky, A.J., 1999. Evidence for oxidative metabolism in the genotoxicity of the atmospheric reaction product 2-nitronaphthalene in human lymphoblastoid cell lines. Mutation Research, 445, 113-125.

Scanlon, J. T., Willis, D. E. 1985. Calculation of flame ionization detector relative response factors using the effective carbon number concept. J. Chromatogr. Sci., 23, 333-340.

Schauer, J. J., Fraser, M. P., Cass, G. R., Simoneit, B. R. T. 2002. Source reconciliation of atmospheric gas-phase and particle-phase pollutants during a severe photochemical smog episode. Environ. Sci. Technol., 36, 3806-3814.

Schmitt, W.J., Moriconi E.J., O'Connor, W.F., 1955. The ozonolysis of phenanthrene. Journal of the American Chemical Society, 77, 5640-5642.

Schuetzle, D., 1983. Sampling of vehicle emissions for chemical analysis and biological testing. Environmental Health Perspectives, 47, 65-80.

Schuetzle, D., Jensen, T.E. 1985. Analysis of nitrated polycyclic aromatic hydrocarbons (Nitro-PAH) by mass spectrometry: In *Nitrated Polycyclic Aromatic Hydrocarbons*, C. M. White (Ed.) Huethig, Heidelberg, pp. 121-167.

Suzuki, H., Mori, T. 1996. Ozone-mediated nitration of naphthalene and some methyl derivatives with nitrogen dioxide. remarkable enhancement of the 1-nitro/2-nitro isomer ratio and mechanistic implications. J. Chem. Soc., Perkin Trans. 2, 677-683.

Taylor, W. D., Allston, T. D., Moscato, M. J., Fazekas, G. B., Kozlowski, R., Takacs, G. A. 1980. Atmospheric photodissociation lifetimes for nitromethane, methyl nitrite, and methyl nitrate. Int. J. Chem. Kinet., 12, 231- 240.

Thiault, G., Mellouki, A., Le Bras, G., Chakir, A., Sokolowski-Gomez, N., Daumont, D. 2004. UV-absorption cross sections of benzaldehyde, ortho-, meta-, and para-tolualdehyde. J. Photochem. Photobiol. A: Chem., 162: 273-281.

Tokiwa, H., Ohnishi, Y. 1986. Mutagenicity and carcinogenicity of nitroarenes and their sources in the environment. CRC Critical Rev. Toxicol., 17, 23-60.

Wang, L. Arey, J., Atkinson, R. 2005. Reactions of chlorine atoms with a series of aromatic hydrocarbons. Environ. Sci. Technol., 39, 5302-5310.

Wang, L., Arey, J., Atkinson, R. 2006. Kinetics and products of photolysis and reaction with OH radicals of a series of aromatic carbonyl compounds. Environ. Sci. Technol., 40, 5465-5471.

Wang, L. Doctor of Philosophy Dissertation in Environmental Toxicology, *Aspects of the Atmospheric Chemistry of Alkylnaphthalenes, Phenanthrene and their Atmospheric Reaction Products,* University of California, Riverside, 2006.

Wang, L., Atkinson, R., Arey, J. 2007a. Formation of 9,10-phenanthrenequinone by atmospheric gas-phase reactions of phenanthrene. Atmos. Environ., 41, 2025-2035. Wang, L., Atkinson, R., Arey, J. 2007b. Dicarbonyl products of the OH radical-initiated reactions of

Wania, F., Mackay, D., 1996. Tracking the distribution of persistent organic pollutants. Environmental Science and Technology, 30, 390A-396A.

Wells, P. R., Alcorn, P.G. E. 1963. Proton magnetic resonance spectra of nitronaphthalenes in dimethylacetamide solution. Aust. J. Chem., 16, 1108-1118.

Wilson, N. K., McCurdy, T. R. , Chuang, J.C. 1995. Concentrations and phase distributions of nitrated and oxygenated polycyclic aromatic hydrocarbons in ambient air. Atmos. Environ., 29, 2575-2584.

Zafonte, L., Rieger, P. L., Holmes, J. R. 1977. Nitrogen dioxide photolysis in the Los Angeles atmosphere. Environ. Sci. Technol., 11, 483-487.

Zetzsch, C. 1982. Predicting the rate of OH-addition to aromatic rings using σ^+-electrophilic substituent constants for mono- and polysubstituted benzene, 15th Informal Conference on Photochemistry, Stanford, CA, June 27-July 1, 1982.

Zheng, M., Cass, G. R., Schauer, J. J., Edgerton, E. S. 2002. Source apportionment of PM2.5 in the southeastern United States using solvent-extractable organic compounds as tracers. Environ. Sci. Technol., 36, 2361-2371.

Zhu, L., Cronin, T. J. 2000. Photodissociation of benzaldehyde in the 280-308 nm region, Chem. Phys. Lett., 317, 227-231.

Zielinska, B., Arey, J., Atkinson, R., Ramdahl, T., Winer, A.M., Pitts, J.N., Jr. 1986. Reaction of dinitrogen pentoxide with fluoranthene. J. Am. Chem. Soc., 108, 4126-4132.

Zielinska, B., J. Arey, W. P. Harger and R. W. K. Lee. 1988. Mutagenic activities of selected nitrofluoranthene derivatives in *Salmonella typhimurium* strains TA98, TA98NR and TA98/1,8-DNP$_6$. Mutat. Res., 206, 131-140.

Zielinska, B., Arey, J., Atkinson, R., McElroy, P.A. 1989. Formation of methylnitronaphthalenes from the gas-phase reactions of 1- and 2-methylnaphthalene with OH radicals and N_2O_5 and their occurrence in ambient air. Environ. Sci. Technol., 23, 723-729.

Zielinska, B., Sagebiel, J., McDonald, J. D., Whitney, K., Lawson, D. R. 2004. Emission rates and comparative chemical composition from selected in-use diesel and gasoline-fueled vehicles. J. Air & Waste Manage. Assoc., 54, 1138-1150.

Zielinska, B, Samy, S. 2006. Analysis of nitrated polycyclic aromatic hydrocarbons. Anal. Bioanal. Chem., 386, 883-890.

V.   PUBLICATIONS RESULTING FROM THIS PROJECT

Kinetics and Products of Photolysis and Reaction with OH Radicals of a Series of Aromatic Carbonyl Compounds.

L. Wang, J. Arey and R. Atkinson, *Environmental Science and Technology*, **40**, 5465-5471 (2006).

Formation of 9,10-Phenanthrenequinone by Atmospheric Gas-phase Reactions of Phenanthrene.

L. Wang, R. Atkinson and J. Arey, *Atmospheric Environment*, **41**, 2025-2035 (2007).

Dicarbonyl Products of the OH Radical-Initiated Reactions of Naphthalene and the C_1- and C_2-Alkylnaphthalenes.

L. Wang, R. Atkinson and J. Arey, *Environmental Science and Technology,* **41**, 2803-2810 (2007).

Synthesis and Identification of Dimethylnitronaphthalenes and Ethylnitronaphthalenes to Aid in their Analysis in Ambient Air.

K. A. Gallagher and J. Arey, *Polycyclic Aromatic Compounds*, in press (2007).

VI. GLOSSARY

API-MS	Atmospheric pressure ionization – mass spectrometry
CAD	Collision-activated dissociation, used in API-MS analyses
CH_3ONO	Methyl nitrite
CO	Carbon monoxide
CO_2	Carbon dioxide
da	Dalton (atomic mass unit)
DMN	Dimethylnaphthalene
DMNN	Dimethylnitronaphthalene
EN	Ethylnaphthalene
ENN	Ethylnitronaphthalene
F	Multiplicative factor to take into account secondary reactions
FT-IR	Fourier transform infrared
GC-FID	Gas chromatography with flame ionization detection
GC/MS	Combined gas chromatography-mass spectrometry
GC/MS-NCI	Combined gas chromatography-mass spectrometry with negative ion chemical ionization
GC/MS-PCI	Combined gas chromatography-mass spectrometry with positive ion chemical ionization
GC-NICIMS	Combined gas chromatography-negative ion chemical ionization mass spectrometry
HO_2	Hydroperoxyl radical
HPLC	High performance liquid chromatography
IR	Infrared

k_a	Rate constant for reaction pathway A
M	molecular weight, molecular mass
$[M]^+$	molecular ion
$[M+H]^+$	protonated molecular ion
MN	Methylnaphthalene
MNN	Methylnitronaphthalene
NCI	Negative chemical ionization
nm	Nanometer (10^{-9} m)
1-NN	1-Nitronaphthalene
2-NN	2-Nitronaphthalene
NO	Nitric oxide
NO_2	Nitrogen dioxide
NO_3	Nitrate radical
1,4-NQ	1,4-Naphthoquinone
OH	Hydroxyl radical
O_3	Ozone
PAH	Polycyclic aromatic hydrocarbon
PDMS/DVB	Polydimethylsiloxane/divinylbenzene
PFBHA	*O*-(2,3,4,5,6-Pentafluorobenzyl)hydroxylamine
$R^\bullet$	Alkyl or substituted alkyl radical
$RC(O)OO^\bullet$	Peroxyacyl radical
$RC(O)OONO_2$	Peroxyacyl nitrate
$RO^\bullet$	Alkoxy radical

ROO$^{\bullet}$ or RO$_2$$^{\bullet}$ Alkyl peroxy radical

SIM   Single ion monitoring

SPME   Solid phase micro extraction

VOC   Volatile organic compound

Absorption coefficients (M^{-1} cm^{-1}), base 10, for phthaldialdehyde, 2-acetylbenzaldehyde,

1,2-diacetylbenzene and phthalide measured in *n*-hexane solution.

wavelength	absorption coefficient (M^{-1} cm^{-1})[a]			
(nm)	phthalide	1,2-diacetylbenzene	2-acetylbenzaldehyde	phthaldialdehyde
205.0	9614[b]	23000[c]	17154 (1120)	12238 (370)
206.0	10089 (956)	22500[c]	18540 (1274)	13873 (292)
207.1	9125 (976)	21600[c]	20132 (1226)	15618 (276)
208.0	8743 (928)	20500[c]	21118 (1230)	17195 (344)
208.9	8351 (764)	22126[b]	20618[b]	19000 (219)
210.0	8168 (818)	20045[b]	21547[b]	20683[b]
211.0	7980 (784)	17153[b]	22426[b]	23053[b]
211.9	7805 (834)	14884[b]	22966[b]	24606[b]
213.0	7530 (710)	13429[b]	23266[b]	26757[b]
214.0	7415 (722)	11880[b]	23680[b]	28521[b]
215.1	7372 (672)	10124 (252)	23577[b]	30490[b]
216.0	7522 (718)	8976 (184)	23281[b]	31998[b]
216.9	7759 (688)	7935 (296)	22761[b]	32496[b]
218.0	8022 (710)	7254 (252)	21502[b]	32604[b]
219.0	8291 (706)	6734 (232)	21628 (952)	31387[b]
219.9	8684 (760)	6245 (200)	19721 (814)	30365[b]
221.0	8945 (754)	5853 (62)	17661 (958)	28641[b]
222.0	9337 (716)	5636 (68)	15625 (690)	26935[b]
223.1	9930 (756)	5472 (66)	13508 (790)	24070[b]
224.0	10066 (814)	5376 (58)	11396 (528)	20378 (82)
224.9	9406 (728)	5357 (72)	10233 (298)	16127 (256)
226.0	8653 (730)	5418 (62)	8493 (216)	11733 (140)
227.0	8039 (614)	5527 (66)	7748 (254)	9884 (56)
228.1	7322 (626)	5717 (62)	7111 (232)	8409 (86)
229.0	7541 (634)	5948 (50)	6792 (222)	7401 (46)
230.0	8207 (704)	6132 (188)	6604 (226)	6868 (104)
231.1	6819 (634)	6535 (184)	6474 (220)	5883 (74)
232.0	4927 (230)	6774 (210)	6431 (226)	5291 (48)
232.9	2907 (154)	7106 (216)	6412 (214)	4896 (68)
234.0	1499 (130)	7433 (250)	6418 (208)	4487 (44)
235.0	859 (62)	7755 (220)	6467 (224)	4369 (54)
236.1	449 (40)	8069 (232)	6590 (216)	4394 (58)
237.0	328 (34)	8196 (286)	6701 (226)	4498 (68)
237.9	250 (26)	8354 (250)	6847 (220)	4666 (64)
239.0	205 (22)	8505 (226)	7036 (222)	4936 (70)

240.0	190 (28)	8550 (210)	7204 (222)	5213 (80)
241.1	186 (26)	8528 (216)	7393 (230)	5570 (62)
242.0	187 (26)	8415 (214)	7491 (232)	5837 (62)
243.0	194 (24)	8242 (218)	7606 (236)	6090 (90)
244.1	198 (24)	7967 (188)	7689 (256)	6437 (82)
245.0	203 (22)	7597 (190)	7731 (239)	6835 (106)
245.9	218 (26)	7159 (216)	7705 (248)	7194 (82)
247.0	238 (26)	6694 (166)	7624 (240)	7514 (76)
248.0	257 (20)	6355 (154)	7531 (240)	7695 (62)
249.1	291 (20)	5823 (48)	7354 (242)	8058 (98)
250.0	315 (26)	5295 (56)	7170 (222)	8303 (106)
250.9	339 (28)	4711 (58)	6966 (220)	8516 (100)
252.0	361 (24)	4093 (58)	6755 (214)	8727 (82)
253.0	392 (24)	3670 (36)	6586 (204)	8825 (90)
253.9	435 (34)	3178 (76)	6322 (190)	8877 (74)
255.0	496 (34)	2518 (16)	5886 (184)	8915 (80)
256.0	539 (34)	2067 (32)	5403 (176)	8860 (62)
257.1	584 (36)	1649 (22)	4825 (174)	8764 (88)
258.0	622 (34)	1404 (24)	4359 (140)	8589 (70)
259.0	662 (42)	1152 (32)	3883 (174)	8341 (66)
260.1	747 (40)	943 (22)	3306 (126)	7997 (74)
261.0	815 (42)	839 (26)	2958 (126)	7726 (88)
261.9	900 (42)	760 (28)	2615 (108)	7351 (56)
263.0	986 (54)	685 (28)	2239 (100)	6811 (54)
264.0	1028 (50)	648 (24)	1936 (96)	6434 (80)
264.9	1033 (52)	632 (22)	1666 (88)	5983 (92)
266.0	1041 (56)	626 (22)	1414 (86)	5459 (60)
267.0	1071 (54)	635 (22)	1262 (74)	5042 (34)
268.1	1282 (68)	653 (22)	1075 (86)	4408 (62)
269.0	1451 (66)	671 (24)	959 (92)	3674 (38)
270.0	1589 (78)	702 (20)	862 (88)	2826 (50)
271.1	1603 (72)	743 (20)	810 (82)	2038 (40)
272.0	1501 (70)	763 (24)	795 (78)	1700 (36)
272.9	1215 (56)	797 (20)	801 (74)	1392 (44)
274.0	937 (46)	832 (18)	820 (74)	1158 (40)
275.0	834 (44)	863 (20)	844 (82)	1039 (40)
275.9	964 (52)	891 (22)	878 (70)	990 (44)
277.0	1566 (78)	915 (20)	911 (74)	986 (38)
278.0	2034 (84)	935 (18)	958 (74)	1003 (34)
279.1	1467 (100)	964 (20)	999 (70)	1056 (30)
280.0	812 (44)	982 (18)	1050 (74)	1107 (38)
280.9	431 (28)	998 (16)	1081 (56)	1167 (48)
282.0	222 (24)	1006 (16)	1125 (68)	1241 (38)
283.0	119 (14)	1007 (16)	1160 (60)	1308 (42)
283.9	67 (20)	1004 (18)	1199 (74)	1386 (42)
285.0	36 (22)	982 (14)	1233 (68)	1485 (44)

286.0	25 (12)	965 (20)	1261 (66)	1554 (44)
287.1	19 (12)	940 (16)	1272 (64)	1641 (44)
288.0	12 (10)	913 (16)	1288 (68)	1711 (44)
288.9	4 (14)	880 (14)	1294 (68)	1779 (44)
290.0		832 (20)	1295 (62)	1849 (42)
291.0		791 (20)	1284 (70)	1914 (48)
292.1		740 (12)	1265 (64)	1977 (46)
293.0		683 (12)	1239 (66)	2042 (46)
294.0		621 (14)	1204 (60)	2118 (48)
295.0		561 (12)	1145 (60)	2174 (48)
296.0		513 (16)	1092 (60)	2205 (54)
296.9		475 (10)	1034 (60)	2247 (40)
298.0		441 (10)	964 (56)	2207 (42)
299.0		403 (12)	878 (58)	2125 (44)
300.1		374 (10)	777 (56)	2009 (54)
301.0		356 (8)	712 (54)	1937 (38)
301.9		347 (12)	659 (52)	1883 (36)
303.0		329 (12)	579 (50)	1818 (42)
304.0		320 (10)	512 (54)	1756 (40)
305.1		301 (14)	445 (48)	1698 (30)
306.0		295 (14)	404 (52)	1664 (36)
306.9		287 (12)	366 (46)	1642 (36)
308.0		274 (12)	307 (40)	1548 (40)
309.0		268 (14)	269 (46)	1343 (20)
310.1		260 (12)	236 (46)	1018 (30)
311.0		255 (14)	208 (38)	758 (20)
311.9		250 (10)	193 (50)	562 (26)
313.0		240 (10)	176 (44)	380 (32)
314.0		231 (8)	176 (40)	262 (22)
315.1		226 (14)	167 (44)	181 (20)
316.0		222 (14)	164 (36)	143 (34)
316.9		215 (12)	158 (38)	113 (22)
318.0		207 (10)	155 (38)	102 (28)
319.0		199 (12)	149 (34)	86 (26)
320.1		194 (16)	148 (34)	82 (24)
321.0		187 (14)	148 (36)	77 (24)
321.9		183 (12)	141 (34)	69 (28)
323.0		172 (14)	145 (34)	71 (26)
324.0		166 (14)	136 (46)	69 (30)
325.1		156 (16)	139 (50)	72 (16)
326.0		151 (8)	132 (34)	72 (22)
326.9		147 (12)	137 (38)	71 (18)
328.0		139 (10)	131 (38)	69 (30)
329.0		132 (6)	128 (34)	63 (24)
330.0		127 (10)	124 (46)	63 (30)
331.0		119 (10)	122 (38)	66 (22)

332.1		111 (12)	120 (36)	62 (22)
333.0		108 (12)	111 (40)	62 (22)
333.9		102 (10)	114 (36)	58 (22)
335.0		92 (8)	104 (38)	59 (26)
336.0		91 (14)	109 (38)	57 (26)
337.1		87 (6)	108 (32)	58 (24)
338.0		82 (12)	109 (32)	52 (28)
338.9		76 (10)	101 (32)	60 (28)
340.0		72 (8)	101 (34)	58 (18)
341.0		71 (8)	94 (36)	58 (18)
342.0		62 (8)	89 (40)	57 (26)
343.0		60 (12)	79 (32)	59 (20)
344.1		53 (12)	87 (34)	53 (22)
345.0		50 (12)	80 (30)	55 (18)
345.9		45 (4)	76 (26)	48 (22)
347.0		41 (6)	71 (34)	56 (24)
348.0		40 (8)	72 (28)	57 (22)
349.0		35 (10)	71 (34)	53 (14)
345.0		32 (6)	68 (28)	51 (24)
351.1		30 (8)	60 (24)	51 (22)
352.0		26 (14)	61 (30)	44 (24)
352.9		22 (12)	62 (28)	42 (22)
354.0		21 (10)	58 (30)	42 (22)
355.0		20 (10)	55 (34)	41 (16)
356.0		19 (10)	51 (28)	43 (20)
357.0		15 (10)	48 (32)	38 (26)
358.1		13 (10)	44 (38)	39 (26)
359.0		9 (10)	46 (30)	36 (24)
359.9		7 (6)	44 (28)	39 (18)
361.0		11 (6)	40 (32)	34 (20)
361.9		10 (12)	47 (30)	39 (22)
363.0		5 (10)	41 (34)	33 (26)
364.0		5 (10)	43 (24)	36 (30)
365.0		7 (6)	35 (34)	34 (22)
366.0		2 (8)	34 (30)	34 (22)
367.1		1 (6)	35 (36)	32 (18)
368.0		5 (6)	31 (28)	33 (24)
368.9		1 (10)	27 (28)	30 (26)
370.0			30 (24)	31 (26)
370.9			27 (26)	30 (22)
372.0			26 (22)	31 (30)
373.0			25 (32)	35 (28)
374.0			20 (24)	30 (26)
375.0			23 (26)	28 (28)
376.1			23 (30)	30 (24)
377.0			19 (24)	27 (24)

378.1			21 (24)	26 (26)
379.0			15 (26)	23 (24)
379.9			17 (26)	27 (24)
381.0			14 (24)	23 (28)
381.9			15 (36)	21 (28)
383.0			13 (24)	25 (26)
383.9			13 (26)	22 (24)
385.0			9 (32)	21 (16)
386.0			10(24)	19 (26)
387.0			16 (28)	20 (26)
388.0			11 (32)	24 (26)
389.1			12 (22)	21 (24)
390.0			15 (18)	17 (24)
391.1			12 (24)	20 (28)
392.0			12 (22)	15 (26)
393.1			8 (22)	16 (24)
394.0			10 (26)	14 (22)
394.9			4 (22)	8 (30)
396.0			7 (16)	9 (26)
396.9			8 (24)	17 (24)
398.0			4 (22)	12 (22)
398.9			8 (18)	13 (30)

[a]Measured using a Varian CARY 50 Bio UV-Vis spectrophotometer with a 1-cm path length quartz cell. For each aromatic carbonyl, absorption spectra of 4 solutions containing different concentrations of the aromatic carbonyl (ranging from 1.21×10^{-5} to 1.67×10^{-4} M) were measured and the absorption coefficient (ε) obtained by least-squares analyses using the Beer-Lambert law, $\log_{10}(I_o/I) = \varepsilon[\text{aromatic carbonyl}]l$ (where l is the pathlength), which was shown to be valid for the wavelength range and concentrations used here. The numbers in parentheses are the 2 standard deviations obtained from least-squares analyses of the absorbance *versus* concentration at each wavelength, excluding absorbances >1.0 and not using the (0,0) point.

[b]Obtained using only the lowest two concentrations because the absorbances were >1.0 at the higher concentrations.

[c]Obtained using only the lowest concentrations plus the (0,0) point, because the absorbances were >1.0 at the higher concentrations.